Mechanisms of complex programmed patterns of anthocyanin pigment formation in *Antirrhinum majus*

A thesis presented in partial fulfilment of the requirements for the degree of

Doctor of Philosophy

in

Plant Molecular Biology

at Massey University, Palmerston North, New Zealand.

Nilangani Nadyeshda Pathirana

2007

Abstract

Antirrhinum majus is a model plant used in flower pigmentation studies. Anthocyanin pigment production is mainly controlled by regulation of transcription of the anthocyanin biosynthetic genes. Two types of transcription factors, MYB and bHLH, together with a WD40 type co-regulator have been shown to regulate the transcription of the anthocyanin biosynthetic genes. In antirrhinum, in addition to the wild type Rosea1 phenotype, in which pigmentation occurs throughout the inner and outer epidermis of the petal, other complex pigmentation patterns are observed, such as anthocyanins being produced only in the outer (abaxial) epidermis of both lobes and upper tube region of the dorsal petals (rosea^{dorsea} phenotype). The major objective of this research project was to understand the genetic regulatory system leading to the development of the two different floral pigmentation patterns in antirrhinum as a means to understanding differential regulation of gene expression in similar cells.

Promoter deletion analysis coupled with linker scanning mutagenesis identified the -162 bp to -120 bp region of the *Rosea1* promoter as important for the regulation of the *Rosea1* gene. Four putative transcription factor-binding sites within this region: a W-box, a pyrimidine box, a DOF and a WRKY transcription factor binding site were shown to be important for *Rosea1* gene regulation.

Promoter deletion analysis carried out on the *rosea1*^{dorsea} promoter showed that the proximal 187 bp deletion was, surprisingly, not responsible for the rosea^{dorsea} phenotype. Cloning and characterisation of the *Rosea1* promoter sequence from various *Antirrhinum* species and accessions verified this finding. The *rosea1*^{dorsea} promoter analysis also indicated that -151 bp of the promoter was sufficient for its expression as well as for the maintenance of petal specific expression. The *rosea1*^{dorsea} allele was also shown to encode a functional protein.

In situ hybridisation analysis showed that *Rosea1* transcripts were present in the inner and outer epidermis of the petal tissue of both wild type and rosea^{dorsea} petal tissue.

Vascular expression of the *Rosea1* mRNA is indicative of regulation of this gene through sugar or hormonal cues. However, *rosea1*^{dorsea} transcript levels (in rosea^{dorsea}) were much lower than *Rosea1* (wild type). Lowered expression of *rosea1*^{dorsea} transcripts may be responsible for the overall weak pigmentation in the rosea^{dorsea} flowers. Analysis of the intron sequences of the two alleles revealed that many sequence changes were present in the intron 2 of *rosea1*^{dorsea}. These changes may lead to instability or the lower expression of the *rosea1*^{dorsea} mRNA and may be responsible for the rosea^{dorsea} phenotype. Another possibility is that a fourth *Myb* gene may be responsible for the rosea^{dorsea} phenotype.

The role of the *Deficiens* gene in direct regulation of Rosea1 was analysed by RNAi and bioinformatics-based methods. The presence of potential MADS box binding sites in the intron 2 region of the *Rosea1* allele indicated that *Rosea1* might be directly regulated by *Deficiens*. Initial experiments using transient assays did not support this suggestion. However, silencing of *Deficiens* in wild type antirrhinum buds led to the loss of anthocyanin pigments in the petals. Further analysis of the RNAi tissue using SEM revealed that the proper development of conical shaped epidermal cells was also affected. The RNAi tissue also developed chlorophyll pigments underscoring the plasticity of petal identity. This work demonstrated that proper expression of *Deficiens* is required throughout flowering for anthocyanin pigment production as well as maintenance of petal cell identity.

The current investigation revealed that the higher order regulation of the *Rosea1* alleles in antirrhinum petals is much more complex than initially postulated.

Dedicated to the loving memory
of Chumpa aunty and Podisudu mami

Acknowledgments

I would like to express my gratitude and heartfelt thanks to my supervisors Professor Paula Jameson, Dr Kathy Schwinn, Dr Kevin Davies and Associate Professor Michael McManus. Thank you very much for your support, guidance, encouragement and faith in me. I am also grateful for the support and advice from Professor Cathie Martin.
I appreciate all the help Steve Arathoon, Jan Manson, Margaret Young and Andrew Mullen have given me in the lab. Special thanks to Erin O'Donoghue, Dave Brummell, Don Hunter, Huaibi Zhang, Lyn Watson, Simon Deroles, Jocelyn Eason, David Lewis and Marian McKenzie for helping with numerous queries, and Ian King and Julie Ryan for looking after my many tobacco plants. I am grateful to Ross Lill and Julian Heyes for letting me work at Crop & Food Research. Thanks to Tatyana, Lia, Anya, Nick, Lei, Margaret B., Margaret T., Sheryl, Phil, Carol, Maryanne, Darren, Trev and everyone in the molecular biology lab for your friendship.

Thathi and ammi, none of this would have been possible without your love, guidance, support and encouragement. You are the best parents in the whole world and I would like to thank you so much for giving me the best of everything, I am very grateful. Thank you John, for your love, support and encouragement. Thanks also to my little sis for her love and support and her faith in me. I'm also grateful to my grandparents, uncles and aunties for their best wishes in my endeavours. I would like to dedicate this thesis to the loving memory of Chumpa aunty and Podisudu mami, two people who would have loved to call me Dr. Nadyeshda.

I also acknowledge the Marsden Fund, the Institute of Molecular BioSciences, The Royal Society of New Zealand and the New Zealand Society of Plant Biologists for contributions made towards research and conference travels. I am grateful for the Bright Future Scholarship from the Tertiary Education Commission for providing me with tuition fees, general living expenses and conference monies.

Table of Contents

List of Figures

List of Tables

Abbreviations

IIA	TFIIA
2-ME	2-mercaptoethanol
3-AT	3-amino 1,2,4-triazole
ANS	Anthocyanidin synthase
BAP	Benzyl Amino Purine
Ω	Omega
bp	base pair
CHI	Chalcone isomerase
CHS	Chalcone synthase
CTAB	Cetyl Trimethyl Ammonium Bromide
Ci	Curie
DNA	DeoxyriboNucleic Acid
dNTP	deoxy Nucleotide TriPhosphate
DMF	Dimethylformamide
DMSO	Dimethyl sulfoxide
DFR	Dihydroflavonol 4-reductase
DTT	Dithiothreitol
EDTA	Ethylenediaminetetra-acetate
F3H	Flavanone 3-β-hydroxylase
F3'H	Flavonoid 3'-hydroxylase
F3'5'H	Flavanoid 3'5'-hydroxylase
g	gram
GFP	Green Fluorescent Protein
GST	Glutathione-*S*-transferase
GMO	Genetically Modified Organism
Hepes	4-(2-hydroxyethyl)-1-piperazineethanesulfonic acid
h	hour
IAA	Isoamylalcohol
IPTG	Isopropyl ß-D-1-thiogalactopyranoside

kPa	kilo Pascal
L	litre
LB	L-Broth
LS	Linsmaier and Skoog
MES	2-(*N*-morpholino)ethanesulfonic acid
min	minutes
ms	miliseconds
N_2	nitrogen
mg	milligram
mL	millilitre
MS	Murshige and Skoog
MOPS	3-(*N*-morpholino)propanesulfonic acid
NAA	Naphthaleneacetic acid
OCS	Octopine synthase
PBS	Phosphate Buffered Saline
PCR	Polymerase Chain Reaction
PIPES	Piperazine-NN'-bis-2-ethanesulphonic acid
PMSF	Phenylmethylsulphonyl fluoride
Poly A	Polyadenylic Acid
PVP	Polyvinylpyrrolidine
rpm	revolutions per minute
3RT	UDP-rhamnose: anthocyanidin-3-*O*-glucoside rhamnosyltransferase
sec	seconds
SD	Synthetic Dropout
SDS	Sodium Dodecyl Sulphate
SEM	Sucrose-EDTA-Morpholinepropanesulfonic acid
SOT	Solenoid Opening Time
TAE	Tris-Acetate-EDTA
TAFs	TBP associated factors
TB	Terrfic Broth
TBP	TATA-box binding protein

TBE	Tris-Borate-EDTA
T_m	melting temperature
µ	micro
UFGT	UDP-Glc:flavanoid 3-*O*-glucosyltransferase
UV	Ultra Violet
w/v	weight by volume
v/v	volume by volume
V	Volume
X-Gal	5-bromo-4-chloro-3-indolyl-beta-D-galactopyranoside
X-GlcA	5-Bromo-4-chloro-3-indolyl β-D-glucuronide cyclohexylamine salt

Chapter 1: Introduction

1.1 Overview

Many flowers have complex anthocyanin pigment patterns such as spots, stripes or irregular patches. All the cell and tissue types in a plant have the potential to produce anthocyanin pigments. However, their synthesis is controlled in a cell autonomous manner in response to various spatial and temporal cues. In most flower petals, anthocyanin pigments are produced only in the epidermal cell layer (Martin and Gerats, 1993). From a gene regulation aspect this raises the fundamental question as to how patterns are formed when all the cell types involved are competent to produce anthocyanin pigments.

This research project is part of a larger study determining the mechanisms by which gene expression in similar cells is differentially regulated, using the formation of different pigmentation patterns in *Antirrhinum majus* as a model system. In all plant systems studied to date, anthocyanin biosynthesis is mainly controlled at the transcriptional level by MYB transcription factors and their co-activators of the basic helix-loop-helix (bHLH) and WD40 type (Schwinn *et al.*, 2006). In this project, two pigmentation patterns in antirrhinum were analysed: the wild type, due to *Rosea1* activity in which pigmentation occurs throughout inner and outer epidermis of the petal; and $rosea^{dorsea}$ in which pigmentation occurs only in the dorsal surface of the corolla (Figure 1.1). It is hypothesised that these two pigmentation patterns are due to the promoter specificities of *Rosea1* alleles. ROSEA1 is an anthocyanin pigment regulator of the MYB transcription factor family (Schwinn *et al.*, 2006).

A second aspect of this project was to characterise pigmentation patterning in relation to development, as it is a poorly understood aspect of plant biology. In the ABC model for flower development three morphogenic functions (A, B and C) determine organ identity, although related genes outside the A, B and C functions have also been identified (Sommer *et al.*, 1990). It is known that some of the ABC genes continue to be expressed late into flower development, even after organ identity has been established. One such gene is *Deficiens,* which belongs to the B class (Schwarz-Sommer *et al.*, 1992). Therefore, it was hypothesised that the class B *Deficiens* gene may control petal

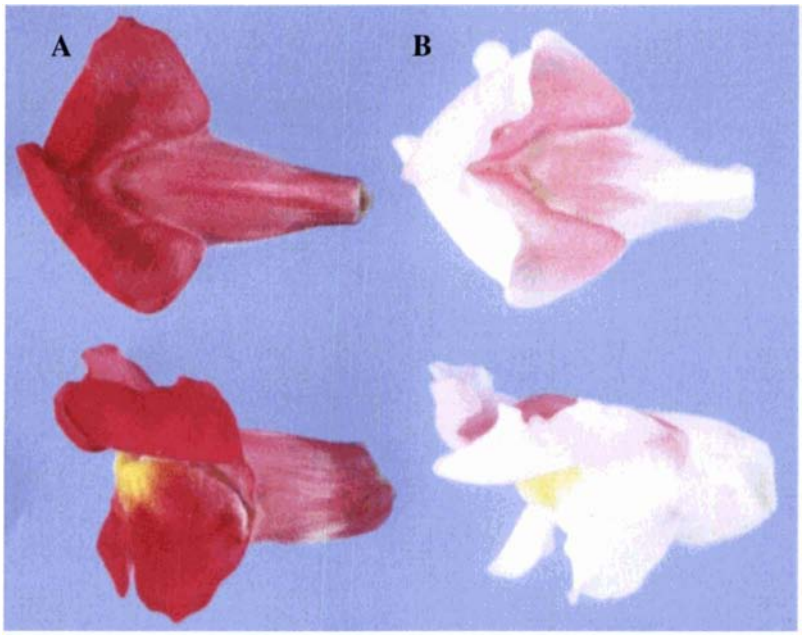

Figure 1.1 Examples of pigmentation patterns in antirrhinum (adapted with permission from Dr Kathy Schwinn).

Rosea1 gives wild type patterning with strong anthocyanin-based pigmentation throughout most of the petal epidermis (A) and rosea^{dorsea} has pigmentation only in the outer epidermis of the dorsal surface of the flower (B).

pigmentation either as a developmental trigger or as a determinant of pigmentation production.

1.2 Plant pigments

The major groups of plant pigments are flavonoids, chlorophylls, carotenoids and betalains. Flavonoids serve diverse functions within the plant including protection against abiotic and biotic stresses, signalling to micro-organisms during nodulation, influencing auxin transport as well as providing most colours in the visible spectrum to the floral organs in order to attract pollinators (Shirley, 1996; Schwinn and Davies, 2004). Anthocyanin pigments are the major class of flavonoids, providing pigmentation to flowers, fruits and leaves. Chlorophylls function as photosynthetic pigments and are widespread across the plant kingdom. They occur in the leaves as well as in flowers and fruits. Carotenoid pigments also function in photosynthesis as well as providing bright yellow to orange colours to flowers and fruits (Davies, 2004). Betalain pigments are restricted to a few families in the order Caryophyllales and their occurrence is mutually exclusive to that of anthocyanins. They provide red, violet, yellow and orange colour to flowers, fruits and vegetative tissue and also occur in some fungi (Piattelli, 1981; Grotewold, 2006).

1.2.1 Anthocyanin pigments

Anthocyanins are water-soluble pigments and are the major contributor of red, purple and blue colours in flowers. Anthocyanins are classified into three major groups according to their base structure with pelargonidin-based pigments producing orange, red or pink colours, cyanidin-based pigments producing red, mauve or magenta colours and the delphinidin-based pigments producing purple, blue or blue-black flower colours (Davies and Schwinn, 1997). In most flower petals anthocyanins occur only in the epidermal layer.

1.2.2 The anthocyanin biosynthetic pathway

The anthocyanin biosynthetic pathway is part of the larger phenylpropanoid metabolic pathway leading to production of lignins, lignans, stilbenes and hydroxycinnamic acids (Schwinn and Davies, 2004). The biochemistry of the major steps for anthocyanin

biosynthesis is well known with the genes/cDNAs for biosynthetic enzymes being cloned and characterised from a wide range of species.

A simplified anthocyanin biosynthetic pathway is presented in Figure 1.2. Anthocyanins are part of the flavonoid pathway and their biosynthesis begins in the cytoplasm with the sequential condensation of one 4-coumaroyl-CoA molecule with three malonyl-CoA molecules catalysed by chalcone synthase (CHS) leading to the production of naringenin chalcone. This is the first commited step for flavonoid biosynthesis. Naringenin chalcone is generally the precursor molecule for all classes of flavonoids including aurones, flavones, flavonols, flaven-diols, flavan-4-ols, proanthocyanidins (condensed tannins), isoflavonoids and anthocyanins. Naringenin chalcone is cyclised to form the flavanone, naringenin, by chalcone isomerase (CHI). Flavonoid 3'-hydroxylase (F3'H) which has broad substrate specificity then introduces a 3'-hydroxyl group to convert naringenin to eriodictyol while flavanoid 3'5'-hydroxylase (F3'5'H) catalyses the formation of petahydroxyflavanone from naringenin. Flavanone 3-β-hydroxylase (F3H) also has broad substrate specificity and catalyses the reduction of naringenin, eriodictyol and pentahydroxyflavanone to dihydrokaempferol, dihydroquercetin, and dihydromyricetin, respectively. Whilst the β-ring hydroxylases may work on more than one type of substrate, the level that they operate will vary depending on the species. Dihydroflavonol 4-reductase (DFR) then catalyses the reduction of these dihydroflavonols to produce the leucoanthocyanidins, 3,4-*cis*-leucopelargonidin, 3,4-*cis*-leucocyanidin and 3,4-*cis*-leucodelphinidin. It should be noted that the F3'H and F3'5'H can also use the dihydroflavanols as substrates, and there is evidence of their ability to use leucoanthocyanidins in some species (Schwinn and Davies 2004). These leucoanthocyanidins are further reduced by anthocyanidin synthase (ANS) to produce the anthocyanidins, pelargonidin, cyanidin and delphinidin (Schijlen *et al.*, 2004).

Anthocyanidins can be further modified by glycosylation, most commonly at C-3 (Grotewold, 2006). The initial glycosylation may be followed by addition of multiple sugar residues, as well as acylation. 3-*O* glycosylation of anthocyanidins is most commonly catalysed by UDP-Glc:-flavanoid 3-*O*-glucosyltransferase (UFGT), which adds a glucose residue (Tanner, 2003). Acylation of anthocyanins by various organic acids is catalysed by a group of enzymes known as anthocyanin acyltransferases and

Figure 1.2 The anthocyanin biosynthetic pathway [adapted from Schwinn and Davies, (2004); Grotewold (2006)].

It should be noted that the pathway shown here is a simplified one for the conversion of leucoanthocyanidins to anthocyanins, rather than the proposed *in vivo* route that occurs via a pseudobase intermediate.

CHS - chalcone synthase, CHI - chalcone isomerase, F3'H - flavonoid 3'-hydroxylase, F3'5'H - flavanoid 3'5'-hydroxylase, F3H - flavanone 3-β-hydroxylase, DFR - dihydroflavonol 4-reductase, ANS - anthocyanidin synthase, UFGT – UDP-Glc:flavanoid 3-*O*-glucosyltransferase , GST - glutathione-*S*-transferase

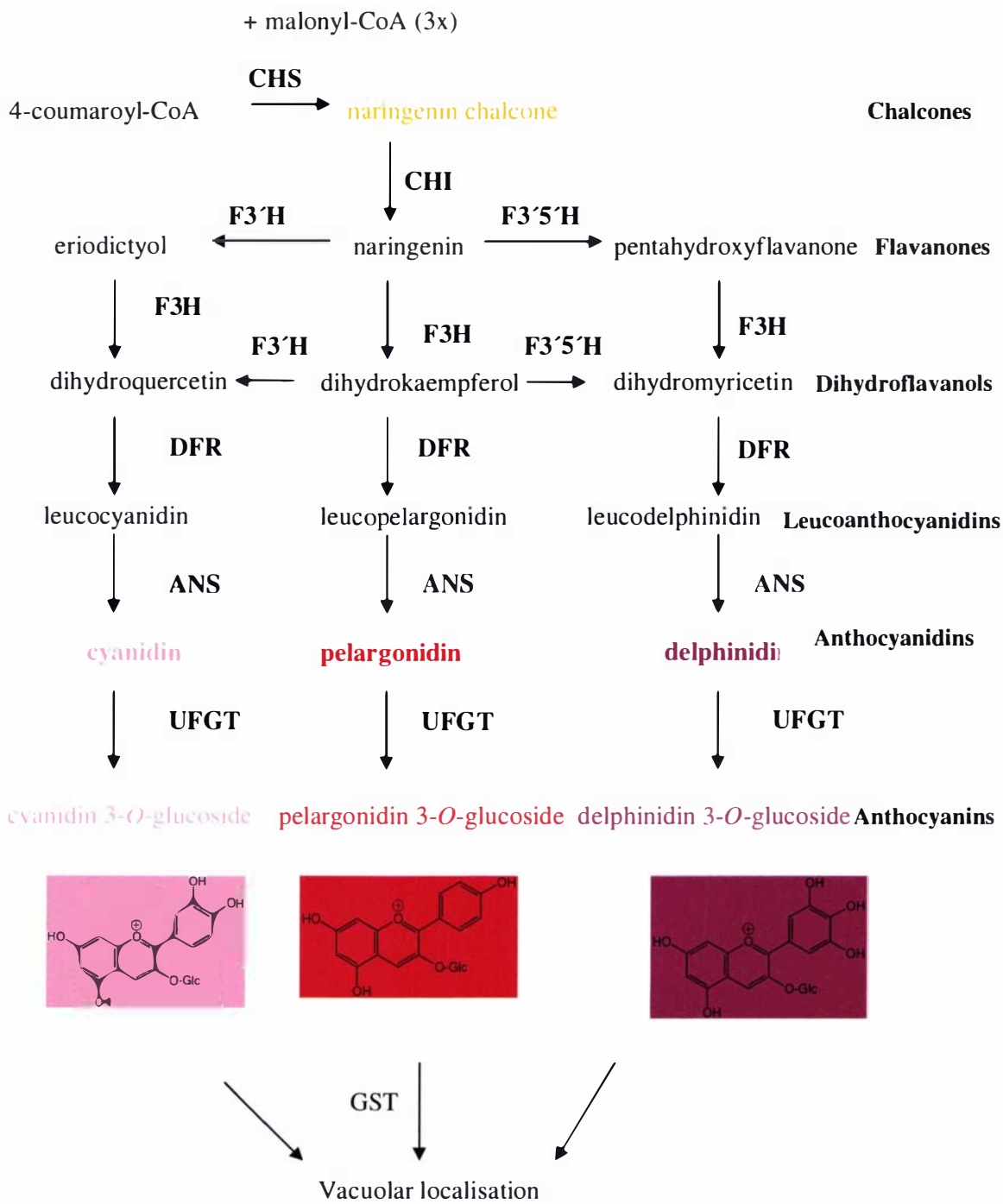
+ malonyl-CoA (3x)
CHS
4-coumaroyl-CoA
naringenin chalcone
Chalcones
CHI
F3´H
F3´5´H
eriodictyol
naringenin
pentahydroxyflavanone
Flavanones
F3H
F3H
F3H
F3´H
F3´5´H
dihydroquercetin
dihydrokaempferol
dihydromyricetin
Dihydroflavanols
DFR
DFR
DFR
leucocyanidin
leucopelargonidin
leucodelphinidin
Leucoanthocyanidins
ANS
ANS
ANS
cyanidin
pelargonidin
delphinidi
Anthocyanidins
UFGT
UFGT
UFGT
cyanidin 3-O-glucoside
pelargonidin 3-O-glucoside
delphinidin 3-O-glucoside
Anthocyanins
GST
Vacuolar localisation

contributes to intramolecular and intermolecular interactions that increase the stability of anthocyanins (Nakayama *et al.*, 2003). The final step of anthocyanin biosynthesis is the transportation of the pigment molecule to the vacuole where the pigments are stabilised and express the full pigment colour. The details of the vacuolar transport process are unclear. However, analysis of mutants in various species have indicated the involvement of glutathione-*S*-transferase (GST) and ABC-type transporters in this process (Grotewold, 2004). There is a wide range of anthocyanin structures identified (>600 known), including variation in the anthocyanidin type through hydroxylation or methylation. The structures characterised for antirrhinum to date are fairly simple and implicate the activities of UFGT and UDP-rhamnose: anthocyanidin-3-*O*-glucoside rhamnosyltransferase (3RT) (Schwinn and Davies, 2004).

1.3 Genetic regulation of the anthocyanin biosynthetic pathway in flowers

Detailed studies of the anthocyanin pathway in different species have shown that transcriptional control is the key regulation point for the control of anthocyanin biosynthetic gene expression. Previous studies have indicated that the expression of anthocyanin biosynthetic genes is co-ordinately regulated in response to various developmental and environmental cues (Martin *et al.*, 1991; Jackson *et al.*, 1992; Albert *et al.*, 1997; Quattrocchio *et al.*, 1998, 1999). Furthermore, the biosynthetic genes have been shown to be regulated in groups, with the specific grouping varying for each species. Studies on the classic model species divided the anthocyanin biosynthetic genes into two major groups, early biosynthetic genes (EBGs) and late biosynthetic genes (LBGs) with the point of division being at either F3H or DFR (Davies and Schwinn, 2003). Whether this division applies to all flowers is uncertain. For example, in the coloured organs of *Anthurium andreanum* (anthurium), the DFR gene is the key regulatory target (Collette *et al.*, 2004). While much is known about the regulation of the LBGs leading to anthocyanin biosynthesis (discussed in the next paragraph), little is known about the main regulators of the EBGs for flower pigmentation. However, for increased anthocyanin production both EBGs and LBGs need to be regulated in a co-ordinated fashion. MYB and bZIP factors have been implicated in the regulation of EBGs, suggesting that different combinations of transcription factors to those controlling

the LBGs may be the main regulators of the EBGs (Sablowski *et al.*, 1994; Sablowski *et al.*, 1995; Moyano *et al.*, 1996).

A common theme emerging from the studies on transcriptional regulation of the anthocyanin biosynthetic pathway is that MYB and bHLH-type transcription factors together with a WD40 co-regulator function in this process (Ramsay and Glover, 2005). The MYB proteins contain either one (R3), two (R2 and R3) or three (R1, R2 and R3) imperfect repeats of the MYB DNA binding motif (Martin and Paz-Ares, 1977). Most of the plant MYB proteins belong to the R2R3 family. The MYB factors directly bind to regulatory elements present in their target promoters. The bHLH partner has been shown to be essential for transcriptional activation of the target genes by MYB factors, although they have not been shown to bind DNA. The precise function of the WD40 co-activator in the MYB-bHLH-WD40 complex is not yet known. WD40 proteins are highly conserved, from algae to humans, with their general function being the facilitation of protein-protein interactions (Ramsay and Glover, 2005). Figure 1.3 shows the current model for the transcriptional regulation of anthocyanin biosynthetic genes by the MYB-bHLH-WD40 complex.

1.3.1 Eukaryotic gene transcription

The initiation of transcription in eukaryotes requires two major components: transcriptional activators and the RNA polymerase II holoenzyme complex. Transcriptional activation of a gene is achieved by the binding of gene-specific transcriptional activators to the *cis*-elements, most commonly present in the promoter region, where they recruit and regulate the activities of chromatin-modifying complexes and the RNA polymerase II holoenzyme transcription apparatus (Berk, 1999). The RNA polymerase II holoenzyme complex is composed of the 12-subunit RNA polymerase II core enzyme, the general transcription factors (GTFs) and one or more of the multi-subunit complexes called co-activators or mediators (Lee and Young, 2000). The GTFs include TFIIA, TFIIB, TFIID, TFIIE, TFIIF and TFIIH. GTFs are essential for specific promoter binding by RNA polymerase II. Co-activators/mediators are all the factors that do not belong to the general GTFs and transcription factors. These form multi-protein complexes that are capable of acetylating histones and play an important role in

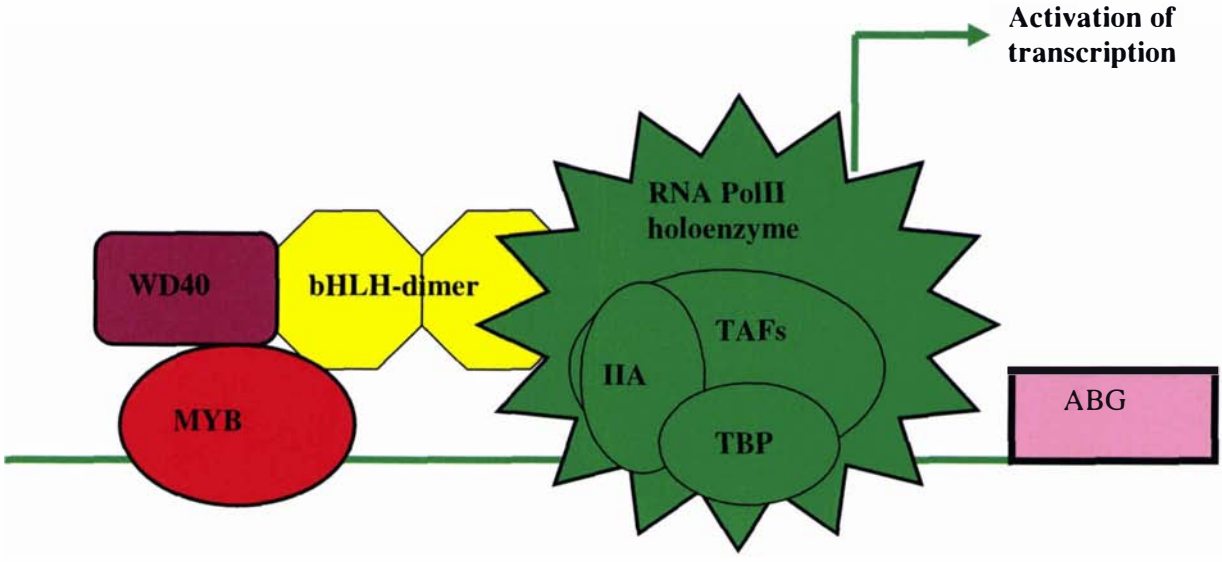

Figure 1.3 Current model for the initiation of transcription of anthocyanin biosynthetic genes.

A complex containing MYB, bHLH and WD40 factors binds to the promoter regions of the anthocyanin biosynthetic genes (ABGs) and interacts with the basal transcription machinery to activate transcription.

It should be noted that all the components of the basal transcription machinery has not been shown for clarity of the figure. TBP - TATA-box binding protein, TAFs - TBP associated factors, IIA-TFIIA.

increasing the accessibility of GTFs to enhancer/promoter regions (Berger, 1999). Co-activators/mediators include TATA-box binding protein (TBP)- associated factors (TAFs) as well as the subunits of the SRB/mediator complex (Meyer and Young, 1998).

Transcription factors are proteins that interact either directly or indirectly with *cis*-regulatory elements and modulate the efficiency of transcription from linked core promoters (Courey, 2001). These can be divided into two broad categories: sequence-specific regulators (e.g. MYB proteins) and the co-regulators (e.g. WD40 proteins). The sequence-specific regulators interact with the *cis*-elements in a sequence-specific manner and are usually modular in nature (i.e. made up of independent structural domains that have specific functions important for the various biochemical functions of the factor) (Courey, 2001; Latchman, 2004). In contrast, co-regulators do not interact with the DNA directly but are directed to their regulatory targets by protein-protein interaction with the sequence-specific regulators. The regulation of gene expression is achieved by an inter-play of transcriptional activators and repressors.

1.3.2 Regulation of anthocyanin biosynthetic genes in model species

Genetic and molecular studies have identified that the *Zea mays* (maize) regulatory factors can be classified into two families: the *R/B* family, which encodes the bHLH factors (Chandler *et al.*, 1989; Ludwig *et al.*, 1989; Tonelli *et al.*, 1991), and the *C1/Pl* family encoding the MYB factors (Cone *et al.*, 1986, 1993; Paz-Ares *et al.*, 1987). Anthocyanin biosynthetic genes in maize are controlled as one regulatory unit with the transcription of all the target genes being regulated in a co-ordinate manner (Davies and Schwinn, 2003).

The *R/B* family includes *R (Red)*, *B (Booster)*, *Lc (Leaf colour)* and *Sn (Sienna)*. These genes show much allelic diversity in terms of both developmental timing and tissue specificity of their expression. The duplicate function of the *R* and *B* genes are apparent in their DNA sequence similarity where the *R* gene sequence was used as a heterologous probe to clone the other members (*B*, *Lc* and *Sn*) of the family (Chandler *et al.*, 1989; Ludwig *et al.*, 1989; Tonelli *et al.*, 1991). The *R* locus is located on chromosome 10 with the *Lc* and *Sn* genes located two map units away from the *R* locus indicating that an

intrachromosomal duplication of the *R* containing region may be responsible for the evolution of the *Lc* and *Sn* alleles (Consonni *et al.*, 1993). The *B* locus is located on chromosome 2 and is more divergent and most likely to have evolved due to a chromosomal duplication event.

Although all of the tissue in the maize plant is competent to produce anthocyanin pigments it has been demonstrated that pigment production is strictly dependent on the specific bHLH factor expressed in a particular tissue. For example, *R* gene expression is required for pigmentation of aleurone, anthers and coleoptiles, *Sn* gene expression is required for pigmentation of mesocotyl, leaf base, pericarp and aleurone, *Lc* expression is required for pigmentation of midrib, ligule, auricle, glume, lemma, palea and pericarp tissue and *B* gene expression is required for pigmentation of the seed (Ludwig *et al.*, 1989; Ludwig and Wessler, 1990; Tonelli *et al.*, 1991; Consonni *et al.*, 1993).

The high degree of sequence similarity in proteins belonging to the *R*-gene family indicates that this phenotypic diversity is due to either minor variations in the *R*-gene family of proteins and/or differences in their patterned expression. Experimental evidence supports the latter view that various proteins of the *R*-gene family are functionally redundant and that pigmentation can be induced in a novel tissue by changing their promoter regions (Ludwig and Wessler, 1990). Therefore, the tissue-specific expression pattern of the genes belonging to the *R* family is mainly due to divergence of their promoter regions allowing distinct spatial and temporal regulation of these genes.

The MYB factors required for regulation of maize anthocyanin biosynthetic genes are encoded by the two closely related and paralogous genes *C1* (*Colourless1*) and *Pl* (*Purple leaf*) (Cone *et al.*, 1986, 1993; Paz-Ares *et al.*, 1987). *C1* regulates anthocyanin production in the aleurone and scutellum while *Pl* controls its production in mature tissue. The MYB proteins activate anthocyanin biosynthetic gene expression at the transcriptional level by interaction with a bHLH partner. This interaction does not increase the DNA binding specificity of the MYB factor (Sainz *et al.*, 1997). Although the MYB proteins can bind to *cis*-elements present in the anthocyanin biosynthetic genes by themselves, they absolutely require the bHLH partner for the activation of transcription of the target genes (Sainz *et al.*, 1997; Lesnick and Chandler, 1998;

Grotewold *et al.*, 2000; Hernandez *et al.*, 2004). This suggests that the interaction of the bHLH factor with the MYB partner is essential for transcriptional activation by this complex (Goff *et al.*, 1992). It is interesting to note that the related MYB proteins for phlobaphene (3-deoxyflavonoids) production can activate some of the same target genes (e.g. DFR) without the need for a bHLH factor (Grotewold *et al.*, 1994). Phlobaphenes are red coloured pigments found in pericarp and seed coat tissue of maize and other monocot species. The WD40 protein regulating anthocyanin biosynthesis in maize is encoded by the *Pac1* (*Pale aleurone colour1*) gene (Carey *et al.*, 2004).

The proteins encoded by *C1* and *Pl* of the MYB family also show a high degree of sequence similarity (Cone *et al.*, 1993a; Consonni *et al.*, 1993). However, the different MYB/bHLH partners have been shown to regulate pigmentation of different tissues in maize and so, as for the *R* gene family, this is explained by the divergence in their promoter regions resulting in differential expression of individual members of each family (Ludwig *et al.*, 1989; Ludwig and Wessler, 1990; Goff *et al.*, 1991, 1992; Consonni *et al.*, 1993).

In *Petunia sp.* the floral organs, stems and leaf petioles may be pigmented. Studies have used a range of petunia species, most notably, *P. hybrida* and petunia 'mitchell' [*Petunia axillaris* x (*P. axillaris* x *P. hybrida*)]. The regulation of anthocyanin biosynthesis in the flower petals is well characterised and is controlled by the positive regulation of LBGs from DFR onwards (Mol *et al.*, 1998). MYB and bHLH transcription factors together with a WD40 co-activator regulate the anthocyanin LBGs in the two petal domains, limb and tube.

An2 (*Anthocyanin2*) and *An4* (*Anthocyanin4*) encode the MYB factors and show spatially distinct expression patterns with *An2* being expressed in the petal limb and *An4* in the anthers (Quattrocchio *et al.*, 1999; Spelt *et al.*, 2002). The bHLH factors are encoded by *An1* and *Jaf13* (Quattrocchio *et al.*, 1998; Spelt *et al.*, 2000, 2002). *An1* controls petal limb colour and *Jaf13* is expressed in limb, tube and anthers, though the spatial domain where it regulates anthocyanin pigmentation is not known (Quattrocchio *et al.*, 1998).

The specific partnerships between the MYB and bHLH factors of *Petunia* are not known. However, transient expression studies using different combinations of the MYB and bHLH factors have shown that they are functionally redundant, indicating that their tissue specific expression pattern is due to divergence of their promoter regions (Quattrocchio *et al.*, 1998; Spelt *et al.*, 2000). Little is known regarding the mechanisms controlling *Myb* and *bHLH* regulation and the modulation of their activity. AN11 encodes a WD40 protein that, from studies on the *an11* mutant, is known to be required for anthocyanin production in the flower. However, it is expressed in many tissues including those that are pigmented and unpigmented (deVetten *et al.*, 1997). Transient experiments also indicate that AN11 acts upstream of AN2 and may regulate the activity of AN2 by post-translational mechanisms.

In addition to regulation of anthocyanin biosynthetic gene expression (Quattrocchio *et al.*, 1998), *An1*, *An2* and *An11* also control intracellular pH and epidermal cell differentiation in petal tissue (Gerats *et al.*, 1989; Quattrocchio, 1994; Spelt *et al.*, 2002). Other factors may also be involved in regulation of pigmentation in petunia flowers. One such factor is that which corresponds to the *An12* gene, which increases pigmentation in regions outside of petal veins and when mutated results in flowers with dark pigmentation in the veins and paler pigmentation throughout the rest of the petal limb (Gerats *et al.*, 1989).

Anthocyanins, as well as another class of pigments called the proanthocyanidins, are present in various tissues of *Arabidopsis thaliana* (arabidopsis) plants. Proanthocyanidin pigments are brown coloured and occur in the seed coat, vegetative tissue and seedlings of arabidopsis. *Transparent testa 2* (*tt2*) encodes a MYB transcription factor important for regulation of pigment biosynthesis in the seed coat (Nesi *et al.*, 2001) and has been shown to regulate BANYULS, which encodes the anthocyanidin reductase that catalyses the first committed step in the proanthocyanidin biosynthetic pathway (Xie *et al.*, 2003). *Transparent testa 8* (*tt8*) encodes a bHLH factor and is required for the activity of TT2 (Nesi *et al.*, 2000, 2002). TRANSPARENT TESTA GLABROUS 1 (TTG1), a WD40 protein, is also important for anthocyanin and proanthocyanidin biosynthesis, as well as seed mucilage and trichome production in arabidopsis (Walker *et al.*, 1999; Western *et al.*, 2001). Recently, using a combination of genetic and molecular approaches Baudry *et*

al. (2004) demonstrated that TT2, TT8 and TTG1 synergistically specify the expression of BANYULS and proanthocyanidin biosynthesis in arabidopsis. Anthocyanin production in vegetative tissue is regulated by two other bHLH proteins, GL3 (GLABROUS3) and EGL3 (ENHANCER OF GLABROUS3), and a homeodomain protein, ANL2 (ANTHOCYANINLESS2) of the GLABARA2 group (Kubo *et al.*, 1999; Payne *et al.*, 2000; Zhang *et al.*, 2003). Overexpression of two *Myb* genes, *PAP1* (*Production of anthocyanin pigment1*) and *Pap2* (*Production of anthocyanin pigment2*) lead to the ectopic accumulation of anthocyanin pigments, as well as flavonol and hydroxycinnamic acid accumulation indicating their role in regulating anthocyanin biosynthesis (Borevitz *et al.*, 2000). Other MYB factors that might be involved in flavonoid gene regulation in arabidopsis are MYB113, MYB114, MYB12, MYB11 and MYB11 (Kranz *et al.*, 1998; Strack *et al.*, 2001; Mehrtens *et al.*, 2005).

There are various additional factors regulating pigmentation in arabidopsis. *Transparent testa glabrous 2* (*ttg2*), which encodes a plant-specific WRKY transcription factor, has been shown to be important for the production of seed coat proanthocyanidins, mucilage and trichomes (Johnson *et al.*, 2002). TRANSPARENT TESTA1 (TT1), representing a new group of zinc finger proteins of the WIP subfamily, is also required for proanthocyanidin expression and BANYULS expression, as well as endothelium development (Sagasser *et al.*, 2002).

A MYB-bHLH and WD40 transcription factor complex has also been shown to regulate pigmentation in *Ipomoea* species including the common morning glory (*Ipomoea purpurea*) and the Japanese morning glory (*Ipomoea nil*). IpMYB1/W and IpbHLH2, the MYB and bHLH factors in *I. purpurea* respectively, have been cloned and characterised (Chang *et al.*, 2005; Park *et al.*, 2007). A MYB factor (InMYB1/C), bHLH factors (InbHLH2 and InbHLH1) as well as the WD40 co-factor (InWDR1) have been cloned and characterised from *I. nil* (Morita *et al.*, 2006).

Negative regulators of anthocyanin biosynthesis have been identified in maize, petunia, arabidopsis and strawberry. The maize *In1* (*Intensifier1*) locus encodes a bHLH protein with similarity to R. The majority of the transcripts for *in1* are mis-spliced and it has been proposed that the truncated proteins encoded by these transcripts might function as

dominant negative inhibitors (Burr *et al.*, 1996). Arabidopsis ICX1 (INCREASED CHALCONE SYNTHASE EXPRESSION1) acts as a negative regulator of several different pathways that regulate the flavonoid biosynthesis genes in an epidermal-specific manner (Jackson *et al.*, 1995; Wade *et al.*, 2003). ICX1 has been shown to act as a negative regulator of cryptochrome 1, phytochrome A, responses to UV-B, low temperature and sucrose, and cytokinin induction of CHS expression and/or anthocyanin accumulation. These results also demonstrate that these different pathways are either directly or indirectly regulated by at least one common component. ICX1 functions in seedlings as well as in mature leaf tissue, mainly in the epidermis, as the *icx1* mutant is altered in epidermal development. Although *icx1* is yet to be cloned, the detailed characterisation of the *icx1* mutant by Wade *et al.* (2003) suggests that it acts upstream of the transcription factors that regulate the flavanoid biosynthetic genes. The *Myb4* gene from arabidopsis has also been shown to repress the transcription of its target genes (Jin *et al.*, 2000). MYB4 belongs to a novel group of plant R2R3 MYB proteins containing a repressor domain and is involved in transcriptional silencing. The strawberry MYB1 suppresses both anthocyanin and flavonol accumulation in transgenic tobacco (Aharoni *et al.*, 2001). Interestingly, the strawberry MYB1 also contains the C-terminal amino acid motif present in the arabidopsis MYB4 that is important for its repressor function.

Table 1.1 summarises the major transcriptional regulators of anthocyanin biosynthesis in model species based on subgrouping of the MYB and bHLH factors according to phylogenetic similarity.

1.4 Regulation of anthocyanin production in *Antirrhinum majus*

Anthocyanin pigments are present in many floral and vegetative tissues of antirrhinum. Petal pigmentation regulation in antirrhinum is similar to that of petunia, where different MYB/bHLH factors regulate pigmentation in the tube and lobes in a spatially distinct manner (Figure 1.4). A WD40 factor involved in pigment production has been isolated from antirrhinum (Dr Kathy Schwinn, personal communication).

Table 1.1 Transcription factors involved in the regulation of the anthocyanin biosynthetic pathway in model species.

Species	R2R3 MYB TF		bHLH TF		WD40 co-activator
	Group 1	Group 2	Group 1	Group 2	
Antirrhinum majus	Rosea1 Rosea2 Venosa		Delila	Mutabilis	
Zea mays		C1 Pl	B Lc	R Sn IN1	Pac1
Petunia hybrida	An2 An4		Jaf13	An1	An11
Arabidopsis thaliana	Pap1 Pap2		GL3 EGL3	TT8	TTG1
Ipomoea nil	InMYB1/C		InbHLH1	InbHLH2	InWDR1
Ipomoea purpurea	IpMYB1/W			IpbHLH2	

Expression of anthocyanin biosynthetic genes in antirrhinum is spatially co-ordinated through the regulation of LBGs beginning with F3H. The known bHLH factors are encoded by *Delila* and *Mutabilis* (Goodrich *et al.*, 1992; Schwinn *et al.*, 2001). *Delila* controls pigmentation of the tube region (Almeida *et al.*, 1989; Goodrich *et al.*, 1992) by activating transcription of DFR, F3H, ANS and UFGT (Jackson *et al.*, 1991). Additionally, *Delila* has been shown to repress the expression of CHS in the mesophyll cells of the corolla lobes, indicating a possible dual role as an activator and repressor in different spatial domains of the antirrhinum flower (Martin *et al.*, 1991). *Mutabilis* encodes for a second bHLH factor and controls pigmentation in the lobe tissue.

The known MYB factors regulating anthocyanin LBGs are encoded by *Venosa* and the complex *Rosea* locus comprised of the two closely linked genes *Rosea1* and *Rosea2.*

Figure 1.4 MYB-bHLH protein interactions in the different spatial domains of the antirrhinum flower (Schwinn *et al.*, 2006).

An outline of the different MYB-bHLH interactions occurring in the two different regions, lobe and tube, of the antirrhinum flower. *Mutabilis* is expressed only in the lobe region while *Delila* is expressed in both tube and lobe regions. ROSEA1 (ROS1) and VENOSA (VE) interact with both MUTABILIS (MUT) and DELILA (DEL) in the lobe and tube tissues while ROSEA2 (ROS2) only interacts with DELILA.

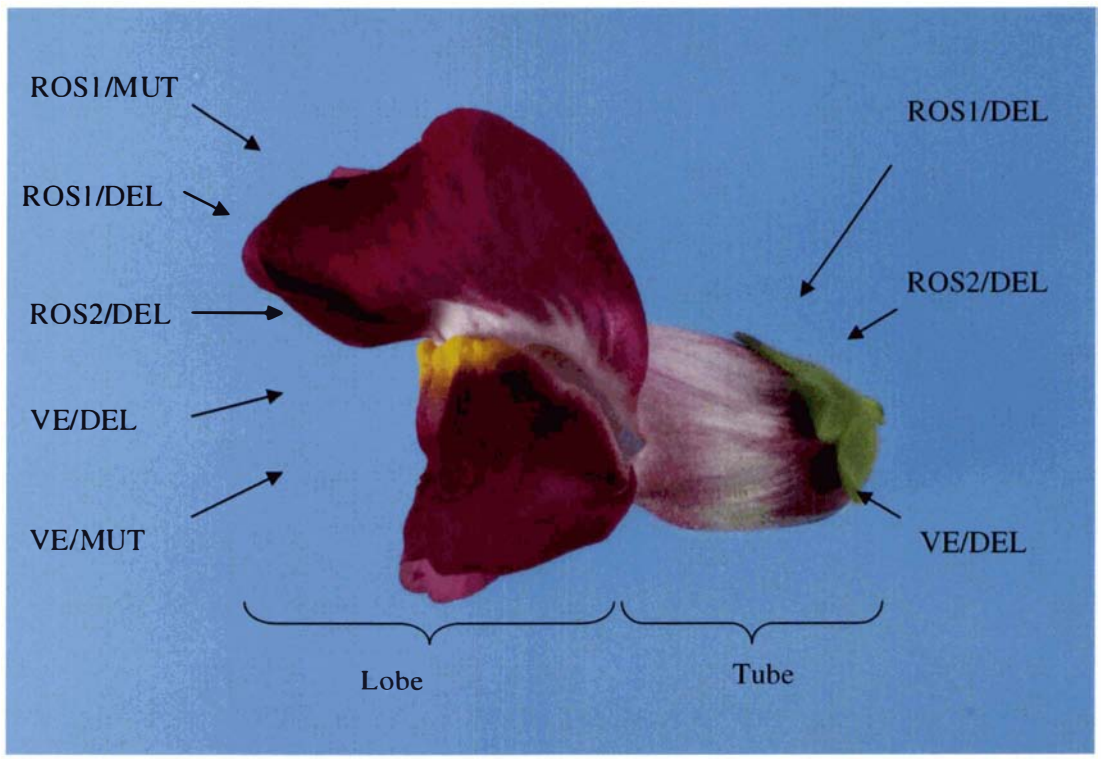
ROS1/MUT
ROS1/DEL
ROS2/DEL
VE/DEL
VE/MUT
ROS1/DEL
ROS2/DEL
VE/DEL
Lobe
Tube

(Schwinn *et al.*, 2006). Expression of the *Venosa* gene leads to pigment production in the inner epidermal tissue overlying the veins of the corolla (Shang, 2007). Mutations affecting these regulatory genes have allowed the identification of the spatial expression domains of these genes in the corolla. *Rosea1* is expressed in both tube and lobe tissue although the steady state transcript level was several times greater in the lobes (Schwinn, 1999). This pattern is also observed for biosynthetic gene expression, as well as the intensity of anthocyanin pigmentation in antirrhinum petals (Jackson *et al.*, 1992). The *Rosea1* transcript can be first detected (by northern blotting) at stage three (bud length 10-15 mm) with a substantial increase occurring by stage five (bud length 20-25 mm) (Schwinn, 1999; Schwinn *et al.*, 2006). In stage five petal tissue, the stage when the petals are reaching full expansion, LBG expression is at maximum, EBG expression is declining and anthocyanin levels are rapidly increasing (Coen *et al.*, 1986; Bartlett, 1989 ; Jackson *et al.*, 1992). *Rosea2* has little or no effect on pigmentation of the central part of the lobe and no effect in other organs of the flower. *Rosea2* also produces a much weaker pigmentation phenotype compared to *Rosea1* and has much lower transcript levels compared to *Rosea1*. This low expression level of the *Rosea2* gene has been attributed to inefficiency in splicing of the large (> 9 kb) second intron (Schwinn *et al.*, 2006). Although functionally equivalent in their ability to induce pigmentation in transient gene assays, *Venosa*, *Rosea1* and *Rosea2*, have different target gene specificity in addition to their different expression patterns in the corolla tissue (Schwinn *et al.*, 2006). Therefore, it is likely that the anthocyanin regulatory factors in antirrhinum have diverged functionally and in their expression pattern (Schwinn *et al.*, 2006). This is different from the situation in maize where C1 and Pl have been shown to be functionally equivalent (Cone *et al.*, 1993a & b).

Genetic and molecular evidence indicate that *Rosea1* is epistatic to *Venosa* and *Rosea2* as the Rosea1 phenotype masks the phenotypes of both rosea2 and venosa mutants (Schwinn *et al.*, 2001). MUTABILIS and DELILA functions in lobe tissue. Their partnership with the *Myb* factors appears to be specific and, therefore, important for the spatial regulation of pigmentation (Schwinn *et al.*, 2001, 2006). For example, mutant analysis indicates that ROSEA2 only interacts with DELILA in the flower petals.

1.4.1 *Antirrhinum* as a model plant for pigmentation patterning studies

Antirrhinum is a perennial eudicot belonging to the Scrophulariaceae (Perry, 1981). Antirrhinum has been used in the earliest of genetic studies by scientists such as Darwin and Mendel and became established as a model system for inheritance studies by Erwin Baur in the early 20th century. Antirrhinum plants are hardy, have a relatively short generation time, and are easily self- and cross-pollinated. These characteristics, as well as the plethora of phenotypic variations available, prompted its use as a model for these early studies. Studies on antirrhinum have contributed much to the understanding of the pigment biosynthetic and photosynthetic pathways, as well as to the establishment of fundamental aspects of developmental genetics of plants (Schwarz-Sommer *et al.*, 2003).

Floral pigmentation in antirrhinum has been studied extensively, leading to isolation and characterisation of the anthocyanin biosynthetic genes as well as their regulatory factors. Mutations that affect the biosynthetic genes include *nivea* (CHS) (Sommer and Saedler, 1986), *incolorata* (F3H) (Martin *et al.*, 1991), *eosinea* (F3′H) (Stickland and Harrison, 1974), *pallida* (DFR) (Martin *et al.*, 1985) and *candica* (ANS) (Martin *et al.*, 1991). For most of these loci mutations lead to acyanic flowers.

The wild type pigmentation pattern of the antirrhinum flower is comprised of yellow (aurone) and magenta (cyanidin). Additional patterning such as the venation pattern of pigmentation, where increased pigmentation occurs in the epidermal region overlying the vascular strands of the petal, was characterised from the early 20th century onwards (Onslow, 1925). Many of the other *Antirrhinum* species also show variation in their floral pigmentation patterns (Schwinn *et al.*, 2006). Most of the native species from Spain, Portugal, France and Italy are either acyanic, palely pigmented or palely pigmented with strong venation pigmentation patterns. Some species have entirely yellow corolla lobes due to enlarged zones of aurone accumulation. In addition to these original species with different pigmentation patterns, many other pigmentation phenotypes have been developed by breeding. The availability of these different pigmentation phenotypes as well as the genetic, biochemical and molecular biological knowledge of anthocyanin biosynthesis and its regulation in *Antirrhinum* makes it an excellent model for pigmentation patterning studies.

1.4.2 *Antirrhinum majus* flower architecture

Antirrhinum flowers have five small sepals. Each flower is born on a short, leafless pedicel that arises from the axil of a short, sessile bract. The flowers point in all directions in the inflorescence, and show bilateral symmetry. The corolla of the flower, fused at the base to form a tube, divides distally to form two lips (Figure 1.1). The upper lip is erect and the lower lip spreads to form a projecting palate that closes the mouth of the corolla tube (Cocksull, 1985). Cell division in the flower bud is complete when it is approximately 10 mm in length with the rest of the growth occurring due to cell expansion (Jackson *et al.*, 1991).

In the wild type flowers, anthocyanins occur in both lobe and the tube tissue, and are located exclusively in the inner and outer epidermis with more abundance in the inner epidermis (Jackson *et al.*, 1992; Martin and Gerats, 1993). Anthocyanins are present at very early stages of bud development and steadily increase to maximum levels when the flower is fully opened and slightly decrease as the flower ages (Coen *et al.*, 1986). Aurones, which provide yellow pigmentation to the face and throat of the corolla, also show similar epidermal-specific localisation as well as similar developmental accumulation patterns as anthocyanin pigments (Geissman *et al.*, 1954; Asen *et al.*, 1972).

1.4.3 Pigmentation patterns conferred by the *Rosea1* alleles

Rosea locus is a key determinant of flower pigmentation and is comprised of two closely linked genes, *Rosea1* and *Rosea2*. An allelic series exists for both of these genes. This study focused on the *Rosea1* and *rosea1*^{dorsea} alleles, the phenotypes of which are shown in Fig. 1.1. In wild type Rosea1 flowers, anthocyanins accumulate in the epidermis of both tube and lobe regions (Jackson *et al.*, 1992). The distribution of anthocyanins is more even in the lobe tissue except for the aurone-producing face of the flower where it is excluded. Also, more anthocyanins accumulate in the inner epidermis than the outer epidermis in the lobes, while in the tube it is more balanced at the base of the tube. The top part of the tube accumulates anthocyanins more weakly and they are found only in

the outer epidermis (Jackson *et al.*, 1992). The wild type flowers are null mutants for *rosea2* (Schwinn *et al.*, 2006). In rosea^{dorsea} flowers, anthocyanins accumulate only on the outer (abaxial) epidermis of both lobes and upper tube region of the dorsal petals. The rest of the tube is unpigmented except for a vestigial ring of pigmentation occurring at the base of the tube (Schwinn *et al.*, 2006).

The two pigmentation genotypes used in this project are those giving wild type and rosea^{dorsea} phenotypes. Northern analysis for *Rosea1* transcripts in rosea^{dorsea} flowers did not detect its expression because its transcript levels were below the detection limit in both tube and lobes. However, RT-PCR was able to amplify the *Rosea1* cDNA from rosea^{dorsea} (Schwinn 1999). All three exons, intron 1 and part of intron 2 of *rosea1*^{dorsea} were also sequenced and compared with the *Rosea1* allele. No obvious mutations were seen in the amino acid sequence that could account for the radical phenotype change seen in the flowers of rosea^{dorsea}. Seventeen differences were found in intron 2 of *rosea1*^{dorsea} with most of them being single bp changes. However, none occurred at the exon/intron border regions. Further analysis of the promoter region led to the identification of a large 187 bp deletion in the *rosea1*^{dorsea} promoter in comparison to the promoter region of the *Rosea1* gene from the wild type. Other changes include an extra 12 bp segment, four single base pair insertions and 11 single base pair changes in the *rosea1*^{dorsea} promoter. Given that the *rosea1* transcript in rosea^{dorsea} appears to be normal, it was postulated that the two distinct pigmentation patterns found in wild type and rosea^{dorsea} could be due to the promoter specificity of the *Rosea1* gene (Schwinn *et al.*, 2006).

1.5 Regulation of the transcription factors controlling the anthocyanin biosynthetic genes

Comprehensive data on the regulatorial hierarchy of *Myb* and *bHLH* gene expression are lacking. Most of the work on regulation of the regulatory factors of the anthocyanin biosynthetic genes has been carried out in maize. In maize, the colourless phenotype of the *viviparous1 (vp1)* mutant was shown to be associated with the failure to express the *C1* gene in the kernel indicating that *Vp1* and *C1* might be part of this regulatory gene hierarchy (McCarty *et al.*, 1989, 1991). The *C1* gene was shown to be regulated by a combination of developmental and environmental signals. Further analysis of the *C1*

promoter region lead to the identification of *cis*-elements that were necessary and sufficient for its activation by abscisic acid (ABA), *VP1* and light (Kao *et al.*, 1996). *VP1* contains four domains: the A1 domain located in the acidic N-terminal region and three basic regions, B1, B2 and B3, in the C-terminal. Studies by Suzuki *et al.* (1997) showed that the B3 domain has highly cooperative DNA binding activity that is specific for the Sph sequence present in the *C1* promoter region.

In addition to *vp1*, *anthocyaninless lethal1* (*anl1*) and *intensifier1* (*in1*) also affect anthocyanin production in the aleurone tissue of maize kernel. The *anl1* gene in recessive form is lethal and lacks anthocyanin pigments and the *in1* gene acts in a recessive intensifier/dominant inhibitor fashion in controlling anthocyanin production in the aleurone (Coe *et al.*, 1988). Studies by Burr *et al.* (1996) showed that *in1* has sequence similarity to the members of the *R/B* family and that its transcripts are mis-spliced. Furthermore, very little functional transcript was made and it is postulated that mis-splicing may be a mechanism for reducing the levels of a transcription factor.
Studies by Procissi *et al.* (1997) have also shown that *Sn* gene expression is enhanced by light while *R* gene expression is not affected. A model has been proposed where the duplication of the bHLH anthocyanin regulators, *R* and *Sn*, lead to the partial silencing of the *Sn* gene expression by methylation of the *Sn* promoter region (Tonelli *et al.*, 1994; Ronchi *et al.*, 1995). In contrast, both *C1* and *Pl* expression are regulated by light at different stages of seed development in the aleurone and pericarp of the maize seed, respectively. Furthermore, the developmental competence of these tissues to respond to light was shown to be limited by the expression of the two *Myb* genes (Procissi *et al.*, 1997).

The *Pl* alleles are phenotypically classified with the dominant *Pl* alleles leading to intense, light-independent pigmentation in vegetative tissue and floral tissue while the recessive, *pl*, "sun-red' alleles, lead to light-dependent pigmentation (Cone *et al.*, 1993b). The proteins encoded by the two distinct alleles were shown to be functionally similar and it has been proposed that the difference in their promoter regions led to the differential expression of the alleles. Another allele of *Pl*, *pl-bol3*, was identified by Pilu *et al.* (2003) and was shown to have a complex molecular structure, containing multiple *p11* gene copies, and was the first complex locus discovered in the *C1/P11* gene family.

While the protein product encoded by the *pl-bol3* allele was functionally similar to the previously identified *pl1* alleles, the promoter region was highly divergent.

Regulation of *Lc* gene expression is achieved by multiple mechanisms. *Lc* expression was reduced by 25-30 fold by the presence of a 235 bp 5'-transcript leader sequence. The leader sequence encoded a 38-codon upstream open reading frame and repressed the transcription of *Lc* (Damiani Jr. and Wessler, 1993). Further analysis of the 5'-untranslated region (UTR) of *Lc* led to the identification of a hairpin structure that acts in an additive manner leading to translational repression (Wang and Wessler, 2001). Two alleles of the *B* gene, *B-Peru* and *B-I*, have markedly different expression patterns in the maize seed. Extensive analysis of the two alleles by Selinger *et al.* (1998) found that the promoter region of the *B-Peru* allele had extensive DNA rearrangements that led to its tissue-specific expression pattern through both positive and negative promoter elements. To summarise, much of the information on the regulatorial hierarchy for the transcriptional factors involved in the anthocyanin biosynthetic pathway has been made available through research carried out in maize, a monocot model species. To date, similar information for dicot species, including antirrhinum, is lacking. This work aims to fill this knowledge gap.

1.6 Role of *Deficiens* in *Antirrhinum majus* flower development

The functions of the A, B and C genes in the establishment of floral identity have been studied extensively and much is known about their role in early flower development. However, many of these genes are continuously expressed, well after floral identity has been established. Therefore, it has been proposed that these genes may play an additional important role in controlling secondary aspects of flower development. A major aim of this project was to analyse the role of the B function gene, *Deficiens*, in regulating the secondary metabolism pathway leading to anthocyanin production.

The morphological and genetic analysis of homeotic floral mutants in antirrhinum and arabidopsis has led to the development of the ABC model for floral development. In this model three morphogenic functions, A, B and C are defined, which alone or in

combination, determine organ identity of the four whorls of the flower (Gutierrz-Cortines and Davies, 2000). Expression of A function alone determines sepal identity, while co-expression of A and B or B and C determines petal or stamen identity, respectively. Expression of C function alone is responsible for carpel formation. Almost all of the A, B and C function genes belong to a class of transcription factors called MADS-box (Schwarz-Sommer *et al.*, 1990).

Several lines of evidence have shown that A, B and C functions are not the sole determinants of floral organ identity. Results from analysis of homeotic mutants and ectopic expression of the A, B and C function genes have shown that organ identity genes are necessary and sufficient to specify organ identity within a floral inflorescence context that is presumably defined by the presence of additional flower-specific factors. Candidates for these flower specific factors belong to the MADS-box family and are required for the activity of A, B and C function genes (Angenent *et al.*, 1994; Pnueli *et al.*, 1994). This class of genes is referred to as *Identity mediating* (*Im*) genes. These genes are necessary for the function of the A, B and C genes by participating in the various complexes formed between the A, B and C factors (Davies *et al.*, 1996).

Deficiens is a B function MADS-box gene in antirrhinum important in the control of petal and stamen development (Sommer *et al.*, 1990; Schwarz-Sommer *et al.*, 1992; Egea-Cortines *et al.*, 1999). *Deficiens* mRNA can be first detected (by *in situ* hybridisation) at the beginning of sepal differentiation and high levels of expression are detected at the time of the appearance of morphologically detectable petal and sepal primordia in the young flower buds. Expression of *Deficiens* is not uniform throughout the entire whorl area and is restricted to the organ primordia. In later stages of organogenesis *Deficiens* expression is not equally distributed in the differentiating organs. For example, in petal tissues *Deficiens* expression is stronger in the upper lobe compared to the lower and is more pronounced in the ventral surface. Once *Deficiens* expression is established, it is maintained throughout the whole period of flower development at a constant well after organ identity has been established (Schwarz-Sommer *et al.*, 1992; Zachgo *et al.*, 1995).

Deficiens was the first floral plant homeotic gene to be cloned and belongs to the *Deficiens* allelic series originally described by Baur in 1924 as a mutant in which the

sepals replace petals and carpels replace stamens (Sommer *et al.*, 1990). The *Deficiens* allelic series, which contains morphologically distinct mutants (morphoalleles), has been vital for the identification of the functional domains of DEFICIENS (DEF) as well as the regulation of *Deficiens* expression. For example, in the globifera (deficiens^{gli}) null mutants, the petals are morphologically indistinguishable from sepals except for the increased size and their position within the flower. In this mutant, the development of a genuine gynoecium is also affected and the stamens show carpelloid features. The *deficiens*^{gli} allele results from the insertion of the Tam7 transposon into the third intron of the *deficiens* gene as well as several point mutations in exons and numerous alterations in the introns compared to the wild type *Deficiens* sequence (Sommer *et al.*, 1990; Schwarz-Sommer *et al.*, 1992). In the chlorantha (deficiens^{chlorantha}) mutant, the flowers are smaller and the petals show weak virescence indicative of sepaloid features and the stamens also develop carpeloid features (Figure 1.5). The *deficiens*^{chlorantha} allele results from mutation of four bp (CGG instead of CCCCTG) 32 bp upstream of a CArG-box [CC(A/T)$_6$GG]. This motif is the consensus-binding site for MADS-box transcription factors and indicates the importance of this promoter region for the proper expression of the *Deficiens* gene. The flowers of the temperature sensitive deficiens-101 mutant also have sepaloid petals and carpelloid stamens, similar to the phenotype of deficiens^{gli} null mutants, but only when grown at the non-permissive temperature of 26°C (Figure 1.5C). Under the permissive temperature of 15°C, deficiens-101 flowers are morphologically similar to wild type flowers (Schwarz-Sommer *et al.*, 1992; Zachgo *et al.*, 1995). The *deficiens-101* allele results from a three bp deletion in the N-terminal end resulting in the loss of a lysine residue in the DEF protein.

Functional analysis of this temperature sensitive deficiens-101 mutant and morphoalleles of the *Deficiens* gene has been used to define the distinct functional domains of DEF (Schwarz-Sommer *et al.*, 1992; Zachgo *et al.*, 1995). The N- terminal MADS-box domain is conserved and is required for DNA binding while the K-box is required for protein-protein interactions and stabilising the heterodimer. The C-terminal domains of MADS box genes are more divergent and are important for ternary complex formation (Egea-Cortines *et al.*, 1999). It is presumed that the C-terminal domain may be important for divergent biological roles of MADS-box proteins and may function to create a network of interactions with other transcription factors.

MADS-box transcription factors bind to two major classes of binding sites that are based on the central CArG-box consensus motif of 5'-CC(A/T)$_6$GG-3' (Serum Response Element [SRE]- like) and 5'-CTA(A/T)$_4$TAG-3' (N10-like) (Shore and Sharrocks, 1995). However, some plant MADS-box transcription factors such as SQUAMOSA (SQUA) have been shown to bind both SRE-like and N10-like sites as well as to novel sites that are not represented by the two consensus DNA recognition sites. Therefore, MADS- box proteins may have dual DNA binding specificity, as well as the potential to bind to a wide variety of promoter sites *in planta* (West *et al.*, 1998). *In vitro* DNA binding studies by Schwarz-Sommer *et al.* (1992) have demonstrated that DEF binds to specific DNA motifs (CArG boxes) as a heterodimer with the protein product of the floral homeotic gene *Globosa.* Furthermore, ternary complex formation between DEF, GLOBOSA (GLO) and the floral meristem identity gene product SQUA has also been demonstrated. These ternary complexes have greater affinity for DNA binding and are proposed to increase the complexity of the regulatory function of these homeotic genes (Egea-Cortines *et al.*, 1999).

The non-cell-autonomous functions of DEF and GLO were studied using somatically stable *deficiens* and *globosa* periclinal chimeras (Perbal *et al.*, 1996). The L1 chimeras (DEF is present only in the L1 layer) developed five petals in the second whorl although the petal lobes were broader than wild type and their shape was distorted. The epidermal cells were pigmented as in wild type petals. However, the mesophyll cells contained chlorophylls indicating that DEF activity was restored only in the L1 layer and not in the L2 and L3 layers. Analysis of L2L3 chimeras showed that the epidermis was pigmented as a result of non-cell autonomous function of the DEF protein. In these chimeras the L1-derived marginal parts of the petal tip still contained green cells confiming that the L1 layer was genetically mutant for the *Deficiens* gene. More importantly this phenotype highlighted the importance of DEF function for anthocyanin pigmentation in the epidermis. These results were further confirmed by Vincent *et al.* (2003) where restoration of DEF expression in the L1 cell layer was shown to restore DEF and GLO functions in the L1 derived cells only while the mutant inner layers retained sepaloid features. DEF was also shown to be important for expansion of the petal lobes by mediating cell proliferation and/or cell shape and elongation in the L1 layer while in the

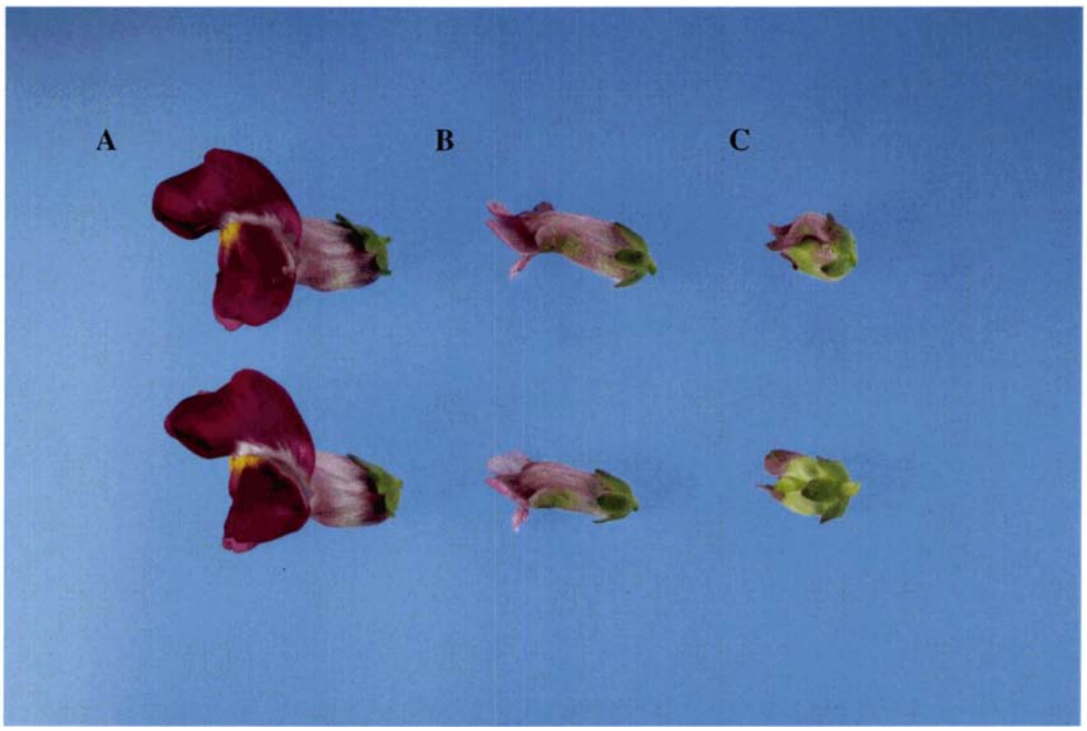

Figure 1.5 Floral phenotypes of deficiens mutants.

Flowers of wild type (A), deficiens^{chlorantha} (B) and deficiens-101 (C) grown at 26°C.

L2 and L3 layers DEF function was important for establishing the petal identity of the epidermal cells (Perbal *et al.*, 1996).

Wild type and deficiens-101 mutant petal tissues used for expression profiling experiments using microarrays comprising of annotated antirrhinum unigenes identified 40 up-regulated and 52 down-regulated petal-expressed genes, which were controlled by DEF (Bey *et al.*, 2002, 2004). Of interest to this project is that two transcription factors of the MADS box family, one of which was *Deficiens* itself, were up-regulated, as well as the *ANS* and *CHS* genes of the anthocyanin biosynthetic pathway (Bey *et al.*, 2004). Furthermore, results from the aforementioned study indicated that DEF performed multiple functions in different petal tissues and that it functioned in a complex manner in regulating diverse and fundamental processes throughout petal morphogenesis including anthocyanin pigment production.

1.7 Aims, objectives and hypothesis

The major objective of this research project was to determine the mechanisms by which genes are differentially regulated, using anthocyanin pigmentation patterning in antirrhinum as the experimental system. As two pigmentation patterns, wild type and rosea^{dorsea}, are thought to occur due to the promoter specificity of the *Rosea1* allele, the main hypothesis in the present work was that the patterns derived from *Rosea1* and *rosea1*^{dorsea} are due to different regulatory systems. A second interlinked hypothesis was that the *Deficiens* gene is a direct regulator of the *Rosea1* gene. The role of this class B function MADS box gene as a developmental trigger or as a determinant of pigment production was analysed, to gain insight into how late developmental processes such as pigmentation are linked to early floral developmental events. Specifically, the aims for this project were to:

1. Use promoter deletion analysis, linker scanning mutagenesis and electrophoretic mobility shift assays to identify key *cis*-elements in the promoter of the wild type *Rosea1* allele that are responsible for the regulation of the *Rosea1* gene.

2. Use promoter deletion analysis to identify whether mutations present in the promoter region of *rosea1*^{dorsea} are responsible for the rosea^{dorsea} phenotype.

3. Identify the role of the *Deficiens* gene in controlling pigment formation in order to gain a better understanding of the link between developmental regulation and pigment production and to specifically determine whether DEFICIENS is involved in the regulation of *Rosea1*.

Chapter 2: Materials and Methods

2.1 Plant material

Transgenic plant material was grown in a PC2 level containment plastic house located at Crop & Food Research, Palmerston North. Non-transgenic tobacco (*Nicotiana tabacum* cv. samsun) and antirrhinum (*Antirrhinum majus*, wild type line #522 and rosea^{dorsea} line #112) plants were grown in a plastic house under prevailing day length and light conditions. Line #522 is a wild type revertant from unstable nivea^{recurrens} mutant (Martin *et al.*, 1991). Mutant F2 plants (Line #112) were obtained from crosses between wild type (line # 522) and rosea^{colorata} (Gatersleben accession). The wild type (line # 522) is homozygous for dominant *Rosea1* allele and recessive for the *rosea2* allele. The rosea^{dorsea} line #112 was homozygous for the recessive alleles *rosea1*^{dorsea} and *rosea2*.

2.2 Nucleic acid manipulation

2.2.1 Plasmid DNA preparation

2.2.1.1 Purification of plasmid DNA using alkaline lysis method

Reagents

- Miniprep solution I - 50 mM glucose, 25 mM Tris-HCl (pH 8.0), 10 mM ethylenediaminetetra-acetate (EDTA) made up to 100 mL with sterile water and stored at 4°C.
- Miniprep solution II - 0.2 M NaOH, 1% (w/v) SDS made up to 20 mL with sterile water. This solution was made fresh as required.
- Miniprep solution III - 60 mL of 5 M potassium acetate, 11.5 mL glacial acetic acid, 28.5 mL of sterile water, pH to 4.8 with acetic acid and stored at 4°C.
- RNAse water - RNAse water contained 20 µL of RNAse (10 mgml^{-1}) diluted to 1 mL with MilliQ water. The solution was stored at 4°C.

This method was routinely used when mini preparations of plasmid DNA was required for diagnostic purposes. Plasmid DNA was isolated from 1 mL of overnight *Escherichia coli* (Novablue from Novagen, Madison, USA) cell culture grown at 37°C or 3-4 mL of

Agrobacterium tumefaciens (strain LBA 4404 from Invitrogen, California, USA) overnight culture grown at 28°C at 250 rpm. The cells were pelleted by centrifugation at 14,000 rpm for 1 min on a bench top centrifuge. Pelleted cells were resuspended in 200 µL of miniprep solution I to which 200 µl of miniprep solution II was added. After mixing of the solution by inversion 200 µL of miniprep solution III was added, solution mixed and debris pelleted by centrifugation at 14,000 rpm for 10 min. The resulting supernatant was removed to a new tube and the plasmid DNA purified as described in Section 2.2.9.1. The purified plasmid DNA was resupended in 60 µL of RNAse water for *E. coli* minipreps or 20 µL of RNAse water for *A. tumefaciens* minipreps.

2.2.1.2 Purification of plasmid DNA using commercial kits

Qiagen™ (Qiagen, Victoria, Australia) and Axygen™ (Axygen Scientific, California, USA) mini and midi plasmid purification kits respectively were used to isolate plasmid DNA when high concentrations of pure DNA were required for sequencing reactions and biolistic-mediated transformation of tissue. Plasmid DNA was isolated from overnight cultures of *E. coli* culture grown at 37°C using the protocol supplied by the manufacturer. The protocol is based on a modified alkaline lysis procedure, followed by binding of the plasmid DNA to an anion-exchange resin under appropriate low-salt and pH conditions. The purified DNA was resuspended in an appropriate volume of water after being precipitated and desalted using isopropanol (Section 2.2.9.1).

2.2.2 Isolation of genomic DNA

2.2.2.1 Cetyl Trimethyl Ammonium Bromide (CTAB)-based DNA extraction protocol

Reagents

DNA extraction buffer - 0.3 g CTAB powder (2%), 0.3 g sodium dodecyl sulphate (SDS) (2%), 0.15 g polyvinylpyrrolidine (PVP), 1.5 ml 1 M Tris-HCl (pH 8.0), 0.75 mL 0.5 M EDTA (pH 8.0) and 6.0 mL 5 M NaCl was added to a 50 mL Nunc tube (Nunc International, New York, USA) mixed well and made up to 15 mL with water

and autoclaved.

This method was based on Zhang (1998). Young tobacco leaf tissue (1-3 g) was ground to a fine powder in liquid N_2 using a pre-cooled mortar and pestle. The DNA extraction buffer (15 mL) was pre-warmed to 55°C and supplemented with 0.3 mL of 2-mercaptoethanol (2 -ME). Powdered tissue was then added to the DNA extraction buffer and mixed completely by inverting the tube followed by vigorous vortexing for 1 min. An equal volume of chloroform:isoamylalcohol (IAA) (24:1 v/v) was added to the DNA extraction buffer, vortexed for 1 min and the sample incubated at 55°C for 15 min. The sample was then centrifuged at 6500 rpm at 4°C for 15 min to separate the phases and the resulting supernatant was removed into a fresh 50 mL Nunc tube. The chloroform:IAA step was repeated and the supernatant was removed to a Corex tube (Fisher Scientific, New Jersey, USA). 1/3 volume of 8 M LiCl (at - 20°C) was added to the supernatant and mixed well. RNA was precipitated by leaving the sample at 4°C overnight. RNA was pelleted by centrifugation of the sample at 10,000 rpm at 4°C for 20 min. The supernatant containing the genomic DNA was removed to a fresh Corex tube and the DNA was precipitated as described in Section 2.2.9.1 using isopropanol. DNA was resuspended in 200 µL of 1 x Tris-EDTA (TE) buffer (Appendix I) and stored at 4°C.

2.2.2.2 Genomic DNA preparation using the Nucleon™ Phytopure™ Genomic DNA Extraction Kit

Nucleon™ PhytoPure™ Genomic DNA Extraction Kit (GE Healthcare, Sydney, Australia) was used for isolating genomic DNA from tobacco leaf tissue for Southern analysis. A pre-cooled mortar and pestle was used to grind 1 g of young leaf tissue to a fine powder in liquid N_2. 2.3 mL of solution 1, 23 µL of 2 -ME and 4.6 µL of RNAse A (10 $mgmL^{-1}$) was added to the powder and mixed well by vortexing. The sample was incubated at 37°C for 30 min and 0.75 mL of solution 2 added, and mixed by inverting the tube. Then the sample was incubated at 65°C for 10 min with mixing of the sample every min by inversion. The sample was then placed on ice for 20 min and 1 mL of chloroform (- 20°C) and 100 µL of PhytoPure™ resin added and mixed by inversion of the tube. The sample was incubated at room temperature for 10 min with mixing every min. The sample was centrifuged at 1300 g for 10 min and the supernatant aspirated to a

fresh tube to which an equal volume of phenol/chloroform was added. This was mixed well by inversion and centrifuged at 4000 g for 30 min. The supernatant was transferred to a Corex tube and an equal volume of isopropanol (- 20°C) added. The sample was mixed by gently swirling the tube. At this point genomic DNA was visible as white strands and was hooked out using a sterile glass rod, left to air dry for 10 min at room temperature and resuspended in 100 µL of water. Genomic DNA was then re-precipitated using 3 M NaAc and ethanol as described in Section 2.2.9.1 and resupended in 100 µL of 1 x TE buffer. Genomic DNA was stored at 4°C.

2.2.3 Restriction enzyme digestion of DNA

Typically 0.5-1 µg of plasmid DNA was digested in a total volume of 20 µL. The appropriate restriction enzyme buffer (10 x), as recommended and supplied by the manufacturer, was matched to the restriction enzyme(s) being used and 2 µL of the buffer and 1 unit of the enzyme were mixed with the DNA. The total volume of the reaction was adjusted to 20 µL using sterile water. The reaction mixture was incubated at 37°C for 2 h and the product checked on 1% (w/v) agarose/Tris-Borate-EDTA (TBE) minigel (Appendix I) as described in Section 2.2.4. For double digestions, the most efficient commercial buffer was identified and 2 µL of the 10 x buffer and 1 µL of each of the restriction enzymes were used. Double digestion reactions were performed at 37°C for 3 h.

2.2.4 Agarose gel electrophoresis for determination of DNA fragment sizes

Horizontal agarose gel electrophoresis was used to separate and quantify DNA fragments generated by restriction digestion and PCR. An appropriate amount of agarose was dissolved in 1 x TBE buffer to give a 1% (w/v) gel solution. This was cooled to 55°C and ethidium bromide added to a final concentration of 0.5 μgmL^{-1}. The gel solution was poured into the gel apparatus and, once set, the gel was covered with 1 x TBE buffer. The samples were loaded onto the gel after the addition of 10 x gel loading dye (Appendix I) to each of the samples to give a final concentration of 1 x. The DNA was separated at 80-100 V until DNA fragments were separated sufficiently. DNA ladders

and concentration standards (Invitrogen Life Technologies, Auckland, New Zealand) were used to estimate the fragment size and their concentration. The DNA fragments were visualised on a short wavelength UV transilluminator (Alpha Innotech Corporation, California, USA) and digital photographs were obtained using the Alpha imager™ 2000 Documentation and Analysis System (Alpha Innotech Corporation).

2.2.5 Insert preparation

Insert fragments for ligations were prepared by restriction digestion (Section 2.2.3) of the plasmid containing the fragment of interest or by PCR (Section 2.4). For restriction digested DNA, the total digest was separated on 1% (w/v) agarose/TBE gel and the fragment of interest was purified from the gel using QIAGEN™ or Axygen™ gel isolation kits as described in Section 2.2.9.2. Insert fragments prepared by PCR were purified using the QIAGEN™ or Axygen™ reaction cleanup kit (Section 2.2.9.2). The purified PCR fragments were then restriction enzyme digested and the restriction enzyme was heat inactivated by incubating the samples at 65°C for 10 min. The concentration of the insert fragment was determined by agarose gel electrophoresis as described in Section 2.2.7.2.

2.2.6 Vector preparation

2.2.6.1 End filling

Vector DNA was restriction enzyme digested (Section 2.2.3) and purified using QIAGEN™ or Axygen™ reaction cleanup kit (Section 2.2.9.2). One µg of the linearised vector DNA was end filled in a total volume of 20 µL. 1/10 volume of each of the required dNTPs at 0.5 mM concentration, 1/10 volume of buffer H and 1 unit of Klenow enzyme (Roche Diagnostics, Auckland, New Zealand) was added and the volume adjusted to 20 µL with sterile water. The mixture was incubated at 30°C for 20 min and the reaction stopped by heat inactivation of the enzyme by incubation at 65°C for 10 min. Vector DNA was quantified using a concentration standard (Section 2.2.7.2).

2.2.6.2 Dephosphorylation

Vector DNA was usually dephosphorylated prior to ligation using shrimp alkaline phosphatase (Roche Diagnostics). Linearised vector DNA (50 ng) was mixed with 1/10 volume of dephosphorylation buffer (Roche Diagnostics) and 1 unit of shrimp alkaline phosphatase and incubated at 37°C for 1 h. The reaction was stopped by incubation of the sample at 65°C for 15 min.

2.2.7 Determination of DNA/RNA concentration

2.2.7.1 Spectrophotometric method

Two µL of the DNA/RNA sample was diluted in water to give a 350-fold diluted solution. The diluted DNA/RNA sample was added to a quartz cuvette and absorbance of the solution determined at 260 nm and at 280 nm using a Shimadzu™ UV visible recording spectrophotometer calibrated with water. DNA concentration was calculated using the assumption that an absorbance reading of 1.0 at 260 nm corresponds to 50 μgmL^{-1} of double-stranded DNA while RNA concentration was calculated using the assumption that an absorbance reading of 1.0 at 260 nm corresponds to a 40 μgmL^{-1} of RNA. The ratio of A_{260}/A_{280} was used to determine the purity of the sample with pure DNA having a value of 1.8 and pure RNA having a value 2.0.

2.2.7.2 Agarose gel concentration standards

One µL of digested plasmid DNA or PCR product was added to 8 µL of water and 1/10 volume of 10 x gel loading dye, mixed thoroughly, and electrophoresed on 1% (w/v) agarose/TBE gel (Section 2.2.4). Four µL of either high mass or low mass ladder (Invitrogen Life Technologies) was run alongside the DNA samples. The concentration of the unknown DNA sample was estimated by visual comparison of the fluorescence intensity and size of the sample band with bands of the mass ladder.

2.2.8 Ligation

Rapid Ligation System (Roche Diagnostics) was routinely used to perform ligation reactions. The following formula was used to determine the ratio of vector DNA and insert DNA to be used in each ligation reaction.

$$\frac{\text{Vector DNA amount (ng) x insert size (kb) x 3 (sticky end)/5 (blunt end)}}{\text{Vector size (kb)}} = \text{Insert DNA amount (ng)}$$

The vector DNA fragment and insert DNA fragment were thoroughly mixed and diluted in 1 x DNA dilution buffer (all buffers were supplied in the kit) in a final volume of 10 µL. T4 DNA ligation buffer was thoroughly mixed and 10 µL was added to the diluted DNA sample. One µL of T4 DNA ligase was then added, the sample mixed and the reaction was incubated for 5-10 min at room temperature. Half of this ligation reaction was used directly afterwards for the transformation of competent *E. coli* cells (Section 2.3.2) and the rest of the reaction mixture was stored at 4°C and was used for repeating the transformation if necessary.

2.2.9 DNA purification

2.2.9.1 Precipitation using ethanol/isopropanol

DNA was precipitated by adding 2.5 volumes of ice-cold 100% ethanol and 1/10 volume of 3 M NaAc (adjusted to pH 6.0 with acetic acid) or 0.7 volumes of isopropanol at room temperature to a known volume of DNA solution. The solution was mixed well and centrifuged at 11,000 rpm in a Sorvall SS-34 rotor for 30 min at 4°C. The supernatant was decanted and the DNA pellet was washed with 1 mL of 70% (v/v) ethanol, centrifuged at 11,000 rpm in a Sorvall SS-34 rotor for 10 min at 4°C. The 70% (v/v) ethanol was then removed and the DNA pellet air-dried for 5-10 min and DNA resuspended in a suitable volume of sterile water.

2.2.9.2 Purification of DNA using commercial kits

Qiagen™ and Axygen™ gel purification and reaction cleanup kits were routinely used for the purification of DNA fragments used for ligation and sequencing reactions using the protocol supplied by the manufacturer.

2.3 Transformation

2.3.1 Preparation of competent *E. coli* cells

100 mL of Luria-Bertani (LB) broth (Appendix I) was inoculated with six fresh colonies of Novablue *E. coli*. Cells were grown overnight at 22°C at 250 rpm in a shaking incubator until an absorbance reading of 0.4-0.8 was reached at 600 nm. The cells were then chilled on ice for 20 min and centrifuged at 5000 rpm for 5 min at 4°C in a Sorvall SS-34 rotor. The supernatant was then removed and the cells were resuspended in 20 mL of ice-cold sucrose - EDTA - morpholinepropanesulfonic acid (SEM) buffer (Appendix I) and left on ice for 10 min. The cells were pelleted using the same centrifugation conditions and the resulting pellet was resuspended in 12 mL of ice-cold SEM buffer. After resuspending the cells, 920 µL of dimethyl sulfoxide (DMSO) was added and 200 µL of cells were aliquoted and snap frozen in liquid N_2. Competent cells were stored at -80°C until required.

2.3.2 Transformation of *E. coli* by the heat shock method

Novablue competent cells were thawed on ice. Half of the ligation reaction or 1 µL of plasmid DNA were thoroughly mixed with 100 µL of competent cells and put on ice for 20 min. The cells were heat shocked by incubating at 42°C for 1.5 min, briefly put on ice and 0.5 mL of LB broth added. The cells were then allowed to recover by incubating at 37°C for 30 min to 1 h. Aliquots of transformed cells were then plated on appropriate selective media using a sterile glass rod, allowed to air dry and incubated at 37°C overnight.

2.3.3 Identification of positive transformants

Antibiotic selection was used for the screening of positive transformants of *E. coli* or *A. tumefaciens*. Transformed cells were plated onto LB-plates supplemented with the appropriate antibiotic (Table 2.1) and incubated overnight (37°C for *E. coli* and 28°C for *A. tumefaciens*). Colonies were picked using sterile toothpicks and were propagated in LB-broth supplemented with the appropriate antibiotic overnight in a shaking incubator set to the appropriate temperature. Plasmid preparations of the cultures were carried out as described in Section 2.2.1.1 and the DNA was then digested by the appropriate restriction enzyme (Section 2.2.3). Agarose gel electrophoresis was then used as described in Section 2.2.4 to visualise DNA fragments and identify positive transformants. Cultures containing positive transformants were streaked on LB plates containing the appropriate antibiotic to obtain single colonies. When appropriate, blue/white selection was also used for identifying positive transformants by supplementing the LB plates with 12 µL of isopropyl ß-D-1-thiogalactopyranoside (IPTG) (20 $mgmL^{-1}$) (Appendix I) and 40 µL of 5-bromo-4-chloro-3-indolyl-beta-D-galactopyranoside (X-Gal) (20 $mgmL^{-1}$) (Appendix I). Plates were stored at 4°C once colonies had sufficiently developed.

Table 2.1. Antibiotic selection used for the screening of positive transformants containing different base vectors.

Vector plasmid	Antibiotic selection
pART7	Ampicillin (100 $mgml^{-1}$)
pGEMT-easy	Ampicillin (100 $mgml^{-1}$)
pBlueScript (KS II +)	Ampicillin (100 $mgml^{-1}$)
pART27	Streptomycin (25 $mgml^{-1}$) for *E. coli*
	Streptomycin/Spectinomycin (200 $mgml^{-1}$ each) for *A. tumefaciens*

2.3.4 Transformation of *A. tumefaciens* by electroporation

Twenty µL aliquots of LBA 4404 (Invitrogen Life Technologies) competent cells were slowly thawed on ice. One µL of plasmid DNA was combined with the competent cells and the mixture was transferred to a chilled Gene Pulser® electroporation cuvette (Bio-Rad Laboratories, California, USA). The Cell-Porator™ electroporation system (BRL Life Technologies) was set to low Ω, 330 capacitance, fast charge rate and booster unit at 4 kΩ. The electroporation cuvette containing the competent cells was placed in the electroporation chamber and the machine was charged up to 12 kV/cm by charging the unit to 300 V and cells transformed by pressing the trigger button for 1 s. Following the electroporation, the cells were resuspended in 1 mL of terrific broth (TB) (Appendix I), and allowed to recover by incubating (with shaking) at 28°C for 4 h. Aliquots of 50 µL, and 100 µL of the culture were plated onto LB-plates supplemented with the appropriate antibiotic and incubated at 28°C for three days or until colonies were visible.

2.4 Polymerase Chain Reaction (PCR)

PCRs were carried out in a Mastercycler® gradient PCR machine by Eppendorf. Taq DNA polymerase (Invitrogen Life Technologies) or Pwo polymerase (Roche Diagnostics) was used for the PCRs. Taq polymerase PCR was used for PCR colony screening and for generating products that were directly ligated into the pGEM-T Easy vector (Promega, Wisconsin, USA). Pwo polymerase was used for the generation of promoter deletion constructs, linker scanning mutagenesis constructs and for cloning of gene/cDNA sequences, where high fidelity and high processivity was required. For each set of PCR using Taq, a master mix of reaction components was prepared for the required number of reactions so that each 50 µL Taq PCR contained: 5 µL of 10 x Taq buffer, 1 µL dNTP (10 mM) (Roche Diagnostics), 1 µL of each of forward and reverse primers (10 µM), and 0.5 units of Taq polymerase and 40.5 µL of sterile water. The master mix was then dispensed in 49 µL aliquots into individual PCR tubes and 1 µL of the template DNA (0.1-0.5 ng) was then added. For each set of PCRs using Pwo polymerase, two master mixes of reaction components was prepared for the required number of reactions.

The first master mix contained 1 μL dNTP (10 mM), 1 μL of each of forward and reverse primers (10 μM) made up to a total volume of 25 μL with sterile water. The second master mix contained 5 μL 10 x Pwo buffer (Roche Diagnostics) and 0.5 units of Pwo polymerase made up to a total volume of 24 μL with sterile water. Twenty five μL of the master mix one and 24 μL of master mix two was then combined in the individual PCR tubes and template DNA (0.1-0.5 ng) was added before the thermal cycling.

PCR conditions were changed according to the T_m of the primers used, expected product size and the polymerase being used for the reaction. Sequences of all the primers used are given in Appendix III. Typically 5 μL of PCR product was run on a gel for visualisation (Section 2.2.4).

2.5 Sequencing

Plasmid DNA at a concentration of 100 ngμL^{-1} and the appropriate primers at a concentration of 3.2 pM were routinely sequenced at Allan Wilson Center at Massey University, Palmerston North. Sequencing was performed using ABI PRISM ™ Dye Terminator Cycle Sequencing Ready Reaction Kit (Perkin Elmer).

2.6 Sequence analysis software

All DNA sequence manipulations and sequence data analysis were performed using the DNASTAR (DNASTAR Inc., Wisconsin, USA) suite of programmes.

2.7 *A. tumefaciens* mediated tobacco transformation protocol

The recipes used for tissue culture media were based on (Murashige and Skoog, 1962) which contains: 1 x Murashige and Skoog (MS salts, Appendix I), B5 vitamins (Appendix I), 3% (w/v) sucrose, and 0.8% (w/v) agar.

- 1702 media also contained naphthaleneacetic acid (NAA) (0.1 mgL^{-1}) and benzyl amino purine (BAP) (1.0 mgL^{-1}).

- 2145 media contained the same hormones as 1702 media as well as kanamycin (500 mgL^{-1}) and ticarcillin disodium (Timentin) (250 mgL^{-1}).
- 1925 media had no hormones and contained kanamycin (300 mgL^{-1}) and ticarcillin disodium (Timentin) (250 mgL^{-1}).

The protocol for *A. tumefaciens* mediated transformation of tobacco leaf tissue was based on the method developed by Horsch *et al.* (1985). A 100 mL overnight culture of *A. tumefaciens* containing the binary vector for transformation of tobacco was set up at 28°C with shaking. Young tobacco leaves were harvested the next day and surface sterilised for 10 min in 15% (v/v) bleach supplemented with a few drops of Tween-20. The leaves were then rinsed three times in sterile water and cut into 5 mm squares using aseptic technique. The discs were transferred into a small sterile beaker containing the *A. tumefaciens* suspension. The leaf discs were allowed to become thoroughly wetted before transferring them onto sterile blotting paper. The discs were blotted to remove excess liquid culture and transferred to plates containing media 1702. Ten leaf disks were transferred into each plate. Leaf disks that had not been inoculated with *A. tumefaciens* were transferred to two plates of media 1702 to be used as controls.

The leaf disks were co-cultivated for two days in a tissue culture room set to 22-26°C under 16/8 h light/dark photoperiod, with 35 $mmolm^{-2}s^{-1}$ cool white fluorescent light. The leaf disks were then transferred to media tubs containing media 2145. Ten leaf disks from the control plates were also transferred to media 2145 to ensure that the selection agent used prevented development of callus or shoots. The other 10 leaf discs were maintained on media 1702 to ensure that callus tissue developed under the hormone regime being used. The leaf discs were allowed to develop callus and shoots for 2-4 weeks. One shoot from each of the leaf discs was then excised and transferred into fresh individually labelled media tub containing media 2145. Shoots were allowed to develop further on media 2145 until it was possible to divide them up once more. Once an independent shoot had proliferated adequately, shoots were transferred to individually labelled media tubs containing media 1925. The clonal shoots of each independent transformant were allowed to develop roots on media 1925. The copies of each independent transformant on media 2145 were maintained for backup purposes. Once the

plants had developed a good mass of roots, they were ex-flasked into soil in the containment house by the technician in charge of the house.

2.8 Biolistic mediated transformation of *A. majus* petal tissue

Media 2 is a solid MS medium modified from Murashige and Skoog (1962) and contains the following: 1/2 x MS macro salts, 1 x MS micro salts (Appendix I), 1 x MS iron (Appendix I), 1 x Linsmaier and Skoog (LS) vitamins (Appendix I), 3% (w/v) sucrose, 0.75% (w/v) agar.

Gold particles (1 μm, BioRad) were sterilised by washing 100 mg of the gold particles with 1 mL of isopropanol in a 1.5 mL microfuge tube. Gold particles were then washed three times with sterile water. Gold particles were then suspended in 1 mL of sterile water and 50 μL portions were aliquoted out into Eppendorf tubes. Sterile gold preparations (5 mg of gold in 50 μL of sterile water) were stored at 4°C.

Gold particles were coated with plasmid DNA as follows: The gold preparation (5 mg of gold in 50 μL of sterile water) was vortexed briefly and 10 μg of each of the plasmid DNA to be used was added. After a brief vortexing step 20 μL of 0.1 M spermidine and 50 μL of 2.5 M $CaCl_2$ were added to the tube, at the same time, and the mixture left on the vortex for 3 min. The mixture was briefly centrifuged and 90 μL of supernatant removed. The gold particles were resuspended by gently flicking the tube. 5 μL of this DNA coated gold mixture was used for each bombardment of antirrhinum petal tissue.

Dorsal petals of antirrhinum were surface sterilised for 15 min in a 15% (v/v) bleach solution supplemented with a few drops of Tween-20. The petals were then washed three times in sterile water. Each surface sterilised petal tissue was placed in a tub containing media 2 and placed in the gene gun chamber with a target distance of 11 cm from the Swinnex (Millipore) unit to the surface of the medium. A modified helium particle inflow gun based on Finer *et al.* (1992) with a high-speed direct current solenoid valve was used for the particle bombardment experiments. The gold particles, loaded onto the Swinnex unit, were accelerated in a helium stream under 400 kPa pressure in a particle vacuum of

- 95 kPa. A standard Solenoid Opening Time (SOT) of 30 ms was used. The trigger in the millisecond timer was then pressed for 1 s to bombard the target tissue. Each petal was bombarded twice. The petals were placed on fresh media 2 and incubated in a tissue culture room set to 22-26°C under 16/8 h light/dark photoperiod, with 35 $mmolm^{-2}s^{-1}$ cool white fluorescent light.

2.9 Histochemical localisation of GUS

Reagents

- Buffer X - 0.2 M $Na_2HPO_4.2H_2O$.
- Buffer Y - 0.2 M $NaH_2PO_4.2H_2O$.
- 50 mM phosphate buffer (pH 7.0) - 32 mL of buffer X was combined with 18 mL of buffer Y and made up to 200 mL with water.
- 5-Bromo-4-chloro-3-indolyl β-D-glucuronide cyclohexylamine salt (X-Gluc) solution – The volume of X-Gluc/ 50 M phosphate buffer required for the assay was calculated and 0.33 mg of X-Gluc was used for every 1 mL of 50 mM phosphate buffer. Each mg of X-Gluc powder was dissolved in 10 µL of dimethylformamide (DMF).

Tobacco petal tissue to be assayed for GUS activity was surface sterilised in 10% (v/v) bleach solution for 15 min and then washed three times with sterile water. Antirrhinum petal tissue that was used in transient assays did not require a surface sterilisation step. The tissue was then transferred into 50 mL Nunc tubes. The tissue was submerged in 50 mM phosphate buffer containing the appropriate amount of X-Gluc solution with 20% (v/v) methanol and vacuum infilterated for approximately 10 min. The tubes were then covered with tin foil and the samples were incubated at 37°C until GUS activity could be detected (usually overnight). Once GUS activity was detected the tissue was destained by incubating at 55°C in 100% ethanol containing 5% (v/v) acetic acid for approximately 30 min. Tissue were stored in 70% (v/v) ethanol solution.

2.10 Light microscopy

An Olympus-SZX12 dissecting microscope with a GFP fluorescence attachment was routinely used for observation of various tissue for reporter gene expression. Image capturing was carried out using a Leica DC 500 digital camera using the software supplied by the manufacturer.

Chapter 3: Characterisation of the *Rosea1* promoter region and analysis of *Rosea1* expression

3.1 Introduction

Previous studies by Schwinn *et al.* (2006) had shown that a 1.2 kb upstream region of the *Rosea1* gene, relative to the translational start site, was sufficient for expression of the *Rosea1* gene (Dr Kathy Schwinn, personal communication). Consequently, the aims of this part of the project were to identify the region/s of the *Rosea1* promoter important for its expression and to identify the spatial expression pattern of *Rosea1* in the antirrhinum flower. To achieve this, promoter deletion analysis was first carried out to identify the key region/s important for regulation of the *Rosea1* gene. The *Rosea1* promoter region was deleted at ~100 bp intervals and was used to drive the GUS reporter gene (Jefferson *et al.*, 1987). As the *Rosea1* promoter provides large areas of pigmentation, the initial promoter deletion analysis was carried out by transient transformation of rosea^{dorsea} (homozygous for the recessive alleles *rosea1*^{dorsea} and *rosea2*) petals using particle bombardment. These assays were conducted by Dr Kathy Schwinn and Mr Michael Bennett. Additional transient assays were carried out to verify their data and are presented in this thesis.

Stable transgenic assays were carried out in *Nicotiana tabacum* (tobacco) to verify the results from the transient assays. Tobacco was used for the generation of stable transgenic plants, as stable transformation of antirrhinum is difficult. Stable transgenic tobacco plants harbouring the promoter deletion constructs were generated by Mr Michael Bennett. The GUS analysis of these lines and the generation and GUS analysis of the stable transgenic tobacco plants harbouring the linker scanning mutagenesis constructs are presented in this thesis. Tobacco is easily transformed and has been successfully used to characterise other MYB transcription factors from antirrhinum (Tamagnone *et al.*, 1998). GUS expression in both antirrhinum petals and tobacco flowers was used to identify a key region in the *Rosea1* promoter important for the regulated expression of the *Rosea1* gene. PCR linker scanning mutagenesis was carried out to further identify the exact elements that are important for the regulated expression of the *Rosea1* gene within this key region. To help with the interpretation of the GUS analyses Southern blotting was carried out on the stably transformed tobacco

plants to determine the copy number of the transgene in individual lines. The spatial expression pattern of *Rosea1* in wild type antirrhinum flowers was analysed using *in situ* hybridisation.

3.2 Materials and Methods

3.2.1 Promoter deletion construct generation

Promoter deletion constructs to be used in transient assays in antirrhinum and for generation of stable tobacco transgenic plants were made using pART 7 and pART 27 binary vectors (Appendix II), respectively. All of the constructs excluding pPN 235 and pPN 245 were made by Mr Michael Bennett. Some transient assays were conducted by Mr Michael Bennett and Dr Kathy Schwinn and additional transient assays were carried out to verify/complete their data. The stable transgenic tobacco plants harbouring the binary vectors were also made by Mr Michael Bennett and the GUS analysis of these plants are presented. The method used for the promoter deletion construct generation is given in Appendix IV and Table 3.1 shows the details of the constructs.

3.2.2 Southern blot analysis

Probe synthesis

Template DNA (25 ng) in a final volume of 11 µL was denatured by heating in a boiling water bath for 10 min and chilled quickly in an ice/water bath. High Prime (Roche Diagnostics) was thoroughly mixed and 4 µL added to the denatured DNA. Five µl of 50 µCi [α^{32}P]dATP was then added and the contents of the tube mixed and incubated for 10 min at 37°C. The reaction was stopped by incubating at 65°C for 10 min.

The labelled insert was purified from the unincorporated labelled nucleotides using a ProbeQuant™ G-50 Micro Column (Amersham Pharmacia Biotech, New Jersey, USA). The resin was resuspended by gently flicking the tube. The cap was loosened one-fourth and the bottom closure was snapped off. The micro column was placed in a 1.5 mL

Table 3.1 Details of *Rosea1* promoter deletion constructs used for transient and stable assays[a].

Name of pART 7 based vector (transient)	Name of pART 27 based vector (stable)	*Rosea1* promoter size (bp)[b]	Primers used
pPN 228	pPN 237	1200	K224.Fwd/K181.Rev
pPN 194	pPN 238	900	K180.Fwd/K181.Rev
pPN 229	pPN 239	809	K214.Fwd/K181.Rev
pPN 230	pPN 240	710	K215.Fwd/K181.Rev
pPN 231	pPN 241	608	K216.Fwd/K181.Rev
pPN 232	pPN 242	493	K266.Fwd/K181.Rev
pPN 233	pPN 243	389	K267.Fwd/K181.Rev
pPN 234	pPN 244	289	K268.Fwd/K181.Rev
pPN 235	pPN 245	189	K269.Fwd/K181.Rev
pPN 257	Ppn 258	120	K277.Fwd/K181.Rev
pPN 236	pPN 246	89	K270.Fwd/K181.Rev

[a] All constructs excluding pPN 235 and pPN 245 were prepared by Mr Michael Bennett.
[b] Promoter size was determined from the NcoI site and includes the 5'UTR region.

screw-cap tube and spun for 2 min at 735 x g. The column was then placed in a fresh screw top microfuge tube and the radiolabelled sample was slowly applied to the top-centre of the resin without disturbing the matrix-bed. The column was then centrifuged at 735 x g for 3 min. The purified probe was collected in the bottom of the support tube and stored at - 20°C until used.

For Southern blot analysis 20 µg of tobacco genomic DNA was completely digested with 80 units of EcoRV in a total reaction volume of 300 µL. The digested DNA was precipitated using NaAc and ethanol as described in Section 2.2.9.1 and resuspended in 25 µL of sterile water. The digested DNA was run on a 0.8% (w/v) agarose/TAE gel overnight at 30 V. 20 ng of the corresponding plasmid containing the promoter deletion construct also digested with EcoRV was used as a positive control and run on the same gel. The DNA was transferred overnight onto a nylon membrane (Hybond N+, Amersham) using downward alkaline (0.4 M NaOH) capillary method (Chomczynski,

1992). The blotting apparatus was set up according to Sambrook *et al.* (1989) with the exception of using 4 M NaOH in place of 10 x SSC. After the DNA was transferred, the membrane was washed in 2 x SSC for 10 min and sealed in a plastic bag.

The expression cassette of each promoter deletion construct (containing the promoter fragment:GUS:OCS) was isolated from each of the corresponding plasmids as a SacI/NotI fragment. Purified expression cassette fragments (Section 2.2.9.2) were then used as templates to generate radiolabelled probes (as described above) for detecting the copy number in the Southern blots.

Radiolabelled probe was denatured by heating at 95°C for 5 min and then quickly chilled on ice. Denatured probe was then added to the hybridising solution and applied to the membrane that had been pre-hybridised at 65°C for 1-3 h in hybridisation solution (Church and Gilbert, 1984). Hybridisation was carried out overnight at 65°C and the membrane washed in 3 x SSC/1% SDS, 2 x SSC/1% SDS, 1 x SSC/1% SDS, 0.1 x SSC/1% SDS and 0.1 x SSC/1% SDS at 65°C for 1 h in each solution. The membranes were then exposed to photographic film for autoradiography at - 80°C overnight (longer exposures were used when required) and developed according to standard procedures.

3.2.3 PCR-based linker scanning mutagenesis of *Rosea1* promoter regions

For the initial mutagenesis of the *Rosea1* promoter, a 60 bp region was mutated, 20 bp at a time, using PCR linker scanning mutagenesis (Table 3.2). The strategy for PCR linker scanning was based on the method used by Barnhart (1999). Figure 3.1 shows the region of *Rosea1* promoter mutated in each of the constructs. The highlighted region in each of the linker scanning constructs was replaced with the random sequence of 5'CTTAGACCTCGAGTGTACCG3' of 20 bp. Two primers were designed with XhoI sites at the 5' end followed by 7 bp of randomly generated mutant nucleotide sequence (Table 3.2 and Appendix III). The last 12 bp of each primer was complimentary to the *Rosea1* promoter sequence. This 20 bp of the mutated promoter region was contained within 289 bp of the *Rosea1* promoter. Two PCRs (using Pwo polymerase) were carried out, the first one was with the K268.Fwd and mutant reverse primer and the second one

was with the mutant forward primer in combination with K181.Rev primer (Appendix III), using pPN 228 plasmid (Appendix II) DNA as the template. The first PCR product was digested with SacI/XhoI and the second product was digested with XhoI/NcoI. A triple ligation reaction (Section 2.2.8) was then used to insert the two PCR fragments into pPN 228 that had been digested with SacI/NcoI to remove the wild type *RoseaI* promoter sequence. Transformation of the ligation products and selection of positive clones were carried out essentially as described in Section 2.3.3. The construction of the mutant promoter constructs in pART 27 binary vector was carried out as described in Appendix IV.

Table 3.2 Details of the constructs used for the initial PCR linker scanning mutagenesis of the *RoseaI* promoter.

Name of pART 7 based vector (transient)	Name of pART 27 based vector (stable)	Primers used
pNNP.ELS1	pNNP.ALS1	K268.Fwd/N4WT.LS and N3WT.LS/K181.Rev
pNNP.ELS2	pNNP.ALS2	K268.Fwd/N6WT.LS and N5WT.LS/K181.Rev
pNNP.ELS3	pNNP.ALS3	K268.Fwd/N8WT.LS and N7WT.LS/K181.Rev

Finer linker scanning mutagenesis was carried out on the LS2 and LS3 regions by mutating 6 bp of the *RoseaI* promoter sequence at a time. The primer sequences used for the initial linker scanning mutants and finer linker scanning mutants are given in Appendix III. Figure 3.2 shows the region mutated in each of the finer linker scanning mutant constructs. The same method that was used for generating 20 bp mutations was used for making the 6 bp mutations except that one mutation (LS 2.1) had a BamHI site and the other (LS 2.3) had a HindIII site incorporated. All the other constructs had XhoI sites as the 6 bp mutant sequence (Table 3.3). A total of eight regions were mutated in the finer linker scanning mutagenesis. The two regions mutated in LS.WRKY and LS.DOF were sites predicted by PLACE database analysis (Section 3.2.4) to bind putative WRKY and DOF transcription factors, respectively. PCR, three-way ligation,

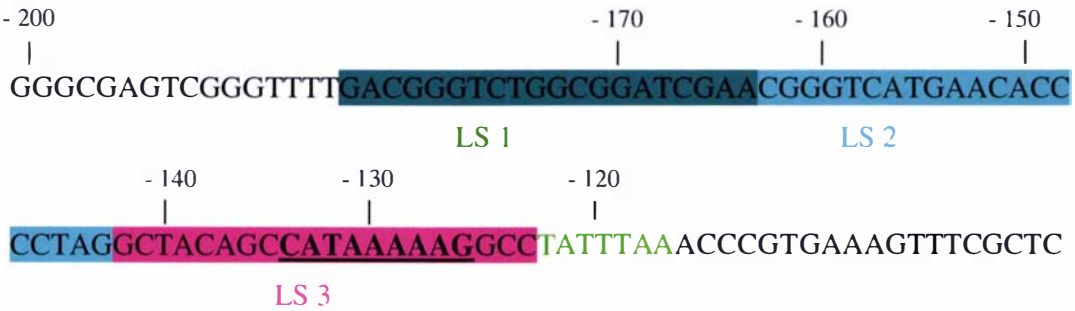

AAGGGGTACTCATTAAAAAAAGGGAAAGAGCAGCTAGACATGTGTTTTCTG

TTTTGACACTTTTAACGAACGGGCATAGTACGTATTAAACGCA**ATG**

Figure 3.1 The initial three regions of the *Rosea1* promoter mutated by PCR linker scanning mutagenesis.

Region highlighted in green (-182 to -163) was mutated in linker scanning construct 1 (LS1), region highlighted in blue (-162 to -143) was mutated in linker scanning construct 2 (LS2) and the region highlighted in purple (-142 to -123) was mutated in linker scanning construct 3 (LS3). A site with similarity to a potential MADS box binding site is in bold font and underlined. This site is not fully conserved with the CArG element bound by plant MADS box proteins. The putative TATA-box is shown in green font and the putative translation start site (ATG) is shown in bold font.

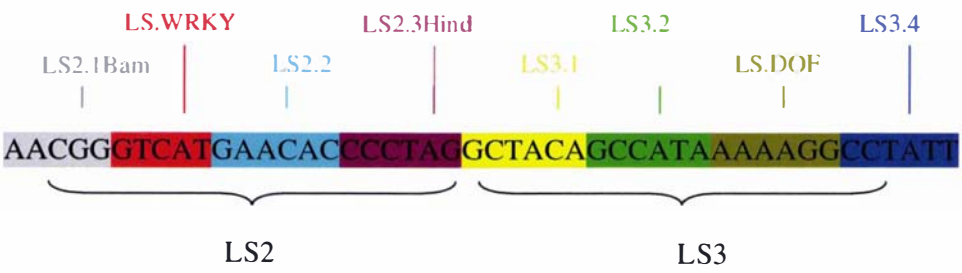

Figure 3.2 The eight regions of the *Rosea1* promoter mutated by finer PCR linker scanning mutagenesis.

The regions mutated in the initial linker scanning mutagenesis are shown as LS2 and LS3. LS.WRKY and LS.DOF are regions with putative WRKY and DOF transcription factor binding sites respectively.

transformation and selection in pART 7 and pART 27 vectors were essentially as described above for the initial linker scanning mutagenesis construct generation.

Table 3.3 Details of the constructs used for the finer PCR linker scanning mutagenesis of the *Rosea1* promoter.

Name of pART 7 based vector (transient)	Name of pART 27 based vector (stable)	Primers used
pNNP.ELS2.1Bam	pNNP.ALS2.1Bam	K268.Fwd/LS2.1Rev, LS2.1Fwd/K181.Rev
pNNP.ELS.WRKY	pNNP.ALS.WRKY	K268.Fwd/WRKY.Rev, WRKY.Fwd/K181.Rev
pNNP.ELS.2.2	pNNP.ALS.2.2	K268.Fwd/LS2.2Rev, LS2.2Fwd/K181.Rev
pNNP.ELS.2.3Hind	pNNP.ALS.2.3Hind	K268.Fwd/LS2.3Rev, LS2.3Fwd/K181.Rev
pNNP.ELS3.1	pNNP.ALS3.1	K268.Fwd/LS3.1Rev, LS3.1Fwd/K181.Rev
pNNP.ELS3.2	pNNP.ALS3.2	K268.Fwd/LS3.2Rev, LS3.2Fwd/K181.Rev
pNNP.ELS.DOF	pNNP.ALS.DOF	K268.Fwd/DOF.Rev, DOF.Fwd/K181.Rev
pNNP.ELS3.4	pNNP.ALS3.4	K268.Fwd/LS3.4Rev, LS3.4Fwd/K181.Rev

3.2.4 Bioinformatic analysis

The -162 to -123 region of the *Rosea1* promoter region identified to be important for expression of *Rosea1* allele was analysed for putative *cis*-elements using the PLACE (plant *cis*-acting regulatory DNA elements) database (http://www.dna.affrc.go.jp/PLACE). The query sequence was uploaded and scanned for motifs that are similar or identical to previously reported *cis*-element motifs in the PLACE database by selecting the signal scan search option (Higo *et al.*, 1999).

3.2.5 Cloning of the 3' UTR of *Rosea1* into pBlueScript vector

Ros3UTR.Fwd and Ros3UTR.Rev primers (Appendix III) were used to amplify a 0.3 kb fragment of the *Rosea1* 3' UTR using Pwo polymerase and pLN81 plasmid as the template (contains a *Rosea1* cDNA under the CAMV 35S promoter). The PCR product was gel purified (Section 2.2.9.2) and digested with Sac1 and Kpn1 and ligated into pBlueScript (KSII +) digested with SacI and KpnI using Roche rapid ligation kit

(Section 2.2.8). Positive clones were selected by isolating the plasmid from a number of colonies followed by restriction digestion. A plasmid giving the expected restriction digestion pattern was verified by sequencing using the T7 primer followed by sequence analysis. The positive clone was named pNNP.RosWT3UTR (Appendix II).

3.2.6 DIG labelled probe synthesis

Two PCR products were generated to use as template for RNA labeling using the DIG RNA labeling kit (Roche Diagnostics). M13.Fwd/T3 primer (Appendix III) combination was used to generate a PCR product that could be used as a template for transcription with T7 polymerase to generate the sense RNA probe and M13.Rev/T7 primer (Appendix III) combination was used to generate a PCR product to be used with T3 polymerase to generate the antisenese RNA probe. PCR was carried out using Pwo polymerase (Section 2.4) and the products were gel purified (Section 2.2.9.2). The RNA labeling reaction contained 200 ng of the appropriate purified PCR product, 2 µl of 10 x NTP labelling mix, 2 µl of 10 x transcription buffer, 1 µL of RNAse inhibitor and 2 µl of T7 or T3 polymerase. The total volume was adjusted to 20 µL using sterile water and the reaction carried out at 37°C for 2 h. 2 µL of DNAse I was added to the reaction and the reaction incubated for an additional 30 min at 37°C. The reaction was stopped by adding 2 µL of 0.2 M EDTA. The DIG-labelled RNA probe was precipitated by adding 2.5 µL of 4 M LiCl and 75 µL ice-cold ethanol and leaving at - 80°C for 1 h after which it was centrifuged for 30 min at 1300 x g at 4°C. The pellet was resuspended in 50 µ of sterile water. The yield of DIG-labelled RNA probe was estimated by a dot blot using the protocol supplied in the DIG application manual (Roche, 2002).

3.2.7 Tissue fixation and sectioning

Freshly harvested antirrhinum flower buds/petal tissue were put into glass vials containing freshly made formalin-alcohol-acetic acid (FAA) fixative and vacuum infiltrated so that the tissue would sink (FAA fixative contained 10:1:2:7 (v/v/v/v) ethanol:acetic acid:formalin (37% formaldehyde):sterile water. The solution was replaced with fresh FAA fixative and the tissue allowed to fix overnight at 4°C. Fixed tissue was then dehydrated in a graded ethanol series by leaving them for 1 h in each of the following ethanol solutions (all v/v); 50%, 50%, 70%, 85%, 95%, 100%, 100% and

100%. The tissue was then left overnight in 3:1 ethanol:xylene (v/v) solution. Next day xylene was substituted for ethanol by leaving the tissue for 1 h in the following ethanol:xylene (v/v) graded series; 3:1, 1:1, 1:3 followed by two 100% xylene steps. Tissue was left overnight in fresh 100% xylene. The next day the tissue was saturated with wax by adding a few paraplast (Oxford Labware, Montana, USA) chips at a time over the course of the day while incubating at 55°C. The tissue was left overnight in paraplast solution and the next day $^{2}/_{3}$ of the wax solution was removed and replaced with fresh molten paraplast wax. This step was repeated five times at 1 h intervals and the tissue was left overnight in fresh molten paraplast wax. Molten wax was replaced about four times with fresh molten wax over the next two days. The tissue was then embedded in wax and stored at 4°C. Wax blocks were attached to metal stubs and 8 µm transverse sections were cut using a Sorvall®Porterblum JB-4 microtome and a stainless steel knife. Ribbons of sections were placed onto drops of sterile water on Superfrost®Plus glass slides (Erie Scientific Company, New Hampshire, USA) and were cured overnight at 42°C and stored at room temperature.

3.2.8 *In situ* RNA hybridisation

Buffers and solutions

- Phosphate buffered saline (PBS) 10 x (pH 7.3): 137 mM NaCl, 2.7 mM KCl, 4.3 mM $Na_2HPO_4.7H_2O$ and 1.4 mM KH_2PO_4.
- 5 x TE: 10 mM Tris-HCl (pH 8.0) and 1 mM EDTA.
- Pronase: Pronase E (Roche Diagnostics) was treated to remove nucleases by dissolving 40 mg in 1 mL of water and incubating for 4 h at 37°C. Stock solutions were stored at - 20°C. 1.08 mL of stock solution was added to 17.5 mL of 1 M Tris and 3.5 mL of 0.5 M EDTA and then diluted to 350 mL with 1 x PBS before use.
- Glycine (2% w/v): dissolved in 1 x PBS.
- Formaldehyde (0.11% v/v): 38.5 mL formaldehyde diluted to 350 mL with 1 x PBS.
- Acetic anhydride (0.005% v/v): was made fresh by adding 1.75 mL acetic anhydride and 0.1 M triethanolamine made up to 350 mL with water

- Denhardt's solution (100%): 2% (w/v) bovine serum albumin (fraction V, nuclease free), 2% (w/v) Ficoll 400 and 2% (w/v) PVP in water.
- tRNA (10 $mgml^{-1}$): Nuclease free tRNA (Roche Diagnostics) in sterile water.
- 10 x Salts (100 mL): 3 M NaCl, 0.1 M Tris-HCl, 0.1M Na_2HPO_4 and 0.5 M Na_2EDTA (pH8).
- Dextran sulphate 50% (w/v): dissolved in water and filter sterilised using a 20 um filter.
- De-ionized formamide: 20 mL of formamide was mixed with 10 g of mixed bed resin TMD-S (Sigma) and stirred in a fume hood for 1 h. The solution was then filtered through Whatman™ filter paper and aliquots stored at - 20°C.
- *In situ* hybridisation buffer: 4 mL of buffer was made fresh for 12 slide pairs. Buffer contained 40 µL Denhardt's solution (100%), 400 µL tRNA (10 $mgmL^{-1}$), 400 µL salts (10 x), 800 µL dextran sulphate (50%), 2 mL deionised formamide and 360 µL sterile water.
- 20 x SSC (pH 7.0): 3 M NaCl and 0.3 M sodium citrate.
- NTE (5 x): 0.5 M NaCl, 0.01 M Tris-HCl and 1 mM EDTA (pH8).
- RNAse: 10 $mgmL^{-1}$ in 1 x NTE.
- Buffer 1: contained 0.1 M maleic acid, 0.15 M NaCl and 0.3% (v/v) Triton X-100. The pH was adjusted to 7.5 with NaOH and the solution was autoclaved. 1% (w/v) BSA fraction V was then added and the total volume was adjusted to 1 L with sterile water.
- BM block: 0.1% (w/v) blocking reagent in buffer 1 was heated to 60-70°C for 1 h and was allowed to cool down to room temperature.
- Buffer 3: contained 0.1 M Tris-base, 0.1 M NaCl and 0.05 M $MgCl_2.6H_20$. The pH was adjusted to 9.5 with NaOH and the solution was autoclaved. The total volume was adjusted to 1 L with sterile water.
- NBT/BCIP: 100 µL of NBT/BCIP (Roche Diagnostics) stock solution was diluted in 5 mL of buffer 1.

Rosea1 transcripts were detected in antirrhinum buds and flower petals using a Digoxigenin (DIG)-labelled probe (Section 3.2.6). DIG- labelled nucleotides are incorporated into the RNA probe during the labelling reaction. Hybridised DIG-

labelled probe is then detected with the high affinity anti-DIG antibody that is conjugated to alkaline phosphatase. A nitro-blue tetrazolium/5-bromo-4-chloro-3-indoylphosphate (NBT/BCIP) colourimetric reaction was then used to detect the DIG-labelled probe. Chalcone synthase probe (gifted by Yongjin Shang) was used as a positive control for each *in situ* hybridisation experiment. Tissue sections from different areas of the lobe tissue were probed with the antisense probe and one slide pair was probed with the sense probe for each *in situ* hybridisation experiment. Both wild type (line#522, Section 2.1) and rosea^{dorsea} (line #112, Section 2.1) tissue sections were cured onto each slide and 12 slide pairs in total were processed for each experiment. Different amounts of the antisense and sense probe (0.3 ng, 0.45 ng and 0.9 ng) were used for the hybridisation.

All the glassware and the 24 position slide rack were baked overnight at 150°C to remove RNAse and precautions were taken to minimise RNAse contamination. Plastic containers reserved solely for *in situ* hybridisation were used to make up the solutions listed in Table 3.4 and Table 3.5. On the first day of the experiment the slides were processed as listed in Table 3.4. A 250 µL aliquot of hybridisation solution (Table 3.4) containing the appropriate amount of probe was spread over one slide and a second slide lowered onto it. The hybridisation reaction was carried out overnight at 50°C in a moist chamber containing 2 x SSC/50% (v/v) formamide.

On the second day of the experiment, the slide pairs were separated and transferred onto the 24-position slide rack to carry out the washing steps listed in Table 3.5. A special container was used for the RNAse wash step. The blocking steps were carried out in a Pyrex dish set on a rocker. Slides were sandwiched together and placed in a high humidity chamber to carry out the anti-DIG antibody binding reaction and the NBT/BCIP colour reaction. The colour reaction was allowed to develop overnight in the dark and the reaction was terminated the next day by washing the slides in sterile water. The slides were mounted using DPX mounting solution (Merck, Auckland, New Zealand). Light microscopy as described in Section 2.10 was used to detect the location of *Rosea1* transcript.

Table 3.4. *In situ* hybridisation protocol for day one.

Step	Solution/solvent (350 ml)	Time (min)
1	Xylene	2 x 10
2	100% EtOH	1.5
3	95% EtOH	0.5
4	85% EtOH + 0.85% NaCl	0.5
5	75% EtOH + 0.85% NaCl	0.5
6	50% EtOH + 0.85% NaCl	0.5
7	30% EtOH + 0.85% NaCl	0.5
8	0.85% NaCl	2
9	PBS	2
10	Pronase	10
11	Glycine	2
12	Formaldehyde	10
13	PBS	2 x 2
14	Acetic anhydride	10
15	PBS	2
16	0.85% NaCl	2
17	Reverse steps 7-2	
18	Air dry slides	
19	Hybridisation solution	o/n

Table 3.5 *In situ* hybridisation protocol for day two.

Step	Solution (350 mL volume)	Time (min)
1	2 x SSC/ 50% formamide at 50°C	2 x 60
2	NTE	5
3	RNAse at 37°C	30
4	NTE	2 x 5
5	0.2 x SSC at 50°C	60
6	PBS	1
	Transfer to glass dish (Following volumes in 100 mL)	
7	BM block/ buffer 1	45
8	Buffer 1	45
9	DIG antibody in buffer 1 (1:2500 dilution)	90
10	Buffer 1	4 x 20
11	Buffer 3	3 x 2
12	NBT/BCIP colour reagent	O/N

3.3 Results

3.3.1 Promoter deletion analysis

Rosea1 promoter deletion constructs (pART 7 based) were initially assayed in rosea^{dorsea} antirrhinum petals using particle bombardment. This experiment was conducted by Dr Kathy Schwinn and Mr Michael Bennett and additional assays were conducted to verify their data. Both inner and outer epidermises were transformed with each of the promoter deletion constructs listed in Table 3.1. Transformed petal tissue was allowed to recover in media 2 (Section 2.8) for two days and stained for GUS expression. Each petal was observed for the number of GUS foci as well as the spatial GUS distribution. The results for the transient assays are given in Table 3.6. It was observed that the shorter promoter fragments [from pPNN 234 (289 bp *Rosea1* promoter) onwards] gave a more restricted GUS expression pattern in the inner epidermis with fewer GUS foci in the lobe region and more GUS foci in the upper tube and the hinge (region between the lobe and tube). Deletion of the *Rosea1* promoter down to the 189 bp (pPN 235 construct) relative to the translational start site was still able to drive GUS expression in both inner and outer epidermis of antirrhinum petals (Figure 3.3A and B). Transient assays carried out by Dr Schwinn showed GUS expression (although relatively weak) with the pPN 257 (harbouring 120 bp of *Rosea1* promoter containing the putative TATA-box and mostly 5' UTR region) construct. However, subsequent assays indicated that this promoter deletion construct was unable to drive GUS expression in both inner and outer epidermis of the petal. pPN 236, where the putative TATA-box was deleted, was unable to drive expression of the GUS reporter gene (Figure 3.3C and D). Therefore, the transient assay results showed that the key *cis*-elements important for the expression of the *Rosea1* gene were present in the -189 bp to -120 bp region of the *Rosea1* promoter.

Transgenic tobacco flowers harbouring the *Rosea1* promoter deletion constructs (listed in Table 3.1) were analysed for GUS expression (Section 2.9). Flowers ranging in size from 1.5 to 7 cm were analysed for temporal and developmental GUS expression pattern. Wild type flowers at the same developmental stages served as a negative control while flowers from plants harbouring pART 27-10 (35S:GUS:OCS) served as

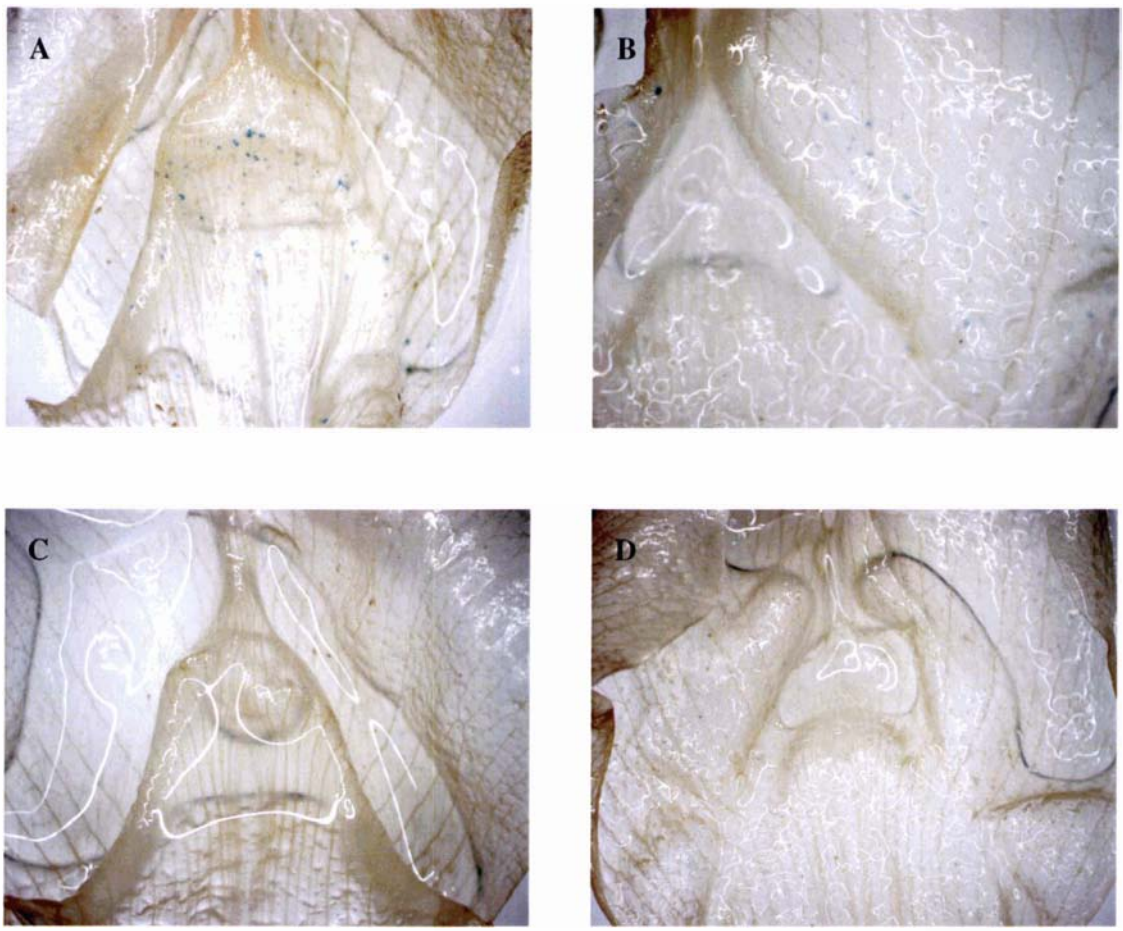

Figure 3.3 Transient GUS assay using particle bombardment transformation of rosea^{dorsea} antirrhinum (line #112) petal tissue with the *Rosea1* promoter deletion constructs listed in Table 3.1.

The pPN 235 construct was able to drive GUS expression in inner (A) and outer (B) epidermis while pPN 236 did not give GUS expression in the inner (C) or outer (D) epidermis. Positive expression is seen as small, multicell blue coloured foci, following histochemical staining for GUS activity and subsequent destaining to remove background colouration.

Table 3.6 GUS expression results of transient assays carried out on rosea[dorsea] antirrhinum petal tissue using the *Rosea1* promoter deletion constructs[a].

Vector	*Rosea1* promoter size (bp)[b]	GUS expression[c]
pPN 228[f]	1200	Yes
pPN 194[f]	900	Yes
pPN 229	809	Yes
pPN 230	710	Yes
pPN 231	608	Yes
pPN 232	493	Yes
pPN 233	389	Yes
pPN 234[f]	289	Yes[e]
pPN 235[f]	189	Yes[e]
pPN 257[f]	120	Yes/No[d]
pPN 236[f]	89	No

[a] These assays were conducted by Mr Michael Bennett and the tissue was observed to verify his results.
[b] Promoter size was determined from the NcoI site and includes the 5'UTR region.
[c] GUS expression in the inner and outer epidermis of the petal.
[d] Transient assays carried out by Dr Kathy Schwinn showed positive GUS expression with this construct. Data were only available for the inner epidermal tissue of the petal. No GUS expression was detected (inner and outer epidermis) when this assay was repeated.
[e] More GUS expression was observed in the upper tube and hinge region compared to the lobe tissue for transient assays carried out on the inner epidermis with these constructs.
[F] Additional transient assays were conducted with these constructs to verify the results obtained by Mr Michael Bennett.

positive controls. After overnight GUS staining, the flowers were analysed for GUS expression using light microscopy (Section 2.10). The stable tobacco transgenic results (Table 3.7 and Appendix V) verified the results from the transient assays as all of the constructs down to pPN 245 (equivalent to pPN 235) showed GUS expression. pPN 258 (equivalent to pPN 257), harbouring 120 bp of the *Rosea1* promoter (contains the putative TATA-box and 5′ UTR region) and pPN 246 (equivalent to pPN 236) (putative TATA-box deleted) gave no GUS expression. GUS expression was most intense in the tips of the flower petals, the lower half of the tube region and in vascular tissue for all of the promoter deletion constructs analysed (Figure 3.4). Leaves and sepals did not show GUS expression indicating that 189 bp of the promoter (promoter size includes

the 5' UTR region) was sufficient for petal specific expression. The temporal GUS expression pattern as observed with staining different developmental stages showed that the GUS expression was much stronger in younger flowers with a gradual decline as the petal matured (Figure 3.5). Anthocyanin pigments are first visible in tobacco flowers that are ~ 4 cm in length. Anthocyanins continue to accumulate in tobacco flowers that are up to about 6 cm in length as observed by the increase in intensity of pink colouration. It was observed that the transgenic tobacco flowers from different independent lines that contained the same construct showed different intensities of GUS expression. Southern blotting (Section 3.3.2) was carried out to investigate whether this was due to differences in the copy number of the transgene in these individual lines. Southern blotting was carried out on different lines of transgenic tobacco plants harbouring pPN 237, 238, 239, 242 and 244 constructs. The copy number of the transgene in these plants varied between 1- 4. Figure 3.6 shows an example Southern blot obtained for ten individual lines harbouring the pPN 242 construct. The copy number data for the other constructs are given in Appendix V. No correlation was observed between the intensity of GUS expression level in individual lines and the transgene copy number.

After GUS staining, the petals were hand sectioned, mounted on a microscope slide and analysed for the tissue specificity of GUS expression. GUS expression was most intense in the inner and outer epidermis of the petal tissue with weaker staining occurring, occasionally, in the vascular tissue (Figure 3.4D).

In summary, the results from both the transient assays of the *Rosea1* promoter deletion constructs in antirrhinum petals and stable transgenic tobacco showed the region between -189 bp to -120 bp of the promoter to be important for expression of the *Rosea1* allele and for maintaining the petal and epidermal specificity of its expression.

3.3.2 Linker scanning mutagenesis of the -189 bp to -123 bp region of the *Rosea1* promoter

The key region (-189 bp to -120 bp) identified by the promoter deletion analysis was further analysed by linker scanning mutagenesis to identify the exact elements

Table 3.7 GUS expression results of stable transgenic tobacco plants harbouring *Rosea1* promoter deletion constructs[a].

Name of pART 27 based vector	*Rosea1* promoter size (bp)[b]	Number of individual transformants analysed for GUS expression	Number of transformants showing positive GUS expression[c]	Number of transformants showing no GUS expression[c]
pPN 237	1200	17	10	7
pPN 238	900	15	12	3
pPN 239	809	11	10	1
pPN 240	710	11	7	4
pPN 241	608	11	4	7
pPN 242	493	15	7	8
pPN 243	389	15	5	10
pPN 244	289	13	5	8
pPN 245	189	13	6	7
pPN 258	120	11	0	11
pPN 246	89	16	0	16

[a] All the constructs excluding pPN 245 were prepared by Mr Michael Bennett. Generation of stable transgenic tobacco containing all the constructs excluding pPN 245 was also carried out by Mr Michael Bennett.
[b] Promoter size was determined from the NcoI site and includes the 5'UTR region.
[c] GUS expression in the inner and outer epidermis of the petal.

important for the regulated expression of the *Rosea1* gene. Linker scanning mutagenesis was chosen as clearly defined region/s of the promoter can be systematically mutated by this method. Furthermore, in this method the mutation is generated while maintaining the original spatial sequence arrangement of the promoter region (Barnhart, 1999). The -189 bp to -120 bp of the *Rosea1* promoter region was divided into three sub-regions for the mutagenesis (Figure 3.1). The region -142 bp to-123 bp was mutated in the LS3 mutant as mutating part of the putative TATA-box (-120 bp to -123bp) would be likely to abolish expression from this construct. This would mask other potential sites important for regulated expression.

Figure 3.4 Typical GUS expression pattern in petals of stably transformed tobacco harbouring the *Rosea1* promoter deletion constructs.

The tissue shown is from a pPN 237 (1.2 kb *Rosea1* promoter:GUS:OCS) transformed line. The spatial expression pattern of the GUS reporter gene (A) with strongest expression observed in the petal tips (B) and the lower portion of the tube region (C). The epidermal specificity of GUS expression is apparent in a petal cross section (D).

A

B

C

D

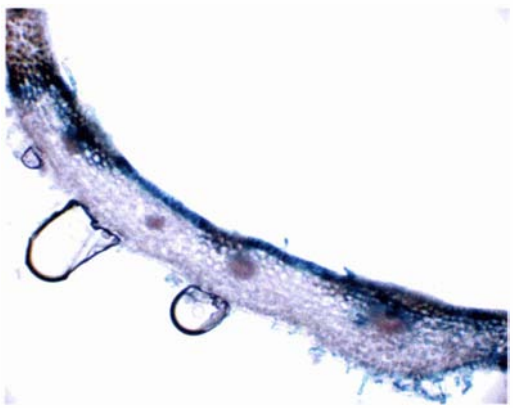

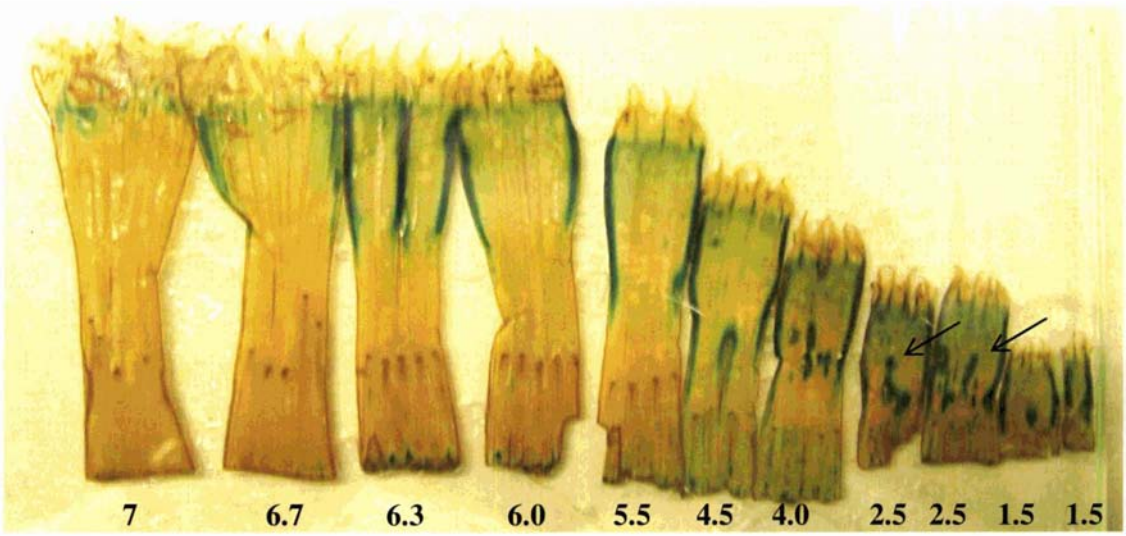

Figure 3.5 Temporal GUS expression pattern over petal development in flowers of stably transformed tobacco plants harbouring the pPN 237 (1.2 kb *Rosea1* promoter:GUS:OCS) construct.

All the flowers shown were obtained from plant line #17 and were stained for GUS expression at the same time. The anthers were removed from the flowers before GUS staining and resulted in wounding damage to the tissue (browning indicated by the arrows). The size of each flower (in cm) is indicated at the bottom of the figure.

Figure 3.6 Southern analysis showing transgene copy number in ten different transgenic lines containing the pPN 242 (0.493 bp *Rosea1* promoter fragment:GUS:OCS) construct.

20 μg of genomic DNA digested with EcoRV was separated on a 0.8% (w/v) agarose/TAE gel. The expression cassette of pPN 242 containing 0.493 bp *Rosea1* promoter fragment:GUS:OCS (Table 3.1) isolated as a SacI/NotI fragment was used for generating the radiolabelled probe. Five EcoRV sites present in the expression cassette containing 0.493 bp *Rosea1* promoter fragment:GUS:OCS gave four internal fragments and served as a positive control for the experiment (indicated by arrows). The sizes of the internal fragments are indicated on the right. The transgene copy number for each plant line was determined by counting the additional junction fragments. For example, line #11 has a single junction fragment (boxed) (in addition to the four internal junction fragments) and therefore, contains a single copy of the transgene.

Line Number	2	7	10	11	19	20	21	25	27	31
Copy Number	1	3	1	1	1	3	4	1	3	2

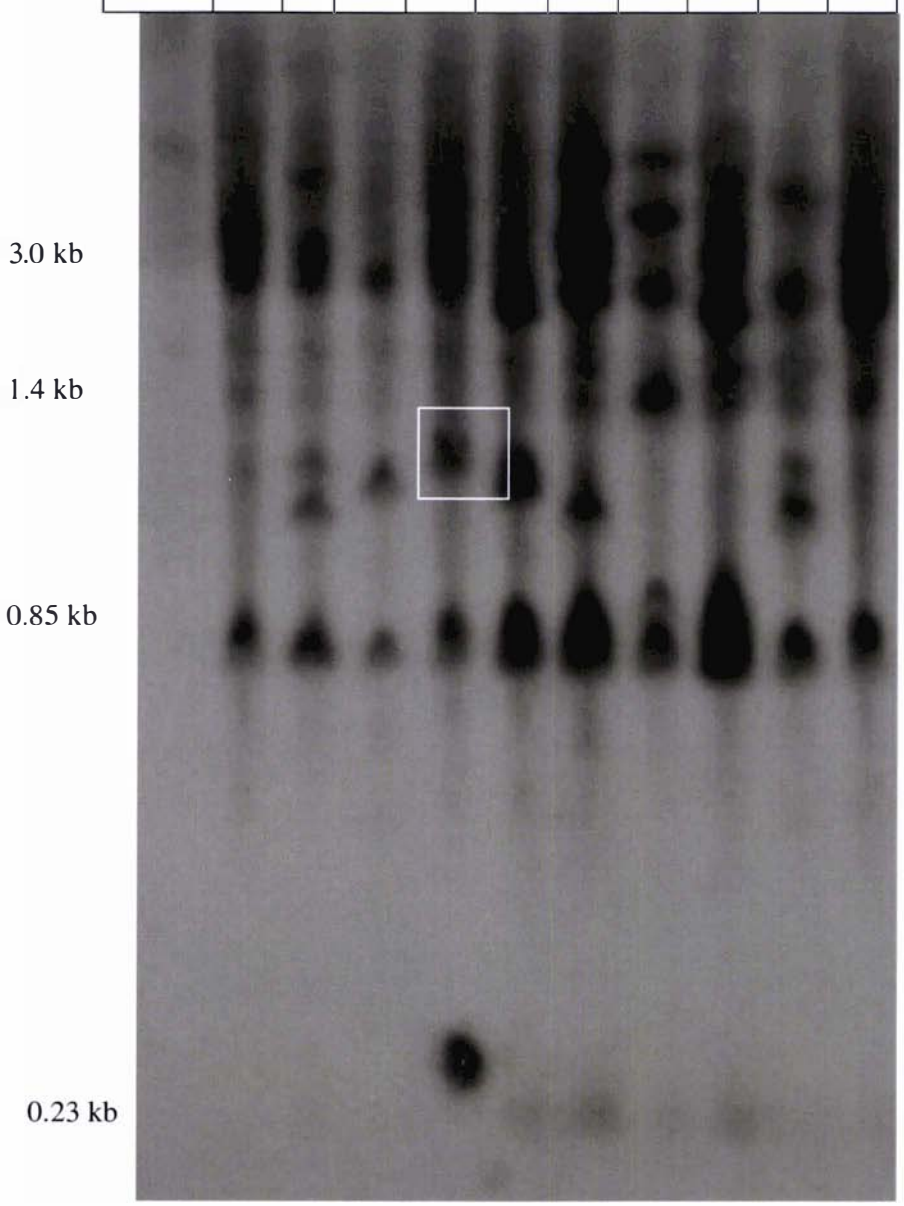

The three linker scanning mutants, ELS1, ELS2 and ELS3 (listed in Table 3.2 and the mutated regions as shown in Figure 3.1) were initially tested for GUS reporter gene activation by transient assays in rosea^{dorsea} petal tissue. Both the inner and outer epidermis of the petal tissue were transformed with the linker scanning constructs. The ELS1 construct gave a similar number of foci (>200 GUS foci) as the positive control used in this experiment, which was construct pPN 234 (289 bp *Rosea1* promoter:GUS:OCS). Transient assays with both ELS2 and ELS3 constructs failed to produce a similar large number of GUS foci as seen for either the ELS1 or pPN 234 constructs, and these few GUS foci (less than 10 foci) had very weak GUS expression.

The effects of the ALS1, ALS2 and ALS3 linker scanning mutations were analysed also in flowers of stably transformed tobacco plants. The flowers from half of the individual lines of stably transformed tobacco plants containing the ALS1 construct showed positive GUS expression (Figure 3.7A). The spatial GUS expression pattern in these flowers was similar to that from plants harbouring the wild type *Rosea1* promoter deletion constructs. The flowers from five individual lines (out of 14 individual lines analysed) harbouring the ALS2 construct also showed a positive GUS phenotype. However, two of these lines had very weak GUS expression and the other three had weak GUS staining only in the tube region of the flowers (Figure 3.7B and C).

Thirteen out of 16 individual lines containing the ALS3 construct also showed positive GUS staining. Out of the 13 lines showing a positive GUS phenotype, five individual lines showed very weak GUS activity with some lines showing weak GUS expression only in the petal tip region (Figure 3.7D). The other eight lines of transformants showing a positive GUS phenotype had the same GUS intensity and spatial GUS expression similar to that observed in plants harbouring the wild type *Rosea1* promoter deletion constructs. The results for the stable tobacco transgenic analysis are presented in Table 3.8 and details are outlined in Appendix VI.

The finer linker scanning mutant constructs listed in Table 3.3 (mutated regions as shown in Figure 3.2) were analysed for GUS reporter gene expression by analysing the flowers from stably transformed tobacco plants. The detailed results are presented in Appendix VII and Table 3.9 summarises the data. All of the finer linker scanning mutant constructs, excluding ALS3.4, showed positive GUS expression in tobacco

flowers. However, some of the constructs only gave very weak GUS expression in tobacco flowers in most of the individual lines analysed (e.g. ALS2.3 and ALSDOF). All of the constructs, excluding ALS3.2 and ALS3.4, also gave GUS expression in the sepal tissue in some of the individual lines (Figure 3.7 E). GUS expression was also seen specifically in either the petal tips or the tube region in the flowers of some lines for most of the constructs analysed except for ALS 2.2, ALS3.2 and ALS3.4 constructs.

3.3.3 Bioinformatic analysis

The *Rosea1* promoter sequence between -162 to -123 bp, identified to be important for its expression through the promoter deletion and linker scanning mutagenesis was analysed for putative *cis*-elements using the PLACE database. Four putative transcription factor-binding sites were predicted to be present in this region (Figure 3.8). These *cis*-elements were: a W box, present in the promoter region of the transcriptional repressor gene *ERF3* of tobacco which may function in the activation of the ERF3 gene in response to wounding (Nishiuchi T *et al.*, 2004); a binding site for WRKY-class of transcription factors, which are involved in plant defence responses (Eulgem *et al.*, 2000); a binding site for DOF-class of transcription factor, a class of plant-specific transcription factors which have been shown to perform diverse regulatory functions (Yanagisawa, 2002, 2004); and a pyrimidine box, a gibberellin-responsive *cis*-element shown to be partially involved in sugar repression (Morita *et al.*, 1998; Mena *et al.*, 2002).

3.3.4 *In situ* hybridisation

The spatial expression pattern of the *Rosea1* gene was analysed in the wild type antirrhinum petal tissue (stage 3, Figure 3.9A) by *in situ* hybridisation. Petal tissue probed with the *CHS* probe served as a positive control for this experiment while tissue sections probed with the *CHS* sense and Rosea1 3'UTR sense probes served as the negative controls. *CHS* positive control was carried out on stage 3 whole buds that were sectioned longitudinally. All other *in situ* hybridisation reactions were carried out on individual petal tissue that was transversely sectioned. *CHS* expression was strong in stage 3 bud tissue and was epidermal specific in both upper and lower petal tissue. The reproductive tissue also showed expression (Figure 3.9B). *Rosea1* gene expression was

observed specifically in both the inner and outer epidermis of the upper and lower lip petal tissue (Figure 3.9C and E). *Rosea1* was also expressed in the vascular tissue of both upper and lower lip petal tissue (Figure 3.9C and E). No signal was observed in the upper and lower petal tissue probed with the sense Rosea1.3'UTR probe (Figure 3.9D and F). However, reproductive tissue showed a weak signal with this probe on some occasions (Figure 3.9F).

Table 3.8 GUS expression results of stable transgenic tobacco plants harbouring the initial linker scanning mutagenesis constructs.

Name of pART 27 based vector	Number of transformants showing positive GUS expression	Number of transformants showing no GUS expression	Comments
ALS1	8	8	GUS expression similar to wild type promoter deletion construct.
ALS2	5	9	Two of the GUS positives had very weak GUS phenotype and three were weakly staining only in the tube region.
ALS3	13	3	Three of the GUS positives had very weak GUS phenotype and two had weak GUS staining only in the petal tip region. Other eight lines had GUS expression similar to wild type promoter deletion construct.

Figure 3.7 Examples of GUS expression pattern in flower tissue of stably transformed tobacco harbouring the linker scanning mutant constructs ALS1, ALS2 and ALS3.

Strong GUS expression was observed in the petals from plants harbouring the ALS1 (line #5) construct (A). Weak GUS expression observed in the petals from plants harbouring the ALS2 (line #9) construct (B). Weak tube-specific GUS expression in petals from plants harbouring the ALS2 (line #12) construct (C). Weak petal tip-specific GUS expression in plants harbouring the ALS3 (line #7) construct (D). GUS expression in the sepal tissue in flowers from tobacco plants harbouring the ALS2.3 (line #6) construct (E).


A


B

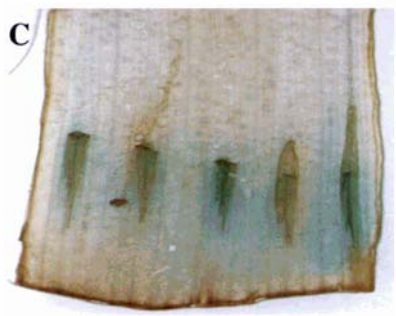
C


D

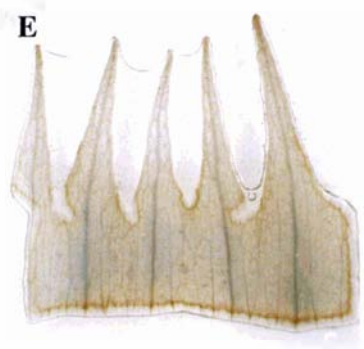
E

Table 3.9 GUS expression results of stable transgenic tobacco plants harbouring the finer linker scanning mutagenesis constructs.

Name of pART 27 based vector	GUS phenotype		Comments
	Positive	Negative	
pNNP.ALS2.1Bam	9	9	Sepals express GUS. Some lines only showed tube or petal tip-specific GUS expression
pNNP.ALS.WRKY	10	7	Sepals express GUS. Some lines only showed tube-specific GUS expression.
pNNP.ALS.2.2	8	7	Sepals express GUS. In most lines GUS expression was very weak.
pNNP.ALS.2.3Hind	12	7	Sepals express GUS. Some lines only showed tube-specific GUS expression and most lines had only weak GUS activity.
pNNP.ALS3.1	7	2	Sepals express GUS. One line had petal tip-specific GUS expression.
pNNP.ALS3.2	7	2	Two lines had very weak GUS expression.
pNNP.ALS.DOF	5	12	Sepals express GUS. Some lines had tube-specific GUS expression. In most lines GUS expression was very weak.
pNNP.ALS3.4	0	14	No GUS expression.

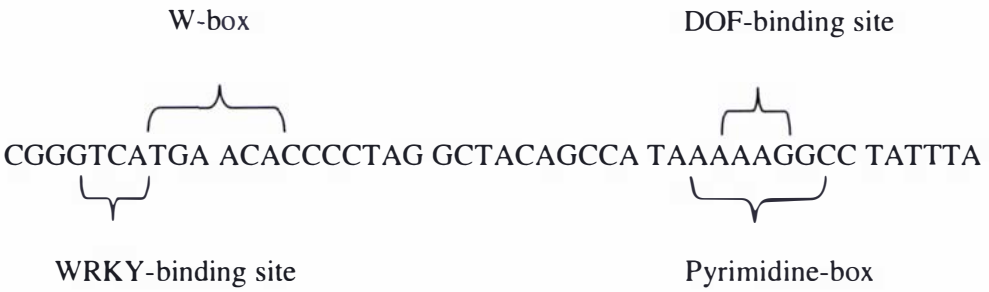

Figure 3.8 Putative *cis*-elements predicted to be present in the region between 162-123 bp of the *Rosea1* promoter.

The nucleotide sequence (+ strand) of -162 bp to -123 bp region of the *Rosea1* promoter region was analysed using the PLACE database. The sequence was then scanned for motifs that are similar or identical to previously reported *cis*-element motifs in the database by selecting the signal scan search option.

Figure 3.9 Analysis of *Rosea1* gene expression in stage 3, wild type antirrhinum flowers (line #522) by *in situ* hybridisation.

Wild type antirrhinum flower at stage 3 (10-15 mm) of development (A). For orientation, cutting plane is shown as a line. Upper and lower lip petal tissues are indicated by arrows. The whole flower was longitudinally sectioned and the lobe tissue probed with the antisense *CHS* probe. Epidermal-specific expression of the *CHS* gene used as a positive control for the *in situ* hybridisation analysis (B). Dissected upper lip petal tissue was transversely sectioned and the lobe tissue probed with the antisense Rosea1.3'UTR probe. Epidermal and vascular tissue-specific expression of the *Rosea1* gene in upper lip petal tissue (C). Upper lip lobe tissue probed with the sense Rosea1.3'UTR probe served as the negative control where no signal is observed (D). Epidermal and vascular tissue-specific *Rosea1* gene expression observed in the lobe region of the lower lip petal tissue probed with the Rosea1.3'UTR antisense probe (E). Lower lip petal tissue probed (lobe region) with the sense Rosea1.3'UTR probe shows no signal in the petal tissue and a weak signal in the reproductive tissue (F).

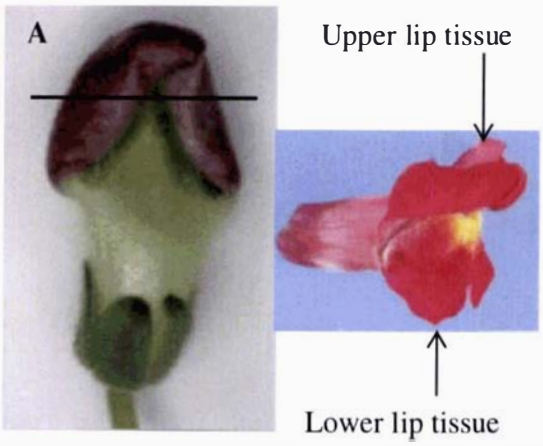
A
Upper lip tissue
Lower lip tissue

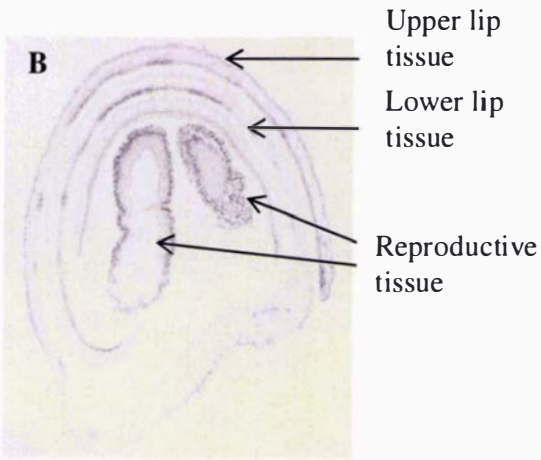
B
Upper lip tissue
Lower lip tissue
Reproductive tissue

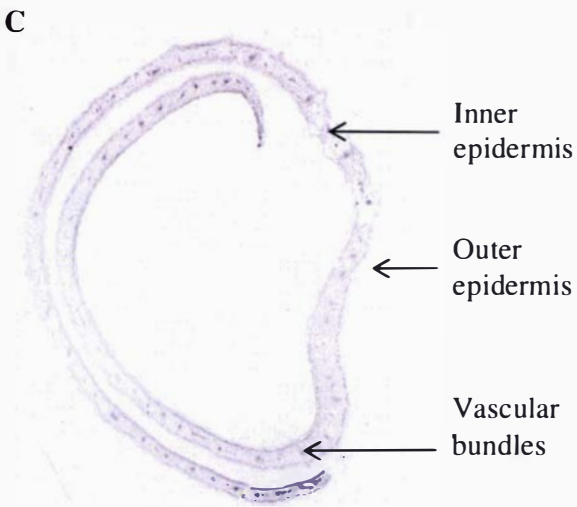
C
Inner epidermis
Outer epidermis
Vascular bundles

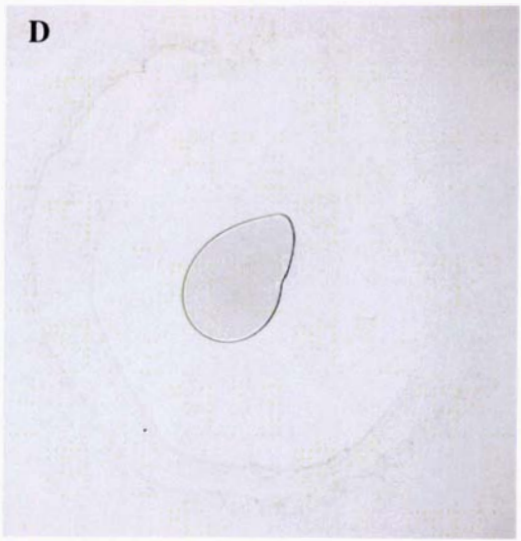
D

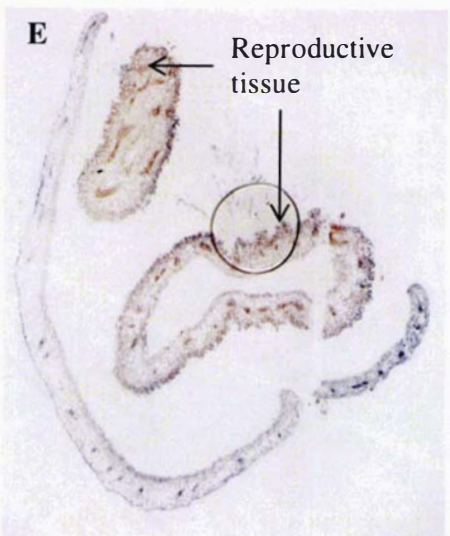
E
Reproductive tissue

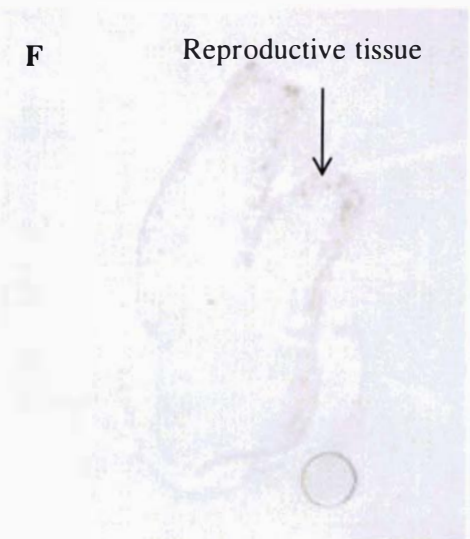
F
Reproductive tissue

3.4 Discussion

The major objective in this chapter was to identify the region/s in the *Rosea1* promoter that is important for expression and to analyse the spatial expression pattern of *Rosea1* in wild type antirrhinum flowers.

Initial promoter deletion analysis was carried out on the 1.2 kb region of the *Rosea1* promoter to find region/s important for expression of *Rosea1* using GUS as the reporter gene. Transient transformation studies are easy to perform, efficient and results are obtained within days. Transient assays have been used successfully for the analysis of genetic regulation of various genes in different species. For example, the promoter region important for the endosperm-specific expression of the rice sucrose synthase gene was identified using promoter deletion analysis carried out using particle bombardment-mediated transient transformation of seed tissue (Rasmussen and Donaldson, 2006). In the rosea^{dorsea} petal tissue, the expression of *Rosea1* is modified and there is no *Rosea2* expression (Schwinn, *et. al.,* 2006). Therefore, the rosea^{dorsea} petal tissue can be used for *Rosea1* gene complementation experiments. Therefore, *Rosea1* promoter deletion constructs were initially assayed by transient transformation of rosea^{dorsea} petal tissue by particle bombardment. These assays showed that the proximal 189 bp of the *Rosea1* promoter region was sufficient to drive GUS expression in both the inner and outer epidermis of antirrhinum petal tissue. Flowers of tobacco plants stably transformed with the promoter deletion constructs were then analysed for GUS reporter gene expression. These assays were performed to verify the results from the transient transformation experiments. Tobacco was chosen for the stable transformation analysis of the *Rosea1* promoter deletion constructs, as stable transformation of antirrhinum is difficult. Tobacco has been used successfully to characterise other antirrhinum *Myb* genes such as *Mixta* (Perez-Rodrigues *et al.,* 2005) and *Mixta-like3* (Jaffe *et al.*, 2007). The tobacco line used (samsun) also has pigmented flowers and a corolla where petals are fused to form a tube and lobe domains (similar to antirrhinum). However, tobacco flowers have radial symmetry rather than the bilateral symmetry present in antirrhinum flowers. The results from the stable transformation assays were consistent with the transient assays. The developmental pattern of GUS expression correlated well with that of anthocyanin accumulation in tobacco. GUS expression was observed to be stronger in the young transgenic tobacco flowers with a

gradual decrease as they mature. The *Rosea1* promoter region down to the proximal 189 bp was able to drive GUS expression in both the inner and outer epidermis of tobacco flowers. The 120 bp proximal region of the *Rosea1* promoter, which contains the putative TATA-box and most of the 5' UTR was not able to drive GUS reporter gene expression in either antirrhinum or tobacco flowers. Taken together, the promoter deletion analysis showed that the *Rosea1* promoter region between -189 bp and -120 bp was important for expression.

Individual transgenic tobacco lines harbouring the same promoter deletion construct showed variations in their floral GUS expression levels. Southern blotting was carried out to analyse whether this was due to variation in the copy number of the transgene between the individual lines. The copy number of the transgene varied between one and four. No correlation was observed between the strength of GUS expression and the copy number. Thus, positional effects from transgene insertion events were more likely to affect GUS expression rather than the copy number of the transgene in these individual lines. Positional effects from different transgene insertion events have been reported previously for tobacco (Hobbs *et al.*, 1990) as well as other plant species such as aspen (Kumar and Fladung, 2001). It was also observed that some transgenic lines did not express GUS. Positional effects from different transgene insertion events may result in weak GUS expression in these lines. It could be possible that this weak expression would be undetectable by histochemical staining for GUS. Thus, while GUS expression analyses of stable tobacco transformants were not suitable for obtaining quantitative data, this system was very useful for qualitative analyses of the *Rosea1* promoter deletion constructs.

Linker scanning mutagenesis is a method used routinely for the identification of various regulatory *cis*-elements in promoter regions. Some examples include the identification of *cis*-elements regulating pollen-specific and quantitative expression of the *ZM13* gene from maize (Hamilton *et al.*, 1998), the identification of two auxin responsive domains in the PS-IAA4/5 gene (encoding a putative auxin inducible transcription factor) from pea (Ballas *et al.*, 1995) and the identification of promoter regions important for the nitrate-dependent expression of two nitrate reductase genes from arabidopsis (Hwang et al., 1997). Consequently, PCR linker scanning mutagenesis was used to identify the exact elements within the -189 bp to -120 bp region that were important for the

regulated expression of the *Rosea1* gene. Initial PCR linker scanning was carried out by mutating 20 bp regions of the *Rosea1* promoter at one time. The region mutated in the LS1 construct (Figure 3.1) did not affect GUS reporter gene expression in either antirrhinum or tobacco petal tissue. This indicated that this region is not important for expression of the *Rosea1* gene. Bioinformatic analysis of the -162 bp to -143 bp region predicted a WRKY and a W-box site to be present in the region mutated in the LS2 construct. A pyrimidine box and a DOF transcription factor binding site were predicted to be present in the region mutated in the LS3 construct (-142 bp to -123 bp). Therefore, it was expected that mutation of either the LS2 or the LS3 region would affect GUS expression. Both ELS2 and ELS3 mutant constructs failed to drive strong GUS expression (compared to the wild type promoter deletion and ELS1 constructs) in the transient assays carried out on antirrhinum petal tissue indicating that this region indeed harboured *cis*-elements important for expression of the *Rosea1* gene.

The three linker scanning mutagenesis constructs were also tested for GUS reporter gene expression by analysing the flowers of stably transformed tobacco plants. The ALS1 construct showed positive GUS expression in tobacco petals further verifying that the region mutated in this construct was not important for expression of the *Rosea1* gene. A few individual lines harbouring the ALS2 construct gave GUS expression in tobacco petals but in all cases this expression was very weak. The ALS3 construct also gave GUS expression in tobacco petals. The GUS expression in five of the individual lines were very weak. However, the other eight lines showed positive GUS expression similar to that obtained from the ALS1 construct. Transient assays carried out with this same construct (ELS3) did not give GUS expression in antirrhinum petals. This contradiction is likely to be a result of using a heterologous stable transgenic system (tobacco) for the identification of the *cis*-elements. The transcription factors present in tobacco flowers are likely to be different from those in antirrhinum petal tissue. It is also likely that homologous transcription factors from tobacco and antirrhinum may have different binding preferences for their target DNA sequence/s. These differences are likely to result in tobacco petal tissue having a different transcriptional regulation mechanism for *Rosea1* compared to that of antirrhinum petal tissue. Thus, for finer promoter analysis, such as linker scanning mutagenesis, the assays conducted in antirrhinum petal tissue should provide more reliable results. Consequently, the two

regions mutated in the LS2 and LS3 constructs are likely to be important for regulating *Rosea1* gene expression.

Finer PCR linker scanning (6 bp segments) was then carried out on the LS2 and LS3 regions to locate the important *cis*-elements. The finer PCR linker scanning constructs were assayed only in flowers of stably transformed tobacco due to time constraints. The region mutated in the ALS 3.4 construct spanned part of the putative TATA-box and served as a negative control for the experiment. The ALS 3.4 construct did not give GUS expression, as expected, and confirmed that the predicted TATA-box is indeed the TATA-box for the *Rosea1* promoter. All of the other finer linker scanning constructs gave GUS expression in tobacco flowers. However, both ALS2.3 and ALSDOF constructs only gave very weak GUS expression indicating that the regions mutated in these constructs contained *cis*-elements that were important for driving *Rosea1* gene expression. All constructs except ALS3.2 and ALS3.4 were also able to drive GUS expression in the sepal tissue. This indicated that mutating these regions affected the ability of the promoter to maintain its petal specificity of expression.

Bioinformatic analysis, carried out on the -162 to -123 bp of the *Rosea1* promoter region, identified four putative transcription factor-binding sites (Figure 3.8). Mutation of the putative W-box (ALS2.2 construct), which may function in wound responses (Nishiuchi *et al.*, 2004), resulted in very weak GUS expression and also affected the petal specificity of expression. The WRKY transcription factor-binding site was also of interest as these factors are mainly involved in plant defence responses (Eulgem *et al.*, 2000). However, the ttg2 gene encoding a WRKY transcription factor in arabidopsis has been shown to function in trichome formation and seed pigmentation (Johnson *et al.*, 2002). Mutagenesis of the WRKY site led to the loss of petal-specific GUS expression indicating that this site may also be important for *Rosea1* gene regulation.

The DOF transcription factor-binding site was of special interest as these proteins are novel, plant-specific transcription factors with many functions, one of which is light regulated expression of genes (Yanagisawa, 2002, 2004). Finer linker scanning mutagenesis of this region (ALSDOF construct) indicated that this site may indeed be an important *cis*-regulatory element of the *Rosea1* gene, especially for petal-specificity.

A pyrimidine-box, a gibberellin-responsive element involved in sugar repression (Morita *et al.*, 1998; Mena *et al.*, 2002), was partially mutated in each of the ALS3.2, ALSDOF and ALS3.4 constructs. Mutating part of this pyrimidine-box in the ALSDOF construct affected GUS expression, especially in maintaining the petal-specificity of expression as previously mentioned. However, in future research the entire region containing this putative pyrimidine-box should be mutated in a single construct to assess the importance of this putative *cis*-element for *Rosea1* regulation. In addition, all the finer linker scanning mutant constructs should also be assayed in antirrhinum petal tissue using particle bombardment to verify the stable tobacco transgenic data.

In situ hybridisation was carried out on stage 3 wild type antirrhinum petal tissue to analyse the spatial expression pattern of the *Rosea1* gene. *Rosea1* transcripts were expressed in the inner and outer epidermal tissue of upper and lower lip petal tissue. This expression pattern was expected, as anthocyanin pigments in the petal are confined to the epidermal tissue (Jackson *et al.*, 1991; Martin and Gerats, 1993). The region around the vascular bundles also showed the presence of *Rosea1* transcript expression. Furthermore, GUS expression was seen in the vascular tissue of tobacco petals harbouring the various *Rosea1* promoter deletion constructs. The *Myb* gene *Venosa* regulates anthocyanin pigment production in the inner epidermal tissue overlying the veins (Schwinn *et al.*, 2006). *Venosa* transcript expression, analysed by *in situ* hybridisation, showed that *Venosa* mRNA was expressed in a zone from the xylem to the adaxial (inner) epidermis, and was controlled spatially and quantitatively by a signal associated with the petal veins (Shang, 2007). This signal might be hormonal, and could be either auxin, cytokinin, gibberellin or cytokinin hormones as the *Venosa* transcripts are specifically associated with the xylem tissue (No and Loopstra, 2000; Hartung *et al.*, 2002). As *Rosea1* is expressed in the vascular tissue, it is possible that it may also be regulated by these hormonal signals. Sugar signals, associated with the phloem tissue may also regulate *Rosea1* expression. A putative pyrimidine-box, which is a gibberellin-responsive element involved in sugar repression (Morita *et al.*, 1998; Mena *et al.*, 2002), is present in the LS3 region of the *Rosea1* promoter. Therefore, the importance of this putative pyrimidine-box should be analysed by linker scanning mutagenesis. The Rosea1.3′UTR sense probe, which served as the negative control, did not give a signal in the epidermal tissue. However, a weak signal was observed in the

reproductive tissue and is due to non-specific binding of the probe to this tissue (Dr Erin O'Donoghue, Crop & Food Research, personal communication).

In conclusion, the *Rosea1* promoter region encompassing -189 bp to -123 bp was shown to be important for the regulated expression of the gene by promoter deletion analysis. Linker scanning mutagenesis was then carried out on this region to identify the exact *cis*-elements important for the regulated expression of the *Rosea1* gene. This analysis identified the -162 bp to -143 bp region as containing the necessary *cis*-elements. Database analysis was used to identify four putative transcription factor-binding sites within this region: a W-box, a pyrimidine box, a DOF and a WRKY transcription factor binding site. Finer linker scanning mutagenesis was used to analyse the importance of these putative transcription factor-binding sites for *Rosea1* gene expression. Mutagenesis of all four sites led to the loss of petal-specific GUS expression indicating that these sites may indeed be important for *Rosea1* gene regulation. Furthermore, mutating the DOF and W-box site resulted in very weak GUS expression indicating that these *cis*-elements may be important for driving high level of *Rosea1* gene expression. *In situ* hybridisation on wild type antirrhinum flower petals showed epidermal and vascular bundle-specific expression of the *Rosea1* mRNA. The epidermal expression of *Rosea1* correlated with the anthocyanin pigment accumulation pattern in wild type antirrhinum flowers. The presence of *Rosea1* mRNA in the vascular bundles indicate that *Rosea1* may also be regulated by hormonal and/or sugar signals.

Chapter 4: Cloning and characterisation of the *rosea1*^{dorsea} gene

4.1 Introduction

Schwinn *et al.* (2006) postulated that the rosea^{dorsea} phenotype is most likely to be due to the differences in the *Rosea1* promoter region, especially the large 187 bp deletion present in the proximal region of the *rosea1*^{dorsea} promoter. In addition to this large deletion, their analysis of the *rosea1* genomic DNA encoding the promoter and the N terminus (up to the second intron) showed nine single nucleotide substitutions, two single nucleotide additions, one single nucleotide loss and a twelve base pair insertion in the promoter region (Figure 4.1). It was decided to analyse the affect of the 187 bp deletion on *rosea1* gene activity using transgenic and genetic approaches. The transgenic approach used standard promoter deletion analysis. Six promoter deletion constructs, where 700 bp of the *rosea1*^{dorsea} promoter were deleted at ~ 100 bp intervals driving the GUS reporter gene, were assayed for promoter activity by transient transformation of rosea^{dorsea} petal tissue by particle bombardment and by assaying the GUS expression of stably transformed tobacco flowers. The promoter deletion constructs and transgenic plants were made by Mr Michael Bennett (Crop & Food Research). Promoter replacement experiments were also conducted to analyse the importance of the intron regions in conferring the wild type and rosea^{dorsea} phenotype.

The genetic test of the importance of the 187 bp deletion made use of the collection of *Antirrhinum* species available at the John Innes Centre. Of the many *Antirrhinum* species that have been described, several of them have strong anthocyanin pigmentation in the corolla, similar to *A. majus*. *A. australe* and *A. barrelieri* are two such examples (Cathie Martin, personal communication). Other closely related *Antirrhinum* species include *A. latifolium*, *A. granaticum*, *A. molle*, *A. mollissimum* and *A. siculum* (Figure 4.2). These species show variation in their corolla pigmentation and typically have pale or no anthocyanin accumulation in the lobe tissue. Although these species have strong self-incompatibility they can be cross-hybridised with *A. majus*. The genetic basis of the weak pigmentation in the aforementioned species was studied by Schwinn *et al.* (2006).

Analysis of the progeny from cross hybridisation of *A. granticum, A, molle, A. mollisimum* to wild type, rosea^{dorsea} and rosea^{colorata} *A. majus* lines showed that the weak pigmentation in these species can be attributed to changes at the *Rosea* locus. To examine the molecular basis of this variation and whether it was due to the 187 bp deletion, the *Rosea1* promoter region was cloned and characterised from two accessions of *A. majus*, Barcelona and Toulouse, and seven *Antirrhinum* species, *A. australe, A. barrelieri*, *A. latifolium*, *A. granaticum*, *A. molle*, *A. mollissimum* and *A. siculum.*

It is possible that other factors besides the promoter variation at the *Rosea* locus may account for the rosea^{dorsea} phenotype. In this regard, it was decided to test the function of the protein encoded by *rosea1*^{dorsea}, the influence of variations in intron sequences, and the pattern of transcript abundance in the rosea^{dorsea} flowers. Previously, Schwinn *et al.* (2006) cloned and characterised the *rosea1*^{dorsea} cDNA and also partially cloned the genomic *rosea1*^{dorsea} allele up to the second intron. The cloned cDNA of *rosea1*^{dorsea} had 11 sequence differences from the wild type, *Rosea1* allele, of which eight affected the identity of the encoded amino acids. Therefore, it was necessary also to test whether the protein product encoded by *rosea1*^{dorsea} was functional. To achieve this, complementation assays were carried out in rosea^{dorsea} petal tissue by particle bombardment of an expression vector containing the *rosea1*^{dorsea} allele. Also the r*osea1*^{dorsea} allele was fully cloned and sequenced to analyse if the intron regions differ from the *Rosea1* allele. The spatial expression of *rosea1* mRNA was also analysed in rosea^{dorsea} petal tissue by *in situ* hybridisation.

Figure 4.1 Sequence alignments between the *Rosea1* and the *rosea1*^{dorsea} promoter regions.

The *Rosea1* promoter sequence is shown on the top strand and the *rosea1*^{dorsea} sequence is shown on the bottom strand. Residues that differ from the *Rosea1* promoter region and the 187 bp deletion in the *rosea1*^{dorsea} promoter are highlighted in red. The putative TATA-box is underlined in green. The start of the proximal -151 bp of the *rosea1*^{dorsea} promoter is indicated. The promoter sequence ends at the proposed translation initiation codon, ATG.

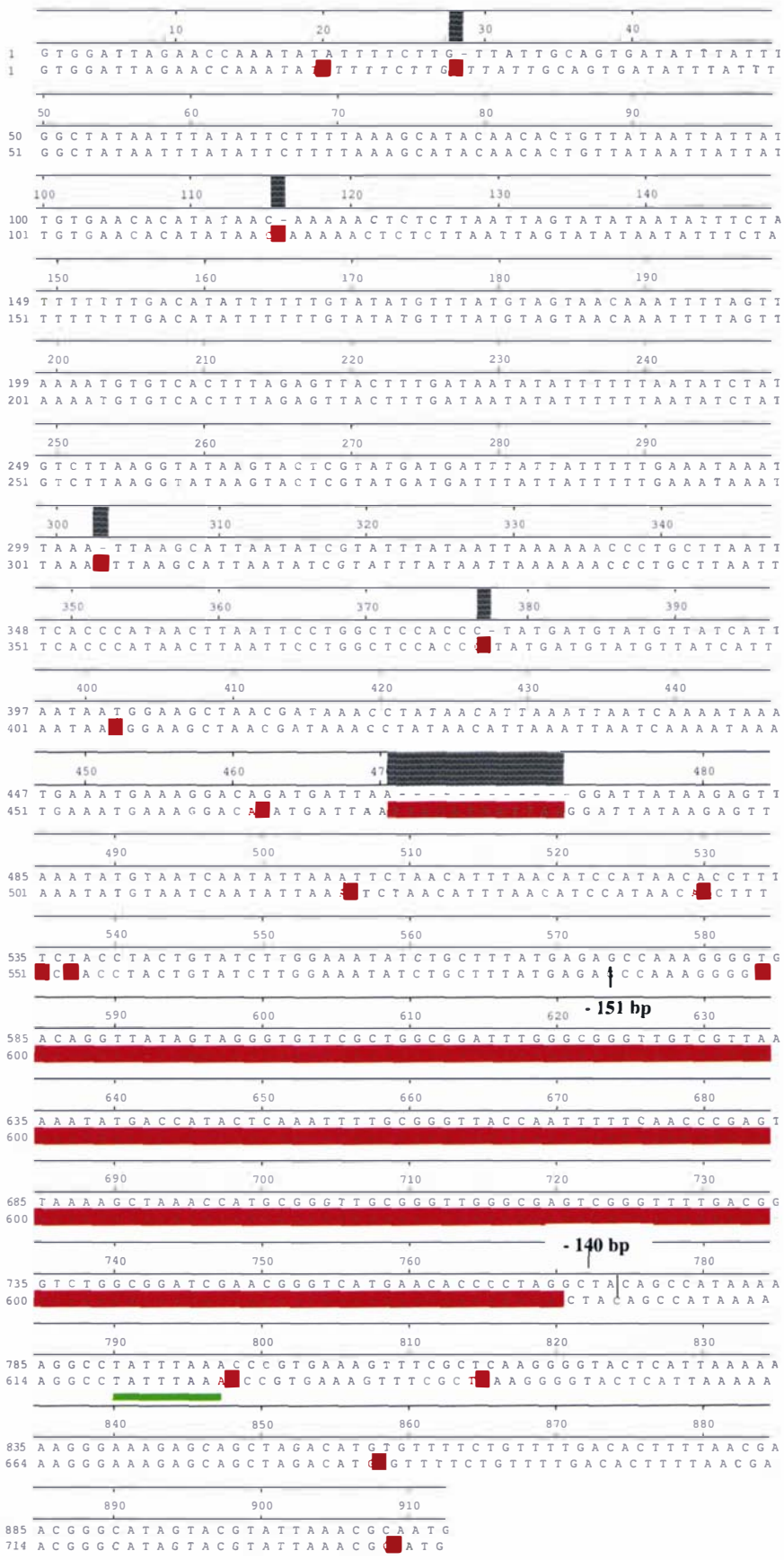
- 151 bp
- 140 bp

Figure 4.2 Floral phenotypes of different species within the *Antirrhinum* genus.

The source of the particular accession is given for some species.
(A) *Antirrhinum majus* (line #522), (B) *Antirrhinum australe*, (C) *Antirrhinum barrelieri*, (D) *Antirrhinum latifolium* (Marseilles), (E) *Antirrhinum molle*, (F) *Antirrhinum mollissimum*, (G) *Antirrhinum meonanthemum*, (H) *Antirrhinum graniticum* and (I) *Antirrhinum siculum* (Syracusa).

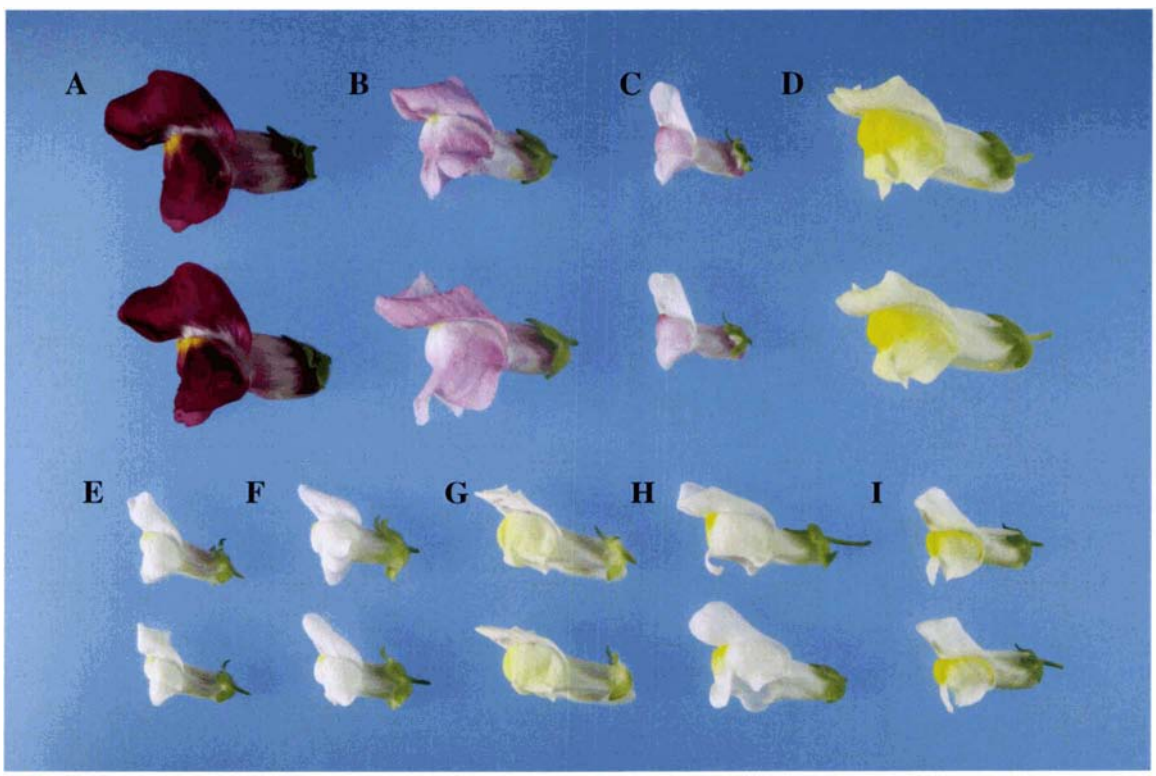
A
B
C
D
E
F
G
H
I

4.2 Materials and Methods

4.2.1 Generation of *rosea1*^{dorsea} promoter deletion constructs

A similar strategy to that outlined in Appendix IV for generation of the *Rosea1* promoter deletion constructs was used for constructing the *rosea1*^{dorsea} promoter deletion constructs in pART 7 and pART 27 (Table 4.1). These constructs were made by Mr Michael Bennett. The transient assays were conducted by Mr Michael Bennett and additional transient assays were carried out to verify/complete his data. Mr Michael Bennett also generated the stable transgenic tobacco plants harbouring the binary vectors. The GUS analysis of these plants were carried out in this thesis. Details of the *rosea1*^{dorsea} promoter deletion construct generation are given in Appendix IV.

Table 4.1 Details of *rosea1*^{dorsea} promoter deletion constructs used for transient and stable assays[a].

Name of pART 7 based vector (transient)	Name of pART 27 based vector (stable)	*rosea1*^{dorsea} promoter size (bp)[b]	Primers used
pPN 195	pPN 247	735	n/a
pPN 208	pPN 248	632	K214.Fwd/K181.Rev
pPN 209	pPN 249	533	K215.Fwd/K181.Rev
pPN 210	pPN 250	431	K216.Fwd/K181.Rev
pPN 211	pPN 251	279	K217.Fwd/K181.Rev
pPN 212	pPN 252	151	K218.Fwd/K181.Rev

n/a - not available
[a] All constructs were prepared by Mr Michael Bennett.
[b] Promoter size was determined from the NcoI site and includes the 5'UTR region.

4.2.2 Cloning of the *Rosea1* promoter region from different *Antirrhinum* species

Genomic DNA from the different *Antirrhinum* species and accessions, grown at the John Innes Centre, Norwich, United Kingdom were isolated by Mr Steven McKay (John Innes

Centre) using a $CsCl_2$ gradient as described by Martin *et al.* (1985). PCR with different forward primers, (Appendix III) and the K181 reverse primer, designed to the *Rosea1* and *rosea1*^{dorsea} promoter regions, were carried out on the genomic DNA templates to amplify the *Rosea1* promoter region from the different species and accessions. PCR was carried out using Taq DNA polymerase using the following conditions; 4 min at 94°C, followed by 35 cycles of 30 s at 94°C, 30 s at 50°C and 1 min at 72°C, and a final extension of 10 min at 72°C. PCR products were purified using the Qiagen PCR product purification kit as described in Section 2.2.4. Sequencing of the purified PCR products was carried out using the primers that were used for the PCR amplification.

4.2.3 Cloning of the *rosea1*^{dorsea} genomic sequence

The full-coding region of the *rosea1*^{dorsea} gene was amplified with Pwo DNA polymerase using genomic DNA isolated from young leaf tissue of rosea^{dorsea} plants. A Mg^{++} titration with 3-8 mM of $MgSO_4$ was used to increase the specificity of the PCR reaction with 5 mM $MgSO_4$ giving the highest product yield. Annealing was carried out at 50°C with K182.Fwd and K183.Rev primers (Appendix III). A total of 30 PCR cycles was carried out with the last 20 cycles having a 5 s time increment increase per cycle. The PCR reaction was gel purified as described in Section 2.2.9.2 and the product cloned into pBluescript (KSII +) vector that had been digested with SmaI and dephosphorylated (Section 2.2.3 and 2.2.6.2, respectively). Ligation reaction, transformation and isolation of positive transformants were carried out as described in Section 2.3.3.

4.2.4 Construction of the *rosea1*^{dorsea} expression vector

A vector was constructed, pPN 345, that contained the *rosea1*^{dorsea} genomic coding region driven by the 700 bp of fragment of the *rosea1*^{dorsea} promoter. 700 bp of the *rosea1*^{dorsea} promoter fragment was isolated from pPN 195 plasmid using a SacI/NcoI digest and the 2.5 kb length *rosea1*^{dorsea} gene was isolated from pPN 282 (35S:*rosea1*^{dorsea}:OCS) with a NcoI/XhoI digest. pART 7 was digested with SacI/XhoI and three-way ligation was then used to insert the 0.7 kb promoter fragment and the *rosea1*^{dorsea} gene into the digested

vector. Plasmid DNA digestion, purification, ligation and selection of positive clones was carried out as essentially as described in Section 2.3.3.

4.2.5 Construction of pPN 371 reporter vector

A vector was constructed, pPN 371, that contained the *rosea1*^{dorsea} genomic coding region driven by the 900 bp fragment of the *Rosea1* promoter. pPN 194 was digested with SacI/NcoI to isolate 900 bp of the *Rosea1* promoter fragment and pPN 282 was digested with NcoI/XhoI to isolate the *rosea1*^{dorsea} gene. Three-way ligation was then used to insert these two fragments into pART 7 vector that had been digested with SacI/XhoI. The general methods as described in Section 2.3.3 for DNA cloning and selection of positive transformants, were used for generation of pPN 371.

4.2.6 *In situ* hybridisation

In situ hybridisation was carried out on stage 3 rosea^{dorsea} petal tissue using DIG-labeled *Rosea1* 3' UTR probe. The techniques used for tissue fixation and *in situ* hybridisation are described in Section 3.2.8.

4.2.7 Bioinformatics

The promoter region of *rosea1*^{dorsea} as well as the intron regions were analysed for putative *cis*-elements using the PLACE website as described in Section 3.2.4.

4.3 Results

4.3.1 *rosea1*^{dorsea} promoter deletion analysis

rosea1^{dorsea} promoter deletion constructs (Table 4.1) were assayed for promoter activity by transient transformation of antirrhinum petals as well as analysis of flowers of stably transformed tobacco plants, essentially as described in Section 3.3.1.

The majority of the transient assays using the *rosea1*^{dorsea} promoter deletion constructs were carried out by Mr Michael Bennett and additional assays were conducted to complete the experiment. The generation of the stable tobacco transformants containing the *rosea1*^{dorsea} promoter deletion constructs were also carried out by Mr Michael Bennett and GUS expression analysis of these plants are presented in this thesis.

All of the *rosea1*^{dorsea} promoter deletion constructs gave similar numbers of GUS foci in transient assays carried out with rosea^{dorsea} petal tissue (Table 4.2). The pPN 212 construct harbouring the -151 bp *rosea1*^{dorsea} promoter:GUS:OCS gave a similar number of GUS foci as the pPN 195 construct (735 bp *rosea1*^{dorsea} promoter:GUS:OCS) in both epidermal layers of antirrhinum flowers (Figure 4.3). It should be noted that the results from the transient assays are based on visual assessment, as sample to sample variation, as well as variation between different assays, prevented quantification.

Flower tissue from tobacco plants stably transformed with the *rosea1*^{dorsea} promoter deletion constructs were analysed for GUS expression. All six promoter deletion constructs were able to drive GUS expression. Strong GUS expression was observed in both petal tips and the tube tissue (Figure 4.4A). Leaf tissue and sepal tissue did not show GUS expression with any of the promoter deletion constructs. Hand sectioning of flower petals stained for GUS expression showed that all six promoter deletion constructs were able to drive GUS expression in the inner and outer epidermis of the petals tissue (example shown in Figure 4.4B). GUS expression was also observed in the vascular tissue. pPN 252, which contains 151 bp of the *rosea1*^{dorsea} promoter region, was capable of driving GUS expression in both the inner and outer epidermis of tobacco petals (Figure 4.4B). Table 4.3 contains the summary of results for the *rosea1*^{dorsea} promoter deletion analysis in tobacco plants. Appendix VIII contains detailed information on the GUS expression in individual lines containing the six *rosea1*^{dorsea} promoter deletion constructs.

Figure 4.3 Transient assay using particle bombardment transformation of rosea^{dorsea} antirrhinum petal (line #112) tissue using the *rosea1*^{dorsea} promoter deletion constructs.

pPN 195 construct (735 bp *rosea1*^{dorsea} promoter:GUS:OCS) was able to drive GUS expression in the inner (A) and outer (B) epidermis. pPN 212 (151 bp *rosea1*^{dorsea} promoter:GUS:OCS) was also able to drive GUS expression in the inner (C) and outer (D) epidermis.

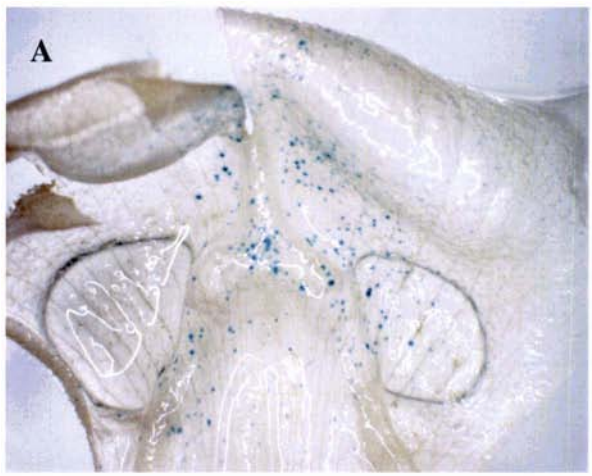
A

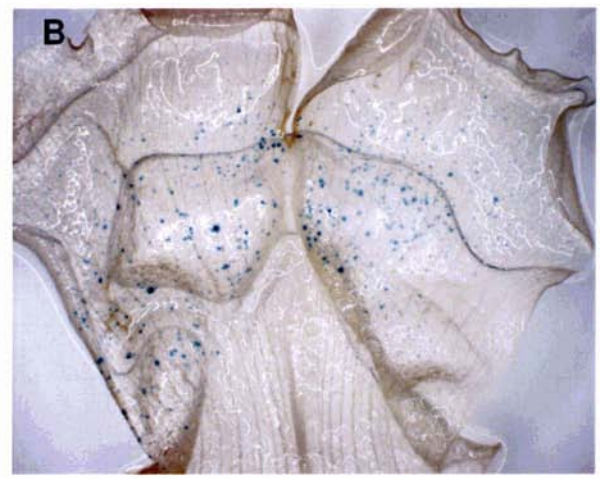
B

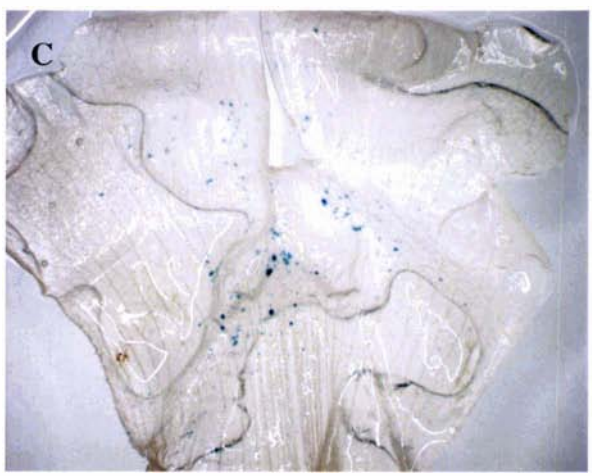
C


D

Table 4.2 GUS expression results of transient assays carried out on rosea[dorsea] antirrhinum petal (line #112) tissue using the *rosea1*[dorsea] promoter deletion constructs[a].

Vector	*rosea1*[dorsea] promoter size (bp)[b]	GUS expression[c]
pPN 195[d]	735	Yes
pPN 208	632	Yes
pPN 209	533	Yes
pPN 210	431	Yes
pPN 211[d]	279	Yes
pPN 212[d]	151	Yes

[a] These assays were conducted by Mr Michael Bennett and the tissue was observed by me to verify his results.
[b] Promoter size was determined from the NcoI site and includes the 5'UTR region.
[c] GUS expression in the inner and outer epidermis of the petal.
[d] I conducted additional transient assays with these constructs to verify the results obtained by Mr Michael Bennett.

4.3.2 Cloning of the *Rosea1* promoter region from different *Antirrhinum* species and accessions

PCR was successfully used to amplify the *Rosea1* promoter region from *A. majus* (*Barcelona*), *A. majus* (Toulouse), *A. australe*, *A. barrelieri*, *A. latifolium* (Julius), *A. molle*, *A. mollissimum*, *A. graniticum* and *A. siculum*. Table 4.4 shows the PCR results with different primers used.

The PCR products were cloned and sequenced. The sequence alignment between the promoter regions for *Rosea1* (line #522) and *rosea1*[dorsea] (line #112) alleles and the different *Antirrhinum* species and accessions, are given in Appendix IX, and Figure 4.5 gives a summary of the alignment results.

Sequence alignment results showed that the *Rosea1* promoter region from *A. majus* (Toulouse) and *A. graniticum* was identical to the wild type *Rosea1* sequence. *A. majus*

Table 4.3 GUS expression results of stable transgenic tobacco plants harbouring *rosea1*^{dorsea} promoter deletion constructs.[a]

Name of pART 27 based vector	*rosea1*^{dorsea} promoter size (bp)[b]	Number of transformants showing positive GUS expression[c]	Number of transformants showing no GUS expression[c]
pPN 247	700	11	3
pPN 248	632	6	6
pPN 249	533	8	0
pPN 250	431	4	1
pPN 251	279	7	5
pPN 252	151	5	8

[a] All the constructs were prepared by Mr Michael Bennett. Generation of stable transgenic tobacco containing all the constructs was also carried out by Mr Michael Bennett. I carried out the GUS analysis of all the plants.
[b] Promoter size was determined from the NcoI site and includes the 5'UTR region.
[c] GUS expression in the inner and outer epidermis of the petal.

(Toulouse) has medium intensity anthocyanin pigmentation and *A. graniticum* has very pale pigmentation /no pigmentation (Figure 4.2 H). The *Rosea1* promoter region from *A. majus* (Barcelona), *A. barrelieri, A. mollissimum* and *A. siculum* was similar in sequence to the wild type *Rosea1* promoter. The *A. majus* (Barcelona) *Rosea1* promoter sequence contained a five bp insertion as well as many sequence differences in the distal part of the promoter as well as in the region corresponding to the 187 bp region missing in the *rosea1*^{dorsea} promoter sequence. *A. majus* (Barcelona) flowers have medium intensity anthocyanin pigmentation. *A. barrelieri* had 13 single bp changes in the promoter region, of which seven were present in the 187 bp region missing in the *rosea1*^{dorsea} promoter. The *Rosea1* promoter from *A. mollissimum* and *A. siculum* contained 16 and 77 single base pair changes, respectively, of which 14 and 71 changes were seen in the 187 bp region missing in the *rosea1*^{dorsea} promoter. *A. barrelieri* flowers have strong background anthocyanin pigmentation (Figure 4.2C), whereas *A.*

Figure 4.4 GUS expression in petal tips of stably transformed tobacco harbouring a transgene containing the GUS reporter gene driven by 151 bp of the *rosea1*^{dorsea} promoter.

Strong GUS expression was observed in the petal tips (A). GUS expression was limited to the inner and outer epidermis of the petal tissue (B).

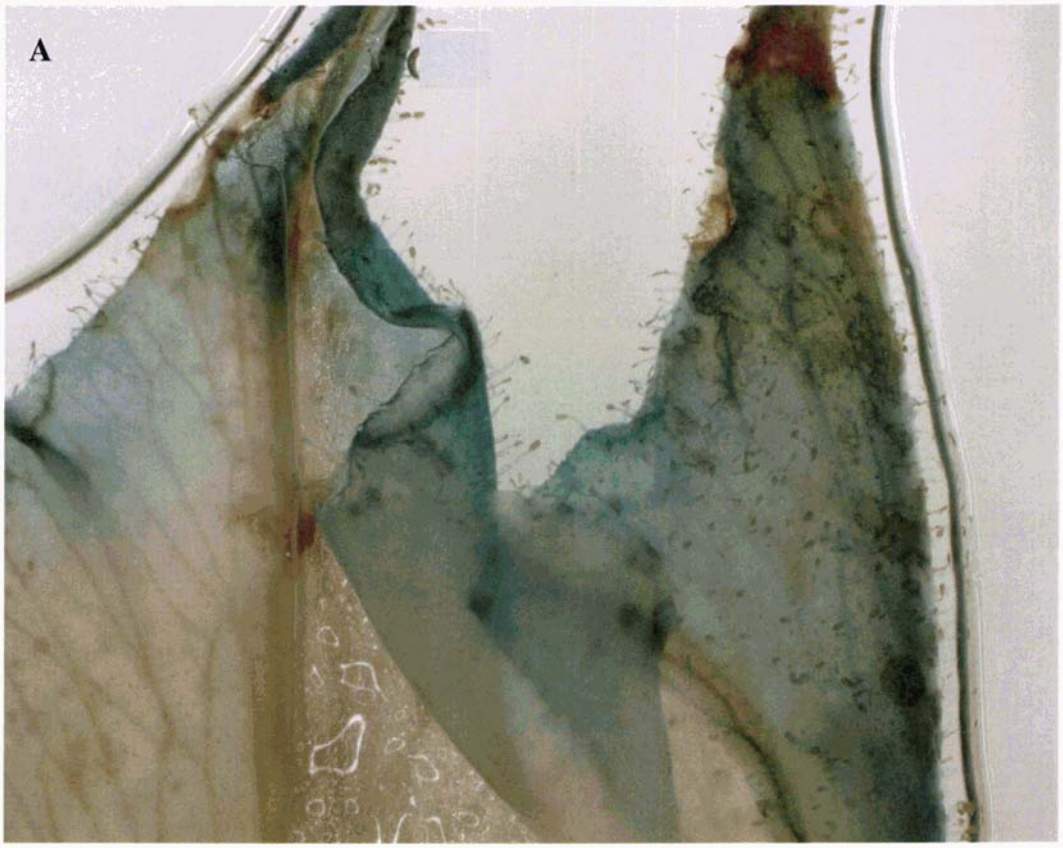
A

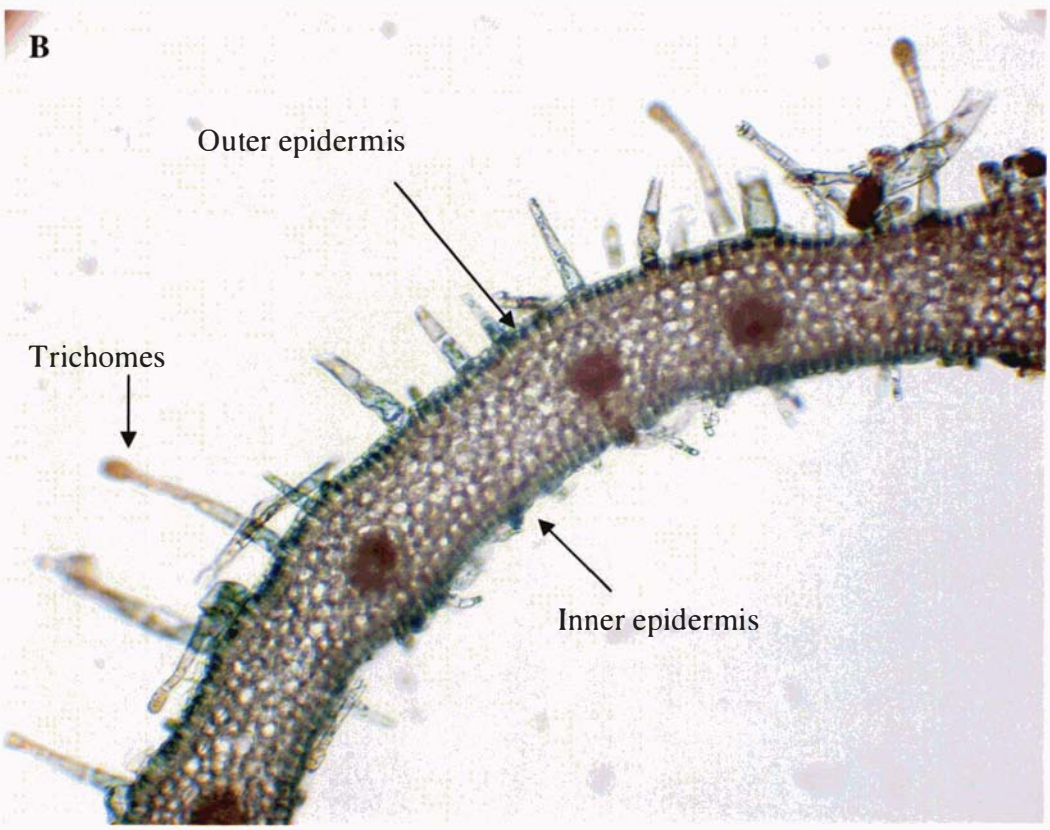
B
Outer epidermis
Trichomes
Inner epidermis

Table 4.4 Results of the PCR amplification of the *Rosea1* promoter region from different *Antirrhinum* species and accessions.

Species	Forward primer		
	K214	K215	K216
A. majus (Barcelona)	X	√	X
A. majus (Toulouse)	√	√	√
A. australe	√	X	X
A. barrelieri	√	√	X
A. latifolium (Julius)	X	√	X
A. molle	X	√	X
A. mollissimum	X	X	√
A. graniticum	√	X	X
A. siculum	X	√	X

√ - indicates that a PCR product was obtained using the forward primer and K181 reverse primer.
X – indicates that PCR was not successful using the forward primer and K181 reverse primer.

mollissimum and *A. siculum* (Figure 4.2F and 2, respectively) flowers have no background anthocyanin pigmentation.

Rosea1 promoter sequences from *A. latifolium* and *A. molle* were more similar to the *rosea1*^{dorsea} sequence than the wild type promoter sequence. In addition to the 187 bp deletion, *A. latifolium* also contained eight single bp changes as well as a 12 bp insertion in the distal part of the promoter. Flowers of *A. latifolium* have no background anthocyanin pigmentation (Figure 4.2D). *A. molle* also has no background anthocyanin pigmentation (Figure 4.2E), and contained six single bp changes, a 10 bp insertion and a single bp and a four bp insertion in its *Rosea1* promoter region. *A. australe* flowers have strong background anthocyanin pigmentation (Figure 4.2B). However, the *Rosea1* promoter region from *A. australe* was more similar to the *rosea1*^{dorsea} promoter and contained 12 single bp changes, the 187 bp deletion and the 12 bp insertion.

Figure 4.5 Graphical representation of the sequence alignment of the *Rosea1* promoter region from wild type (line #522), rosea^{dorsea} (line #112) and other *Antirrhinum* species and accessions.

The horizontal red line represents the 187 bp deletion present in the *Rosea1* promoter region in *rosea1*^{dorsea}, *A. australe, A. latifolium* and *A. molle.* Single base pair changes from the *Rosea1* promoter sequences are represented by red lines, and insertions and deletions are represented by green triangles. (some photos were adapted with permission from Dr Kathy Schwinn)

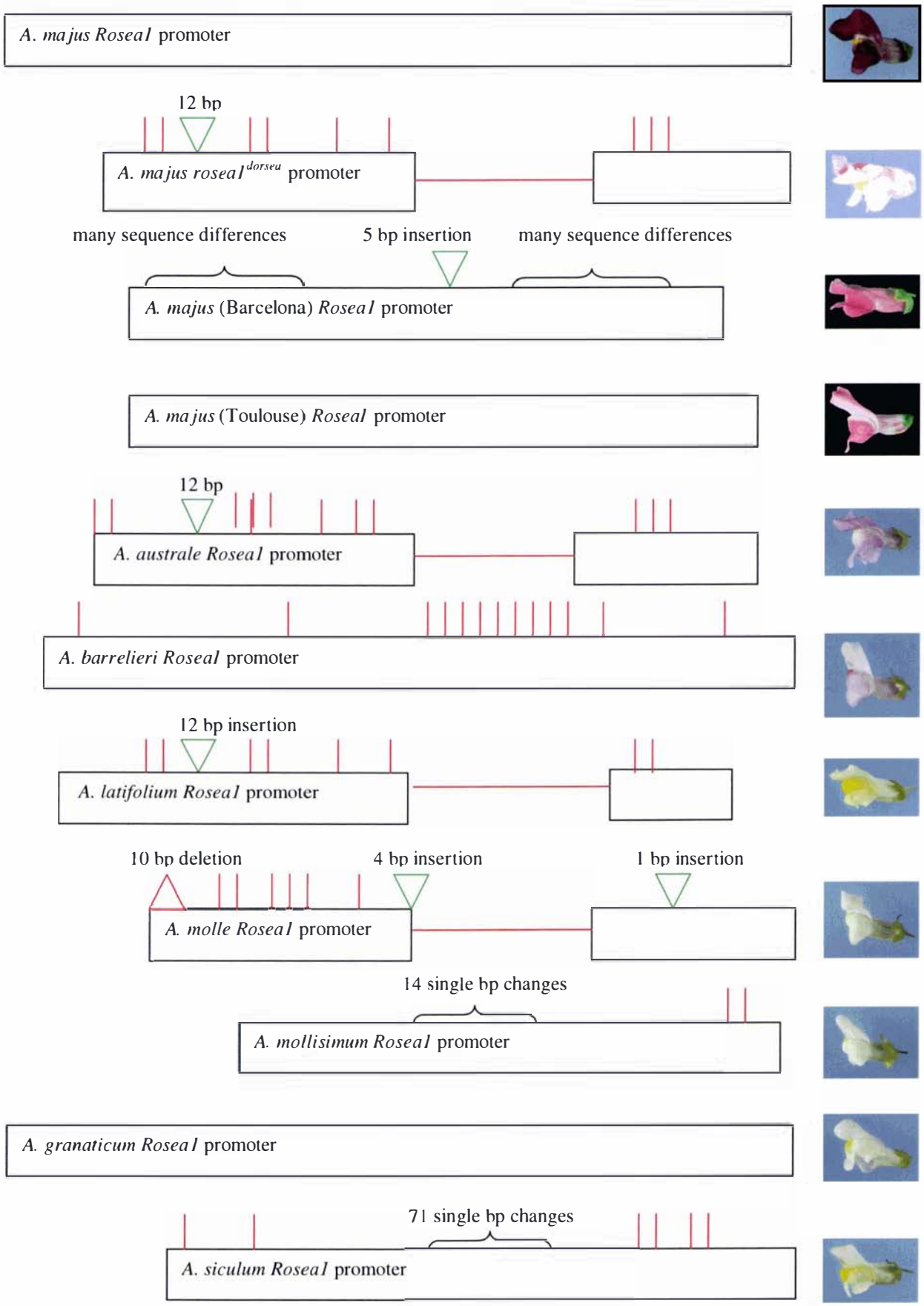
A. majus Rosea1 promoter
12 bp
A. majus rosea1 dorsea promoter
many sequence differences
5 bp insertion
many sequence differences
A. majus (Barcelona) Rosea1 promoter
A. majus (Toulouse) Rosea1 promoter
12 bp
A. australe Rosea1 promoter
A. barrelieri Rosea1 promoter
12 bp insertion
A. latifolium Rosea1 promoter
10 bp deletion
4 bp insertion
1 bp insertion
A. molle Rosea1 promoter
14 single bp changes
A. mollisimum Rosea1 promoter
A. granaticum Rosea1 promoter
71 single bp changes
A. siculum Rosea1 promoter

4.3.3 Cloning, characterising and testing the functionality of the *rosea1*^{dorsea} allele

The *rosea1*^{dorsea} allele was successfully amplified by PCR and was cloned into the pBluescript (KSII +) vector as described in Section 4.2.3. The sequence of the *rosea1*^{dorsea} allele was then compared to the *Rosea1* allele using the SeqMan (DNASTAR) programme. The sequence alignment between the *Rosea1* and *rosea1*^{dorsea} allele is given in Appendix X and Table 4.5 gives a summary of these results. The single bp changes within the coding region of the two alleles affected the identity of 11 deduced amino acids as described by Schwinn *et al.* (2006). The intron 1 of the *rosea1*^{dorsea} allele was the same length as the *Rosea1* intron 1 (231 bp) and contained a few sequence differences as well as single insertion and deletion events compared to the *Rosea1* intron 1 sequence. The intron 2 region of the *Rosea1* and *rosea1*^{dorsea} alleles contained many sequence differences as well as insertion and deletion events. The *Rosea1* intron 2 region was 1498 bp in length while the intron 2 region from *rosea1*^{dorsea} was smaller, being 1447 bp in length. It was also observed that neither of the *rosea1*^{dorsea} introns had sequence alterations near the intron/exon boundary, which could affect the splicing of the mRNA transcript.

Due to the sequence alterations present in the *rosea1*^{dorsea} allele, it was necessary to identify whether it still encoded a functional protein. To test this, the pPN 345 (700 bp *rosea1*^{dorsea} promoter:genomic *rosea1*^{dorsea}:OCS, Section 4.2.4) construct was used to transform *rosea1*^{dorsea} petal tissue by particle bombardment (Section 2.8). Transformed petals produced red-coloured foci in both epidermal layers, confirming that the *rosea1*^{dorsea} allele was indeed capable of producing a functional protein that can up-regulate the anthocyanin biosynthetic pathway. The number of anthocyanin-producing foci was similar to those obtained from using pPN 182 (900bp WT promoter:genomic *Rosea1*:OCS gifted by Dr Kathy Schwinn).

4.3.4 Analysis by promoter replacement of the importance to gene expression of the intron regions in *rosea1*^{dorsea}

pPN 371 (900 bp *Rosea1* promoter: genomic *rosea1*^{dorsea}:OCS) and pPN 182 (900 bp *Rosea1* promoter:genomic *Rosea1*:OCS constructs were used to transform both the inner and outer epidermis of rosea^{dorsea} petal tissue using particle bombardment. This experiment was carried out to analyse whether the intron regions of two *Rosea1* alleles, *Rosea1* and *rosea1*^{dorsea}, can confer spatial specificity of their expression. Both constructs gave a similar number of anthocyanin producing cells in inner and outer epidermis of the antirrhinum petal.

Table 4.5 Summary of sequence differences, insertions and deletions present between the *Rosea1 and rosea1*^{dorsea} alleles.

Region	Sequence differences	Insertions*		Deletions*	
Exon 1	1	0		0	
Intron 1	4	1 (1)		1 (1)	
Exon 2	0	0		0	
Intron 2	94	41 (1)	10 (2)	14 (1)	1 (3)
		1 (3)	1 (4)	1 (4)	2 (8)
		1 (6)	1 (7)	1 (12)	
		1 (18)		Total deletions =	
		Total insertions = 56		19	
Exon 3	11	0		0	

* The number within the parentheses indicates the number of nucleotide insertions/deletions i.e. (1) indicates a single bp insertion

4.3.5 *In situ* hybridisation

In situ hybridisation was carried out on both upper and lower lip tissue of stage 3, wild type and rosea^{dorsea} petal tissue (Figure 3.9A). The upper lip petal tissue of rosea^{dorsea}

showed transcripts of the *rosea1*^{dorsea} allele in both the inner and outer epidermis (Figure 4.6A and B). The upper lip petal tissue in this mutant produces anthocyanin pigments only in the outer epidermal layer. The lower lip tissue of rosea^{dorsea} petal does not produce anthocyanin pigments. However, the *rosea1*^{dorsea} transcript was seen in both epidermal layers of this tissue as well (Figure 4.6C and D). The *rosea1*^{dorsea} allele had the same spatial expression pattern as the *Rosea1* allele. The transcript abundance of the *rosea1*^{dorsea} allele in both the upper and lower lip tissue was much weaker compared to the expression of the *Rosea1* allele in the wild type tissue. *Rosea1* expression was also observed in the vascular tissue of both wild type and rosea^{dorsea} petal tissue.

4.3.6 Bioinformatic analysis

The 151 bp of the proximal region of the *rosea1*^{dorsea} promoter region was analysed for putative *cis*-elements using the PLACE database to see whether additional/different *cis*-elements might be present in this region compared to the *Rosea1* promoter. Figure 4.7 shows the results of the PLACE database analysis. The region between 151 bp and the putative TATA-box contained an additional DOF-binding site compared to the *Rosea1* promoter.

Both intron 1 and intron 2 regions from *rosea1*^{dorsea} allele were also analysed for putative *cis*-elements using the PLACE database. Intron 1 had the same putative *cis*-elements as those predicted for the *Rosea1* intron 1. The intron 2 region of the *rosea1*^{dorsea} allele contained different putative *cis*-elements from those predicted to be present in the *Rosea1* intron 2.

4.4 Discussion

One of the major objectives in this project was to analyse whether differences in the promoter of the *rosea1*^{dorsea} allele, compared to the *Rosea1* promoter, are responsible for the rosea^{dorsea} phenotype. The effect of the 187 bp deletion, 141 bp proximal to the translation start site, was the first difference investigated (Figure 4.1).

Promoter deletion analysis carried out on the 700 bp *rosea1*^{dorsea} promoter region showed that the proximal -151 bp of the promoter region [the region -141 bp upstream of the transcription site plus ten nucleotides after the site of the deletion (Figure 4.1)] was able to drive GUS expression in antirrhinum and tobacco petal tissue. This 151 bp region of the *rosea1*^{dorsea} promoter maintained epidermal and petal specificity and drove reporter gene expression in both the inner and outer epidermis of antirrhinum and tobacco petals, a characteristic of the wild type *Rosea1* promoter. The ability of this region to still drive reporter gene expression in both the inner and outer epidermis indicates that the 187 bp deletion in the *rosea1*^{dorsea} promoter region is not essential for the expression of the gene and is not responsible for the rosea^{dorsea} phenotype. There are only four single bp changes from -1 to -141 bp of the *rosea1*^{dorsea} and *Rosea1* promoter. All four changes occur in the 5' UTR of the promoter. Therefore, the differences in the *rosea1*^{dorsea} promoter are unlikely to confer the rosea^{dorsea} phenotype.

This conclusion was further supported by the analysis of the *Rosea1* promoter region from different *Antirrhinum* species and accessions. These different *Antirrhinum* species and accessions had varying levels of anthocyanin pigmentation intensity and patterning. No previous sequence data on the *Rosea1* promoter was available for these species and accessions which led to difficulty in designing primers for cloning. Degenerate PCR primers could not be used for the same reason. It was hoped that of three different forward primers, initially used for generating the *Rosea1* promoter deletion constructs, at least one would anneal to the different *Rosea1* promoter regions of these species and accessions. This method was successful at amplifying varying lengths of the *Rosea1* promoter regions from the species and accessions listed in Table 4.4. Their sequences were then compared against the *Rosea1* (line # 522) and *rosea1*^{dorsea} (line # 112) promoter sequence. Sequence analysis showed that the *Rosea1* promoter region from pigmented (medium-level pigment intensity) accessions of *A. majus* (Toulouse) and *A. majus* (Barcelona), and *A. barrelieri* (strong background anthocyanin colouration) have identical or very similar sequences to the wild type *Rosea1* promoter sequence. However, some species such as *A. mollissimum* and *A. siculum* with either very pale

Figure 4.6 *In situ* hybridisation on stage 3 (10-15 mm) wild type (line #522) and rosea^{dorsea} (line #112) antirrhinum petal tissue.

All sections are transverse sections through the lobe region (cutting plane is indicated in Figure 3.9A). Wild type upper lip petal tissue (A) showed higher levels of *Rosea1* transcript abundance compared to rosea^{dorsea} upper lip petal tissue (B). Higher amounts of *Rosea1* transcript was also seen in the lower lip tissue of wild type flower petals (C) in comparison to rosea^{dorsea} lower lip petal tissue (D). In all cases *Rosea1* transcript was observed to be in epidermal layers and also in the vascular tissue.

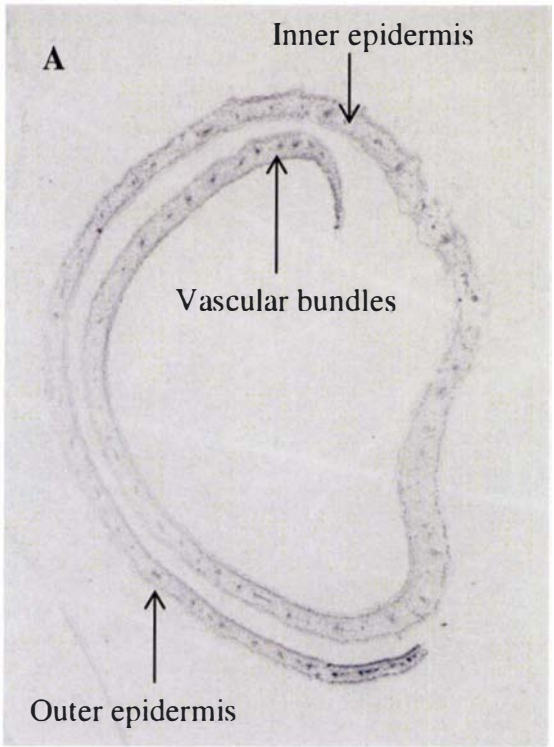
A
Inner epidermis
Vascular bundles
Outer epidermis

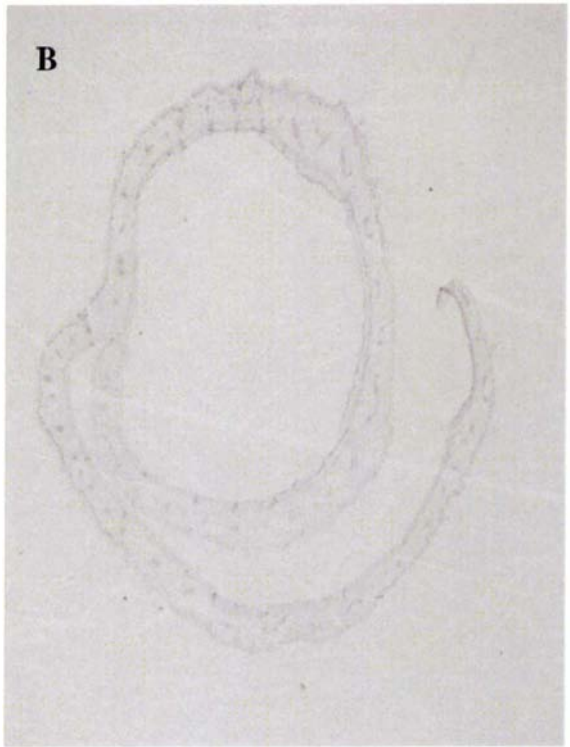
B

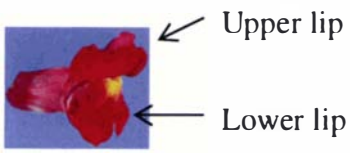
Upper lip
Lower lip

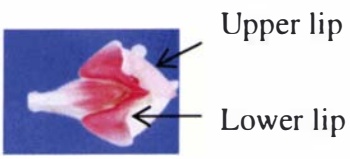
Upper lip
Lower lip

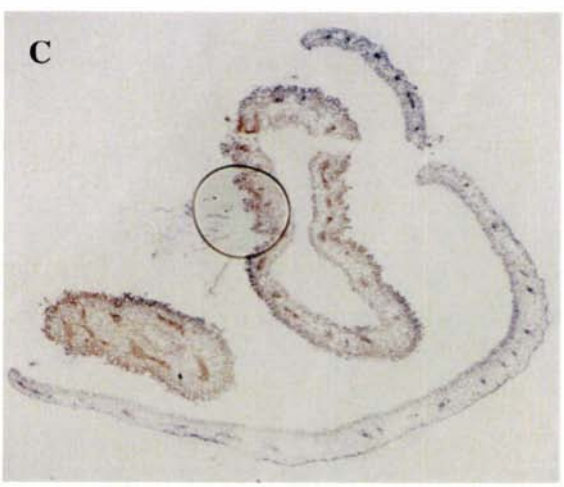
C

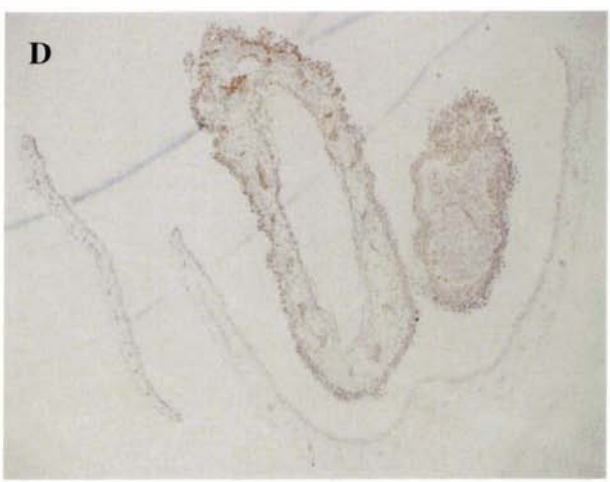
D

AGAGCC[redacted]GGGTCTACAGCCATAAAAAGGCCTATTTAAATCCGTGAAAGT
TTCGCTTAAGGGGTACTCATTAAAAAAAGGGAAAGAGCAGCTAGACATGAGT
TTTCTGTTTTGACACTTTTAACGAACGGGCATAGTACGTATTAAACGCCATAG
G

Figure 4.7 PLACE database analysis of the proximal 151 bp region of the *rosea1*^{dorsea} promoter.

The putative TATA-box is highlighted in green. The putative DOF-binding site common to both *Rosea1* and *rosea1*^{dorsea} is underlined while the unique DOF-binding site is highlighted in red.

anthocyanin pigmentation or no background anthocyanin pigmentation also had sequences similar to the wild type *Rosea1* promoter. These weakly pigmented antirrhinum species show a rosea^{dorsea}-like phenotype in their lobe tissue (Prof. Cathie Martin, personal communication). While the F1 progeny obtained from crosses between wild type *A. majus* and *A. mollissimum* gave fully coloured flowers, crosses of *A. mollissimum* to rosea^{dorsea} mutants were unable to complement pigmentation (Schwinn *et al.*, 2006). This lack of complementation indicated that changes at the *Rosea* locus were responsible for the weak pigmentation in this species. The fact that *A. mollissimum* contains a wild type-like *Rosea1* promoter region indicates that changes in the actual ROSEA1 protein might be responsible for the weak pigmentation phenotype rather than a promoter change causing changes in the transcription of the *Rosea1* gene in this species.

The *Rosea1* promoter sequences of *A. latifolium* and *A. molle* were more similar to the *rosea1*^{dorsea} sequence than the wild type promoter sequence. The flowers of both these species have no background anthocyanin pigmentation. The F1 progeny obtained from crosses between wild type *A. majus* and *A. latifolium* and wild type *A. majus* and *A. molle* gave fully coloured flowers, while crosses of either species to rosea^{dorsea} mutants were unable to complement pigmentation (Schwinn *et al.*, 2006). This result indicates that changes in the *Rosea* locus are responsible for their lack of background pigment production.

The *Rosea1* promoter region from *A. australe* was also similar to the *rosea1*^{dorsea} promoter sequence. The flowers of *A. australe* have strong background anthocyanin pigmentation. The fact that *A. australe*, which can produce fully pigmented flowers, still contains a promoter sequence similar to *rosea1*^{dorsea} allele confirmed that the changes in this promoter were not responsible for the rosea^{dorsea} phenotype. These data further support the suggestion that the large 187 bp deletion in the proximal region of the *rosea1*^{dorsea} promoter does not affect the expression of the *rosea1* gene, as *A. australe* can produce fully pigmented flowers despite the fact that it has a *rosea1*^{dorsea}-like promoter region.

Previous studies by Schwinn *et al.* (2006) showed that the *Rosea1* cDNA from the rosea^{dorsea} mutant has several bp changes compared to that of the wild type cDNA, which leads to a total of eight amino acid changes in the deduced peptide. Comparison of these changes to the other two MYB factors regulating anthocyanin biosynthesis in antirrhinum, ROSEA2 and VENOSA, indicated that these changes were unlikely to contribute to the rosea^{dorsea} phenotype. However, there was no experimental evidence available on the functionality of the ROSEA1 protein in rosea^{dorsea} mutants. To test the functionality of the ROSEA1 protein in rosea^{dorsea} mutants, the full genomic sequence of *rosea1*^{dorsea} allele was successfully cloned and sequenced. The functionality of the ROSEA1 protein encoded by the *rosea1*^{dorsea} allele was tested by transient assays where the *rosea1*^{dorsea} allele driven by a fragment of its native promoter was introduced to both the inner and outer epidermis of the petal tissue from rosea^{dorsea} mutants. This construct was able to upregulate anthocyanin production in both epidermal layers of the rosea^{dorsea} mutant petal tissue to the same extent as the wild type *Rosea1* allele. This indicated that the *rosea1*^{dorsea} allele indeed encodes for a fully functional protein. The changes within the *rosea1*^{dorsea} allele do not seem to confer the rosea^{dorsea} phenotype, as anthocyanin production was upregulated in the inner epidermis as well as the outer epidermis by this construct.

The sequence of intron 1 in the *rosea1*^{dorsea} allele was similar to that of the *Rosea1* allele. However, intron 2 had many sequence differences including insertions and deletions. Bioinformatic analysis of the intron 2 region indicated that the putative *cis*-elements present in the *rosea1*^{dorsea} allele were quite different from those present in the *Rosea1* allele. Promoter replacement experiments were carried out using biolistics to see whether differences in the intron regions might confer the rosea^{dorsea} phenotype. The pPN 371 construct which has the cassette of 900 bp of the *Rosea1* promoter:genomic *rosea1*^{dorsea}:OCS, gave a similar number of anthocyanin producing foci as the pPN 182 construct (900bp *Rosea1* promoter:genomic *Rosea1*:OCS) in both the inner and outer epidermis of rosea^{dorsea} petals.

In situ hybridisation experiments carried out on stage 3 rosea^{dorsea} petal tissue showed that the spatial expression of the *rosea1*^{dorsea} allele was similar to *Rosea1*. The *rosea1*^{dorsea} allele was transcribed in both the inner and outer epidermis of the upper lip petal, which produces anthocyanin pigments in the outer epidermis only (i.e. rosea^{dorsea} phenotype); it was also transcribed in both epidermal layers of the lower lip petal tissue, which does not produce anthocyanin pigments. These results show that the *rosea1*^{dorsea} promoter is capable of driving the transcription of the *rosea1*^{dorsea} allele in the rosea^{dorsea} background. However, the transcript level of the *rosea1*^{dorsea} allele in rosea^{dorsea} petals was much weaker in comparison to that of *Rosea1* transcript levels. This may be due to changes that occur in intron 2 of the *rosea1*^{dorsea} allele such as the absence of potential MADS box binding sites (Appendix X). For instance, these changes might affect the stability of the mRNA transcript or even the expression level of the actual *rosea1*^{dorsea} allele itself (Larkin *et al.*, 1993; Chen *et al.*, 1998; Deyholos and Sieburth, 2000; Jeon *et al.*, 2000).

The promoter replacement experiments argue against the expression of the allele being affected by the intron sequences. However, these results might be an actual artifact of the biolistic experiment. In this method, large numbers of the reporter construct are introduced into single cells and, therefore, allow much higher levels of expression of the introduced gene compared to its normal expression level in the *in vivo* situation (Mehlo *et al.*, 2000; Dai *et al.*, 2001; Shou *et al.*, 2004). Hence, this might over-ride the effects of the intron regions on expression of the *rosea1*^{dorsea} allele. The strength of the GUS expression in the transient and stable promoter deletion assays also supports the notion that intron regions of the *rosea1*^{dorsea} allele might be affecting mRNA expression or stability. GUS expression in petals harbouring the various *rosea1*^{dorsea} promoter deletion constructs were similar to those harbouring the *Rosea1* promoter deletion constructs. The expression cassettes consisted of promoter:GUS:terminator and did not contain the different intron regions of the *Rosea1* alleles negating their effects on expression. To define the role of intron 2 in transcript expression/stability, GUS reporter genes containing these different allelic introns could be used in stable and transient experiments and expression observed. Alternatively the native *Rosea1* alleles could have their introns swapped and their affects on expression could be analysed in a similar way.

Chapter 5: Analysis of the regulation of *Rosea1* gene expression by the *Deficiens* gene

5.1 Introduction

The class-B function MADS-box gene, *Deficiens,* plays an important role in antirrhinum flower development by establishing petal and stamen identity during early flower development. In this Chapter the role of the *Deficiens* gene in anthocyanin pigment formation in antirrhinum flowers was investigated. Two approaches were used to provide evidence of the requirement of *Deficiens* activity for *Rosea1* expression. Firstly, bioinformatics-based methods were used to identify putative DEFICIENS binding sites in the promoter and intron regions of the *Rosea1* and *rosea1*^{dorsea} alleles. The effect of mutating/deleting the putative DEFICIENS-binding sites were then analysed by biolistic assays. Secondly, two methods were used to study the impact of a loss of *Deficiens* expression on anthocyanin pigment production: RNAi was used to silence *Deficiens* expression in young antirrhinum flower buds using a transient technique (Shang, *et. al.,* 2007) and the phenotype of the *Deficiens* RNAi tissue was compared to that of the deficiens^{chlorantha} mutant using microscopy techniques.

In situ hybridisation analysis of *Deficiens* gene expression has shown that the transcript is present in the petal and sepal primordia at very early stages of flower development. In the petal tissue, expression of *Deficiens* continues at a constant level right throughout the whole period of flowering, well after organ identity has been established (Schwarz-Sommer *et al.*, 1992; Zachgo *et al.*, 1995). Analysis of *A. majus* deficiens mutants as well as petal tissue derived from periclinal chimeras of *deficiens* have shown that proper expression of *Deficiens* is also essential for the establishment and maintenance of the petal identity of the epidermal cells (Schwarz-Sommer *et al.*, 1992; Zachgo *et al.*, 1995; Perbal *et al.*, 1996). For example, the petal tissues of deficiens null mutants (deficiens^{gli}) are morphologically identical to sepal tissue except for their increased size and their position within the flower (Schwarz-Sommer *et al.*, 1992). Petal tissues of deficiens^{chlorantha} and deficiens-101 mutants also have sepaloid petals providing further

evidence that proper expression of *Deficiens* is essential for the establishment of petal cell identity (Schwarz-Sommer *et al.*, 1992; Zachgo *et al.*, 1995). Analysis of periclinal chimeras of *deficiens* by Perbal *et al.* (1996) showed the development of chlorophyll containing epidermal cells in the petal tissue, indicating the requirement of DEFICIENS activity for maintenance of the petal cell identity. Although the early functions of *Deficiens* are well characterised, less is known about its possible roles in regulating processes in the later stages of flower development, such as anthocyanin pigmentation. This work was aimed at filling this knowledge gap.

5.2 Materials and Methods

5.2.1 Bioinformatics

Both intron 1 and intron 2 sequences, the 189 bp of the proximal region of the *Rosea1* promoter and 151 bp of the proximal region of *rosea1*^{dorsea} promoter were analysed for putative MADS-box binding sites using the PLACE database as described in Section 3.2.4.

5.2.2 Deletion of the intron 2 region of *Rosea1* and expression vector construction

A vector, named pNNP.WT.Int2.Del was constructed that contained 0.9 kb of the *Rosea1* promoter and all of the *Rosea1* gene excluding the region of intron 2 that contains two putative MADS-box binding sites (Figure 5.1). Two primers, WT.Int2.Rev and WT.Int2.Fwd were designed (with 5′ XbaI sites) to PCR amplify 0.9 kb of the *Rosea1* promoter region and all of the *Rosea1* gene except for part of intron 2 harbouring the putative MADS box-binding site using the K180.Fwd (designed with a 5′ SacI site) and K183.Rev (designed with a 5′ BamHI) primers with pPN 182 (900 bp *Rosea1* promoter:*Rosea1* gene:OCS) as the template. 1124 bp of the 1498 bp region encoding the *Rosea1* intron 2 sequence was removed by this method. PCR with WT.Int2.Rev and K180.Fwd was used to amplify the *Rosea1* promoter, exons 1 and 2, intron 1 and

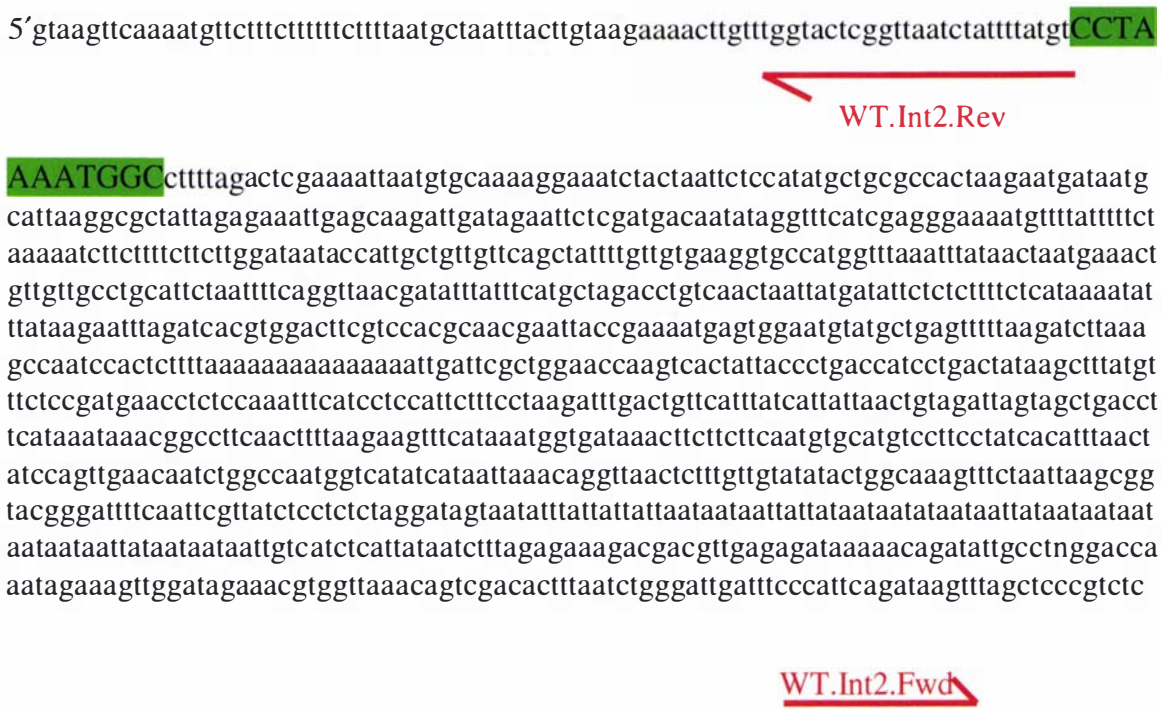

Figure 5.1 Sequence of the intron 2 region of the *Rosea1* allele and the location of the two putative MADS box protein binding sites.

The two regions highlighted in green are the putative MADS-box protein-binding sites. Binding sites for WT.Int2.Rev and WT.Int2.Fwd primers are shown in red.

proximal part of intron 2 as a SacI/XbaI fragment and PCR with WT.Int2.Fwd and K183.Rev was used to amplify the distal part of intron 2 and exon 3 as a second PCR fragment with XbaI/BamHI sites. PCR was carried out using Pwo polymerase (Roche Diagnostics) essentially as described in Section 2.4 with an annealing temperature of 55°C. The two PCR products were digested with SacI/XbaI and XbaI/BamHI, respectively (Section 2.2.3). A triple ligation reaction (Section 2.2.8) was then used to insert the two PCR fragments into pART 7 (Appendix II) that had been digested with SacI/BamHI. Transformation of the ligation products and selection of positive clones were carried out essentially as described in Section 2.3.3.

5.2.3 Mutation of a site similar to a MADS box binding site in the *Rosea1* promoter and expression vector construction

A region with close similarity [C(A/T)$_7$G] to a MADS-box binding site [C(A/T)$_8$G], present in the *Rosea1* promoter (shown in Figure 3.1), was mutated by PCR linker scanning mutagenesis essentially as described in Section 3.2.3. Primers (MADS.Fwd and MADS.Rev, Appendix III) designed with a 5′ BamHI site followed by two mutated bp in each of the forward and reverse primers was used to replace the 10 bp region the *Rosea1* promoter using PCR. The 10 bp region of the *Rosea1* promoter, with similarity to a MADS box binding site, was replaced with the AGGGATCCCT sequence in the mutant construct. The 10 bp mutated region was constructed in the context of the 289 bp of the *Rosea1* promoter using K268.Fwd and K181.Rev primers. A reporter construct with the mutated promoter region driving the GUS reporter gene (ALS.MADS) was constructed by triple ligation of the two PCR products as described in Section 3.2.3.

5.2.4 *Deficiens* RNAi vector construction

5.2.4.1 *Deficiens* inverted NOS construct

The initial *Deficiens* RNAi experiments were carried out using an inverted NOS approach as only a single ligation event is required allowing rapid construct generation for the experiment (Brummell *et al.*, 2003). Def.RNAi.Fwd and Def.RNAi.Rev primers

(Appendix III) were designed to amplify 0.5 kb of the *Deficiens* cDNA from pJAM 1182 plasmid (Appendix II). PCR using Taq polymerase (Section 2.4) was successfully used to amplify the correct sized fragment. The purified PCR product (Section 2.2.9.2) was then ligated into pDAH1 vector (Shang *et al.*, 2007) that had been digested with XcmI and dephosphorylated (Sections 2.2.3 and 2.2.6.2, respectively). Novablue cells were transformed with the ligation reaction as described in Section 2.3.2 and plated on LB ampicillin (100 $mgmL^{-1}$) plates. Positive clones were selected by digesting plasmid DNA with BamHI and XbaI and verified by sequencing with the 35S primer (Appendix III). The resulting plasmid containing *Deficiens* cDNA fragment driven by the 35S promoter was named pNNP.Def.RNAi.

5.2.4.2 *Deficiens* hairpin construct

Def.Hairpin.Fwd and Def. Hairpin.Rev primers, designed to generate a 5' XbaI and a 3' BamHI site (Appendix III), were used to amplify 0.45 kb of the *Deficiens* cDNA from pJAM 1182 plasmid using Taq polymerase (Section 2.4). The purified PCR product was digested with XbaI and BamHI and ligated into pDAHCROP 13 vector (Appendix II) that had been digested with XbaI and BglII (compatible with BamHI). Novablue cells were transformed and selected using ampicillin as described in Section 2.3.2 and 2.3.3, respectively. Positive clones were identified using XbaI and BamHI digestion of the plasmid DNA followed by sequencing with the 35S primer (Appendix III). The resulting plasmid containing *Deficiens* cDNA in the sense orientation driven by the 35S promoter was then digested with BamHI and NheI (compatible with XbaI). A second ligation reaction was used to introduce *Deficiens* cDNA (digested with XbaI and BamHI) in the antisense orientation to this vector to generate the hairpin construct. This hairpin construct was named pNNP.Def.Hairpin (Appendix II).

5.2.5 Transient transformation of antirrhinum buds with the RNAi constructs

The method developed by Shang *et al.* (2007) was used for transformation of 5 mm length, un-pigmented, wild type antirrhinum buds (line #522) with the RNAi constructs.

The sepals were dissected and the buds were surface sterilised by washing in 10% (v/v) bleach solution supplemented with a few drops of Tween-20 for 10 min. Buds were then rinsed 3 x with sterile water. The buds were placed on the center of tubs containing media 2 (Section 2.8) and bombarded using the conditions described in Section 2.8. Each bud was shot on the top and on the sides eight times for the transient transformation of the immature petal tissue. Un-shot buds and buds shot with gold preparation without any plasmid DNA were used as negative controls for each experiment. The petiole of the flower buds were embedded into fresh media 2 and the buds allowed to develop in a tissue culture room set to 22-26°C under 16/8 h light/dark photoperiod, with 35 mmolm^{-2}s^{-1} cool white fluorescent light.

5.2.6 Scanning electron microscopy

The inner epidermis of the antirrhinum deficiens^{chlorantha} petal tissue (Schwarz-Sommer *et al.*, 1992) was observed using a CamScan mark IV scanning electron microscope with a Hexland cryostage (Oxford Instruments, Oxford, UK) at the John Innes Centre with the help of Prof. Cathie Martin. The deficiens^{chlorantha} petal tissue was quickly dissected by hand under a light microscope and rapidly frozen in liquid N_2 slush. Dissected tissue was sputter coated with 25 nm gold and then observed whilst being maintained in its frozen state on the cold stage of the SEM. Images were recorded at 16 kV using Ilford FP120 roll film.

Petal tissue from the RNAi experiment was fixed and analysed with the help of Mr Doug Hopcroft at the Manawatu Microscopy & Imaging Centre at Massey University. Tissue was fixed in 3% (v/v) glutaraldehyde and 2% (v/v) paraformaldehyde in 0.1 M phosphate buffer. Samples were dehydrated in acetone, critical-point dried in liquid CO_2 and sputter coated with 25 nm gold using a Polaron E 5400 sputter coater (SCD-050; Bal-Tec, Balzers, Liechtenstein). Specimens were examined on a Cambridge 250 Mark III scanning electron microscope (Cambridge Instruments, Cambridge, UK) operated at 20 kV, and images were captured on 35 mm film.

5.3 Results

5.3.1 Bioinformatics

Analysis of the *Rosea1* and *rosea1*^{dorsea} proximal promoter regions (-189 bp and -156 bp region, respectively) and intron 1 sequences using the PLACE database showed no sequences exactly matching the known MADS-box protein binding sites (called CArG boxes). However, two CArG boxes [CC(A/T)$_6$GG and C(A/T)$_8$G] were found in the intron 2 sequence of the *Rosea1* gene but not that of *rosea1*^{dorsea} (Figure 5.1). A MADS box-like site that had some, but not all of common nucleotides [C(A/T)$_7$G], was present in the proximal region of both *Rosea1* and *rosea1*^{dorsea} promoters (Figure 3.1). PCR linker scanning mutagenesis (Section 5.2.3) was used to analyse the importance of this site for *Rosea1* expression, the results of which are discussed in Section 5.3.3.

5.3.2 Intron 2 deletion analysis

Transient assays (Section 2.8) were carried out in rosea^{dorsea} (line #112) antirrhinum petals using the pNNP.WTInt2.Del construct to analyse the importance of the two putative MADS-box protein binding sites of intron 2 for *Rosea1* expression. pPN 182 (900 bp *Rosea1* promoter:*Rosea1* gene:OCS) was used as a positive control for this experiment. After two days the petal tissue was observed for the production of pigmented foci. It was observed that the expression of *Rosea1* from the pNNP.WTInt2.Del construct was similar to that obtained from the full-length gene. Furthermore, this construct was able to drive pigment production in both inner and outer epidermis of antirrhinum petal tissue.

5.3.3 Mutation analysis of a site similar to a MADS box binding site in the *Rosea1* promoter

Transgenic tobacco flowers harboring the ALS.MADS construct were analysed for GUS expression. The temporal and developmental GUS expression pattern in flowers

ranging in size from 1.5 - 7 cm was analysed by light microscopy (Section 2.12). Seven out of the eighteen individual lines that were analysed showed positive GUS expression. The GUS expression patterns and intensity in these lines were similar to those obtained with the *Rosea1* and *rosea1*^{dorsea} promoter deletion constructs, with intense GUS staining in the tips of the flower petals, the lower half of the tube region and in vascular tissue.

5.3.4 RNAi

The inverted NOS construct, pNNP.Def.RNAi (Section 5.2.5.1), was initially used for RNAi of the *Deficiens* gene in wild type antirrhinum buds using transient transformation (Section 5.2.6). This construct uses a hairpin of the transcript terminator region (NOS) for easier construct generation. Developing flower buds and petals were observed daily for morphological changes over a two week period. Developing flower buds and petal tissue showed wild type-like pigmentation and morphology and no alteration to pigmentation patterning was observed.

The hairpin *Deficiens* RNAi construct, pNNP.Def.Hairpin (Section 5.2.5.2), was then used to transform wild type antirrhinum buds (Section 5.2.6). This construct would generate hairpin RNA of the *Deficiens* transgene. Un-shot buds and buds shot with gold-only preparation served as controls. Both controls developed into wild type-like flowers with normal pigmentation. Transformed flower buds were observed daily for about three weeks for alteration in their pigmentation pattern (Figure 5.2). Aas the flower petals shot with the pNNP.Def.Hairpin developed, areas of reduced/no anthocyanin pigmentation was apparent. This alteration of pigmentation was observed in both the outer epidermis and inner epidermis (Figure 5.3A & B). Furthermore, the areas with reduced/no anthocyanin pigments started accumulating chlorophyll pigments leading to greening of these areas (Figure 5.3C). The areas accumulating chlorophyll pigments showed red auto-fluorescence under UV light (Figure 5.3D). The un-shot buds and buds shot with gold-only preparation did not show any of these phenotypes and had fully pigmented inner and outer epidermal tissue.

The pPN283 (*CHS* inverted NOS construct) was used as the positive control for the RNAi assays. RNAi of the *CHS* gene led to regions in the petal tissue where anthocyanin pigments were not produced leading to white patches in the petals, in comparison to the fully pigmented phenotype of wild type tissue (Figure 5.4A). The white patches were present in both the outer and inner epidermis similar to the phenotype obtained with the *Deficiens* RNAi. It was noted that the areas of reduced pigmentation obtained with RNAi of *CHS* gene were much whiter compared to those obtained from *Deficiens* RNAi, which were more greenish-brown in colour (Figure 5.4 B).

SEM analysis was performed on areas of the RNAi tissue that had reduced/ no anthocyanin pigmentation to observe if other morphological alterations were present. The SEM photographs are presented in Figure 5.5. The anthocyanin-containing border sectors of the sections had conical cells, typical of wild type inner epidermal petal tissue (Figure 5.5A). However, the areas that had reduced/ no anthocyanin pigments had flat inner epidermal cells (Figure 5.5B &C). SEM analysis was carried out on petal tissue of wild type, 5 mm antirrhinum buds (i.e. the stage when they are normally biolistically transformed). The epidermal petal cell shape at this stage was observed to be almost flat-shaped, although the cells were beginning to develop a slightly conical shape (Figure 5.5D).

Light microscopy and SEM analysis were carried out on deficiens^{chlorantha} petals (phenotype is described in Section 1.6) to see whether morphological alterations similar to those seen in the *Deficiens* RNAi tissue were present in this tissue. Light microscopy showed that areas of the petal tissue, where *Deficiens* activity was lacking, had chlorophyll-containing, green inner epidermal cells (Figure 5.6A) similar to that of the *Deficiens* RNAi tissue (Figure 5.4B). SEM analysis of the same region revealed that the inner epidermal cells in the areas lacking *Deficiens* activity were flat (Figure 5.6B) like the *Deficiens* RNAi tissue (Figure 5.5 B and C). These mutant cells were bordered by wild type, anthocyanin-containing cells expressing *Deficiens*. SEM analysis of the wild type sectors of the deficiens^{chlorantha} petal showed the presence of conical cells in these

areas (Figure 5.6B). In the deficiens^{chlorantha} petal tissue, the sectors that were lacking *Deficiens* activity contained trichomes, unlike the *Deficiens* RNAi tissue.

5.4 Discussion

A major objective in this project was to analyse the role of the *Deficiens* gene in regulating anthocyanin pigmentation in antirrhinum flowers. It was hypothesised that *Deficiens* may either function as a developmental trigger or act as a determinant of anthocyanin pigmentation patterning in the antirrhinum flowers.

Bioinformatics-based methods were used to analyse whether *Deficiens* was directly regulating *Rosea1* expression by binding to the regulatory regions of the *Rosea1* gene. Bioinformatic analysis of the proximal *Rosea1* and *rosea1*^{dorsea} promoter regions and the intron 1 of both alleles did not reveal any known MADS-box protein binding sites. However, two CArG boxes, which are known to bind MADS box proteins, were present in the intron 2 sequence of *Rosea1* but not in *rosea1*^{dorsea}. The pNNP.WTInt2.Del construct was used to analyse whether the absence of these two sites in intron 2 of *rosea1*^{dorsea} leads to the rosea^{dorsea} phenotype. This did not seem to be the case as removal of the two CArG boxes from the *Rosea1* intron 2 did not affect production of pigmented foci in the inner or outer epidermis of rosea^{dorsea} antirrhinum petals. However, it should be noted that transient assays using particle bombardment could lead to artifacts in the experiment. A major issue with biolistic transformation is that many copies of the transgene are introduced to a single cell (Mehlo *et al.*, 2000; Dai *et al.*, 2001; Shou *et al.*, 2004). This high copy number may override the true genetic regulation of the gene of interest (Dai *et al.*, 2001). Therefore, using this method it is rather difficult to assess the importance of single/few potential *cis*-elements for gene regulation. It was also observed that variation of transgene expression occurred within the replicate samples of a single experiment. Transgene expression using particle bombardment is dependent on many variables including the development stage of the tissue, the particle delivery method and the parameters used for the bombardment experiment (Nan and Kuehnle, 1995; Cai *et al.*, 1996). The optimal parameters for bombardment such as the helium pressure, target

distance and vacuum pressure were optimised for antirrhinum petal tissue. Although the optimal parameters were used it was difficult to ensure that all petals used for the transient assays were at stage 3. Also due to limited availability of flowers, petal tissue from different plants was used for the experiment. These two factors are likely to lead to sample-to-sample variation in the experiment. Thus, the results from these assays could not be quantified in a reliable fashion. Therefore, for future experiments, pNNP.WTInt2.Del construct should be co-bombarded with a second reporter construct that can be used to normalise for variability. This method has been used successfully to obtain quantitative data on transient assays using particle bombardment experiments conducted in soybean and maize seeds (Iida *et al.*, 1995; Grotewold *et al.*, 2000). A site very similar to a MADS-box protein binding site was present in both *Rosea1* and *rosea1*^{dorsea} promoters. Mutating this region did not affect GUS expression in tobacco flowers indicating that this site is unlikely to bind DEFICIENS.

RNAi was used to analyse the importance of the *Deficiens* gene for pigment formation in developing antirrhinum flowers. Initial RNAi experiments were conducted using an inverted NOS construct, pNNP.Def.RNAi. No affect on pigmentation was observed on the developing flowers that were transformed with this construct. RNAi from inverted NOS constructs can be sequence dependent i.e., some genes can be easily silenced by this method compared to others depending on the gene sequence that is used for generating the construct (Dr David Brummell, personal communication). Therefore, a second RNAi construct (pNNP.Def.Hairpin) to produce hairpin *Deficiens* mRNA was constructed, as hairpin of the target gene sequence directly is more efficient in gene silencing (Brummell *et al.*, 2003). RNAi experiments performed with this hairpin construct resulted in development of areas with reduced/no anthocyanin pigmentation in antirrhinum flower petals. This effect on pigmentation was observed in both the outer and inner epidermis. This indicated that the silencing signal was moving from the outer epidermis (biolistically transformed tissue) to the inner epidermis. The regions where *Deficiens* was silenced also produced chlorophyll leading to greening of these areas. Chlorophyll pigments (which are normally produced in the sepal tissue of the flower) were produced well after the petal identity had been established and demonstrated the developmentally flexible nature of

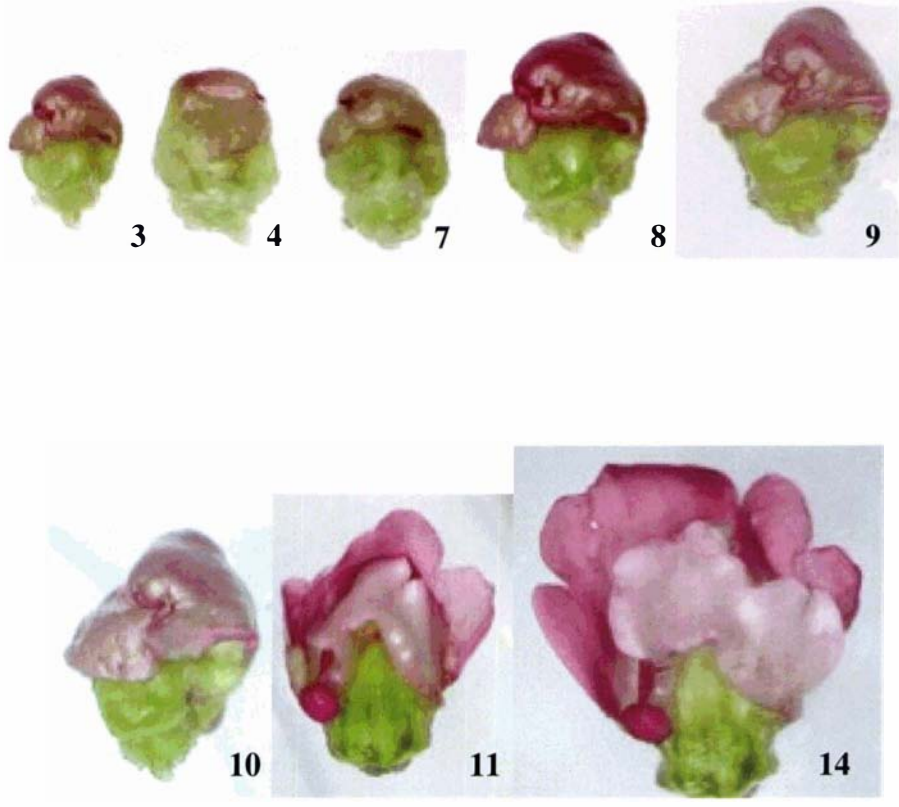

Figure 5.2 Development of antirrhinum flower buds (line #522) shot with gold-only preparation cultured *in vitro* over a 14-day period.

The number below each figure indicates the number of days after bombardment.

Figure 5.3 Inhibition of *Deficiens* activity in developing antirrhinum flower buds (line #522) using transient RNAi.

The inner epidermal tissue (A) and outer epidermal tissue (B) and (C) of a petal biolistically transformed with pNNP.Def.Hairpin construct (flower buds were cultured *in vitro* for nine days after bombardement). Areas with reduced/no anthocyanin pigments and accumulation of chlorophyll pigments can be seen as green-brown patches against the pink anthocyanin producing regions (D). Auto-fluorescence under UV- light observed as red colour, associated with the regions of the petal tissue accumulating chlorophyll pigments seen as green-brown patches in (C).

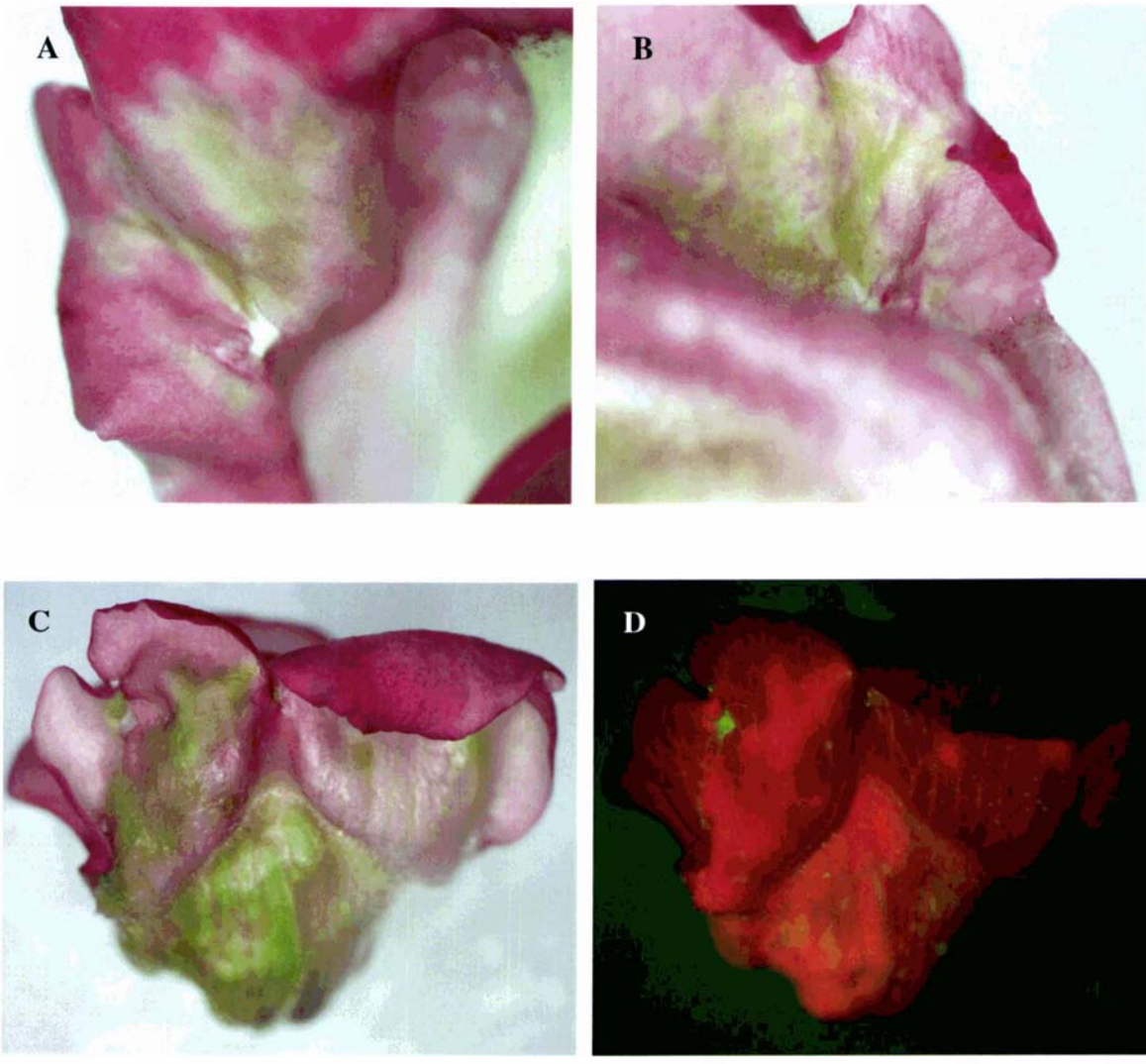
A
B
C
D

Figure 5.4 Phenotype of antirrhinum flower buds (line #522) silenced for *CHS* and *Deficiens* genes using transient RNAi.

Outer epidermis of a petal tissue silenced for *CHS* gene expression showing the development of areas with no anthocyanin pigments that are white (A). Petal tissue silenced for *Deficiens* gene expression, showing development of areas with no anthocyanin pigments and a green-brown colouration (B).

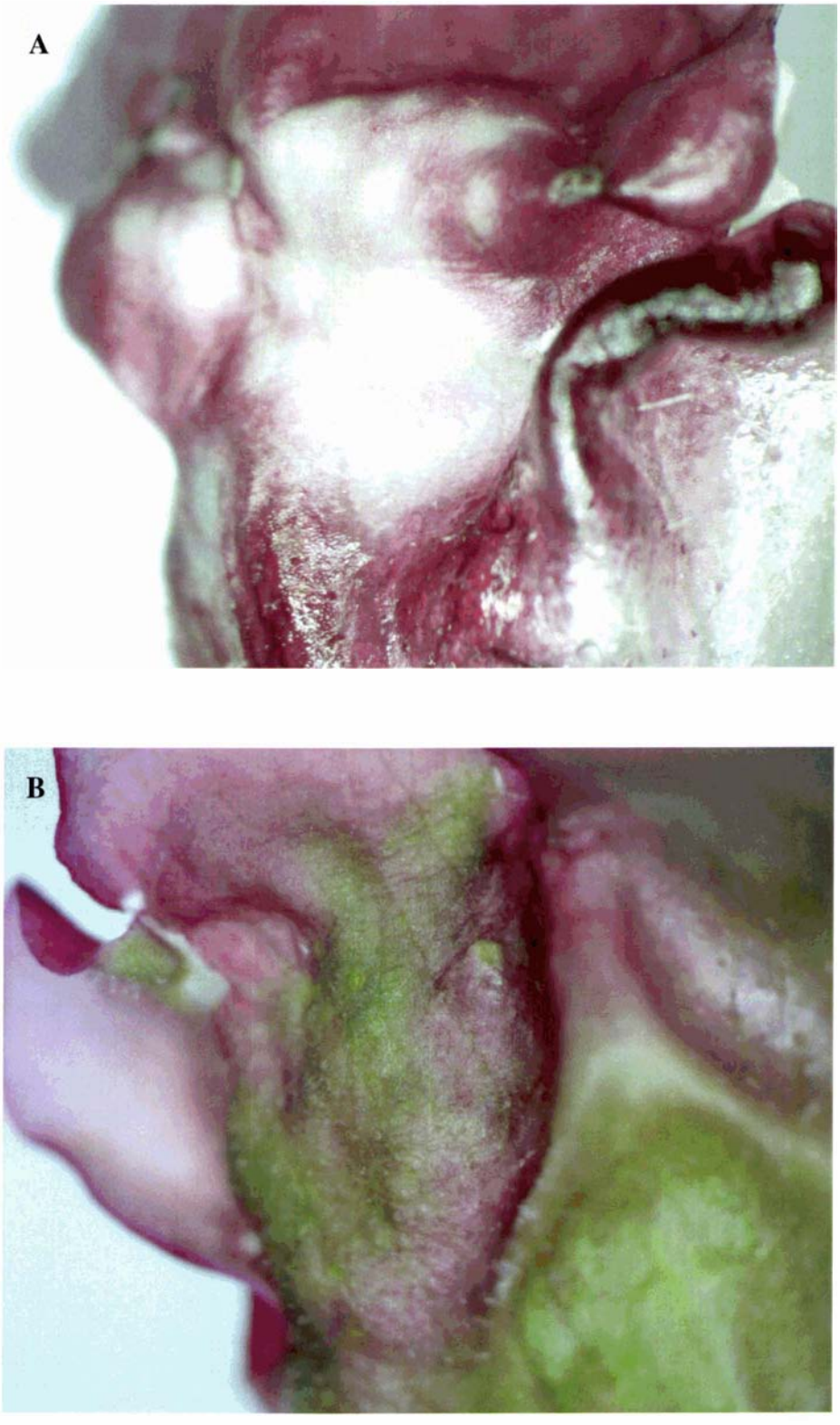
A
B

Figure 5.5 SEM analysis of *Deficiens* RNAi petal tissue of antirrhinum (line #522).

The border sector of *Deficiens* RNAi tissue containing anthocyanin pigments showing conical inner epidermal cells (x 1000 magnification) (A). A border sector with wild type, conical cells and a *Deficiens* silenced area with no/reduced anthocyanin pigments showing flat inner epidermal cells (x 200 magnification) (B). Higher magnification (x 1000) of a *Deficiens* silenced area with the flat inner epidermal cells (C). Wild type, inner epidermal cells of antirrhinum buds (5 mm) are mostly flat with beginnings of conical cell shape development (x 1000 magnification) (D).

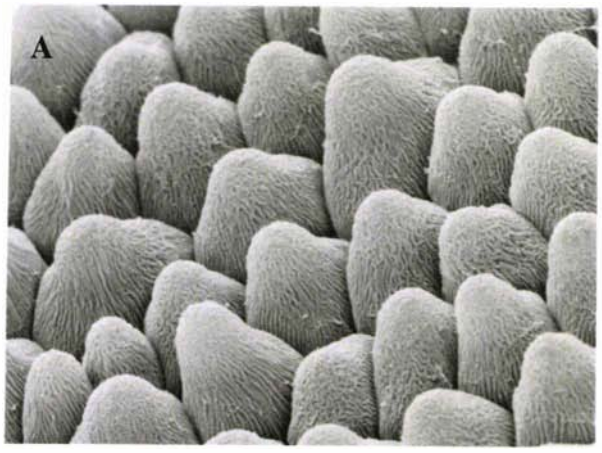
A

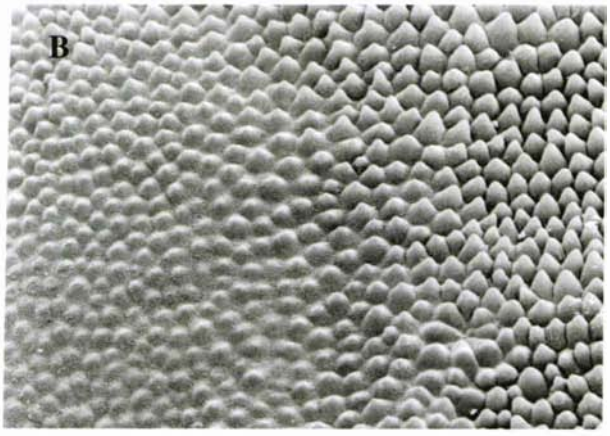
B

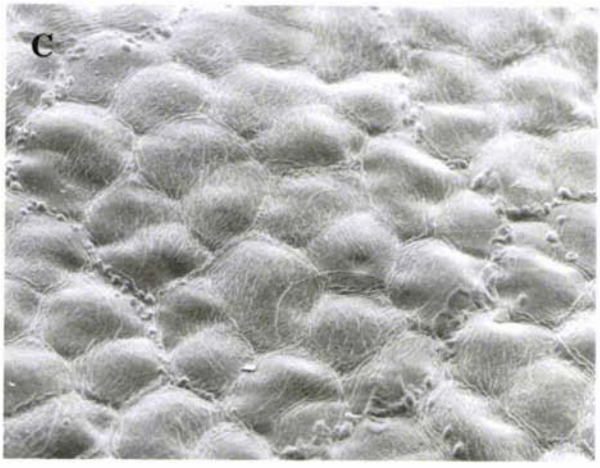
C

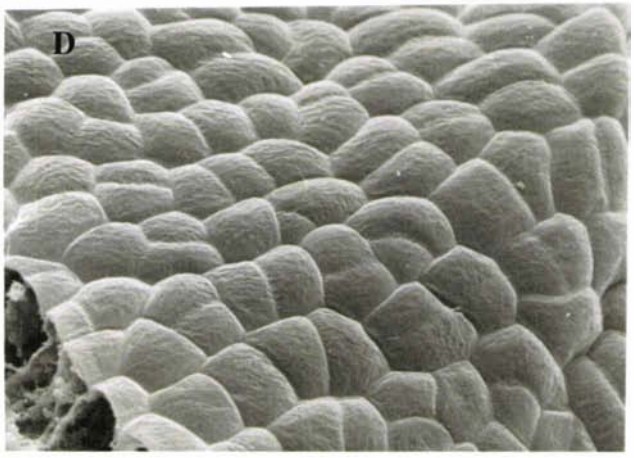
D

Figure 5.6 Light microscopy and SEM analysis of deficiens^{chlorantha} antirrhinum petal tissue.

Light photograph of deficiens^{chlorantha} petal showing patches lacking *Deficiens* activity which have chlorophyll-containing, green inner epidermal cells, bordered by wild type, pigmented cells (A). SEM photograph of the area boxed in (A) showing flat inner epidermal cells and the presence of trichomes in areas where *Deficiens* activity is lacking are bordered by wild type, conical shaped cells (B).

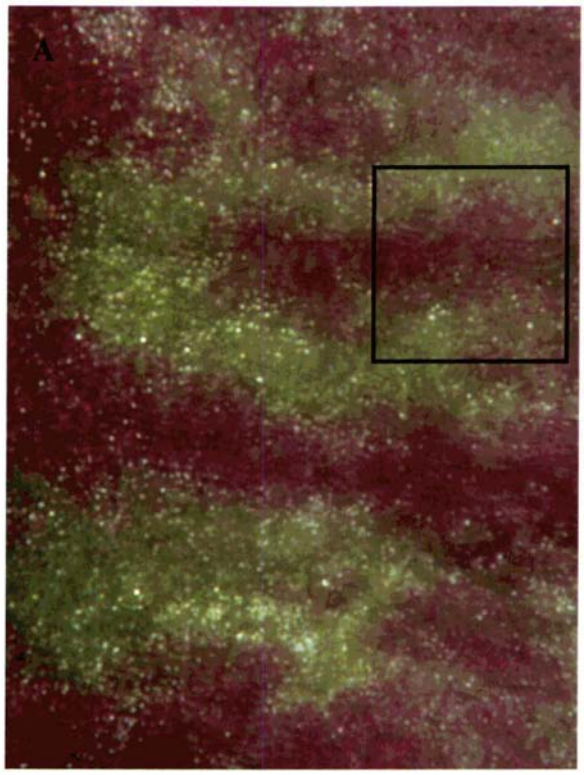
A

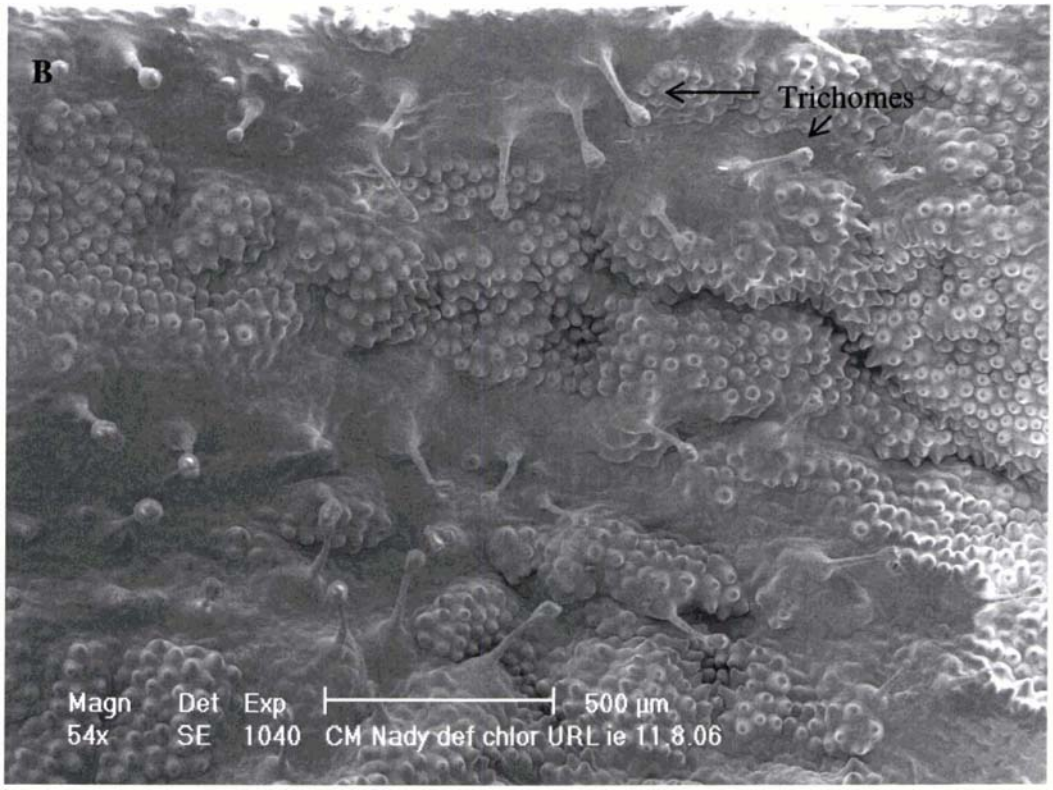
B
Trichomes
Magn Det Exp
500 µm
54x SE 1040 CM Nady def chlor URL ie 11.8.06

floral tissue. These results confirmed that expression of *Deficiens* is not only important for maintenance of petal identity but also for anthocyanin pigment formation in both inner and outer epidermis of antirrhinum petals.

It has been shown that *Deficiens* may also have other roles in epidermal cell development, such as development of the conical cell shape in the inner epidermis (Martin and Paz-Ares, 1997; Perez-Rodrigues *et al.*, 2005). Therefore, SEM analysis was carried out on areas of the RNAi petal tissue that had reduced/no anthocyanin pigmentation to see the effect on other morphological traits such as the inner epidermal cell shape. The inner epidermal cells in the *Deficiens* silenced areas failed to develop the normal conical cell shape. Studies by Schwarz-Sommer *et al.* (1992) showed that the deficiens^{chlorantha} mutant had lower *Deficiens* transcript levels in the petal and stamen tissue compared to that of the wild type. Their study further identified that this down-regulation of the *Deficiens* transcript levels was due to a mutation in the promoter region. In the deficiens^{chlorantha} mutant, patchy expression of *Deficiens* has also been shown to result in development of sepaloid features in the petal (Bey *et al.*, 2002). However, no further analysis of the petal morphology was carried out on this mutant.

SEM analysis and light microscopy of the deficiens^{chlorantha} petal tissue in the present study confirmed that proper expression of *Deficiens* is indeed required for the production of anthocyanin pigments in the petal as well as the proper development of the conical cell shape of the inner epidermal tissue. Furthermore, trichomes were present in the inner epidermis indicating that the areas lacking *Deficiens* activity had developed sepal-like characters. However, the RNAi tissue did not develop trichomes. In the deficiens^{chlorantha} mutant, *Deficiens* activity is likely to be lacking at very early stages of flower development, before petal identity has been established. Therefore, regions of the petal tissue of this mutant are likely to develop trichomes due to homeotic conversion of these regions into sepaloid structures. In the RNAi experiments, *Deficiens* expression is abolished well after the petal identity has been established. Therefore, the RNAi tissue is unlikely to develop trichomes. RNAi can be further used to induce phenotypic changes at later stages of antirrhinum flower development to allude to the dependence of petal tissue identity on *Deficiens* expression. *Deficiens* RNAi and deficiens^{chlorantha} petal tissue can be

also used to analyse the coincidence of *Deficiens* and *Rosea1* transcript expression by *in situ* hybridisation. This experiment would be useful to analyse whether *Deficiens* is likely to directly regulate the expression of *Rosea1*.

In conclusion, it was shown that the *Deficiens* gene activity is required for anthocyanin production as well as the development of the conical shape of inner epidermal cells in antirrhinum petals. The two potential MADS box protein binding sites present in the intron 2 of the *Rosea1* gene were shown to be not important for the expression of *Rosea1*. However, it should be noted that this might be due to the nature of the transient assay method used. Although transient assays with particle bombardment are very useful for qualitative experiments such as analysis of gene function, it is much more difficult to obtain quantitative data on experiments on gene expression and mutation studies (Dai *et al.*, 2001). The region of the *Rosea1* promoter that was similar to the MADS box protein binding site was also shown to be not important for driving expression of the GUS reporter gene. RNAi experiments coupled with SEM analysis showed that proper expression of *Deficiens* is indeed required for anthocyanin pigment formation as well as for maintaining the petal identity in antirrhinum petals during the late developmental stages of the petal. The absence of potential MADS box binding sites in the proximal part of the *Rosea1* and *rosea1*^{dorsea} promoters suggest that DEFICIENS may not regulate anthocyanin pigment production via *Rosea1*. It is possible that DEFICIENS may not be directly regulating *Rosea1* expression but regulates one or more of the anthocyanin biosynthetic genes directly. Therefore, the regulatory region of the anthocyanin biosynthetic genes should be analysed for potential MADS box binding sites. The possibility also exists that DEFICIENS may directly regulate the expression of a transcription factor regulating *Rosea1* expression or that it is required for the activation of other components of the anthocyanin regulatory machinery, such as the bHLH factors or the (unknown) factors required for EBG activation. Previous work by Schwarz-Sommer *et al.* (1992) and Perbal *et al.* (1996) has shown that DEFICIENS activity is required for the establishment and maintenance of the petal cell identity in antirrhinum. Therefore, DEFICIENS may provide only the base line signal for maintaining the petal epidermal cell identity while the timing of pigmentation may be independently controlled. In this

regard DEFICIENS activity would regulate pigmentation but not the actual timing of pigment production.

Chapter 6: General discussion and conclusions

The major objective of this research project was to understand the genetic regulatory system leading to the development of two different floral pigmentation patterns in antirrhinum: wild type and rosea^{dorsea}. This would provide a better understanding of the regulatory mechanisms leading to differential gene expression. Previous studies by Schwinn *et al.* (2006) suggested that these two pigmentation patterns occur due to changes in the promoter region of the *Rosea1* gene. *Rosea1* encodes a MYB transcription factor regulating anthocyanin biosynthesis in antirrhinum. Studies by Schwinn *et al.* (2006) demonstrated that variation in the activities of the *Rosea* and *Venosa* (which also encodes for a MYB transcription factor regulating anthocyanin biosynthesis) loci, were responsible for the differences in anthocyanin pigmentation between at least six species of *Antirrhinum.* Variation in anthocyanin patterns has been attributed to variation in MYB activity in other species including petunia (Quattrocchio *et al.*, 1999), grape (Kobayashi *et al.*, 2004, 2005) and potato (De Jong *et al.*, 2004). Therefore, it was hypothesised that the pigmentation patterns derived from wild type and rosea^{dorsea} in antirrhinum are due to different regulatory systems.

Sequence analysis of the *Rosea1* and *rosea1*^{dorsea} promoter regions showed that the *rosea1*^{dorsea} promoter had a large 187 bp deletion in the proximal region (in addition to other sequence changes), which may lead to the loss of *cis*-elements important for *Rosea1* expression in the inner epidermis of the antirrhinum petal tissue (Schwinn *et al.*, 2006). Promoter deletion analysis has been successfully used by Kao *et al.* (1996) to identify the *cis*-elements necessary and sufficient for the activation of the *C1* gene by absicic acid, VP1 and light in maize. The *C1* gene encodes a *Myb* regulator of anthocyanin biosynthesis in maize. Therefore, the effect of the 187 bp deletion on *rosea1* gene activity was first analysed by deletion analysis of the *Rosea1* and *rosea1*^{dorsea} promoters. Promoter deletion analysis in the present study demonstrated that the 151 bp proximal region of the *rosea1*^{dorsea} promoter can still drive GUS reporter gene expression in both inner and outer epidermal cells of flower petals of antirrhinum (using transient assays)

and tobacco (through stable transgenic assays) while maintaining petal specificity of expression as well. This proximal -151 bp of the promoter contained -141 bp region upstream of the transcription site plus ten bps after the site of the deletion (Figure 4.1). Thus, the promoter deletion analysis of the *rosea1*^{dorsea} promoter showed that the nucleotide sequence that is deleted in the 187 bp proximal region is not essential for the expression of the gene and is not responsible for the rosea^{dorsea} phenotype.

Further analysis of the importance of the 187 bp deletion in the *rosea1*^{dorsea} promoter in conferring the rosea^{dorsea} phenotype was tested by genetic analysis of a collection of *Antirrhinum* species available at the John Innes Centre. Previous work by Schwinn *et al.* (2006) showed that the weak floral pigmentation in *A. granticum, A. molle* and *A. mollisimum* species, which is very similar to the rosea^{dorsea} phenotype in *A. majus*, occurs due to changes at the *Rosea* locus. The *Rosea1* promoter regions from two accessions of *A. majus*, Barcelona and Toulouse, and seven *Antirrhinum* species were cloned and characterised in order to analyse if the weakly pigmented species carried the same 187 bp promoter deletion. The results from the sequence analysis of the *Rosea1* promoter region from the different antirrhinum species indicated that the proximal 187 bp deletion in the *rosea1*^{dorsea} promoter is not important for expression of the *rosea1* gene. Together, promoter deletion analysis and sequence analysis of the *Rosea1* gene from different *Antirrhinum* species thus prompt the conclusion that the changes in the *rosea1*^{dorsea} promoter region are not responsible for the rosea^{dorsea} phenotype.

Studies by Schwinn *et al.* (2006) also identified several nucleotide changes in the *rosea1*^{dorsea} cDNA that lead to eight amino acid changes in the deduced peptide. As there were no previous experimental data on the functionality of the ROSEA1 protein in rosea^{dorsea} mutants of *A. majus*, the full genomic sequence of the *rosea1*^{dorsea} allele was analysed. The functionality of the encoded protein was determined by complementation assays carried out on rosea^{dorsea} petal tissue. These assays showed that the *rosea1*^{dorsea} allele encodes for a functional protein and that changes in the coding region do not confer the rosea^{dorsea} phenotype.

In situ hybridisation analysis was performed on rosea^{dorsea} petal tissue to determine the expression pattern of the *rosea1*^{dorsea} allele. *rosea1*^{dorsea} transcript was present in both epidermal layers of the upper and lower lobe petal tissue and the vascular bundles. Thus, the *rosea1*^{dorsea} promoter was demonstrated to be capable of driving expression of the *rosea1*^{dorsea} allele in the rosea^{dorsea} petal tissue. These *in situ* results further verified the results obtained from the *rosea1*^{dorsea} promoter deletion analysis and *Rosea1* promoter sequence analysis of the *Antirrhinum* species. However, the expression level of *rosea1*^{dorsea} transcript in rosea^{dorsea} petals was much lower than that of *Rosea1* in wild type petal tissue. This low level of *rosea1*^{dorsea} transcript expression may indeed be responsible for the weak anthocyanin pigmentation in the rosea^{dorsea} flowers. It is proposed that an unidentified *MYB* factor may be responsible for the dorsal pigmentation pattern in rosea^{dorsea} with the activity of this fourth MYB being 'unmasked' by the loss of the strong wild type pigmentation pattern.

The transcript abundance of the *rosea1*^{dorsea} allele was much weaker in the rosea^{dorsea} petal tissue compared to that of wild type *Rosea1* transcript abundance. Yet the promoter deletion analysis of the *Rosea1* and *rosea1*^{dorsea} suggested equivalent promoter activity. Therefore, it was possible that regulation of *rosea1*^{dorsea} expression occurs via the intron and/or UTR sequences. There are many examples where intron regions and the untranslated regions regulate the transcription of an associated gene (Larkin *et al.*, 1993; Chen *et al.*, 1998; Deyholos and Sieburth, 2000; Jeon *et al.*, 2000). Sequence analysis revealed that the intron 2 region of the *rosea1*^{dorsea} allele contains many sequence differences from the *Rosea1* allele. Promoter replacement experiments were carried out to analyse if these changes were affecting the mRNA stability or expression level of the gene *in planta* and leading to the rosea^{dorsea} phenotype. The results of the promoter replacement experiments suggested that these changes might not be affecting the expression of the *rosea1*^{dorsea} allele. However, it should be mentioned that this result might not be reliable as it is difficult to obtain quantitative data due to the inherent nature of particle bombardment experiments. During particle bombardment a single cell may receive as many as one hundred copies of the plasmid being introduced and therefore might mask the finer regulation of a gene that occurs in the *in vivo* situation (Mehlo *et al.*,

2000; Dai *et al.*, 2001; Shou *et al.*, 2004). Therefore, to confirm these results, the pNNP.WTInt2.Del construct should be co-bombarded with a second reporter construct that can be used to normalise for the variability, allowing quantitative gene expression analysis from this construct.

The combined results from promoter deletion analysis of *Rosea1* and *rosea1*^{dorsea} promoters were also used to identify a key region of the *Rosea1* promoter that is important for its expression. The proximal -162 to -123 bp region of the *Rosea1* promoter was shown to be important for the regulated expression of the GUS reporter gene using transient and stable transgenic assays of the various promoter deletion constructs. This promoter region was also shown to be sufficient for maintaining the epidermal specificity as well as the petal specificity of reporter gene expression. PCR linker scanning mutagenesis was used to verify that this region is indeed important for expression of the *Rosea1* gene and to further define the *cis*-elements. Transient assays using rosea^{dorsea} petal tissue and analysis of flowers from transgenic tobacco plants harbouring the linker scanning constructs showed that mutating this region affected the expression of the GUS reporter gene dramatically. Finer linker scanning mutagenesis of the -162 to -123 bp region combined with bioinformatics-based methods were then used to identify the presence of *cis*-elements in this 40 bp region of the *Rosea1* promoter.

Bioinformatics analysis revealed the presence of a W-box, a pyrimidine box, and DOF and WRKY transcription factor binding sites in this promoter region. W-boxes have been shown to function in wound responses (Nishiuchi *et al.*, 2004). Mutation of this putative W-box resulted in very weak GUS expression and also affected the petal specificity of expression. This indicated that this W-box is important for regulation of the *Rosea1* gene.

Anthocyanin pigments are synthesised in response to hormonal signals and various environmental cues such as light, temperature and stresses induced by, for example, pathogen attack (Schwinn and Davies, 2004). DOF transcription factors belong to a recently identified novel class of DNA binding proteins and are important for light-

regulated expression and gibberellin responsive expression of genes (Mena *et al.*, 2002; Yanagisawa, 2004). DOF transcription factors are unique to the plant kingdom and, therefore, may perform unique and, as yet, unidentified roles in plant gene regulation (Yanagisawa, 2002, 2004). The major known role of the WRKY transcription factors in plants is in defence responses (Eulgem *et al.*, 2000). However, the *ttg2* gene encodes a WRKY transcription factor that functions in at least three morphogenic processes in the L1-derived cells in arabidopsis: trichome formation and the production of mucilage and proanthocyanidin in the seed coat (Johnson *et al.*, 2002). These authors proposed that TTG2 may directly regulate the proanthocyanidin biosynthesis gene, *Banyuls*. Thus, it is likely that WRKY transcription factors may function in responses other than stress, one of which may be in the regulation of pigment production. Therefore, it was of interest to analyse if the putative DOF and WRKY transcription factor binding sites present within the -162 to -123 bp of the *Rosea1* promoter region are important for its expression. This was done by mutating the putative DOF and WRKY transcription factor binding sites by finer linker scanning mutagenesis. Mutating the putative DOF binding site prevented strong GUS expression, whereas mutating the WRKY site led to the loss of petal-specific GUS expression. These results indicated that the putative DOF and WRKY transcription factor binding sites are important for the regulation of *Rosea1*.

A pyrimidine-box which is involved in gibberellin-related sugar repression (Morita *et al.*, 1998; Mena *et al.*, 2002), was mutated using three linker scanning constructs. Mutating part of this pyrimidine-box affected normal GUS expression as well as the petal-specificity of expression. Future work should involve mutating the entire region containing this putative pyrimidine-box to assess the importance of this putative *cis*-element for *Rosea1* regulation. Mutating the other regions within -162 bp to -123 bp of the *Rosea1* promoter by finer linker scanning mutagenesis led to the GUS reporter gene being expressed in sepal tissue indicating that petal specific elements are also present within this region. Interestingly, this also suggests that petal specificity of *Rosea1* expression may be achieved by a combination of activation in petals and repression in other organs. In summary, promoter deletion analysis combined with linker scanning

mutagenesis was successful in identifying key *cis*-elements for regulation of the *Rosea1* gene.

Preliminary experiments were conducted in order to identify regulatory proteins that interact with the -162 bp to -123 bp region of the *Rosea1* promoter. This was approached by two methods. In the first method, EMSA was carried out with nuclear proteins isolated from stage 3-5 antirrhinum flowers on LS2 (-162 bp to -143 bp region of the *Rosea1* promoter) and LS3 (-142 bp to -123 bp region of the *Rosea1* promoter) oligonucleotides. Preliminary EMSA assays indicated that both oligonucleotide sequences may bind antirrhinum petal nuclear proteins in a specific manner. This suggested that the -162 bp to -123 bp region of the *Rosea1* promoter harbours *cis*-elements that may regulate gene activity through interaction with nuclear proteins. The second approach utilised yeast-one hybrid screening using the -162 bp to -123 bp region of the *Rosea1* promoter as the DNA bait and a cDNA library made from antirrhinum flowers at stage 3-5 as the potential DNA-binding protein source. Methods for yeast one-hybrid library generation and screening were successfully set up in the laboratory as part of this project. Only 48 colonies were screened for the presence of a putative DNA-binding function due to time limitations. Most of the PCR products that were successfully sequenced encoded ribosomal RNA and for chloroplast proteins. tBLASTx analysis of one clone (#7) revealed that the encoded protein might be similar to the beta subunit of transcription initiation factor IIE from *Oryza sativa* (rice). Three other clones with good sequence identity to ESTs in the *A. majus* database were identified. However, the functions of the encoded proteins are, as yet, unidentified. The results from the one hybrid screen should be approached with some caution however, as transformation efficiencies were very low. This work should be repeated with a freshly prepared library. While regulatory factors of the *Rosea1* transcription factor were not identified, preliminary EMSA showed that nuclear proteins isolated from antirrhinum petal tissue may bind to the -162 bp to -123 bp *Rosea1* promoter region in a sequence-specific manner. Some expressing proteins, which might interact with the -162 bp to -123 bp region of the *Rosea1* promoter were identified through the yeast one-hybrid analysis. It should be noted however that protein-DNA interactions were very weak and these experiments need to be repeated.

The final objective of this project was to identify whether the *Deficiens* gene directly regulates *Rosea1* expression in antirrhinum. Not much is known about how early developmental pathways might regulate late developmental events such as anthocyanin biosynthesis. Therefore, the results from this objective would give an insight into the role of regulators active in early floral developmental stages in controlling late developmental pathways.

Two main approaches were used to analyse the importance of the *Deficiens* gene for anthocyanin pigmentation in antirrhinum. In the first approach, RNAi was used to silence the expression of the *Deficiens* gene in young antirrhinum flower buds. Silencing *Deficiens* expression led to development of areas with no/reduced anthocyanin pigments in the flower petals. Further analysis of the RNAi tissue and the deficiens^{chlorantha} mutant by light microscopy and SEM analysis revealed that, in addition to production of anthocyanin pigments, *Deficiens* expression was also required for the conical cell shape development of the inner epidermis of petals. The deficiens^{chlorantha} mutant also produced trichomes in the regions of the inner epidermis of the petal that were lacking *Deficiens* activity. This indicated that homeotic reversion of these petal regions into sepals was occurring in these regions. These results were consistent with previous work showing the importance of the *Deficiens* gene for maintaining petal cell identity (Perez-Rodriguez *et al.,* 2005). Therefore, it was concluded that *Deficiens* is an important factor required for anthocyanin pigment production as well as development of inner epidermal cell shape in antirrhinum.

Deficiens might regulate anthocyanin pigment production in many ways: firstly, it might function as a transcriptional activator of the regulator of the anthocyanin biosynthetic pathway (i.e. *Rosea1*); secondly, it might function as a transcriptional activator of the actual anthocyanin biosynthetic genes; thirdly, it may directly regulate the expression of the regulator of *Rosea1* or may be required for the activation of other components of the anthocyanin regulatory machinery, such as the bHLH factors or some unknown factors required for EBG activation.

The first scenario was further investigated by using bioinformatics-based search tools to identify potential DEFICIENS binding sites (i.e. MADS box protein binding sites) in the proximal region of the *Rosea1* promoter as well as the intron regions of *Rosea1* and *rosea1*^{dorsea} alleles. It was of interest that the *Rosea1* intron 2 contained two putative MADS box protein binding sites while *rosea1*^{dorsea} allele did not contain any. This was further pursued as it was possible that the absence of these putative MADS box protein binding sites might be responsible for the rosea^{dorsea} phenotype. However, this was shown not to be the case as removal of the two sites by deleting a large part of the intron 2 of the *Rosea1* gene did not affect the expression of *Rosea1*. As this experiment was carried out by complementation analysis of rosea^{dorsea} petals by particle bombardment, obtaining quantitative data was difficult (Mehlo *et al.*, 2000; Dai *et al.*, 2001; Shou *et al.*, 2004). Therefore, more direct methods, such as EMSA performed on the *Rosea1* promoter and the intron 2 regions with the DEFICIENS protein should provide more conclusive data on *Deficiens* as a direct regulator of *Rosea.* DEFICIENS requires its partner GLO for the recognition and binding of its target DNA (Schwarz-Sommer *et al.*, 1992). Furthermore, ternary complex formation between DEFICIENS, GLO and SQUA has also been demonstrated (Egea-Cortines *et al.*, 1999). Therefore, *in vitro* assays such as EMSA may pose potential problems as all the proteins required for DEFICIENS activity will need to be present in their native configuration in the assay.

The absence of potential *Deficiens* binding sites in the proximal region of the *Rosea1* promoter does not support *Deficiens* as a direct transcriptional activator of *Rosea1,* but leaves open the suggestions that *Deficiens* may function as a direct transcriptional activator of the anthocyanin biosynthetic genes. However, it seems unlikely that *Deficiens* is a direct regulator of the anthocyanin biosynthetic genes as the Myb-bHLH-WD40 proteins are thought to be necessary and sufficient for the regulation of anthocyanin biosynthesis (Ramsay and Glover, 2005). Also, anthocyanin pigments are produced in a wide variety of tissue and, therefore it is unlikely that a MADS box gene expressed mainly in the floral tissue would act as a regulator.

In situ hybridisation experiments on deficiens^{chlorantha} and *Deficiens* RNAi tissue should be carried out in the future to analyse the coincidence of *Deficiens* and *Rosea1* gene expression. This will allow the monitoring of *Rosea1* transcript levels in relation to *Deficiens* expression and can be used to identify whether *Deficiens* is a direct regulator of *Rosea1*. This will also enable to overcome the difficulties associated with using DEFICIENS for EMSA. The transient RNAi method also has several advantages over the use of deficien*s* mutants for this study. With RNAi the function of several genes can be analysed by silencing them simultaneously. Also the gene/s can be silenced in later stages of flower development. This would provide larger areas of tissue that can be used for further analysis such as microscopy.

Overall, the aim of this project was to understand the genetic regulatory system leading to the development of wild type and rosea^{dorsea} floral pigmentation patterns in antirrhinum. This would allow a better understanding of the regulatory mechanisms leading to differential gene expression. The differences in the promoter region of *rosea1*^{dorsea} (particularly the 187 bp proximal deletion) were shown not to be responsible for the rosea^{dorsea} phenotype. Two major mechanisms are proposed that may be responsible for the rosea^{dorsea} phenotype: firstly, the changes occurring in the intron 2 region of the *rosea1*^{dorsea} allele may lead to instability of the mRNA leading to lower expression of *rosea1*^{dorsea} and, secondly, an unidentified fourth *Myb* gene may be responsible for the dorsal pigmentation in rosea^{dorsea} flowers. This study also demonstrated that the higher level regulation of a regulator such as *Rosea1* is much more complex than postulated. The *Deficiens* gene may function as a higher order regulator with DOF and WRKY transcription factors regulating the *Rosea1* gene directly. Attempts were also made to identify the role of early developmental pathways in regulating late developmental events. The role of the floral identity gene, *Deficiens,* in pigment production was analysed in antirrhinum flowers. This work demonstrated that *Deficiens* is important for anthocyanin production as well as for the maintenance of petal cell identity in antirrhinum.

Appendix 1: Buffers and solutions

- AB salts (20 x): 1000 mg NH_4Cl, 300 mg $MgSO_4$, 150 mg KCl, 10 mg $CaCl_2$.

- 1% agarose/TBE minigel: 1 g of agarose in 100 mL of 1 x TBE buffer. The solution was autoclaved and cooled to 50°C before pouring the gel.

- B5 vitamins: Inositol 100 mgL^{-1}, nicotinic acid 1 mgL^{-1}, pyridoxine.HCl 1 mgL^{-1}, Thiamine.HCl 10 mgL^{-1}, Kinetin 0.1 mgL^{-1} and 2,4-dichlorophenoxyacetic acid 1 mgL^{-1}.

- 10 x gel loading dye: 20% Ficoll 400, 0.1 M EDTA (pH 8.0), 1% SDS, 0.25% bromophenol blue and 0.25% xylene cyanol made upto 20 mL with sterile water.

- IPTG: IPTG (20 $mgmL^{-1}$) was dissolved in sterile water and filter sterilised. Aliquots were stored at - 20°C.

- LB broth: contained Difco Bactotryptone (BD Diagnostics, Maryland, USA), 10 gL^{-1}, Difco yeast extract (BD Diagnostics) 5 gL^{-1} and NaCl 10 gL^{-1}. For solid media 1.5% (w/v) agar (Progen Pharmaceuticals Limited, Queensland, Australia) was added.

- LS vitamins: Inositol 100 mgL^{-1} and Thiamine.HCl 400 mgL^{-1}.

- MS salts: NH_4NO_3 1650 mgL^{-1}, KNO_3 1900 mgL^{-1}, $CaCl_2.2H_2O$ 440 mgL^{-1}, $MgSO_4.7H_2O$ 370 mgL^{-1} and KH_2PO_4 170 mgL^{-1}, KI 0.83 mgL^{-1}, H_3BO_3 6.2 mgL^{-1}, $MnSO_4.4H_2O$ 22.3 mgL^{-1}, $ZnSO_4.7H_2O$ 8.6 mgL^{-1}, $Na_2MoO_4.2H_2O$ 0.25 mgL^{-1}, $CuSO_4.5H_2O$ 0.025 mgL^{-1} and $CoCl_2.6H_2O$ 0.025 mgL^{-1}.

- MS micro salts: KI 0.83 mgL^{-1}, H_3BO_3 6.2 mgL^{-1}, $MnSO_4.4H_2O$ 22.3 mgL^{-1}, $ZnSO_4.7H_2O$ 8.6 mgL^{-1}, $Na_2MoO_4.2H_2O$ 0.25 mgL^{-1}, $CuSO_4.5H_2O$ 0.025 mgL^{-1} and $CoCl_2.6H_2O$ 0.025 mgL^{-1}.

- MS macro salts: NH_4NO_3 1650 mgL^{-1}, KNO_3 1900 mgL^{-1}, $CaCl_2.2H_2O$ 440 mgL^{-1}, $MgSO_4.7\ H_2O$ 370 mgL^{-1} and KH_2PO_4 170 mgL^{-1}.

- MS iron: $FeSO_4.7H_2O$ 27.8 mgL^{-1} and $Na_2EDTA.2H_2O$ 37.3 mgL^{-1}.

- 1.2% (w/v) MOPS denaturing gel: For 150 mL of denaturing gel solution 1.95 g of agarose, was melted in 15 mL of 10 x MOPS solution (0.4 M MOPS, 0.1 M NaAc, 10 mM EDTA with the pH adjusted to 7.2 with NaOH) and 135 mL of sterile water. The solution was then allowed to cool to 50°C and 7.65 mL of formaldehyde added before pouring the gel.

- Phenol/chloroform solution: Sterile water (250 mL) was added to 500 g of phenol crystals and melted at 65°C for 4 h. Phenol solution was then transferred to a 1 L Schott bottle containing 0.5 g 8-hydroxy chinoline and 250 mL of 1M Tris-HCl (pH 8.0) added. The contents were mixed thoroughly and the top layer was removed after allowing the two phases to separate. Two washes of 250 mL of 1M Tris-HCl (pH 8.0) were carried out and the top layer removed at each wash. Ten mL of *iso*-amyl alcohol and two volumes of chloroform were added to the phenol and thoroughly mixed and phases allowed to separate overnight. Some Tris-HCl was removed from the top layer before using the phenol/chloroform.

- 2 x RNA denaturing solution: Contained 5 µL of ethidium bromide, 500 µL of 10 x MOPS, 500 µL of formamide and 150 µL of formaldehyde.

- SEM buffer: 10 mM PIPES, 55 mM $MnCl_2$, 15 mM $CaCl_2$ and 250 mM KCl. All ingredients except $MnCl_2$ was dissolved in water and pH adjusted to 6.7 with KOH. $MnCl_2$ was then added, dissolved and volume adjusted to 1 L and the solution filter sterilised.

- 10 x TAE: 0.4 M Tris, 0.2 M Acetic acid and 0.01 M EDTA. The solution was autoclaved.

- TB (Terrific Broth): contained Difco Bactotryptone (BD Diagnostics) 12 gL^{-1}, Difco yeast extract 24 gL^{-1} and 4 mL glycerol. The volume was adjusted to 900 mL with sterile water and the soluton autoclaved. After cooling to toom temerature the volume was adjusted to 1 L with 100ml of filter sterilised solution of 0.17 M KH_2PO_4 and 0.72 M K_2HPO_4.

- 10 x TBE: 1 M Tris, 1 M Boric Acid and 20 mM EDTA. The solution was autoclaved.

- 1 x TE: 10 mM Tris and 1 mM EDTA. The pH was adjusted to 7.5 with HCl.

- X-Gal: X-Gal (20 $mgmL^{-1}$) was dissolved in DMF and aliquots were stored at - 20°C in foil wrapped containers.

Appendix II: Plasmid Maps

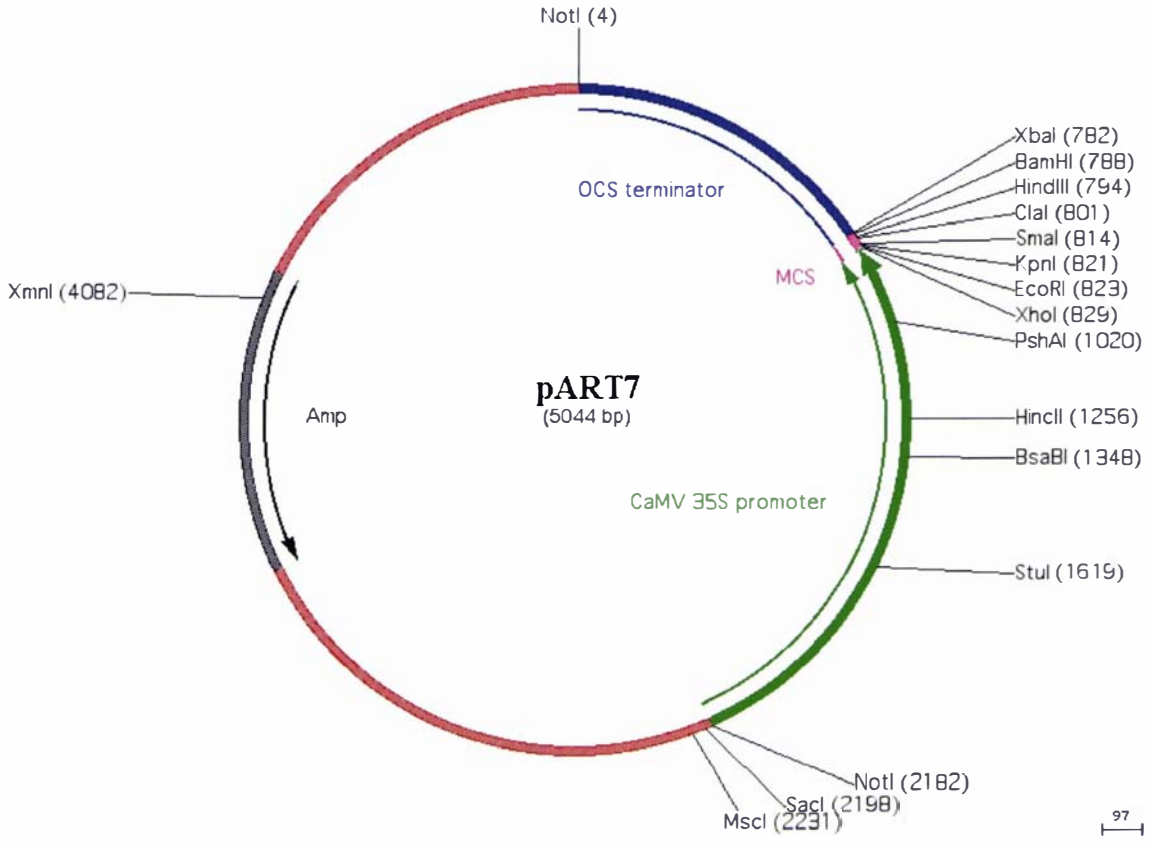

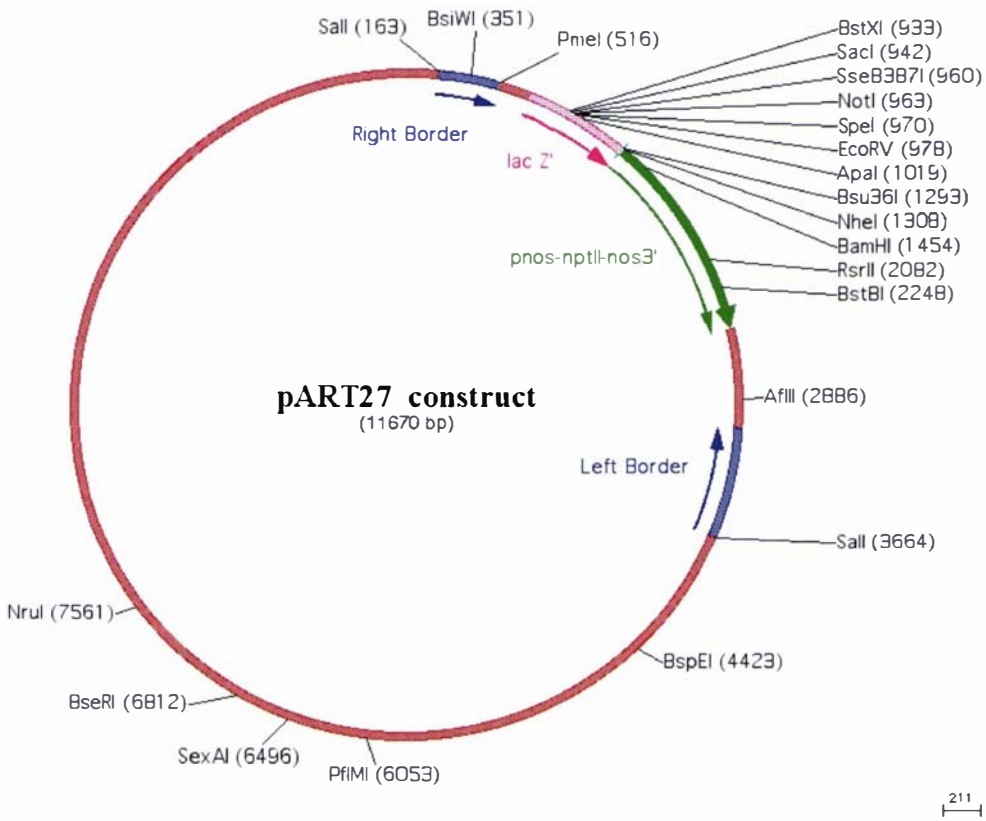
SalI (163)
BsiWI (351)
PmeI (516)
BstXI (933)
SacI (942)
SseB387I (960)
NotI (963)
SpeI (970)
EcoRV (978)
ApaI (1019)
Bsu36I (1293)
NheI (1308)
BamHI (1454)
RsrII (2082)
BstBI (2248)
Right Border
lac Z'
pnos-nptII-nos3'
pART27 construct
(11670 bp)
AflII (2886)
Left Border
SalI (3664)
NruI (7561)
BspEI (4423)
BseRI (6812)
SexAI (6496)
PflMI (6053)
211

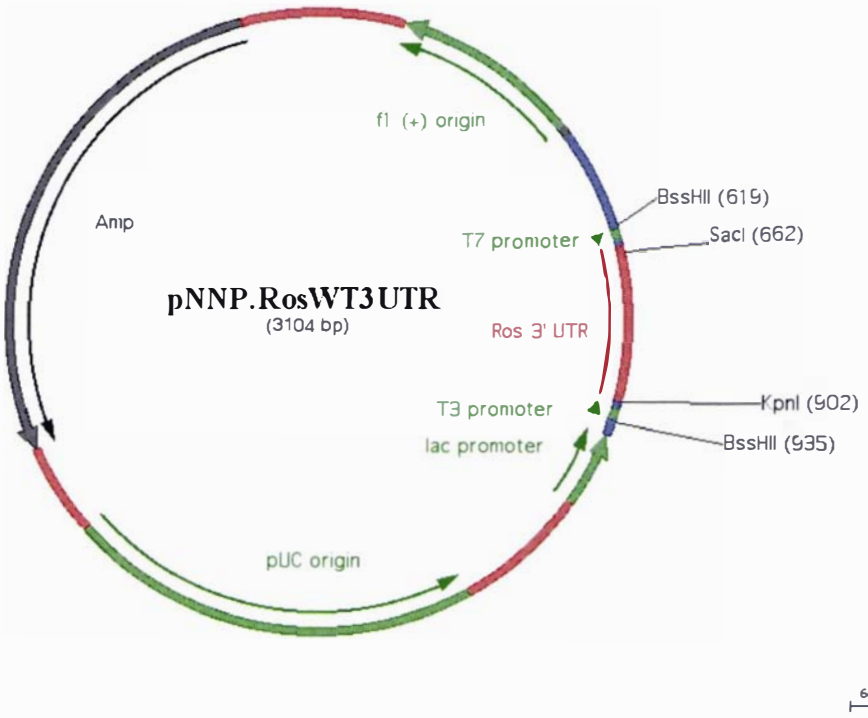
f1 (+) origin
BssHII (619)
SacI (662)
Amp
T7 promoter
pNNP.RosWT3UTR
(3104 bp)
Ros 3' UTR
T3 promoter
KpnI (902)
lac promoter
BssHII (935)
pUC origin
60

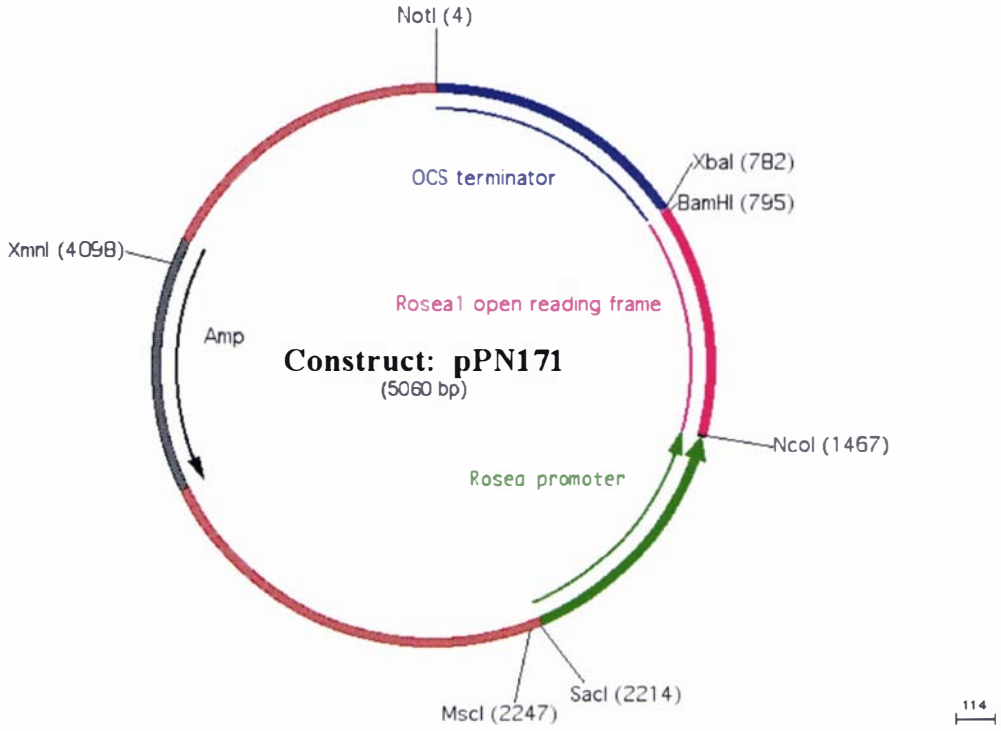
NotI (4)
XbaI (782)
BamHI (795)
OCS terminator
XmnI (4098)
Rosea1 open reading frame
Amp
Construct: pPN171
(5060 bp)
NcoI (1467)
Rosea promoter
SacI (2214)
MscI (2247)
114

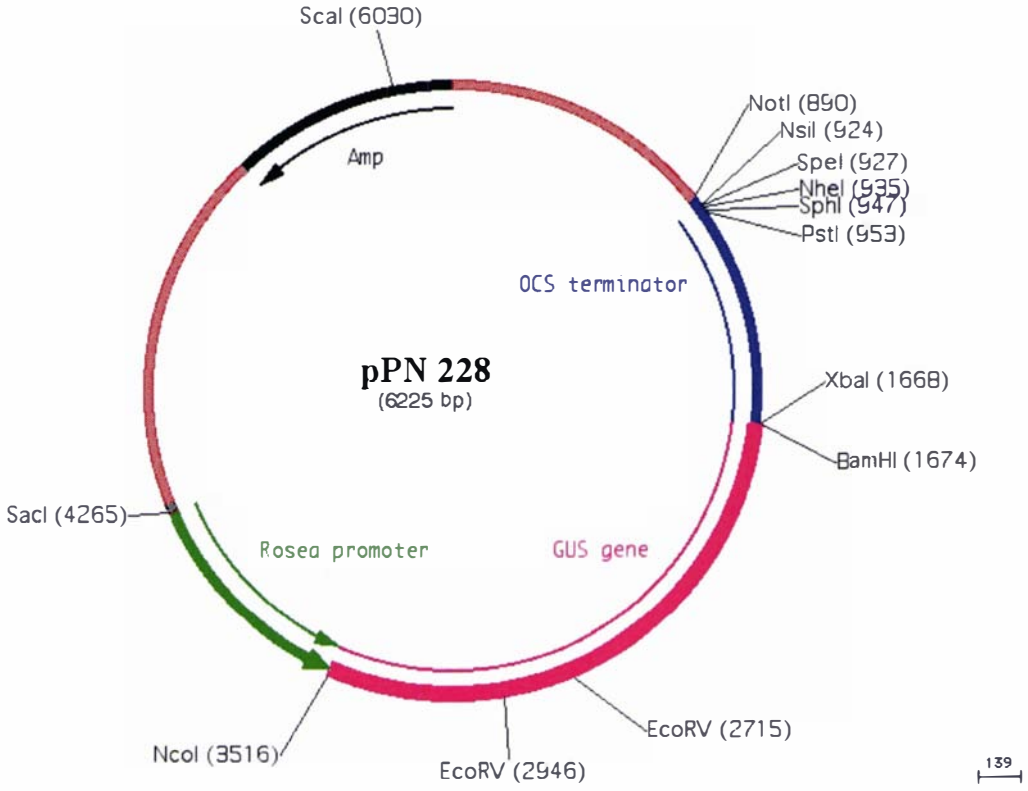
ScaI (6030)
NotI (890)
NsiI (924)
SpeI (927)
NheI (935)
SphI (947)
PstI (953)
Amp
OCS terminator
pPN 228
(6225 bp)
XbaI (1668)
BamHI (1674)
SacI (4265)
Rosea promoter
GUS gene
EcoRV (2715)
NcoI (3516)
EcoRV (2946)
139

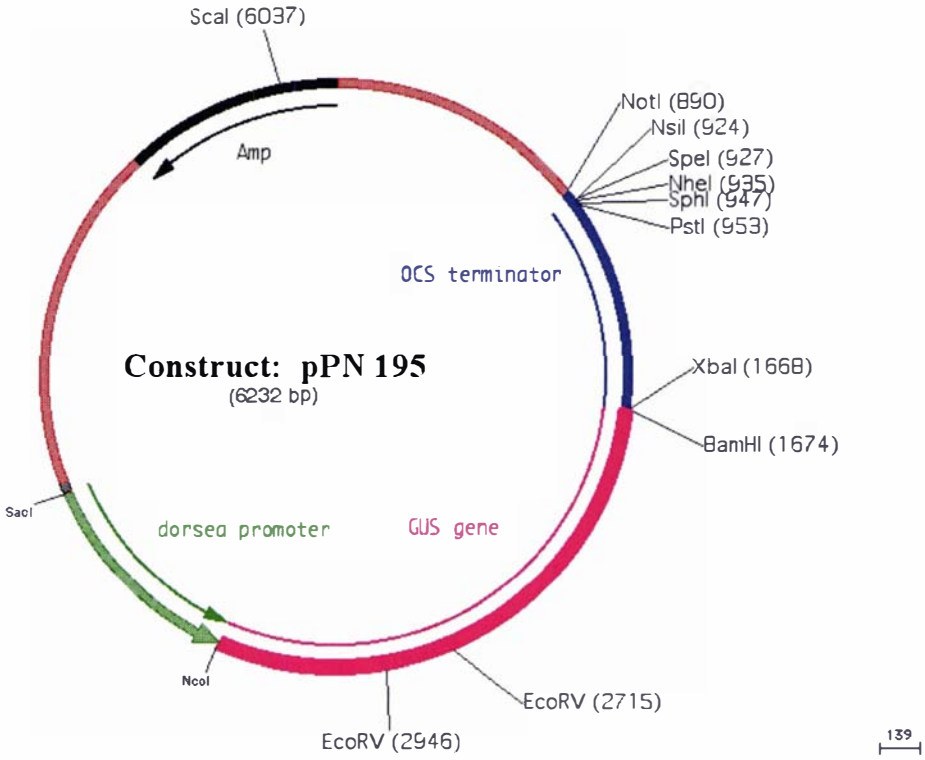
ScaI (6037)
NotI (890)
NsiI (924)
SpeI (927)
NheI (935)
SphI (947)
PstI (953)
Amp
OCS terminator
Construct: pPN 195
(6232 bp)
XbaI (1668)
BamHI (1674)
SacI
dorsea promoter
GUS gene
NcoI
EcoRV (2715)
EcoRV (2946)
139

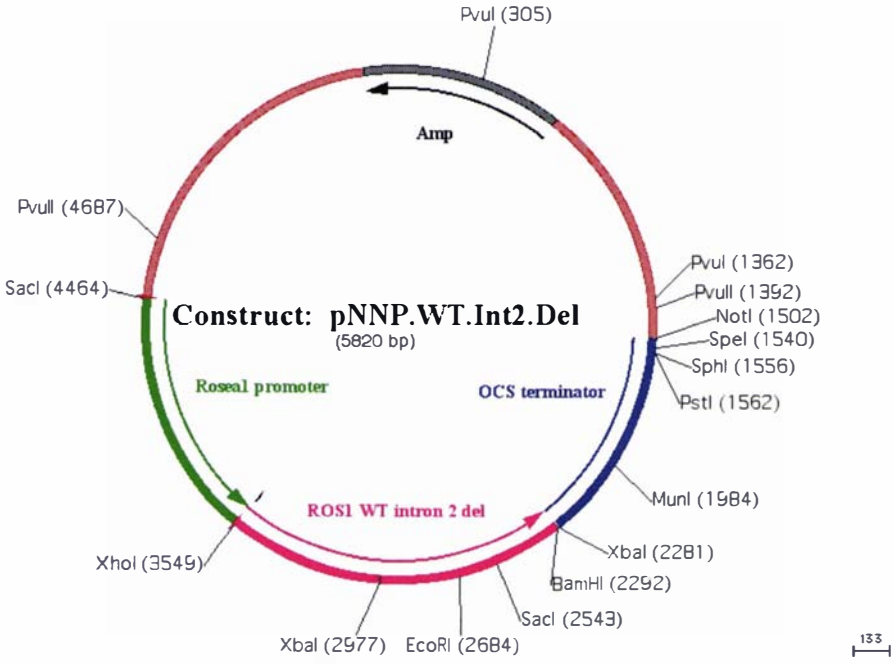
PvuI (305)
Amp
PvuII (4687)
SacI (4464)
Construct: pNNP.WT.Int2.Del
(5820 bp)
Roseal promoter
OCS terminator
ROS1 WT intron 2 del
PvuI (1362)
PvuII (1392)
NotI (1502)
SpeI (1540)
SphI (1556)
PstI (1562)
MunI (1984)
XbaI (2281)
BamHI (2292)
SacI (2543)
XbaI (2977)
EcoRI (2684)
XhoI (3549)
133

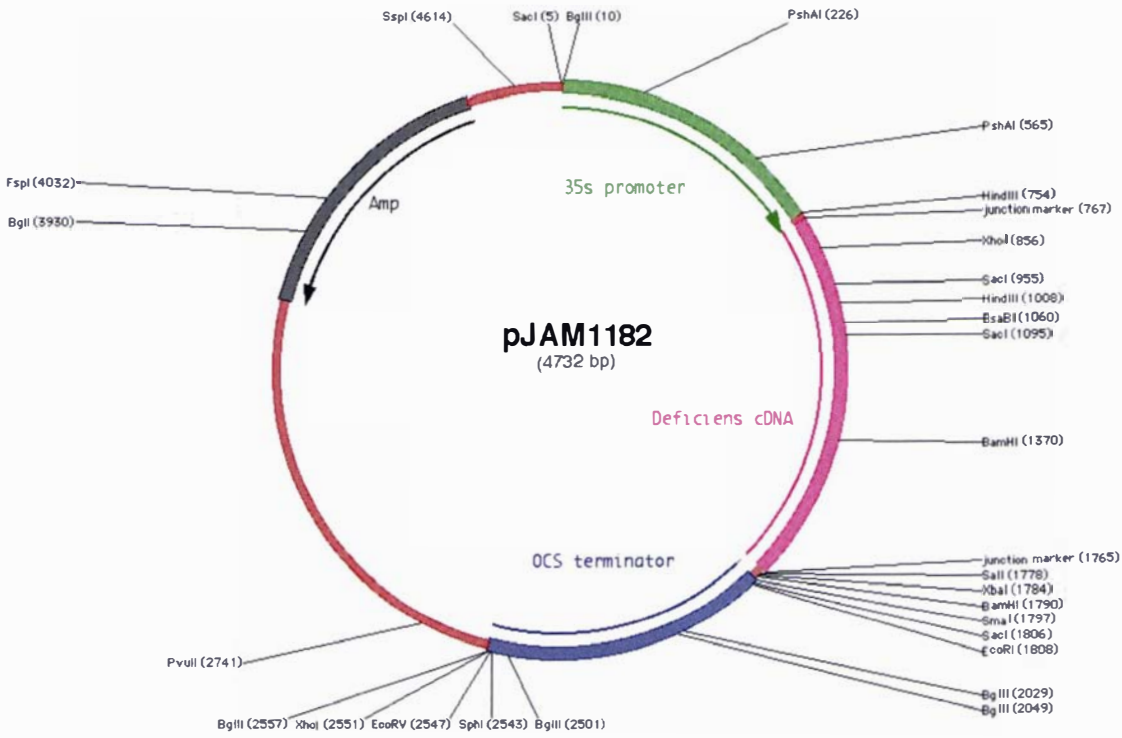
SspI (4614)
SacI (5)
BglII (10)
PshAI (226)
PshAI (565)
HindIII (754)
junction marker (767)
XhoI (856)
SacI (955)
HindIII (1008)
BsaBI (1060)
SacI (1095)
BamHI (1370)
junction marker (1765)
SalI (1778)
XbaI (1784)
BamHI (1790)
SmaI (1797)
SacI (1806)
EcoRI (1808)
BglII (2029)
BglII (2049)
BglII (2501)
SphI (2543)
EcoRV (2547)
XhoI (2551)
BglII (2557)
PvuII (2741)
FspI (4032)
BglI (3930)
Amp
35s promoter
pJAM1182
(4732 bp)
Deficiens cDNA
OCS terminator

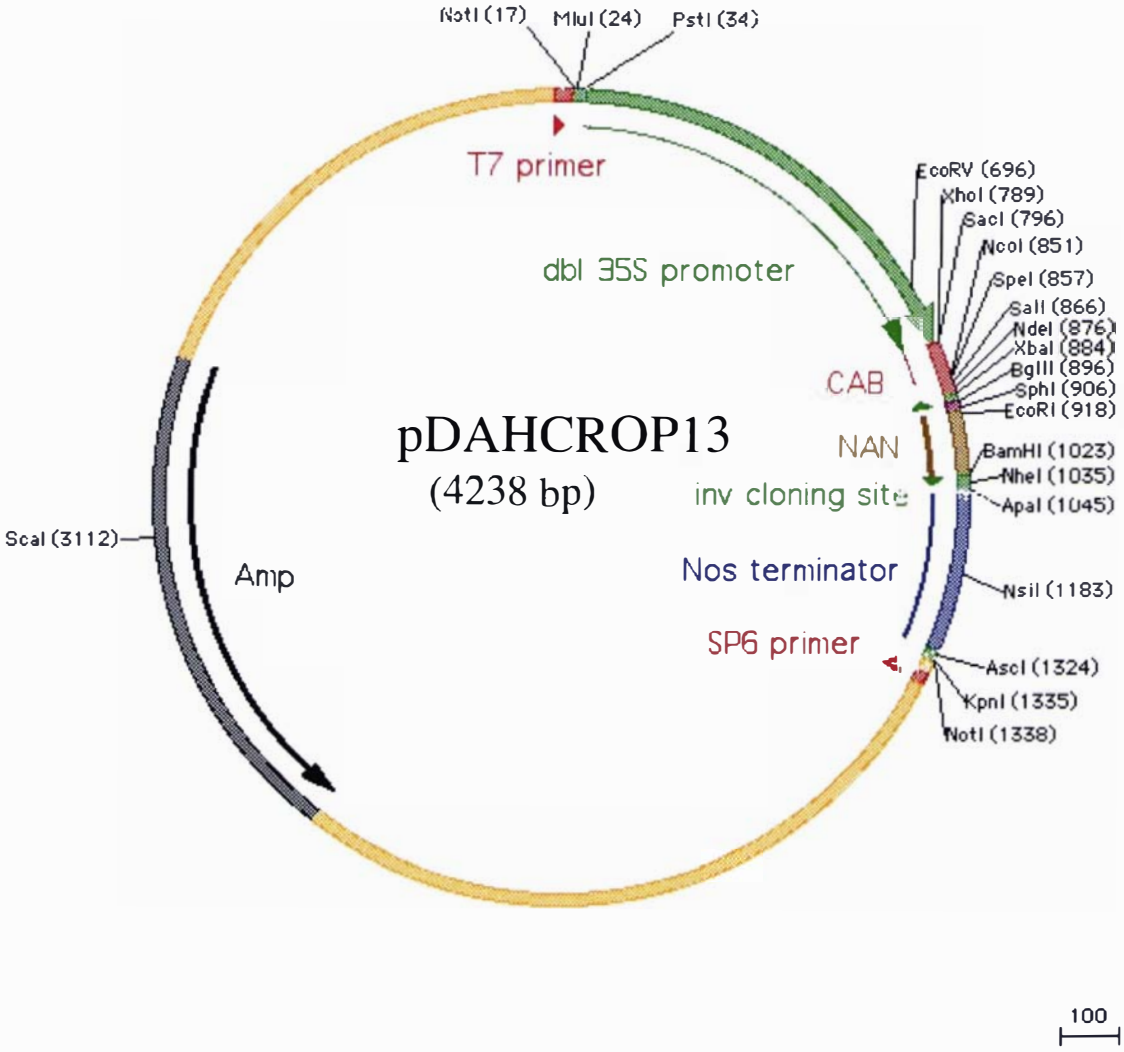
NotI (17)
MluI (24)
PstI (34)
T7 primer
EcoRV (696)
XhoI (789)
SacI (796)
NcoI (851)
SpeI (857)
SalI (866)
NdeI (876)
XbaI (884)
BglII (896)
SphI (906)
EcoRI (918)
dbl 35S promoter
CAB
NAN
pDAHCROP13
(4238 bp)
BamHI (1023)
NheI (1035)
ApaI (1045)
inv cloning site
ScaI (3112)
Amp
Nos terminator
NsiI (1183)
SP6 primer
AscI (1324)
KpnI (1335)
NotI (1338)
100

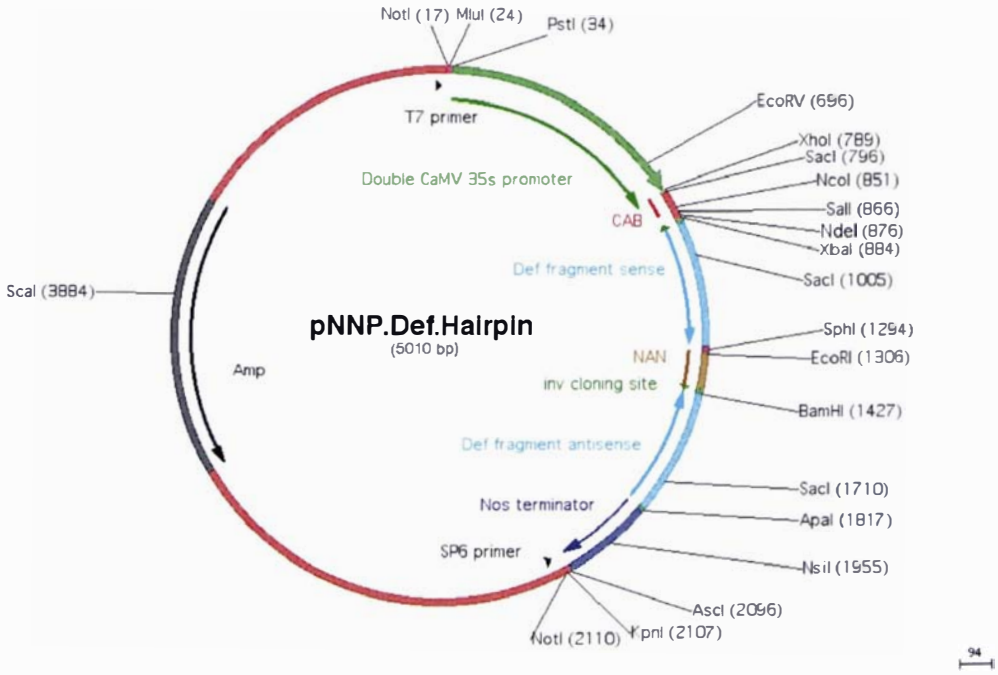
NotI (17)
MluI (24)
PstI (34)
T7 primer
EcoRV (696)
XhoI (789)
SacI (796)
NcoI (851)
SalI (866)
NdeI (876)
XbaI (884)
SacI (1005)
Double CaMV 35s promoter
CAB
Def fragment sense
ScaI (3884)
pNNP.Def.Hairpin
(5010 bp)
Amp
NAN
inv cloning site
SphI (1294)
EcoRI (1306)
BamHI (1427)
Def fragment antisense
SacI (1710)
ApaI (1817)
Nos terminator
SP6 primer
NsiI (1955)
AscI (2096)
NotI (2110)
KpnI (2107)
94

Appendix III: Primer sequences

Primer name	Sequence
K157.Gus	ACCAGACGTTGCCCGCAT
K180.Fwd	GATCGGAGCTCGTGGATTAGAACCAAATATATT
K181.Rev	GATCTACCATGGCGTTTAATACGTACTATGCCC
K182.Fwd	GATCTACCATGGAAAAGAATTGTCGTGGAGTGA
K183.Rev	GACTAGGATCCTTAATTTCCAATTTGTTGGGCC
K214.Fwd	GATCGGAGCTCGAACACATATAACAAAAACTCT
K215.Fwd	GATCGGAGCTCATGTGTCACTTTAGAGTTACTT
K216.Fwd	GATCGCAGCTCTAAGCATTAATATCGTATTTAT
K217.Fwd	GATCGGAGCTCAGGACATATGATTAATTACATG
K218.Fwd	GATCGGAGCTCAGCCAAAGGGGTCTACAGCCAT
K260.Fwd	ACTGACCCATGGGTCAGTCCCTTATGTTA
K261.Rev	ACGTAGGATCCTCATTGTTTGCCTCCCTG
K266.Fwd	GATCGGAGCTCCCTATAACATTAAATTAATCAA
K267.Fwd	GATCGGAGCTCCATAACACCTTTTCTACCTACT
K268.Fwd	GATCGGAGCTCGGTTGTCGTTAAAAATATGACC
K269.Fwd	GATCGGAGCTCGGGTTTGACGGGTCTGGCGGA
K270.Fwd	GATCGGAGCTCACTCATTAAAAAAAGGGAAAGA
K277.Fwd	GATCGGAGCTCTATTTAAACCNGTGNAAGTTT
Ros3UTR.Fwd	ATTATGAGCTCAGGAAACCTATTCGAGGAG
Ros3UTR.Rev	ATTGGTACCCCGTGATGATCTACTCTTAGA
N3.WT/LS	CTCGAGTGTACCGCGGGTCATGAAC
N4.WT/LS	CTCGAGGTCTAAGAAAACCCGACTC
N5.WT/LS	CTCGAGTGTACCGGCTACAGCCCTA
N6.WT/LS	CTCGAGGTCTAAGTTCGATCCGCCA
N7.WT/LS	CTCGAGTGTACCGTATTTAAACCCG
N8.WT/LS	CTCGAGGTCTAAGCTAGGGGTGTTC
WRKY.Fwd	CCGCTCGAGGAACACCCCTA
WRKY.Rev	CCGCTCGAGCGTTCGATCCG
DOF.Fwd	CCGCTCGAGCCTATTTAAC

Primer name	Sequence
DOF.Rev	CCGCTCGAGTATGGCTGTAG
LS2.1.Fwd	CGCGGATCCTCATGAACAC
LS2.1.Rev	CGCGGATCCGCCAG
LS2.2.Fwd	CCGCTCGAGCCCTAGGCTAC
LS2.2.Rev	CCGCTCGAGATGACCCGTTC
LS2.3.Fwd	CCCAAGCTTGCTACAGCCAT
LS2.3.Rev	CCCAAGCTTGTGTTCATGAC
LS3.1.Fwd	CCGCTCGAGGCCATAAAAAG
LS3.1.Rev	CCGCTCGAGCTAGGGGTGTT
LS3.2.Fwd	CCGCTCGAGAAAAGGCCTAT
LS3.2.Rev	CCGCTCGAGTGTAGCCTAGG
LS3.4.Fwd	CCGCTCGAGTAAACCCGTGA
LS3.4.Rev	CCGCTCGAGCCTTTTTATGG
T3	CCCTTTAGTGAGGGTTAATT
T7	GTAATACGACTCACTATAGG
M13.Fwd	TAAAACGACGGCCAGTG
M13.Rev	CAGGAAACAGCTATGAC
EMSA.LS2.fwd	ATGTCTCGAACGGGTCATGAACACCCCTAG
EMSA.LS2.rev	ATGTCCTAGGGGTGTTCATGACCCGTTCGA
EMSA.LS3.fwd	ATGTCGCTACAGCCATAAAAAGGCCTATTT
EMSA.LS3.rev	ATGTCAAATAGGCCTTTTTATGGCTGTAGC
WT.Int2.Fwd	GCTCTAGAGCTGAGAGAGACTATAC
WT.Int2.Rev	GCTCTAGAGCATTAACCGAGTACCA
MADS.Fwd	CGCGGATCCCTCCTATTTAAAC
MADS.Rev	CGCGGATCCCTGCTGTAGCCTA
Def.RNAi.Fwd	TCCAGTACTCAGAAGCTTCA
Def.RNAi.Rev	CTACTCAAGCAAAGCAAAAG
Def.Hairpin.Fwd	CTAGTCTAGATCCAGTACTCAGAAG
DEF.Hairpin.Rev	CGCGGATCCTATCGATCATACCAT
35S	ATGTGATATCTCCACTGACG

Appendix IV: Cloning strategy for generating *Rosea1* and *rosea1*^{dorsea} promoter deletion constructs

Rosea1 promoter deletion constructs:

Rosea1 promoter (isolated from *A. majus* wild type line #522) deletion constructs (Table 3.1) were based on the pPN 171 construct (Appendix II). To generate the promoter deletion constructs for transient assays, *Rosea1* reporter gene in pPN 171 was replaced with the GUS reporter gene by removing the *Rosea1* gene with a NcoI and BamHI digest (Section 2.2.3) followed by ligation (Section 2.2.8) of the GUS reporter gene into the NcoI and BamHI sites as a PCR product amplified using the K260.Fwd and K261.Rev primers (Appendix III). The resulting plasmid, pPN 228 (Appendix II), was then used as a template for PCR reactions with different forward primers designed to amplify different lengths of the *Rosea1* promoter in combination with K181.Rev primer. Pwo polymerase was used in the PCR as described in Section 2.4. The figure outlining the cloning strategy used for generating the *Rosea1* promoter deletion constructs is given in this Appendix. The sequences for the primers are given in Appendix III. The forward and reverse primers were designed such that the resulting PCR products would contain a SacI site and a NcoI site at the 5' end and at the 3' end of the *Rosea1* promoter fragments, respectively. The PCR products were digested with SacI and NcoI and ligated in to pPN 228 that has been digested with SacI and NcoI to remove the 1.2 kb *Rosea1* promoter fragment. Ligation products were transformed into Novablue competent cells as described in Section 2.3.2 and selected on LB plates supplemented with ampicillin at 100 mgmL^{-1}.

The expression cassette containing *Rosea1* promoter:GUS:OCS terminator was isolated from the pART 7 based vectors using SacI and NotI digest. The digest was run on a gel and the band corresponding to the expression cassette was gel purified as described in Section 2.2.9.2. The expression cassette was then ligated into pART 27 vector digested with SacI and NotI as described in Section 2.2.3. Positive plasmid clones were isolated by transforming the ligation reaction into Novablue cells as described in Section 2.3.3 using streptomycin (25 mgmL^{-1}) as the antibiotic selection. Once a positive clone was identified, it was then used to transform competent *Agrobacterium tumefaciens*

(LBA4404 cells) as described in Section 2.3.4 and antibiotic screening carried out using streptomycin/spectinomycin (200 $mgmL^{-1}$). Screening for positive clones were carried out by isolation of plasmid DNA from single colonies growing on selection followed with digestion with SacI and NotI as described in Section 2.3.3. Once a positive clone was identified, the results were verified by sequencing the plasmid (Section 2.5) using K157.Gus primer (Appendix III) followed by sequence analysis.

rosea1^{dorsea} promoter deletion constructs :

The *Rosea1* reporter gene in pPN 134 (700 bp *rosea1*^{dorsea} promoter:*Rosea1*:OCS) was removed by digesting it with NcoI and BamHI. The GUS reporter gene was PCR amplified with K260.Fwd and K261.Rev primers (Appendix III) and inserted into the NcoI/BamHI site of pPN 134 to generate pPN 195 (Appendix II). pPN 195 was then used as the template for subsequent PCR amplification of *rosea1*^{dorsea} promoter fragments using different forward primers (Appendix III) coupled with the K181.Rev primer. The PCR products containing SacI and NcoI ends were ligated into pPN 195 plasmid prepared with a SacI/NcoI digestion as described above for the *Rosea1* promoter deletion construct generation. Subsequent selection of positive clones as well as the generation of the *rosea1*^{dorsea} promoter deletion constructs in pART 27 vector followed the same strategy as that used for generation of *Rosea1* promoter deletion constructs (described above).

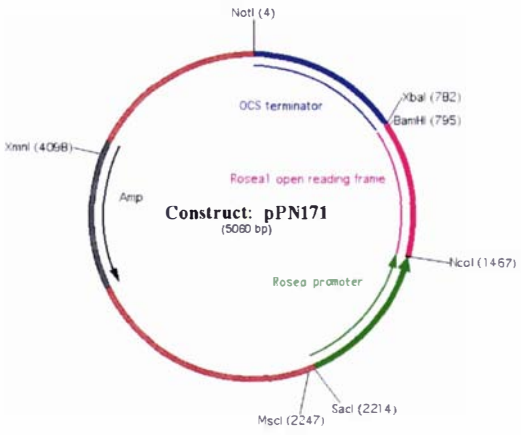

+

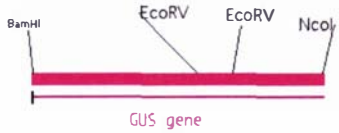

Rosea1 open reading frame was removed from pPN171 vector by NcoI/BamHI digestion followed by ligation of the GUS gene as a NcoI/BamHI fragment to generate pPN228

Vector backbone (4.38 kb) →

Rosea1 open reading frame → (0.65 kb)

Gel photograph showing pPN 171 digested with NcoI/BamHI. The vector backbone is 4.38 kb and the *Rosea1* open reading frame is 0.65 kb in size.

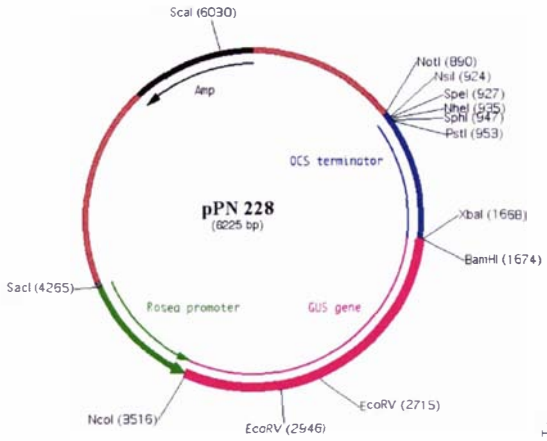

GUS gene (1.8 kb) →

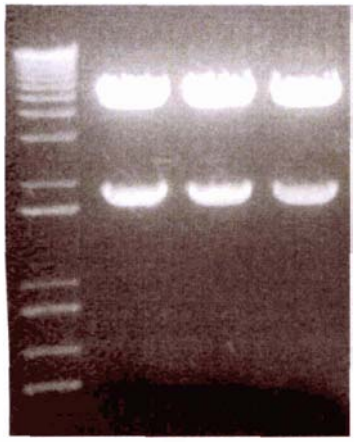

Plasmid DNA was prepared from three *E. coli* colonies transformed with the ligation reaction. Digestion with NcoI/BamHI showed that all four colonies contain the GUS reporter gene (1.8 kb).

Figure continued in the next page

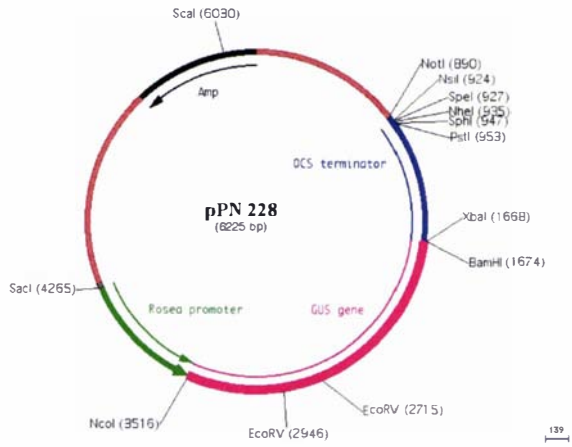

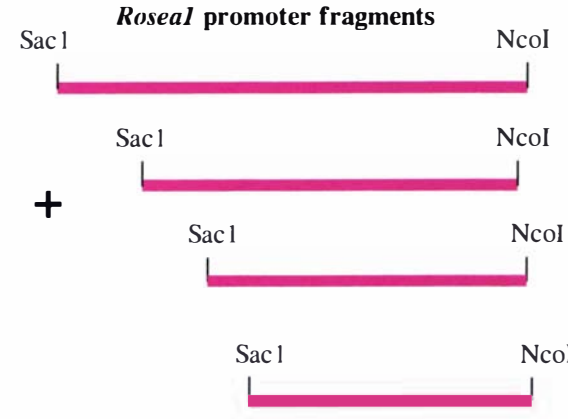

Rosea1 promoter region was removed by SacI/NcoI digestion and the *Rosea1* promoter fragments were cloned in as SacI/NcoI fragments to generate *Rosea1* promoter deletion constructs driving the GUS reporter gene.

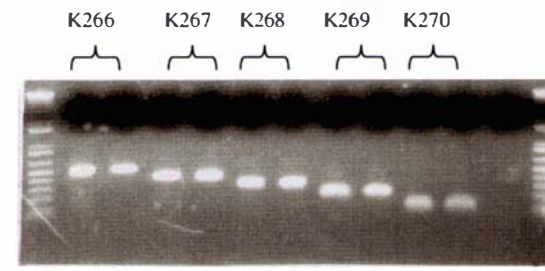

PCR products obtained from amplification of the *Rosea1* promoter fragments using different froward primers and the K181 reverse primer.

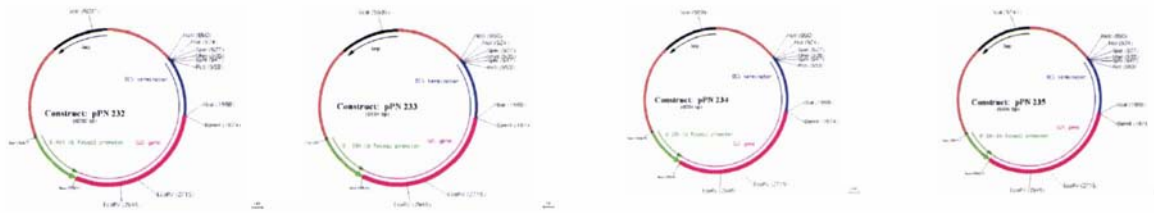

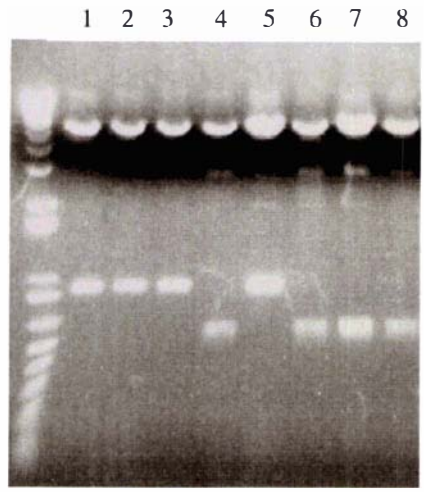

Plasmid DNA was prepared from eight *E. coli* colonies transformed with each of the ligation reactions. Digestion with SacI/BamHI was carried out to identify positive clones containing the corresponding *Rosea1* promoter fragment. This gel photo is for analysis of pPN 232 construct with clones #4, 6, 7 and 8 dropping the correct 0.489 kb *Rosea1* promoter fragment.

Appendix V: GUS phenotype and transgene copy number data for the *Rosea1* promoter deletion constructs analysed in tobacco.

	Construct name										
	pPN237	pPN238	pPN239	pPN240	pPN241	pPN242	pPN243	pPN244	pPN245	pPN258	pPN246
Promoter size(bp) / Line number	1200	900	809	710	608	493	389	289	189	120	89
1	(1)	+	+ (4)	+	-					-	-
2				-	-	- (1)				-	
3				-		-	+			-	-
4							+	+ (1)	-		
5	- (0)	-			-		-			-	
6	- (1)		+				-				
7	- (1)		+ (2)	+		+ (3)		-	+	-	
8		- (2)			-		+	-			-
9		(2)	+ (1)			-		+ (3)		-	
10	- (2)					+ (1)					-
11			+ (1)			+ (1)					-
12		+ (*)							+		
13				-	-		-	-	-	-	
14	+ (4)			+			-		+		-
15	(1)		+				-				
16	+ (1)	+ (*)			+		-		-		
17	+ (2)				+		-				-
18	+ (1)						-		+	-	
19		+ (3)	(1)			+ (1)				-	
20		+		+		+ (3)	-		-		
21	+ (4)	+	+ (1)			+ (4)				-	
22	+ (2)		-		-		+	(1)		-	
23	- (1)	+ (2)				-		- (1)	-		-
24		+						+ (2)			
25						+ (1)					-
26		+ (2)		-					-		-
27		+	(2)	+		- (3)			+		-
28	- (*)		+ (1)	+	+			+ (1)			
29	- (*)	+ (1)	+ (1)				-	- (1)	-		-
30		+ (1)						-			
31	+ (*)					- (2)		(1)			-
32				+	+	-	+	+ (1)			-
33	+ (2)							- (1)			-
34	+ (*)	- (*)	+ (4)		-	-					
35	+ (2)							-	+		-

(*) – Copy number could not be determined.

Appendix VI: GUS phenotype data for the *Rosea1* linker scanning mutant constructs analysed in tobacco.

	Construct name		
Line number	**ALS 1**	**ALS 2**	**ALS 3**
1	+		+
2			-
3	+		
4	-		+
5	+	+#	-
6			+
7	+	-	+^
8			+^
9	+	+#	
10	-		+
11	-	-	+#
12	+	+*	-
13			+
14	-	-	+
15	-		+
16	+	+*	
17	+		
18	-		
19			+
20		-	
21			+#
22			
23	-	-	+#
24			
25		-	
26			
27	-	-	
28		-	
29		-	
30		+*	

- GUS staining is very weak.
* - GUS staining only in the tube and very weak.
^ - GUS staining only in petal tips and very weak.

Appendix VII: GUS phenotype data for the *Rosea1* finer linker scanning mutant constructs analysed in tobacco.

Linc number	Construct name							
	ALS 2.1Bam	ALS WRKY	ALS 2.2	ALS 2.3Hind	ALS 3.1	ALS 3.2	ALS DOF	ALS 3.4
1	+			-		+	-	-
2	+s	Did not flower			+			-
3		+t	+					-
4					+*p	+		-
5	+p	+		+	+	-		-
6	+s	-		+s		+	-	-
7	-	+	-	-	+	+	-	-
8		-	+		+s	+	-	-
9	-	+t	-	-	-	+*	+*	-
10	+						+	-
11	-	-		+	+	+*	+t	-
12			-	-	+		-	-
13		+		-	-	-	+*ts	-
14		-		-			+s	
15		+	+	+			-	
16		Did not flower	+	+t*			-	
17	-	+t*	-	-			-	
18	+s*	+t	-	+			-	
19		+ts	+*	+			-	-
20	+s	-	-	+*			-	
21	+t		-	+*			-	
22	-		+s					
23	-			+s				
24	-	+t	+*	+s				
25		-	+*					
26	-	-						
27	+s							
28	-							
29								
30								
31				+t*				

s - Sepals also show GUS positive phenotype.
* - GUS staining is very weak.
p - GUS staining only in the petal tips.
t - GUS staining only in the tube.

Appendix VIII: GUS phenotype data for the *rosea1*^{dorsea} promoter deletion constructs analysed in tobacco.

	Construct name					
	pPN 247	pPN 248	pPN 249	pPN 250	pPN 251	pPN 252
Promoter size (bp) / Line number	700	632	533	432	279	151
1	+			-		
2			+		+	-
3	+	+				
4	-	-	+	+		
5	+	+				
6	+					
7				+		+
8	+	-			-	
9					+	+
10		-			+	
11		+			-	-
12	+	-				+
13			+	+		
14	-	+				-
15		-		+		
16	+					-
17					+	+
18			+			-
19	+		+		+	-
20	+		+			-
21	+	+	+			
22		-			+	-
23	-		+			+
24	+	+			-	
25					-	
26					+	
27					-	

Appendix IX: Sequence alignment between the promoter regions from the different *Antirrhinum* species and accessions, for *Rosea1* and *rosea1*^{dorsea}


140 150 160
TTAATATCTATGTCTTAAGGTATAAGT
1.2KbRos1 promoter(1>1200) → TTAATATCTATGTCTTAAGGTATAAGT
A. granticum(1>812) → TTAATATCTATGTCTTAAGGTATAAGT
A. barrelieri(1>715) → TTAATATCTATgTCTTAAGGTATAAGT
A. majus (Barcelona)(1>513) → TTAATATCTATGTCTTAAGGTATAAGT
A. latifolium (julius)(1>476) → TTAATATCTATGTCTTAAGGTATAAGT
A. australe(1>469) → ATCTATGTCTTAAGGTATAAGT
170 180
ACTCGTATGATGATTTATTATTTTTGA
1.2KbRos1 promoter(1>1200) → ACTCGTATGATGATTTATTATTTTTGA
A. granticum(1>812) → ACTCGTATGATGATTTATTATTTTTGA
A. barrelieri(1>715) → ACTCGTATGATGATTTATTATTTTTGA
A. majus (Barcelona)(1>513) → ACTCGTATGATGATTTATTATTTTTGA
A. latifolium (julius)(1>476) → ACTCGTATGATGATTTATTATTTTTGA
A. australe(1>469) → ACTCGTATGATGATTTATTATTTTTGA
190 200 210
AATAAATTAAAaTTAAGCATTAATATC
1.2KbRos1 promoter(1>1200) → AATAAATTAAA-TTAAGCATTAATATC
A. majus (Toulouse)(1>574) → AGCATTAATATC
A. granticum(1>812) → AATAAATTAAA-TTAAGCATTAATATC
A. barrelieri(1>715) → AATAAATTAAAATTAAGCATTAATATC
A. majus (Barcelona)(1>513) → AATAAATTAAAATTAAGCATTAATATG
A. latifolium (julius)(1>476) → AATAAATTAAAATTAAGCATTAATATC
A. australe(1>469) → AATAAATTAAAATTAAGCATTAATATC
220 230 240
GTATTTATAATTAAAAAACCCTGCTTA
1.2KbRos1 promoter(1>1200) → GTATTTATAATTAAAAAACCCTGCTTA
A. majus (Toulouse)(1>574) → GTATTTATAATTAAAAAACCCTGCTTA
A. granticum(1>812) → GTATTTATAATTAAAAAACCCTGCTTA
A. barrelieri(1>715) → ATATTTATAATTAAAAAACCCTGCTTA
A. majus (Barcelona)(1>513) → GTATTTATAATTAAAAAACCCTGCTTA
A. latifolium (julius)(1>476) → GTATTTATAATTAAAAAACCCTGCTTA
A. australe(1>469) → GTATTTATAATTAAAAAACCCTGCTTA
250 260 27(
ATTTCACCCATAACTTAATTCCTGGCT
1.2KbRos1 promoter(1>1200) → ATTTCACCCATAACTTAATTCCTGGCT
A. majus (Toulouse)(1>574) → ATTTCACCCATAACTTAaTTCCTGGCT
A. granticum(1>812) → ATTTCACCCATAACTTAATTCCTGGCT
A. barrelieri(1>715) → ATTTCACCCATAACTTAATTCCTGGCT
A. majus (Barcelona)(1>513) → ATTTCACCCATAACTTAATTCCTGGCT
A. siculum(1>574) → CATAACTTAATTCCTGGCT
ros1dorpromoter(1>393) → TCACCCATAACTTAATTCCTGGCT
A. latifolium (julius)(1>476) → ATTTCACCCATAACTTAATTCCTGGCT
A. australe(1>469) → ATTTCACCCATAACTTAATTCCTGGCT

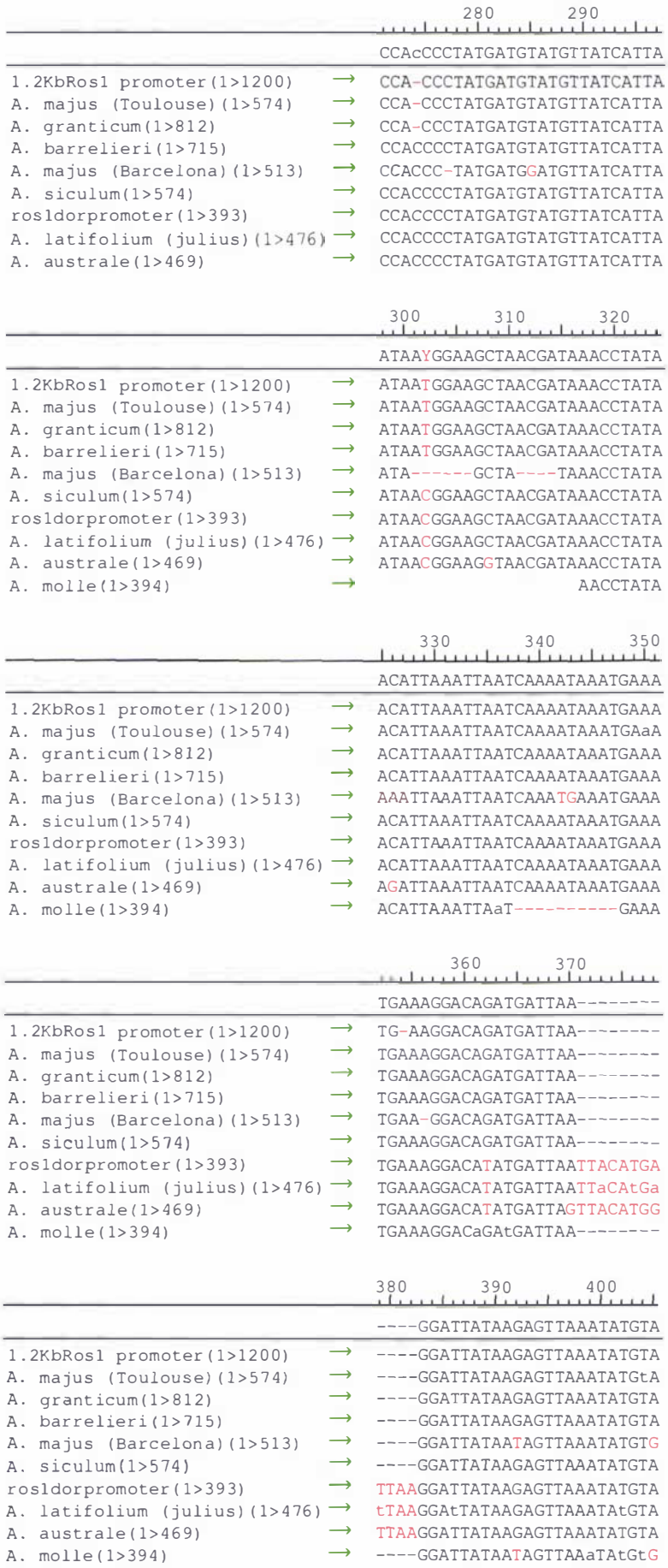
280 290
CCAcCCCTATGATGTATGTTATCATTA
1.2KbRos1 promoter(1>1200) CCA-CCCTATGATGTATGTTATCATTA
A. majus (Toulouse)(1>574) CCA-CCCTATGATGTATGTTATCATTA
A. granticum(1>812) CCA-CCCTATGATGTATGTTATCATTA
A. barrelieri(1>715) CCACCCCTATGATGTATGTTATCATTA
A. majus (Barcelona)(1>513) CCACCC-TATGATGGATGTTATCATTA
A. siculum(1>574) CCACCCCTATGATGTATGTTATCATTA
rosldorpromoter(1>393) CCACCCCTATGATGTATGTTATCATTA
A. latifolium (julius)(1>476) CCACCCCTATGATGTATGTTATCATTA
A. australe(1>469) CCACCCCTATGATGTATGTTATCATTA
300 310 320
ATAAYGGAAGCTAACGATAAACCTATA
1.2KbRos1 promoter(1>1200) ATAATGGAAGCTAACGATAAACCTATA
A. majus (Toulouse)(1>574) ATAATGGAAGCTAACGATAAACCTATA
A. granticum(1>812) ATAATGGAAGCTAACGATAAACCTATA
A. barrelieri(1>715) ATAATGGAAGCTAACGATAAACCTATA
A. majus (Barcelona)(1>513) ATA------GCTA----TAAACCTATA
A. siculum(1>574) ATAACGGAAGCTAACGATAAACCTATA
rosldorpromoter(1>393) ATAACGGAAGCTAACGATAAACCTATA
A. latifolium (julius)(1>476) ATAACGGAAGCTAACGATAAACCTATA
A. australe(1>469) ATAACGGAAGGTAACGATAAACCTATA
A. molle(1>394) AACCTATA
330 340 350
ACATTAAATTAATCAAAATAAATGAAA
1.2KbRos1 promoter(1>1200) ACATTAAATTAATCAAAATAAATGAAA
A. majus (Toulouse)(1>574) ACATTAAATTAATCAAAATAAATGAaA
A. granticum(1>812) ACATTAAATTAATCAAAATAAATGAAA
A. barrelieri(1>715) ACATTAAATTAATCAAAATAAATGAAA
A. majus (Barcelona)(1>513) AAATTAAATTAATCAAATGAAATGAAA
A. siculum(1>574) ACATTAAATTAATCAAAATAAATGAAA
rosldorpromoter(1>393) ACATTAAATTAATCAAAATAAATGAAA
A. latifolium (julius)(1>476) ACATTAAATTAATCAAAATAAATGAAA
A. australe(1>469) AGATTAAATTAATCAAAATAAATGAAA
A. molle(1>394) ACATTAAATTAaT----------GAAA
360 370
TGAAAGGACAGATGATTAA--------
1.2KbRos1 promoter(1>1200) TG-AAGGACAGATGATTAA--------
A. majus (Toulouse)(1>574) TGAAAGGACAGATGATTAA--------
A. granticum(1>812) TGAAAGGACAGATGATTAA--------
A. barrelieri(1>715) TGAAAGGACAGATGATTAA--------
A. majus (Barcelona)(1>513) TGAA-GGACAGATGATTAA--------
A. siculum(1>574) TGAAAGGACAGATGATTAA--------
rosldorpromoter(1>393) TGAAAGGACATATGATTAATTACATGA
A. latifolium (julius)(1>476) TGAAAGGACATATGATTAATTaCAtGa
A. australe(1>469) TGAAAGGACATATGATTAGTTACATGG
A. molle(1>394) TGAAAGGACaGAtGATTAA--------
380 390 400
----GGATTATAAGAGTTAAATATGTA
1.2KbRos1 promoter(1>1200) ----GGATTATAAGAGTTAAATATGTA
A. majus (Toulouse)(1>574) ----GGATTATAAGAGTTAAATATGtA
A. granticum(1>812) ----GGATTATAAGAGTTAAATATGTA
A. barrelieri(1>715) ----GGATTATAAGAGTTAAATATGTA
A. majus (Barcelona)(1>513) ----GGATTATAATAGTTAAATATGTG
A. siculum(1>574) ----GGATTATAAGAGTTAAATATGTA
rosldorpromoter(1>393) TTAAGGATTATAAGAGTTAAATATGTA
A. latifolium (julius)(1>476) tTAAGGAtTATAAGAGTTAAATAtGTA
A. australe(1>469) TTAAGGATTATAAGAGTTAAATATGTA
A. molle(1>394) ----GGATTATAATAGTTAAaTAtGtG

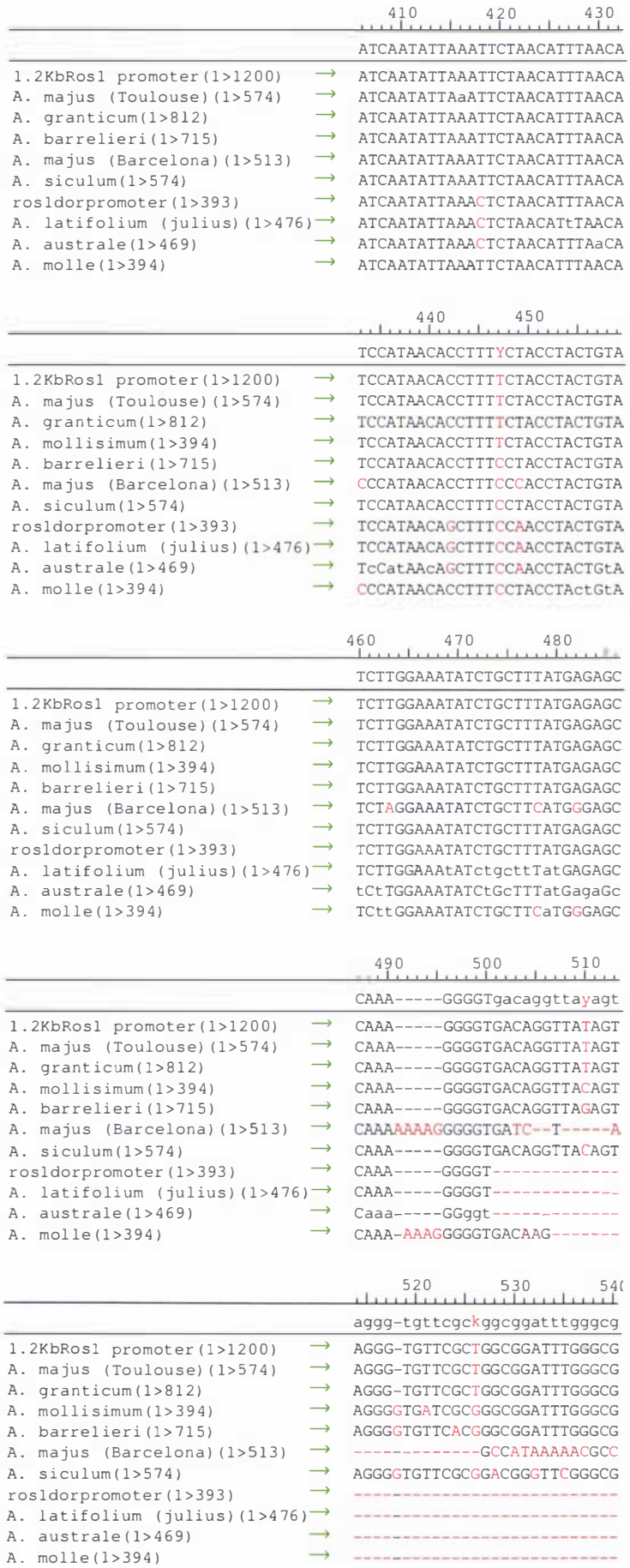
410 420 430
ATCAATATTAAATTCTAACATTTAACA
1.2KbRos1 promoter(1>1200) → ATCAATATTAAATTCTAACATTTAACA
A. majus (Toulouse)(1>574) → ATCAATATTAaATTCTAACATTTAACA
A. granticum(1>812) → ATCAATATTAAATTCTAACATTTAACA
A. barrelieri(1>715) → ATCAATATTAAATTCTAACATTTAACA
A. majus (Barcelona)(1>513) → ATCAATATTAAATTCTAACATTTAACA
A. siculum(1>574) → ATCAATATTAAATTCTAACATTTAACA
ros1dorpromoter(1>393) → ATCAATATTAAACTCTAACATTTAACA
A. latifolium (julius)(1>476) → ATCAATATTAAACTCTAACATtTAACA
A. australe(1>469) → ATCAATATTAAACTCTAACATTTAaCA
A. molle(1>394) → ATCAATATTAAATTCTAACATTTAACA
440 450
TCCATAACACCTTTYCTACCTACTGTA
1.2KbRos1 promoter(1>1200) → TCCATAACACCTTTTCTACCTACTGTA
A. majus (Toulouse)(1>574) → TCCATAACACCTTTTCTACCTACTGTA
A. granticum(1>812) → TCCATAACACCTTTTCTACCTACTGTA
A. mollisimum(1>394) → TCCATAACACCTTTTCTACCTACTGTA
A. barrelieri(1>715) → TCCATAACACCTTTCCTACCTACTGTA
A. majus (Barcelona)(1>513) → CCCATAACACCTTTCCCACCTACTGTA
A. siculum(1>574) → TCCATAACACCTTTCCTACCTACTGTA
ros1dorpromoter(1>393) → TCCATAACAGCTTTCCAACCTACTGTA
A. latifolium (julius)(1>476) → TCCATAACAGCTTTCCAACCTACTGTA
A. australe(1>469) → TcCatAAcAGCTTTCCAACCTACTGtA
A. molle(1>394) → CCCATAACACCTTTCCTACCTActGtA
460 470 480
TCTTGGAAATATCTGCTTTATGAGAGC
1.2KbRos1 promoter(1>1200) → TCTTGGAAATATCTGCTTTATGAGAGC
A. majus (Toulouse)(1>574) → TCTTGGAAATATCTGCTTTATGAGAGC
A. granticum(1>812) → TCTTGGAAATATCTGCTTTATGAGAGC
A. mollisimum(1>394) → TCTTGGAAATATCTGCTTTATGAGAGC
A. barrelieri(1>715) → TCTTGGAAATATCTGCTTTATGAGAGC
A. majus (Barcelona)(1>513) → TCTAGGAAATATCTGCTTCATGGGAGC
A. siculum(1>574) → TCTTGGAAATATCTGCTTTATGAGAGC
ros1dorpromoter(1>393) → TCTTGGAAATATCTGCTTTATGAGAGC
A. latifolium (julius)(1>476) → TCTTGGAAAtATctgcttTatGAGAGC
A. australe(1>469) → tCtTGGAAATATCtGcTTTatGagaGc
A. molle(1>394) → TCttGGAAATATCTGCTTCaTGGGAGC
490 500 510
CAAA-----GGGGTgacaggttayagt
1.2KbRos1 promoter(1>1200) → CAAA-----GGGGTGACAGGTTATAGT
A. majus (Toulouse)(1>574) → CAAA-----GGGGTGACAGGTTATAGT
A. granticum(1>812) → CAAA-----GGGGTGACAGGTTATAGT
A. mollisimum(1>394) → CAAA-----GGGGTGACAGGTTACAGT
A. barrelieri(1>715) → CAAA-----GGGGTGACAGGTTAGAGT
A. majus (Barcelona)(1>513) → CAAAAAAAGGGGGTGATC--T-----A
A. siculum(1>574) → CAAA-----GGGGTGACAGGTTACAGT
ros1dorpromoter(1>393) → CAAA-----GGGGT----------
A. latifolium (julius)(1>476) → CAAA-----GGGGT----------
A. australe(1>469) → Caaa-----GGggt----------
A. molle(1>394) → CAAA-AAAGGGGGTGACAAG-------
520 530 540
aggg-tgttcgckggcggatttgggcg
1.2KbRos1 promoter(1>1200) → AGGG-TGTTCGCTGGCGGATTTGGGCG
A. majus (Toulouse)(1>574) → AGGG-TGTTCGCTGGCGGATTTGGGCG
A. granticum(1>812) → AGGG-TGTTCGCTGGCGGATTTGGGCG
A. mollisimum(1>394) → AGGGGTGATCGCGGGCGGATTTGGGCG
A. barrelieri(1>715) → AGGGGTGTTCACGGGCGGATTTGGGCG
A. majus (Barcelona)(1>513) → ----------GCCATAAAAACGCC
A. siculum(1>574) → AGGGGTGTTCGCGGACGGGTTCGGGCG
ros1dorpromoter(1>393) → ----------
A. latifolium (julius)(1>476) → ----------
A. australe(1>469) → ----------
A. molle(1>394) → ----------

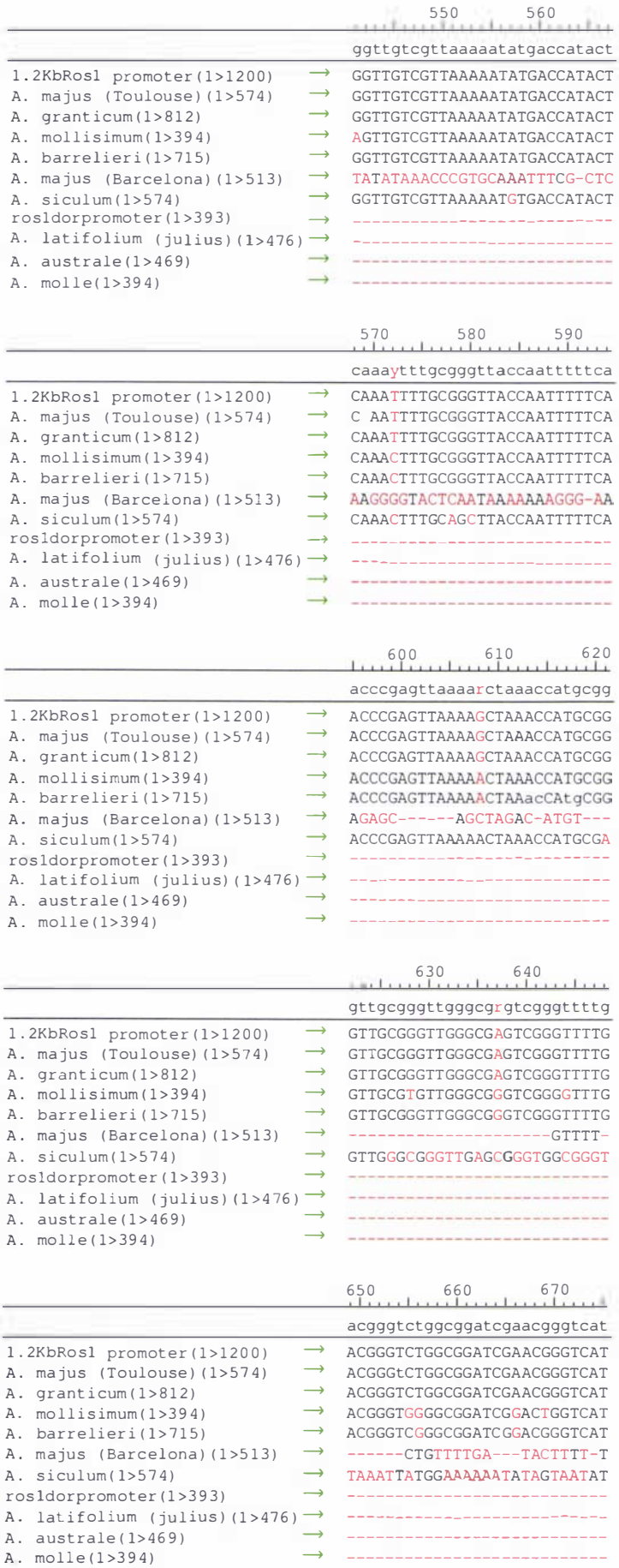
550 560
ggttgtcgttaaaaatatgaccatact
1.2KbRos1 promoter(1>1200) GGTTGTCGTTAAAAATATGACCATACT
A. majus (Toulouse)(1>574) GGTTGTCGTTAAAAATATGACCATACT
A. granticum(1>812) GGTTGTCGTTAAAAATATGACCATACT
A. mollisimum(1>394) AGTTGTCGTTAAAAATATGACCATACT
A. barrelieri(1>715) GGTTGTCGTTAAAAATATGACCATACT
A. majus (Barcelona)(1>513) TATATAAACCCGTGCAAATTTCG-CTC
A. siculum(1>574) GGTTGTCGTTAAAAATGTGACCATACT
ros1dorpromoter(1>393)
A. latifolium (julius)(1>476)
A. australe(1>469)
A. molle(1>394)
570 580 590
caaaytttgcgggttaccaatttttca
1.2KbRos1 promoter(1>1200) CAAATTTTGCGGGTTACCAATTTTTCA
A. majus (Toulouse)(1>574) C AATTTTGCGGGTTACCAATTTTTCA
A. granticum(1>812) CAAATTTTGCGGGTTACCAATTTTTCA
A. mollisimum(1>394) CAAACTTTGCGGGTTACCAATTTTTCA
A. barrelieri(1>715) CAAACTTTGCGGGTTACCAATTTTTCA
A. majus (Barcelona)(1>513) AAGGGGTACTCAATAAAAAAAGGG-AA
A. siculum(1>574) CAAACTTTGCAGCTTACCAATTTTTCA
ros1dorpromoter(1>393)
A. latifolium (julius)(1>476)
A. australe(1>469)
A. molle(1>394)
600 610 620
acccgagttaaaarctaaaccatgcgg
1.2KbRos1 promoter(1>1200) ACCCGAGTTAAAAGCTAAACCATGCGG
A. majus (Toulouse)(1>574) ACCCGAGTTAAAAGCTAAACCATGCGG
A. granticum(1>812) ACCCGAGTTAAAAGCTAAACCATGCGG
A. mollisimum(1>394) ACCCGAGTTAAAAACTAAACCATGCGG
A. barrelieri(1>715) ACCCGAGTTAAAAACTAAacCAtgCGG
A. majus (Barcelona)(1>513) AGAGC------AGCTAGAC-ATGT---
A. siculum(1>574) ACCCGAGTTAAAAACTAAACCATGCGA
ros1dorpromoter(1>393)
A. latifolium (julius)(1>476)
A. australe(1>469)
A. molle(1>394)
630 640
gttgcgggttgggcgrgtcgggttttg
1.2KbRos1 promoter(1>1200) GTTGCGGGTTGGGCGAGTCGGGTTTTG
A. majus (Toulouse)(1>574) GTTGCGGGTTGGGCGAGTCGGGTTTTG
A. granticum(1>812) GTTGCGGGTTGGGCGAGTCGGGTTTTG
A. mollisimum(1>394) GTTGCGTGTTGGGCGGGTCGGGGTTTG
A. barrelieri(1>715) GTTGCGGGTTGGGCGGGTCGGGTTTTG
A. majus (Barcelona)(1>513) ----------GTTTT-
A. siculum(1>574) GTTGGGCGGGTTGAGCGGGTGGCGGGT
ros1dorpromoter(1>393)
A. latifolium (julius)(1>476)
A. australe(1>469)
A. molle(1>394)
650 660 670
acgggtctggcggatcgaacgggtcat
1.2KbRos1 promoter(1>1200) ACGGGTCTGGCGGATCGAACGGGTCAT
A. majus (Toulouse)(1>574) ACGGGtCTGGCGGATCGAACGGGTCAT
A. granticum(1>812) ACGGGTCTGGCGGATCGAACGGGTCAT
A. mollisimum(1>394) ACGGGTGGGGCGGATCGGACTGGTCAT
A. barrelieri(1>715) ACGGGTCGGGCGGATCGGACGGGTCAT
A. majus (Barcelona)(1>513) ------CTGTTTTGA---TACTTTT-T
A. siculum(1>574) TAAATTATGGAAAAAATATAGTAATAT
ros1dorpromoter(1>393)
A. latifolium (julius)(1>476)
A. australe(1>469)
A. molle(1>394)

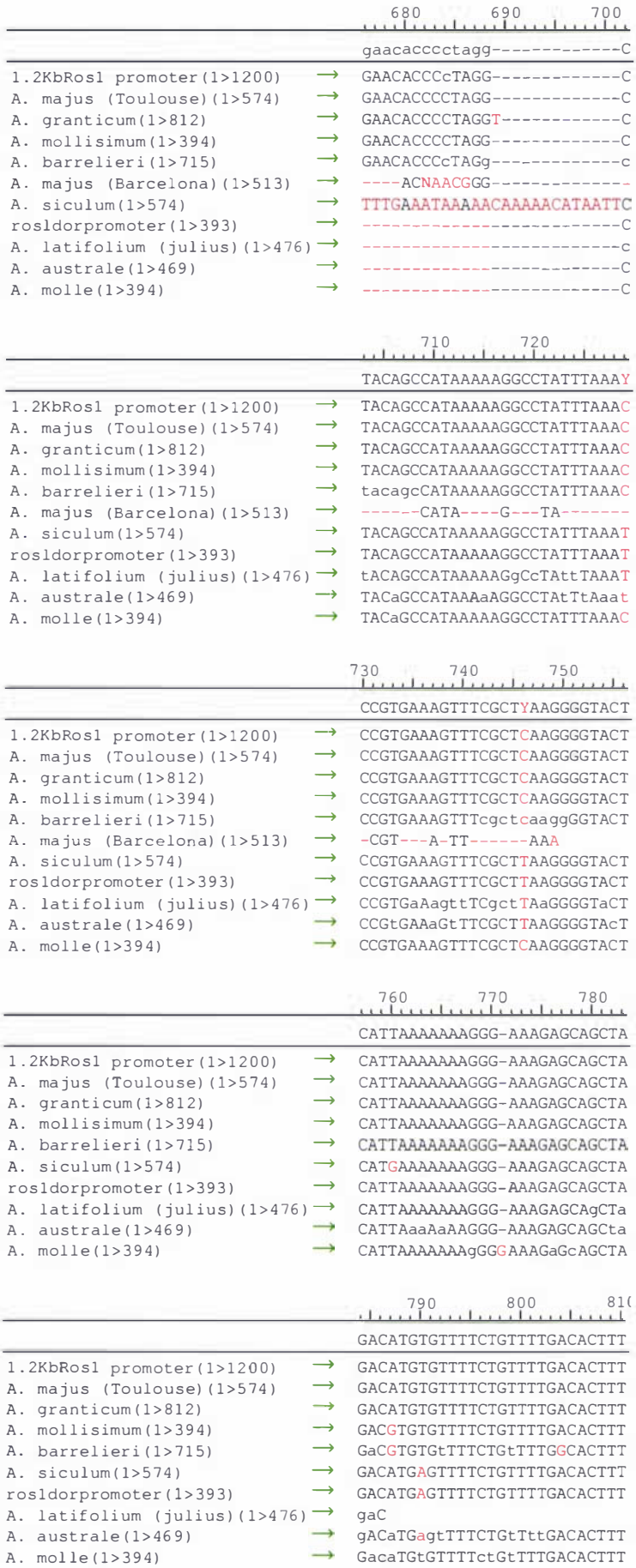
680 690 700
gaacaccctagg----------C
1.2KbRos1 promoter(1>1200) GAACACCCcTAGG----------C
A. majus (Toulouse)(1>574) GAACACCCCTAGG----------C
A. granticum(1>812) GAACACCCCTAGGT----------C
A. mollisimum(1>394) GAACACCCCTAGG----------C
A. barrelieri(1>715) GAACACCCcTAGg----------c
A. majus (Barcelona)(1>513) ----ACNAACGGG----------
A. siculum(1>574) TTTGAAATAAAAACAAAAACATAATTC
rosldorpromoter(1>393) ----------C
A. latifolium (julius)(1>476) ----------c
A. australe(1>469) ----------C
A. molle(1>394) ----------C
710 720
TACAGCCATAAAAAGGCCTATTTAAAY
1.2KbRos1 promoter(1>1200) TACAGCCATAAAAAGGCCTATTTAAAC
A. majus (Toulouse)(1>574) TACAGCCATAAAAAGGCCTATTTAAAC
A. granticum(1>812) TACAGCCATAAAAAGGCCTATTTAAAC
A. mollisimum(1>394) TACAGCCATAAAAAGGCCTATTTAAAC
A. barrelieri(1>715) tacagcCATAAAAAGGCCTATTTAAAC
A. majus (Barcelona)(1>513) ------CATA----G---TA-------
A. siculum(1>574) TACAGCCATAAAAAGGCCTATTTAAAT
rosldorpromoter(1>393) TACAGCCATAAAAAGGCCTATTTAAAT
A. latifolium (julius)(1>476) tACAGCCATAAAAAGgCcTAttTAAAT
A. australe(1>469) TACaGCCATAAAaAGGCCTAtTtAaat
A. molle(1>394) TACaGCCATAAAAAGGCCTATTTAAAC
730 740 750
CCGTGAAAGTTTCGCTYAAGGGGTACT
1.2KbRos1 promoter(1>1200) CCGTGAAAGTTTCGCTCAAGGGGTACT
A. majus (Toulouse)(1>574) CCGTGAAAGTTTCGCTCAAGGGGTACT
A. granticum(1>812) CCGTGAAAGTTTCGCTCAAGGGGTACT
A. mollisimum(1>394) CCGTGAAAGTTTCGCTCAAGGGGTACT
A. barrelieri(1>715) CCGTGAAAGTTTcgctcaaggGGTACT
A. majus (Barcelona)(1>513) -CGT---A-TT------AAA
A. siculum(1>574) CCGTGAAAGTTTCGCTTAAGGGGTACT
rosldorpromoter(1>393) CCGTGAAAGTTTCGCTTAAGGGGTACT
A. latifolium (julius)(1>476) CCGTGaAagttTCgctTAaGGGGTaCT
A. australe(1>469) CCGtGAAaGtTTCGCTTAAGGGGTAcT
A. molle(1>394) CCGTGAAAGTTTCGCTCAAGGGGTACT
760 770 780
CATTAAAAAAAGGG-AAAGAGCAGCTA
1.2KbRos1 promoter(1>1200) CATTAAAAAAAGGG-AAAGAGCAGCTA
A. majus (Toulouse)(1>574) CATTAAAAAAAGGG-AAAGAGCAGCTA
A. granticum(1>812) CATTAAAAAAAGGG-AAAGAGCAGCTA
A. mollisimum(1>394) CATTAAAAAAAGGG-AAAGAGCAGCTA
A. barrelieri(1>715) CATTAAAAAAAGGG-AAAGAGCAGCTA
A. siculum(1>574) CATGAAAAAAAGGG-AAAGAGCAGCTA
rosldorpromoter(1>393) CATTAAAAAAAGGG-AAAGAGCAGCTA
A. latifolium (julius)(1>476) CATTAAAAAAAGGG-AAAGAGCAgCTa
A. australe(1>469) CATTAaaAaAAGGG-AAAGAGCAGCta
A. molle(1>394) CATTAAAAAAAgGGGAAAGaGcAGCTA
790 800 81(
GACATGTGTTTTCTGTTTTGACACTTT
1.2KbRos1 promoter(1>1200) GACATGTGTTTTCTGTTTTGACACTTT
A. majus (Toulouse)(1>574) GACATGTGTTTTCTGTTTTGACACTTT
A. granticum(1>812) GACATGTGTTTTCTGTTTTGACACTTT
A. mollisimum(1>394) GACGTGTGTTTTCTGTTTTGACACTTT
A. barrelieri(1>715) GaCGTGTGtTTTCTGtTTTGGCACTTT
A. siculum(1>574) GACATGAGTTTTCTGTTTTGACACTTT
rosldorpromoter(1>393) GACATGAGTTTTCTGTTTTGACACTTT
A. latifolium (julius)(1>476) gaC
A. australe(1>469) gACaTGagtTTTCTGtTttGACACTTT
A. molle(1>394) GacaTGtGTTTTctGtTTTGACACTTT


820
830
TAACGAACGGGCATAGTACGTATTAAA
1.2KbRos1 promoter(1>1200) → TAACGAACGGGCATAGTACGTATTAAA
A. majus (Toulouse)(1>574) → T
A. granticum(1>812) → TAACGAACGGGCATAGTACGTATTAAA
A. mollisimum(1>394) → TAACGAACGGGCATAGTACGTATTAAA
A. barrelieri(1>715) → TAACGAACGGgcaTAGTACGtAttaaa
A. siculum(1>574) → TAACGAACGGGCATAGTACGTATTAAA
ros1dorpromoter(1>393) → TAACGAACGGGCATAGTACGTATTAAA
A. australe(1>469) → TAACGA
A. molle(1>394) → TAACGAACGGgcATAGTACGtATtaaa
840
CGCCATG
1.2KbRos1 promoter(1>1200) → CGCAATG
A. granticum(1>812) → CGCCATG
A. mollisimum(1>394) → CGCCATG
A. barrelieri(1>715) → CGcCATG
A. siculum(1>574) → CGCCAT
ros1dorpromoter(1>393) → CGCCATG
A. molle(1>394) → cGcc

Appendix X: Sequence alignment between the *Rosea1* and *rosea1*^{dorsea} alleles

Alignment for exon 1 with the *Rosea1* sequence shown on the top strand and the *rosea1*^{dorsea} sequence shown on the bottom strand.

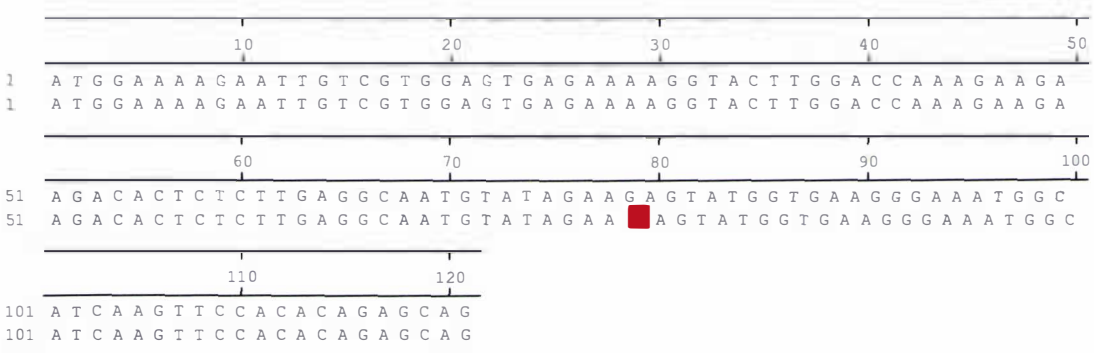

Alignment for intron 1 with the *Rosea1* sequence shown on the top strand and the *rosea1*^{dorsea} sequence shown on the bottom strand.

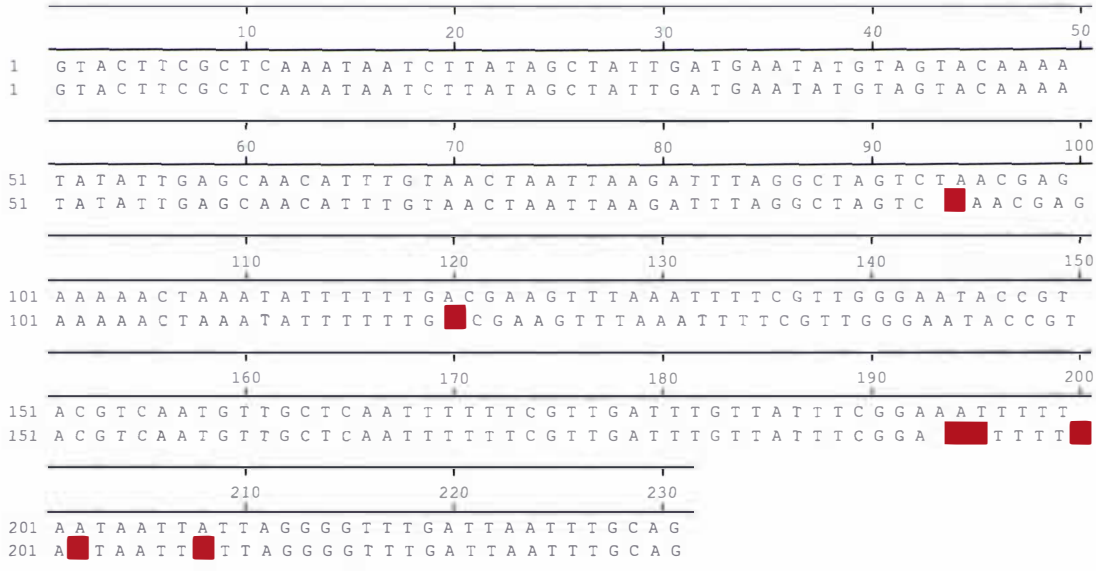

Alignment for exon 2 with the *Rosea1* sequence shown on the top strand and the *rosea1*^{dorsea} sequence shown on the bottom strand.

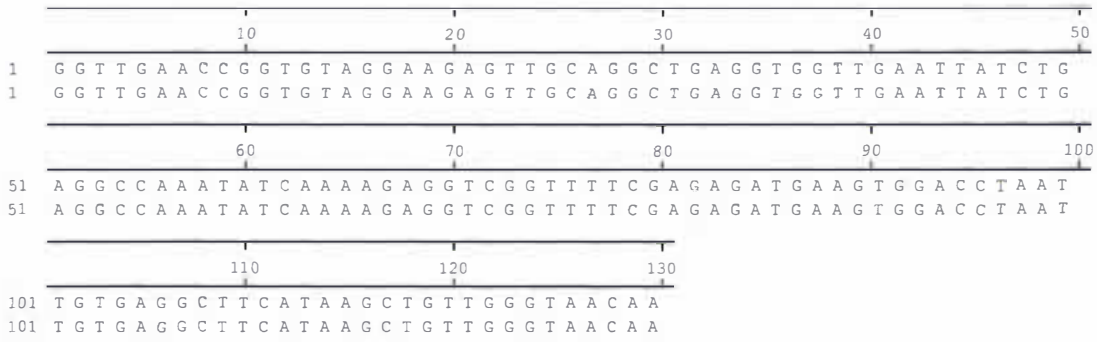

Alignment for intron 2 with the *Rosea1* sequence shown on the top strand and the *rosea1*^{dorsea} sequence shown on the bottom strand.

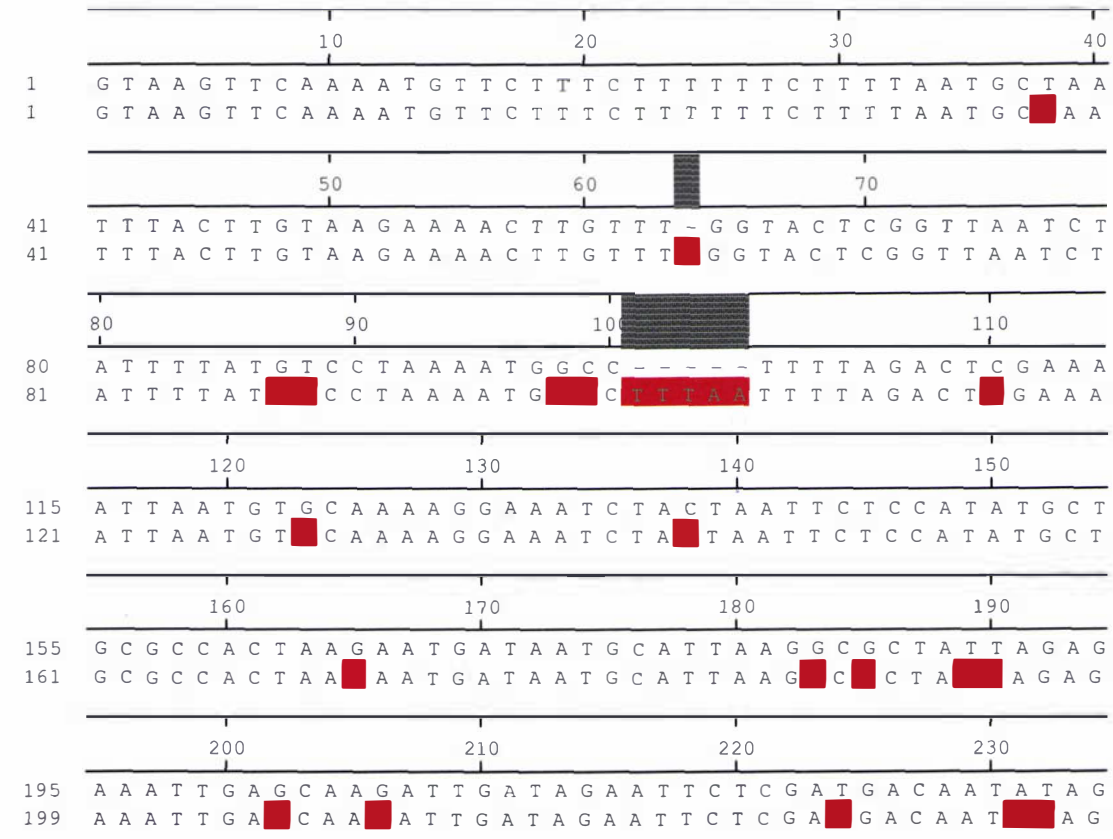

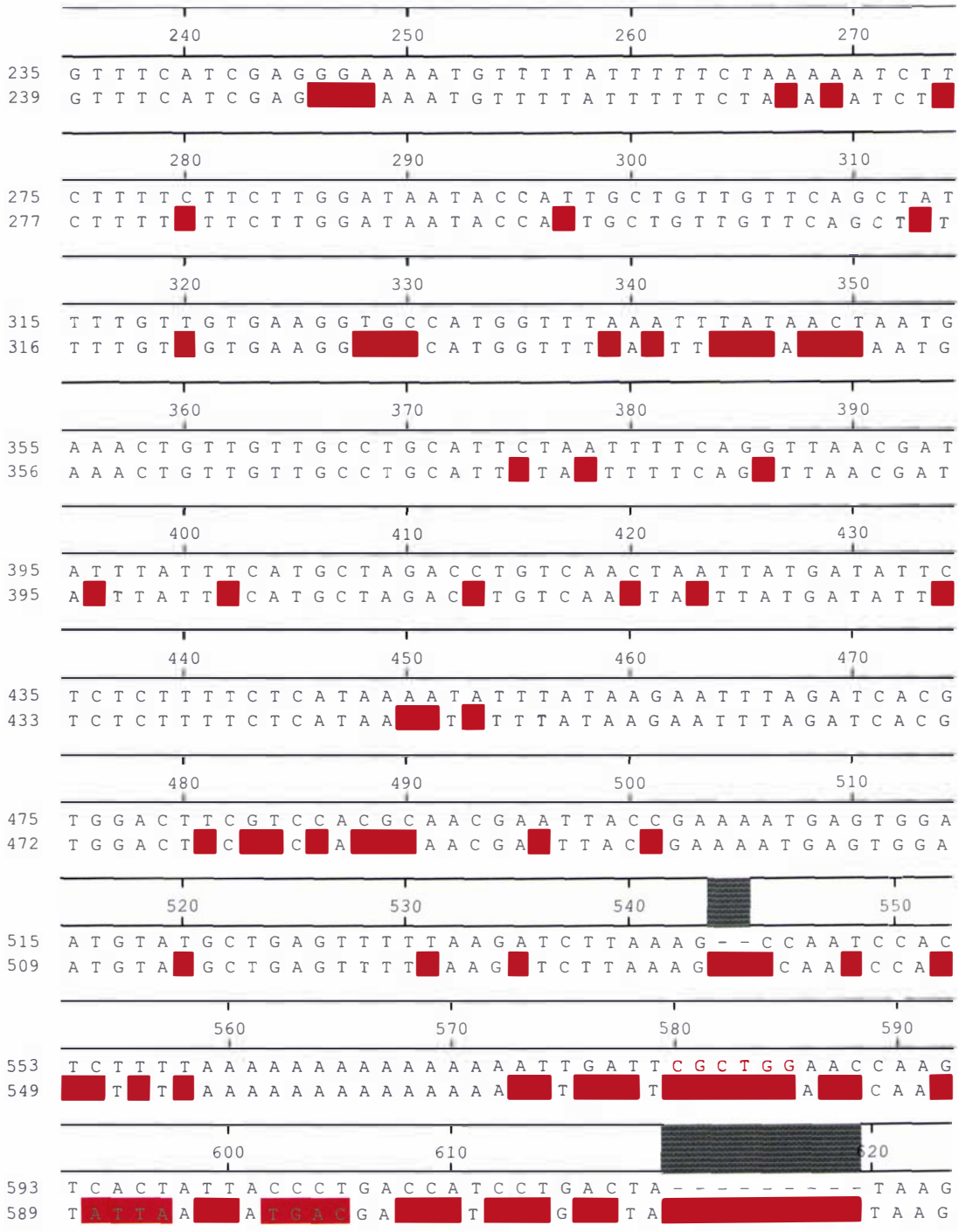

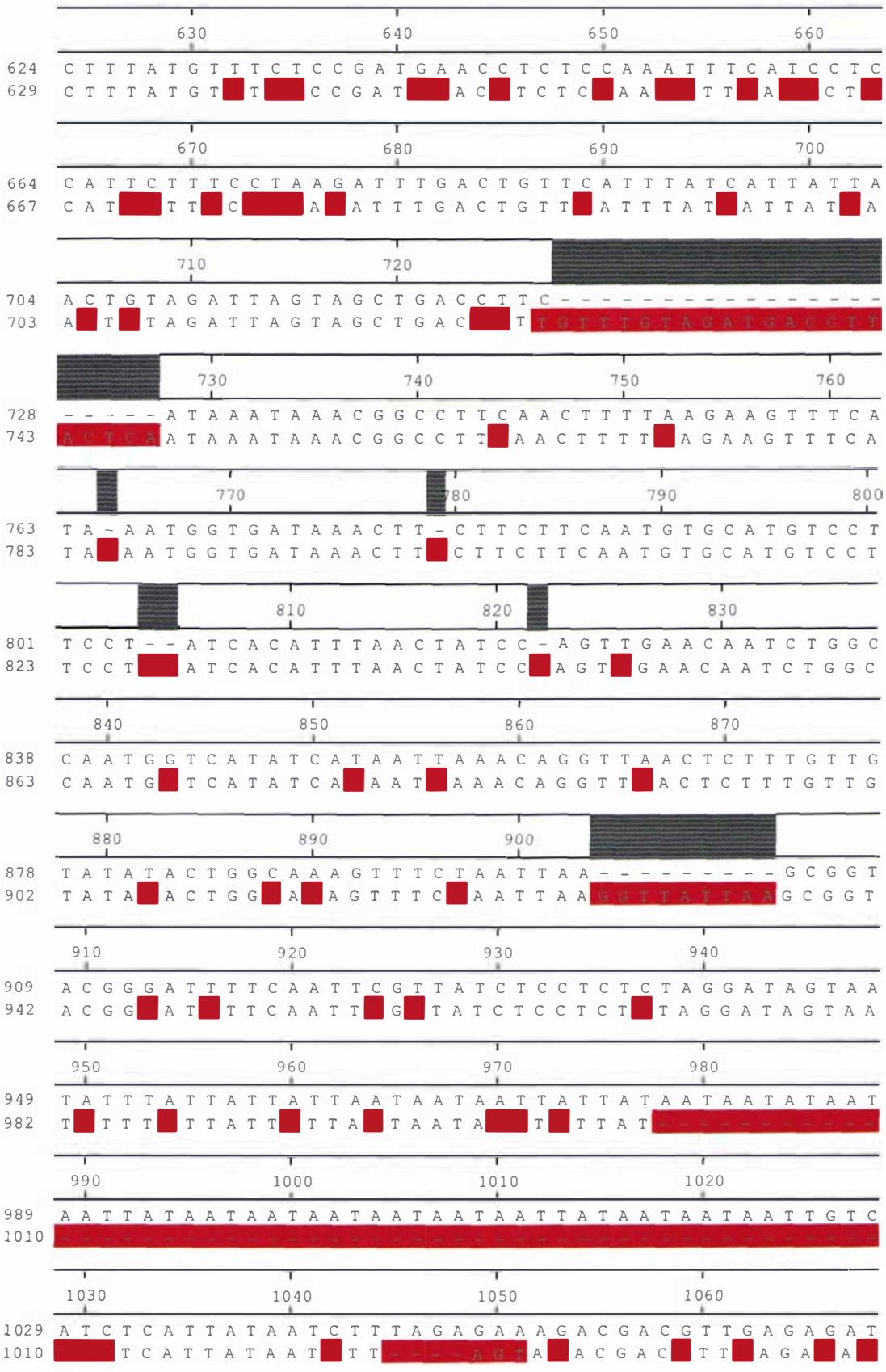

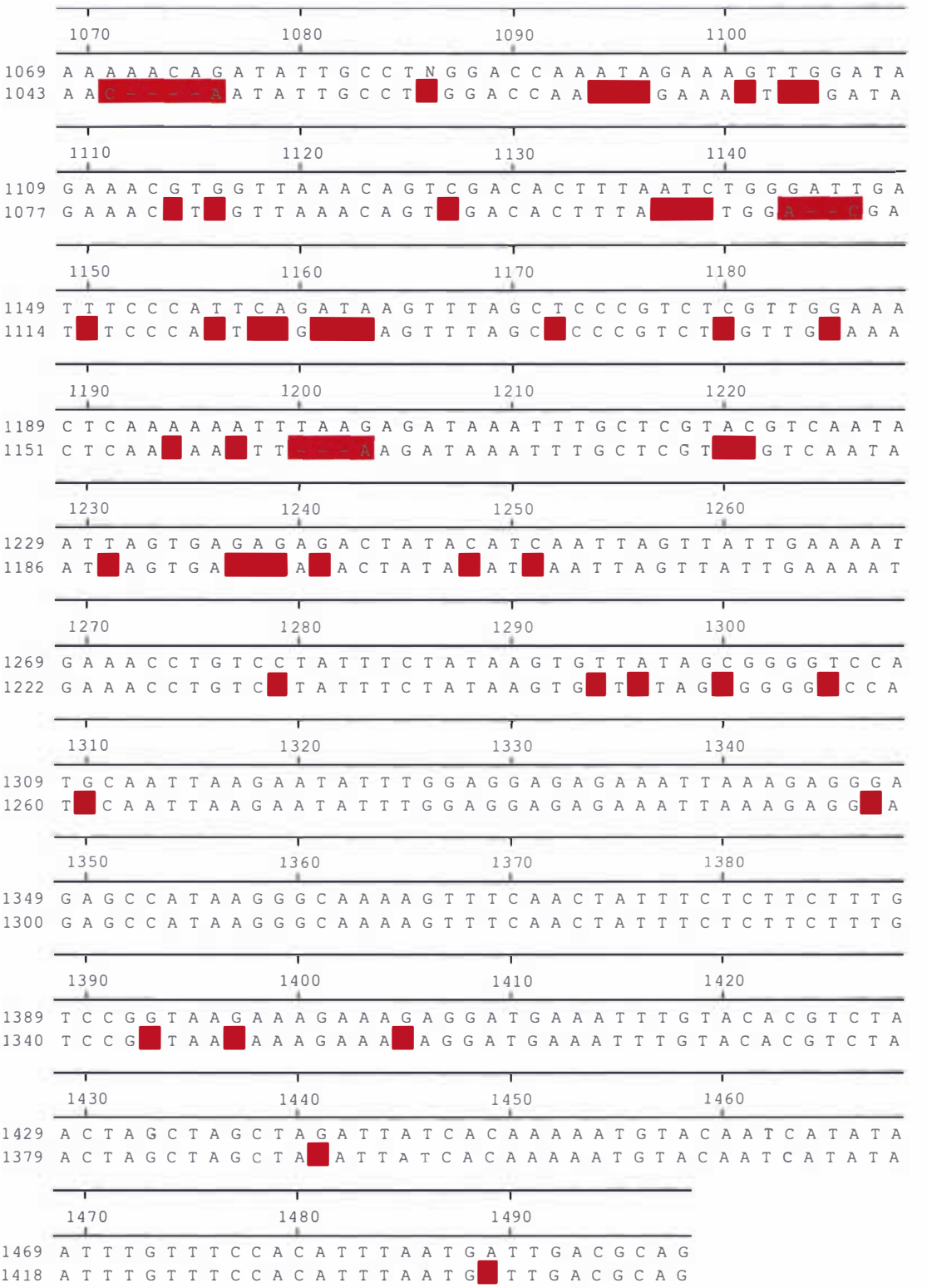
1070 1080 1090 1100
1069 AAAAACAGATATTGCCTNGGACCAAATAGAAAGTTGGATA
1043 AAC----ATATTGCCTGGACCAAGAAATGATA
1110 1120 1130 1140
1109 GAAACGTGGTTAAACAGTCGACACTTTAATCTGGGATTGA
1077 GAAACTGTTAAACAGTGACACTTTAGGA--CGA
1150 1160 1170 1180
1149 TTTCCCATTCAGATAAGTTTAGCTCCCGTCTCGTTGGAAA
1114 TTCCCATGAGTTTAGCCCCGTCTGTTGAAA
1190 1200 1210 1220
1189 CTCAAAAAATTTAAGAGATAAATTTGCTCGTACGTCAATA
1151 CTCAAAATT----AAGATAAATTTGCTCGTGTCAATA
1230 1240 1250 1260
1229 ATTAGTGAGAGAGACTATACATCAATTAGTTATTGAAAAT
1186 ATAGTGAAACTATAATAATTAGTTATTGAAAAT
1270 1280 1290 1300
1269 GAAACCTGTCCTATTTCTATAAGTGTTATAGCGGGGTCCA
1222 GAAACCTGTCTATTTCTATAAGTGTTAGGGGGCCA
1310 1320 1330 1340
1309 TGCAATTAAGAATATTTGGAGGAGAGAAATTAAAGAGGGA
1260 TCAATTAAGAATATTTGGAGGAGAGAAATTAAAGAGGA
1350 1360 1370 1380
1349 GAGCCATAAGGGCAAAAGTTTCAACTATTTCTCTTCTTTG
1300 GAGCCATAAGGGCAAAAGTTTCAACTATTTCTCTTCTTTG
1390 1400 1410 1420
1389 TCCGGTAAGAAAGAAAGAGGATGAAATTTGTACACGTCTA
1340 TCCGTAAAAAGAAAAGGATGAAATTTGTACACGTCTA
1430 1440 1450 1460
1429 ACTAGCTAGCTAGATTATCACAAAAATGTACAATCATATA
1379 ACTAGCTAGCTAATTATCACAAAAATGTACAATCATATA
1470 1480 1490
1469 ATTTGTTTCCACATTTAATGATTGACGCAG
1418 ATTTGTTTCCACATTTAATGTTGACGCAG

Alignment for exon 3 with the *Rosea1* sequence shown on the top strand and the *rosea1*^{dorsea} sequence shown on the bottom strand.

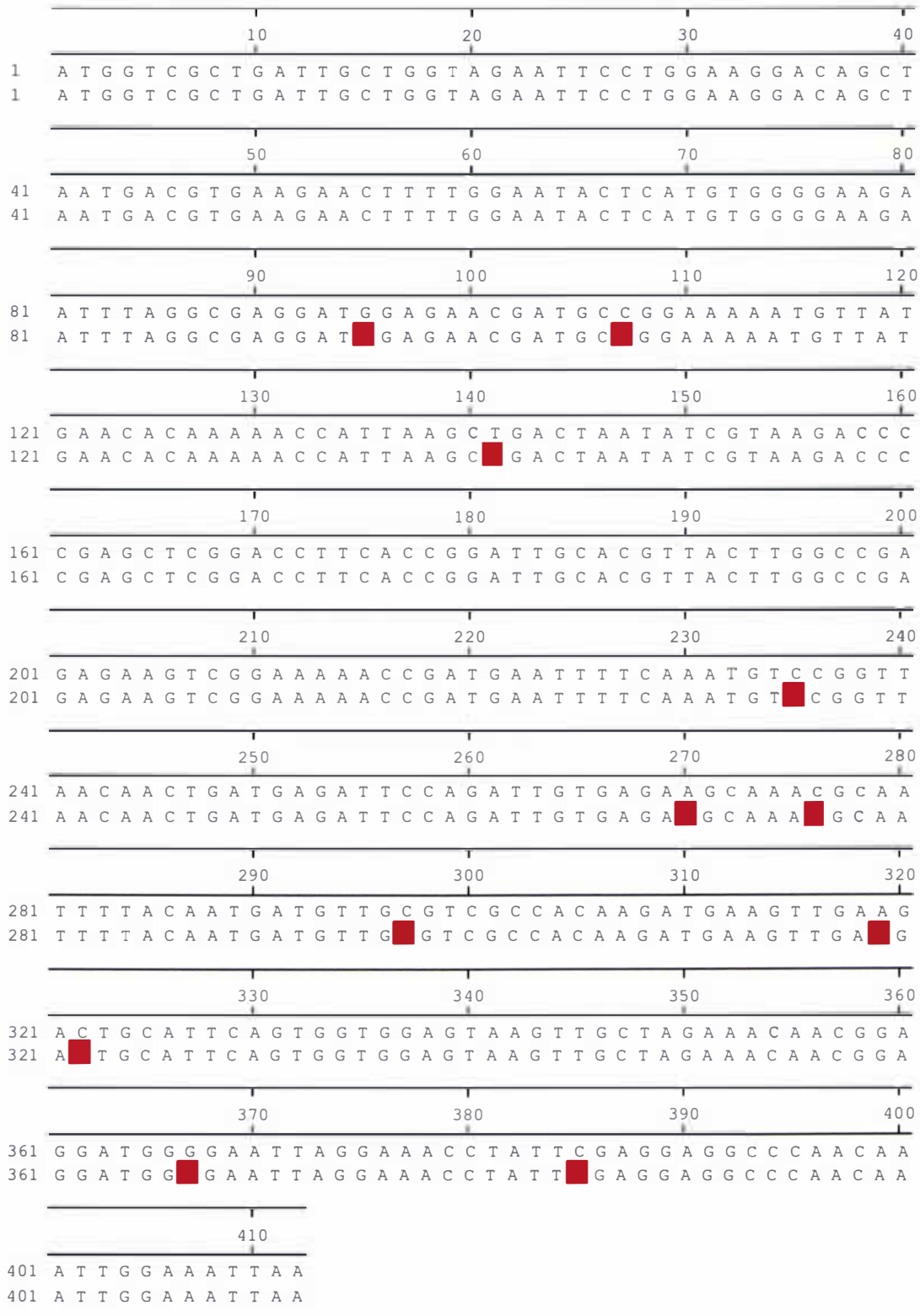

Bibliography

Aharoni, A., Vos, C. H. R. D., Wein, M., Sun, Z., Greco, R., Kroon, A., Mol, J. N. M. and O'Connell, A. P. (2001). The strawberry FaMYB1 transcription factor suppresses anthocyanin and flavonol accumulation in transgenic tobacco. Plant Journal *28*: 319-332.

Albert, S., Delseny, M. and Devic, M. (1997). BANYULS, a novel negative regulator of flavonoid biosynthesis in the *Arabidopsis* seed coat. Plant Journal *11*: 289-299.

Almeida, J., Carpenter, R., Robbins, T. P., Martin, C. and Coen, E. (1989). Genetic interactions underlying flower colour patterns in *Antirrhinum majus*. Genes & Development *3*: 1758-1767.

Angenent, G. C., Franken, J., Busscher, M., Weiss, D. and Vantunen, A. J. (1994). Co-suppression of the petunia homeotic gene *fbp2* affects the identity of the generative meristem. Plant Journal *5*: 33-44.

Asen, S., Norris, K. H. and Stewart, R. N. (1972). Copigmentation of aurone and flavone from petals of *Antirrhinum majus*. Phytochemistry *11*: 2739-2741.

Ballas, N., Wong, L. M., Ke, M. and Theologis, A. (1995). Two auxin-responsive domains interact positively to induce expression of the early indoleacetic acid-inducible gene *Ps-Iaa4/5*. Proceedings of the National Academy of Sciences of the United States of America *92*: 3483-3487.

Barnhart, K. N. (1999). Simplified PCR-mediated, linker-scanning mutagenesis. Biotechniques *26*: 624-625.

Bartlett, J. (1989). The genetic control of anthocyanin biosynthesis in *A. majus*. PhD Thesis, University of East Anglia, Norwich, United Kingdom.

Baudry, A., Heim, M. A., Durbreucq, B., Caboche, M., Weisshaar, B. and Lepiniec, L. (2004). TT2, TT8, and TTG1 synergistically specify the expression of BANYULS and proanthocyanidin biosynthesis in *Arabidopsis thaliana*. Plant Journal *39*: 366-380.

Berger, S. (1999). Histone acytylases and transcriptional activation. Current Opinion in Cell Biology *11*: 336-341.

Berk, A. J. (1999). Activation of RNA polymerase II transcription. Current Opinion in Cell Biology *11*: 330-335.

Bey, M., Mueller, B. M., Lauri, A. and Zachgo, S. (2002). Downstream of DEFICIENS: towards the isolation of target genes. Flowering Newsletter *34*: 19-26.

Bey, M., Stuber, K., Fellenberg, K., Schwarz-Sommer, Z., Sommer, H., Saedler, H. and Zachgo, S. (2004). Characterization of *Antirrhinum* petal development and identification of target genes of the class B MADS box gene DEFICIENS. Plant Cell *16*: 3197-3215.

Borevitz, J. O., Xia, Y. J., Blount, J., Dixon, R. A. and Lamb, C. (2000). Activation tagging identifies a conserved MYB regulator of phenylpropanoid biosynthesis. Plant Cell *12*: 2383-2393.

Brummell, D. A., Balint-Kurti, P. J., Harpster, M. H., Palys, J. M., Oeller, P. W. and Gutterson, N. (2003). Inverted repeat of a heterologous 3'-untranslated region for high-efficiency, high-throughput gene silencing. Plant Journal *33*: 793-800.

Burr, F. A., Burr, B., Scheffler, B. E., Blewitt, M., Wienand, U. and Matz, E. C. (1996). The maize repressor-like gene *intensifier1* shares homology with the *r1/b1* multigene family of transcription factors and exhibits missplicing. Plant Cell *8*: 1249-1259.

Busk, P. K. and Pages, M. (1997). Microextraction of nuclear proteins from single maize embryos. Plant Molecular Biology Reporter *15*: 371-376.

Cai, G. P., Shen, Z. W., Yu, X. L., Zheng, C. X., Liu, S. R., Liang, J. F., Zhao, N. M., Lin, Z. P., Yu, C. H., Peng, L. H., Ma, M., Wang, H. and Lai, B. T. (1996). Biolistic process and factors influencing its validity. Progress in Natural Science *6*: 577-585.

Carey, C. C., Strahle, J. T., Selinger, D. A. and Chandler, V. L. (2004). Mutations in the pale aleurone color1 regulatory gene of the *Zea mays* anthocyanin pathway have distinct phenotypes relative to the functionally similar TRANSPARENT TESTA GLABRA1 gene in *Arabidopsis thaliana*. Plant Cell *16*: 450-464.

Chandler, V. L., Radicella, J. P., Robbins, T. P., Chen, J. C. and Turks, D. (1989). Two regulatory genes of the maize anthocyanin pathway are homologous-isolation of *B* utilizing *R* genomic sequences. Plant Cell *1*: 1175-1183.

Chang, S. M., Lu, Y. and Rausher, M. D. (2005). Neutral evolution of the nonbinding region of the anthocyanin regulatory gene *Ipmyb1* in *Ipomoea*. Genetics *170*: 1967-1978.

Chen, R., Silver, D. L. and de Bruijn, F. J. (1998). Nodule parenchyma-specific expression of the *Sesbania rostrata* early nodulin gene SrEnod2 is mediated by its 3' untranslated region. Plant Cell *10*: 1585-1602.

Chomczynski, P. (1992). One hour downward alkaline capillary transfer for blotting DNA and RNA. Analytical Biochemistry *201*: 134-139.

Church, G. M. and Gilbert, W. (1984). Genomic sequencing. Proceedings of the National Academy of Science of the United States of America *81*: 1991-1995.

Cocksull, K. E. (1985). *Antirrhinum majus*. In:Handbook of flowering. Halevy, A. H. (ed.) CRC Press Inc, Florida: 476-481.

Coe, E. H., Jr., Neuffer, M. G. and Hoisington, D. A. (1988). The genetics of corn. In: Corn and Corn Imporvement. Sprague, G. F. and Dudley, J. (eds.) American Society of Agronomy, Madison: 81-258.

Coen, E. S., Carpenter, R. and Martin, C. (1986). Transposable elements generate novel spaial patterns of gene expression in *Antirrhinum majus*. Cell *47*: 285-296.
Collette, V. E., Jameson, P. E., Schwinn, K. E., Umaharan, P. and Davies, K. M. (2004). Temporal and spatial expression of flavonoid biosynthetic genes in flowers of *Anthurium andraeanum*. Physiologia Plantarum *122*: 297-304.

Cone, K. C., Burr, F. A. and Burr, B. (1986). Molecular analysis of the maize anthocyanin regulatory locus *C1*. Proceedings of the National Academy of Sciences of the United States of America *83*: 9631-9635.

Cone, K. C., Cocciolone, S. M., Burr, F. A. and Burr, B. (1993a). Maize anthocyanin regulatory gene *P1* is a duplicate of *C1* that functions in the plant. Plant Cell *5*: 1795-1805.

Cone, K. C., Cocciolone, S. M., Moehlenkamp, C. A., Weber, T., Drummond, B. J., Tagliani, L., Bowen, B. and Perrot, G. H. (1993b). Role of the regulatory gene *pl* in the photocontrol of maize anthocyanin pigmentation.Plant Cell *5*: 1807-1816.

Consonni, G., Geuna, F., Gavazzi, G. and Tonelli, C. (1993). Molecular homology among members of the *R* gene family in maize. Plant Journal *3*: 335-346.

Courey, A. J. (2001). Regulatory transcription factors and cis-regulatory regions. In: Tanscription factors. Locker, J. (ed.) BIOS Scientific Publishers, Oxford No 1: 336.

Dai, S. H., Zheng, P., Marmey, P., Zhang, S. P., Tian, W. Z., Chen, S. Y., Beachy, R. N. and Fauquet, C. (2001). Comparative analysis of transgenic rice plants obtained by *Agrobacterium*-mediated transformation and particle bombardment. Molecular Breeding *7*: 25-33.

Damiani Jr., R. D. J. and Wessler, S. R. (1993). An upstream open reading frame represees expression of *Lc,* a member of the *R/B* family of maize transcriptional activators. Proceedings of the National Academy of Sciences of the United States of America *90*: 8244-8248.

Davies, B., Egea Cortines, M., Silva, E. D., Saedler, H. and Sommer, H. (1996). Multiple interactions amongst floral homeotic MADS box proteins. EMBO *15*: 4330-4343.

Davies, K. M. and Schwinn, K. E., Eds. (1997). Flower colour. In: Biotechnology of Ornamental Plants. CAB International, London.

Davies, K. M., Ed. (2004). An introduction to plant pigments in biology and commerce. In: Plant Pigments and Their Manipulation, Blackwell Publishing, London.

De Jong, W. S., Eannetta, N. T., De Jong, D. M. and Bodis, M. (2004). Candidate gene analysis of anthocyanin pigmentation loci in the *Solanaceae*. Theoretical and Applied Genetics *108*: 423-432.

deVetten, N., Quattrocchio, F., Mol, J. and Koes, R. (1997). The *an11* locus controlling flower pigmentation in petunia encodes a novel WD-repeat protein conserved in yeast, plants, and animals. Genes & Development *11*: 1422-1434.

Deyholos, M. K. and Sieburth, L. E. (2000). Seperable whorl-specific expression and negative regulation by enhancer elements within the AGAMOUS second intron. The Plant Cell *12*: 1799-1810.

Durfee, T., Becherer, K., Chen, P. L., Yeh, S. H., Yang, Y., Killburn, A. E., Lee, W. H. and Elledge, S. J. (1993). The retinoblastoma protein assocaites with the protein phosphatase type 1 catalytic subunit. Genes & Development *7*: 555-569.

Egea-Cortines, M., Saedler, H. and Sommer, H. (1999). Ternary complex formation between MADS-box proteins SQUAMOSA, DEFICIENS and GLOBOSA is involved in the control of floral architeciture in *Antirrhinum majus*. EMBO *18*: 5370-5379.

Eulgem T, Rushton P. J, Robatzek S and Somssich, S. I. (2000). The WRKY superfamily of plant transcription factors. Trends in Plant Science *5*: 199-206.

Finer, J. L., Vain, P., Jones, M. W. and McMullen, M. D. (1992). Development of the particle inflow gun for DNA delivery to plant cells. Plant Cell Reports *11*: 323-328.

Geissman, T. A., Jorgensen, E. C. and Johnson, B. L. (1954). The chemistry of flower pigmentation in *Antirrhinum majus*. Arch. Biochem. Biophys *49*: 368-388.

Gerats, A. G. M., Beld, M., Huits, H. and Prescott, A. (1989). Gene tagging using homologous and heterologous transposable elements. Developmental Genetics *10*: 561-568.

Goff, S. A., Cone, K. C. and Fromm, M. E. (1991). Identification of functional domains in the maize transcriptional activator C1 - comparison of wild-type and dominant inhibitor proteins. Genes & Development *5*: 298-309.

Goff, S. A., Cone, K. C. and Chandler, V. (1992). Functional analysis of the transcriptional activator encoded by the maize B gene: evidence for a direct functional interaction between two classes of regulatory proteins. Genes & Development *6*: 864-875.

Goodrich, J., Carpenter, R. and Coen, E. S. (1992). A common gene regulates pigmentation pattern in diverse plant-species. Cell *68*: 955-964.

Grotewold, E., Drummond, B. J., Bowen, B. and Peterson, T. (1994). The *myb*-homologous P gene controls phlobaphene pigmentation in maize floral organs by directly activating a flavonoid biosynthetic gene subset. Cell *76*: 543-553.

Grotewold, E., Sainz, M. B., Tagliani, L., Hernandez, J. M., Bowen, B. and Chandler, V. L. (2000). Identification of the residues in the Myb domain of maize C1 that specify the interaction with the bHLH cofactor R. Proceedings of the National Academy of Sciences of the United States of America *97*: 13579-13584.

Grotewold, E. (2004). The challanges of moving chemicals within and out of cells: insights into the transport of plant natural products. Planta *219*: 906-909.

Grotewold, E. (2006). The genetics and biochemistry of floral pigments. Annual Review of Plant Biology *57*: 761-780.

Gutierrz-Cortines, M. E. and Davies, B. (2000). Beyond the ABCs: ternary complex formation in the control of floral organ identity. Trends in Plant Science *5*: 471-476.

Hartung, W., Sauter, A. and Hose, E. (2002). Abscisic acid in the xylem: where does it come from, where does it go to? Journal of Experimental Botany *53*: 27-32.

Hamilton, D. A., Schwarz, Y. H. and Mascarenhas, J. P. (1998). A monocot pollen-specific promoter contains separable pollen-specific and quantitative elements. Plant Molecular Biology *38*: 663-669.

Hernandez, J. M., Heine, G. F., Irani, N. G., Feller, A., Kim, M. G., Matulnik, T., Chandler, V. L. and Grotewold, E. (2004). Different mechanisms participate in the R-dependent activity of the R2R3 MYB transcription factor C1. Journal of Biological Chemistry *279*: 48205-48213.

Higo, K., Ugawa, Y., Iwamoto, M. and Korenaga, T. (1999). Plant cis-acting regulatory DNA elements (PLACE) database. Nucleic Acids Research *27*: 297-300.

Hobbs, S. L. A., Kpodar, P. and Delong, C. M. O. (1990). The effect of T-DNA copy number, position and methylation on reporter gene-expression in tobacco transformants. Plant Molecular Biology *15*: 851-864.

Horsch, R. B., Fry, J. E., Hoffmann, N. L., Eichholtz, D., Rogers, S. G. and Fraley, R. T. (1985). A simple and general-method for transferring genes into plants. Science *227*: 1229-1231.

Hwang, C. F., Lin, Y., Dsouza, T. and Cheng, C. L. (1997). Sequences necessary for nitrate-dependent transcription of *Arabidopsis* nitrate reductase genes. Plant Physiology *113*: 853-862.

Iida, A., Nagasawa, A. and Oeda, K. (1995). Positive and negative *cis*-regulatory regions in the soybean glycinin promoter identified by quantitative transient gene-expression. Plant Cell Reports *14*: 539-544.

Jackson, D., Culianezmacia, F., Prescott, A. G., Roberts, K. and Martin, C. (1991). Expression patterns of *myb* genes from *Antirrhinum* flowers. Plant Cell *3*: 115-125.

Jackson, D., Roberts, K. and Martin, C. (1992). Temporal and spatial control of expression of anthocyanin biosynthetic genes in developing flower of *Antirrhinum*. Plant Journal *2*: 425-434.

Jackson, J. A., Fuglevand, G., Brown, B. A., Shaw, M. J. and Jenkins, G. I. (1995). Isolation of *Arabidopsis* mutants altered in the light-regulation of chalcone synthase gene expression using a transgenic screening approach. Plant Journal *8*: 369-380.

Jaffe, F. W., Tattersall, A. and Glover, B. J. (2007). A truncated MYB transcription factor from *Antirrhinum majus* regulates epidermal cell outgrowth. Journal of Experimental Botany *58*: 1515-1524.

Jefferson, R. A., Kavanagh, T. A. and Bevan, M. W. (1987). GUS Fusions: β–Glucoronidase as a sensitive and versatile gene marker in higher plants. EMBO *6*: 3901-3907.

Jeon, J. S., Lee, S., Jung, K. H., Jun, S. H., Kim, C. and An, G. (2000). Tissue-preferential expression of a rice alpha-tubulin gene, OsTubA1, mediated by the first intron. Plant Physiology *123*: 1005-1014.

Jin, H., Cominelli, E., Bailey, P., Parr, A., Mehrtens, F., Jones, J., Tonelli, C., Weisshaar, B. and Martin, C. (2000). Transcriptional repression by AtMYB4 controls production of UV-protecting sunscreens in *Arabidopsis*. EMBO *19*: 6150-6161.

Johnson, C. S., Kolevski, B. and Smyth, D. R. (2002). TRANSPARENT TESTA GLABARA2, a trichome and seed coat development gene of *Arabidopsis*, encodes a WRKY transcription factor. Plant Cell *14*: 1359-1375.

Kao, C. Y., Cocciolone, S. M., Vasil, I. K. and McCarty, D. R. (1996). Localization and interaction of the cis-acting elements for abscisic acid, VIVIPAROUS1, and light activation of the *C1* gene of maize. Plant Cell *8*: 1171-1179.

Kingston, R. E., Ed. (2001). DNA-Protein interactions. In: Current Protocols in Molecular Biology. John Wiley & Sons, Inc., New York.

Kobayashi, S., Goto-Yamamoto, N. and Hirochika, H. (2004). Retrotransposon-induced mutations in grape skin color. Science *304*: 982.

Kobayashi, S., Yamamoto, N. G. and Hirochika, H. (2005). Association of VvmybA1 gene expression with anthocyanin production in grape (*Vitis vinifera*) skin - color mutants. Journal of the Japanese Society for Horticultural Science *74*: 196-203.

Kranz, H., Denekamp, M., Greco, R., Jin, H. and Levya, A. (1998). Towards functional characterisation of the memebers of the *R2R3-MYB* gene family from *Arabidopsis thaliana*. Plant Journal *16*: 236-276.

Kubo, H., Peeters, A. J. M., Aarts, M. G. M., Pereira, A. and Koornneef, M. (1999). ANTHOCYANINLESS2, a homeobox gene affecting anthocyanin distribution and root development in *Arabidopsis*. Plant Cell *11*: 1217-1226.

Kumar, S. and Fladung, M. (2001). Gene stability in transgenic aspen (*Populus*). II. molecular characterization of variable expression of transgene in wild and hybrid aspen. Planta *213*: 731-740.

Larkin, J. C., Oppenheimer, D. G., Pollock, S. and Marks, M. D. (1993). *Arabidopsis* GLABROUS1 gene requires downstream sequences for function. Plant Cell *5*: 1739-1748.

Latchman, D. S. (2004). Eukaryotic transcription factors. Elsever Academis Press, London.

Lee, T. I. and Young, R. A. (2000). Transcription of eukaryotic protein-coding genes. Annual Review of Genetics *34*: 77-137.

Lesnick, M. L. and Chandler, V. L. (1998). Activation of the maize anthocyanin gene *a2* is mediated by an element conserved in many anthocyanin promoters. Plant Physiology *117*: 437-445.

Lodish, H., Berk, A. J., Zipursky, S. L., Matsudaira, P., Baltimore, D. and Darnell, J. (2001). Recombinant DNA and genomics. In: Molecular Cell Biology. Lodish, H. Berk, A. J., Zipursky, S. L.*et al.* (eds.). W. H. Freeman and Company, New York.

Ludwig, S. R., Habera, L. F., Dellaporta, S. L. and Wessler, S. R. (1989). *Lc*, a member of the maize *R*-gene family responsible for tissue-specific anthocyanin production, encodes a protein similar to transcriptional activators and contains the Myc-homology region. Proceedings of the National Academy of Sciences of the United States of America *86*: 7092-7096.

Ludwig, S. R. and Wessler, S. R. (1990). Maize *R* gene family: tissue-specific helix-loop-helix proteins. Cell *62*: 849-851.

Martin, C., Carpenter, R., Sommer, H., Saedler, H. and Coen, E. (1985). Molecular analysis of instability in flower pigmentation of *Antirrhinum majus*, following isolation of the pallida locus by transposon tagging. EMBO *4*(*7*): 1625-1630.

Martin, C., Prescott, A., Mackay, S., Bartlett, J. and Vrijlandt, E. (1991). Control of anthocyanin biosynthesis in flowers of *Antirrhinum majus*. Plant Journal *1*: 37-49.

Martin, C. and Gerats, T. (1993). Control of pigment biosynthesis genes dring petal development. Plant Cell *5*: 11253-1264.

Martin, C. and Paz-Ares, J. (1997). MYB transcription factors in plants. Trends in Genetics *13*: 67-73.

McCarty, D. R., Carson, C. B., Stinard, P. S. and Robertson, D. S. (1989). Molecular analysis of viviparous-1: An abscisic acid-insensitive mutant of maize. Plant Cell *1*: 523-532.

McCarty, D. R., Hattori, T., Carson, C. B., Vasil, V., Lazar, M. and Vasil, I. K. (1991). The *Viviparous-1* developmental gene of maize encodes a novel transcriptional activator. Cell *66*: 895-905.

Mehlo, L., Mazithulela, G., Twyman, R. M., Boulton, M. I., Davies, J. W. and Christou, P. (2000). Structural analysis of transgene rearrangements and effects on expression in transgenic maize plants generated by particle bombardment. Maydica *45*: 277-287.

Mehrtens, F., Kranz, H., Bednarek, P. and Weisshaar, B. (2005). The *Arabidopsis* transcription factor MYB12 is a flavonol-specific regulator of phenylpropanoid biosynthesis. Plant Physiology *138*: 1083-1096.

Meijer, A. H., de Kam, R. J., d'Erfurth, I., Shen, W. and Hoge, J. H. C. (2000). HD-Zip proteins of families I and II from rice: interactions and functional properties. Molecular & General Genetics *263*: 12-21.

Mena, M., Cejudo, F. J., Isabel-Lamoneda, I. and Carbonero, P. (2002). A role for the DOF transcription factor BPBF in the regulation of gibberellin-responsive genes in barley aleurone. Plant Physiology *130*: 111-119

Meyer, V. E. and Young, R. A. (1998). RNA polymerase II holoenzyme and subcomplexes. Journal of Biological Chemistry (*273*): 27757-27760.

Mol, J., Grotewold, E. and Koes, R. (1998). How genes paint flowers and seeds. Trends in Plant Science *3*: 212-217.

Morita, A., Umemura, T., Kuroyanagi, M., Futsuhara, Y., Perata, P. and Yamaguchi, J. (1998). Functional dissection of a sugar-repressed alpha-amylase gene (*RamyIA*) promoter in rice embryos. FEBS Letters *423*: 81-85

Morita, Y., Saitoh, M., Hoshino, A., Nitasaka, E. and Lida, S. (2006). Isolation of cDNAs for R2R3-MYB, bHLH, and WDR transcriptional regulators and identification of *c* and *ca* mutations conferring white flowers in the japanese morning glory. Plant and Cell Physiology *47*: 457-470.

Murashige, T. and Skoog, F. (1962). A revised medium for rapid growth and bioassays with tobacco tissue cultures. Physiologia Plantarum *15*: 743-747.

Nakayama, T., Suzuki, H. and Nishino, T. (2003). Anthocyanin acyltransferases: specificities, mechanisms, phylogenetics and applications. Journal of Molecular Catalysis. B, Enzymatic *23*: 117-132.

Nan, G. L. and Kuehnle, A. R. (1995). Factors affecting gene delivery by particle bombardment of *Dendrobium* orchids. In Vitro Cellular & Developmental Biology-Plant *31*: 131-136.

Nesi, N., Debeaujon, I., Jond, C., Pelletier, G., Caboche, M. and Lepiniec, L. (2000). The TT8 gene encodes a basic helix-loop-helix domain protein required for expression of DFR and BAN genes in *Arabidopsis* siliques. Plant Cell *12*: 1863-1878.

Nesi, N., Jond, C., Debeaujon, I., Caboche, M. and Lepiniec, L. (2001). The Arabidopsis TT2 gene encodes an R2R3 MYB domain protein that acts as a key determinant for proanthocyanidin accumulation in developing seed. Plant Cell *13*: 2099-2114.
Nishiuchi T, Shinshi H and K., S. (2004). Rapid and transient activation of transcription of the *ERF3* gene by wounding in tobacco leaves: Possible involvement of NtWRKYs and autorepression. Journal of Biological Chemistry *279*: 55355-55361.

Nesi, N., Debeaujon, I., Jond, C., Stewart, A. J., Jenkins, G. I., Caboche, M. and Lepiniec, L. (2002). The TRANSPARENT TESTA16 locus encodes the ARABIDOPSIS BSISTER MADS domain protein and is required for proper development and pigmentation of the seed coat. Plant Cell *14*: 2463-2479.

Nishiuchi, T., Shinshi, H., and Suzuki, K. (2004). Rapid and transient activation of transcription of the ERF3 gene by wounding in tobacco leaves - Possible involvement of NtWRKYs and autorepression. Journal of Biological Chemistry *279*): 55355-55361.

No, E. G. and Loopstra, C. A. (2000). Hormonal and developmental regulation of two arabinogalactan-proteins in xylem of loblolly pine (*Pinus taeda*). Physiologia Plantarum *110*: 524-529.

Onslow, M. W. (1925). The anthocyanin pigments of plants. Cambridge University Press, Cambridge.

Park, K.-I., Ishikawa, N., Morita, Y., Cho, J.-D., Hoshino, A. and Iida, S. (2007). A *bHLH* regulatory gene in the common morning glory, *Ipomoea purpurea*, controls

anthocyanin biosynthesis in flowers, proanthocyanidin and phytomelanin pigmentation in seeds, and seed trichome formation. Plant Journal *47*: 641-654.

Payne, C. T., Zhang, F., Lloyd, A. M. and (2000). GL3 encodes a bHLH protein that regulates trichome development in *Arabidopsis* through interaction with GL1 and TTG1. Genetics *156*: 1349-1362.

Paz-Ares, J., Ghosal, D., Wienand, U., Peterson, P. A. and Saedler, H. (1987). The regulatory C1 locus of *Zea mays* encodes a protein with homology to *myb* proto-oncogene products and with structural similairites to transcriptioanl activators. EMBO *6*: 3553-3558.

Perbal, M., Haughn, G. W., Saedler, H. and Schwarz-Sommer, Z. (1996). Non-cell-autonomous function of the *Antirrhinum* floral homeotic proteins DEFICIENS and GOLBOSA is exerted by their polar cell-to-cell trafficking. Development *122*: 3433-3441.

Perez-Rodrigues, M., Jaffe, F., Butelli, E., Glover, B. and Martin, C. (2005). Development of three different cell types is associated ith the activity if a spcific MYB transcription factor in the ventral petal of *Antirrhinum majus* flower. Development *132*: 359-370.

Perry, F., Ed. (1981). The Macdonald encyclopedia of plants & flowers. Macdonald general books, London.

Piattelli, M. (1981). The betalains: structure, biosynthesis and chemical taxonomy. In: The biochemistry of plants: A comprehensive treatise. Conn, E. E. (ed.). Acedemic Press, New York: 557-575.

Pilu, R., Piazza, P., Petroni, K., Ronchi, A., Martin, C. and Tonelli, C. (2003). *pl-bol3*, a complex allele of the anthocyanin regulatory *pl1* locus that arose in a naturally occurring maize population. Plant Journal *36*: 510-521.

Pnueli, L., Hareven, D., Broday, L., Hurwitz, C. and Lifschitz, E. (1994). The TM5 MADS box gene mediates organ differentiation in the three inner whorls of tomato flowers. Plant Cell *6*: 175-186.

Procissi, A., Dolfini, S., Ronchi, A. and Tonelli, C. (1997). Light-dependent spatial and temporal expression of pigment regulatory genes in developing maize seeds. Plant Cell *9*: 1547-1557.

Quattrocchio, F. (1994). Regulatory genes controlling flower pigmentaion in *Petunia hybrida*. PhD Thesis, Vrije University, Amsterdam, Holland.

Quattrocchio, F., Wing, J. F., van der Woude, K., Mol, J. N. M. and Koes, R. (1998). Analysis of bHLH and MYB domain proteins: species-specific regulatory differences are caused by divergent evolution of target anthocyanin genes. Plant Journal *13*: 475-488.

Quattrocchio, F., Wing, J., van der Woude, K., Souer, E., de Vetten, N., Mol, J. and Koes, R. (1999). Molecular analysis of the anthocyanin2 gene of petunia and its role in the evolution of flower color. Plant Cell *11*: 1433-1444.

Ramsay, N. A. and Glover, B. (2005). MYB-bHLH-WD40 protein complex and the evolution of cellular diversity. Trends in Plant Science *10*: 63-70.

Rasmussen, T. B. and Donaldson, I. A. (2006). Investigation of the endosperm-specific sucrose synthase promoter from rice using transient expression of reporter genes in guar seed tissue. Plant Cell Reports *25*: 1035-1042.

Ronchi, A., Petroni, K. and Tonelli, C. (1995). The reduced expression of endogenous duplications (REED) in the maize *R* gene family is mediated by DNA methylation. EMBO *14*: 5318-5328.

Sablowski, R. W. M., Moyano, E., Culianezmacia, F. A., Schuch, W., Martin, C. and Bevan, M. (1994). A flower-specific Myb protein activates transcription of phenylpropanoid biosynthetic genes. EMBO *13*: 128-137.

Sablowski, R. W. M., Baulcombe, D. C. and Bevan, M. (1995). Expression of a flower-specific Myb protein in leaf-cells using a viral vector causes ectopic activation of a target promoter. Proceedings of the National Academy of Sciences of the United States of America *92*: 6901-6905.

Sagasser, M., Lu, G. H., Hahlbrock, K. and Weisshaar, B. (2002). *A. thaliana* TRANSPARENT TESTA1 is involved in seed coat development and defines a WIP subfamily of plant zinc finger proteins. Genes & Development *16*: 138-149.

Sainz, M. B., Grotewold, E. and Chandler, V. (1997). Evidence for direct activation of an anthocyanin promoter by the maize C1 protein and comparsion of DNA binding by related Myb proteins. Plant Cell *9*: 611-625.

Sambrook, J., Fritsch, E. F. and Maniatis, T. (1989). Molecular cloning: A laboratory manual. Cold Spring Harbour Laboratory Press, New York.

Schijlen, E. G. W. M., Ric de Vos, C. H., van Tunen, A. J. and Bovy, A. G. (2004). Modification of flavonoid biosynthesis in crop plants. Phytochemistry *65*: 2631-2648.

Schwarz-Sommer, Z., Huijser, P., Nacken, W., Saedler, H. and Sommer, H. (1990). Genetic control of flower development by homeotic genes in *Antirrhinum majus*. Science *250*: 931-936.

Schwarz-Sommer, Z., Hue, I., Huijser, P., Flow, P. J., Hansen, R., Tetens, F., Lonnig, W., Saedler, H. and Sommer, H. (1992). Characterization of the *Antirrhinum* floral homeotic MADS-box gene *deficiens*: evidence for DNA binding and autoregulation of its persistent expression throughout flower development. EMBO *11*: 251-263.

Schwarz-Sommer, Z., Davies, B. and Hudson, A. (2003). An everlasting pioneer: the stroy of *Antirrhinum* research. Nature Reviews, Genetics *4*: 655-664.

Schwinn, K. E. (1999). Regulation of anthocyain biosynthesis in *Antirrhinum majus*. PhD thesis, University of East Anglia, Norwich, United Kingdom.

Schwinn, K. E., Davies, K. M., Alm, V., Mackay, S. and Martin, C. (2001). Regulation of anthocyanin biosynthesis in antirrhinum. IV International Symposium on *In Vitro* Culture and Horticultural Breeding, Acta Horticulutre.

Schwinn, K. E. and Davies, K. M., Eds. (2004). Flavonoids. In: Plant pigments and their manipulation. Blackwell Publishing, Oxford. No:14.

Schwinn, K., Venail, J., Shang, Y. J., Mackay, S., Alm, V., Butelli, E., Oyama, R., Bailey, P., Davies, K. and Martin, C. (2006). A small family of MYB-regulatory genes controls floral pigmentation intensity and patterning in the genus *Antirrhinum*. Plant Cell *18*: 831-851.

Selinger, D. A., Lisch, D. and Chandler, V. L. (1998). The maize regulatory gene *B-Peru* contains a DNA rearrangement that specifies tissue-specific expression through both positive and negative promoter elements. Genetics *149*: 1125-1138.

Shang, Y. (2007). How the pigment stripes form in snapdragon (*Antirrhinum majus*) flowers: the study of the molecular mechanism of venation pigmentation patterning in flowers. PhD thesis, Massey University, Palmerston North, New Zealand.

Shang, Y., Schwinn, K. E., Bennett, M. J., Hunter, D. A., Waugh, T. L., Pathirana, N. N., Brummell, D. A., Jameson, P. E. and Davies, K. M. (2007). Methods for transient assay of gene function in floral tissues. Plant Methods *(3)* (online).

Shirley, B. W. (1996). Flavonoid biosynthesis: 'new' functions for an 'old' pathway. Trends in Plant Science *1*: 377-382.

Shore, P. and Sharrocks, A. D. (1995). The MADS-box family of transcription factors. European Jounral of Biochemistry *229*: 1-13.

Shou, H. X., Frame, B. R., Whitham, S. A. and Wang, K. (2004). Assessment of transgenic maize events produced by particle bombardment or *Agrobacterium*-mediated transformation. Molecular Breeding *13*: 201-208.

Sommer, H. and Saedler, H. (1986). Structure of the chalcone synthase gene of *Antirrhinum majus*. Molecular & General Genetics *202*: 429-434.

Sommer, H., Beltran, J. P., Huijser, P., Pape, H., Lonnig, W., Saedler, H. and Schwarz-Sommer, Z. (1990). *Deficiens*, a homeotic gene involved in the control of flower morphogenesis in *Antirrhinum majus*. EMBO *9*: 605-613.

Spelt, C., Quattrocchio, F., Mol, J. N. M. and Koes, R. (2000). *Anthocyanin1* of petunia encodes a basic helix-loop-helix protein that directly activates transcription of structural anthocyanin genes. Plant Cell *12*: 1619-1631.

Spelt, C., Quattrocchio, F., Mol, J. and Koes, R. (2002). ANTHOCYANIN1 of Petunia controls pigment synthesis, vacuolar pH, and seed coat development by genetically distinct mechanisms. Plant Cell *14*: 2121-2135.

Steiner, J. M., Yusa, F., Pompe, J. A. and Loffelhardt, W. (2005). Homologous protein import machineries in chloroplasts and cyanelles. Plant Journal *44*: 646-652.

Stickland, R. G. and Harrison, B. J. (1974). Precursors and genetic control of pigmentation: Induced biosynthesis of pelargonidin, cyanidin and delphinidin in *Antirrhinum majus*. Heredity *33*: 108-112.

Strack, R., Werber, M. and Weisshaar, B. (2001). The *R2R3-MYB* gene family in *Arabidopsis thaliana*. Current Opinion in Cell Biology *4*: 447-456.

Suzuki, M., Kao, C. Y. and McCarty, D. R. (1997). The conserved B3 domain of VIVIPAROUS1 has a cooperative DNA binding activity. The Plant Cell *9*: 799-807.

Tamagnone, L., Merida, A., Parr, A., Mackay, S., Culianez-Macia, F. A., Roberts, K. and Martin, C. (1998). The AmMYB308 and AmMYB330 transcription factors from antirrhinum regulate phenylpropanoid and lignin biosynthesis in transgenic tobacco. Plant Cell *10*: 135-154.

Tanner, G. (2003). Condensed tannins. In: Plant pigments and their manipulation. Davies, K. M. (ed.). Blackwell Publishing, Oxford. No:14.

Tonelli, C., Consonni, G., Dolfini, S. F., Dellaporta, S. L., Viotti, A. and Gavazzi, G. (1991). Genetic and molecular analysis of Sn, a light-inducible, tissue specific regulatory gene in maize. Molecular & General Genetics *225*: 401-410.

Tonelli, C., Dolfini, S., Ronchi, A., Consonni, G. and Gavazzi, G. (1994). Light inducibility and tissue specificity of the *R* gene family in maize. Genetica *94*: 225-234.

Vojta, A., Alavi, M., Becker, T., Hormann, F., Kuchler, M., Soll, J., Thomson, R. and Schleiff, E. (2004). The protein translocon of the plastid envelopes. Journal of Biological Chemistry *279*: 21401-21405.

Wade, T., Sohal, A. K. and Jenkins, G. I. (2003). Arabidopsis ICX1 is a negative regulator of several pathways regulating flavanoid biosynthesis genes. Plant Physiology *131*: 707-715.
Walker, A. R., Davison, P. A., Bolognesi-Winfield, A. C., James, C. M., Srinivasan, N., Blundell, T. L., Esch, J. J., Marks, M. D. and Gray, J. C. (1999). The TRANSPARENT TESTA GLABARA1 locus, which regulates trichome differentiation and anthocyanin biosynthesis in *Arabidopsis*, encodes a WD40 repeat protein. Plant Cell *11*: 1337-1349.

Wang, L. and Wessler, S. R. (2001). Role of mRNA secondary structure in translational repression of the maize transcriptional activator *Lc*. Plant Physiology *125*: 1380-1387.

Wei, G. H., Liu, D. P. and Liang, C. C. (2004). Charting gene regulatory networks: strategies, challenges and perspectives. Biochemical Journal *381*: 1-12.

West, A. G., Causier, B. E., Davies, B. and Sharrocks, A. D. (1998). DNA binding and dimerisation determinants of *Antirrhinum majus* MADS-box transcription factors. Nucleic Acids Research *26*: 5277-5287.

Western, T. L., Burn, J., Tan, W. L., Skinner, D. J., Martin-McCaffrey, L., Moffatt, B. A. and Haughn, G. W. (2001). Isolation and characterization of mutants defective in seed coat mucilage secretory cell development in *Arabidopsis*. Plant Physiology *127*: 998-1011.

Wu, Y., Liu, Y., Lee, L., Miner, Z. and Kulesz-Martin, M. (1994). Wild-type alternatively spliced p53: binding to DNA and interaction with the major p53 protein *in vitro* and in cells. EMBO *13*: 4823--4830.

Xie, D. Y., Sharma, S. B., Paiva, N. L., Ferreira, D. and Dixon, R. A. (2003). Role of anthocyanin reducatse, encoded by BANYULS in plant flavonoid biosynthesis. Science *299*: 396-399.

Yanagisawa, S. (2002). The DOF family of plant transcription factors. Trends in Plant Science *7*: 555-560.

Yanagisawa, S. (2004). DOF domain proteins: Plant-specific transcription factors associated with diverse phenomena unique to plants. Plant and Cell Physiology *45*: 386-391.

Zachgo, S., Silva, E. D., Motte, P., Trobner, W., Saedler, H. and Schwarzsommer, Z. (1995). Functional analysis of the *Antirrhinum* floral homeotic DEFICIENS gene in-vivo and in-vitro by using a temperature-sensitive mutant. Development *121*: 2861-2875.

Zhang, F., Gonzalez, A., Zhao, M., Payne, C. T. and Lloyd, A. M. (2003). A network of redundant bHLH proteins functions in all TTG1-dependent pathways in *Arabidopsis*. Development *130*: 4859-4869.

Zhang, H. (1998). Cytokinins and phase change in *Pinus radiata*: morphological, physiological and molecular studies. PhD Thesis, Massey University, Palmerston North, New Zealand.